DEVELOPMENT AND APPLICATIONS OF NOVEL MONOLITHIC STATIONARY PHASES FOR LIQUID PHASE SEPARATIONS

By

VENKATA RAMANA MURTHY JONNADA

Bachelor of Science
Andhra University
Vishakhapatnam, A.P., India
2005

Master of Science
Jawaharlal Nehru Technological University
Hyderabad, A.P., India
2007

Submitted to the Faculty of the
Graduate College of the
Oklahoma State University
in partial fulfillment of
the requirements for
the Degree of
DOCTOR OF PHILOSOPHY
July, 2016.

DEVELOPMENT AND APPLICATIONS OF NOVEL

MONOLITHIC STATIONARY PHASES FOR

LIQUID PHASE SEPARATIONS

Dissertation Approved:

Dr. Ziad El Rassi

Dissertation Adviser

Dr. Barry K Lavine

Dr. Nicholas Materer

Dr. Richard Bunce

Dr. Ranjith Ramanathan

Outside committee member

ACKNOWLEDGEMENTS

First of all, my sincere appreciation goes to my advisor, Dr. Ziad El Rassi, for his guidance, advice, sincerity and dedication to his work, which has made this dissertation possible. I consider myself fortunate to work under him where I was constantly nurtured with ideas and suggestions. This was an unforgettable experience as a student where I blossomed in to total new researcher. I am very great full to him for providing me this opportunity and I will be always indebted to him.

I would also like to convey my thankfulness towards my committee members, Dr. Lavine, Dr. Materer, Dr. Bunce and Dr. Ramanathan for their support and suggestions. It's been a great privilege to attend course work taught by Dr. El Rassi, Dr. Lavine and Dr. Materer. I would like to express my sincere gratitude towards our collaborators from the Robert M. Kerr Food & Agricultural Products Center, Oklahoma State University, especially Dr. Guadalupe Davila El Rassi for the support in my PhD work.

I would like express my gratitude to my former and current lab members Shantipriya Khadka, Renuka Rathnasekara, Sarah Alharthi, Nisansala Ganewatta, and Subhashini Selvaraju for a friendly lab atmosphere. I would like to thank Dr. Nammalwar and Dr. Handa for their help in the synthesis part of the current work.

I am very great full to my wife Shantipriya, without the support of whom this work would not be possible. I would like to cherish the moments of her unconditional love and support during my graduate studies throughout my life. I am blessed to have my

two loving elder sisters Lavanya and Sowjanya, without whose constant support and motivation I would not have completed my PhD. I would like to acknowledge my nephew Varshu and nieces Sumana and Vibhi, who bring a lot of cheer to my life. I would also like to convey my sincere gratitude towards my brothers-in-law Nayudu Ayyala and Dr. Venkat Sakhireddy and my cousin Nalini Rama for their support. I sincerely thank my in-laws Govinda Bahadur and Kavita Khadka for their support.

I would like to acknowledge the support of M N Rao, Praveen Relangi, Anup Kumar, Narasimha Cingitham, Kasi Viswanath Kollati and Ramya Ayyalasomayajula for their constant support and help. My heartfelt gratefulness to my uncle Dr. S. Vijaya Babu for his support in the hard times that our family has faced during these years. I am greatly indebted to him. I would also like to thank my uncle Late S Haranadha Baba, whose memories I would like to cherish throughout my life.

Finally, I would like to dedicate my thesis to my parents Rama Gopala Raju and Surya Rani Jonnada, who are the constant force that drives me forward in my life. I am very lucky to have them as my parents. Their constant support and suggestions both surprise me and guide me towards the destination which I always wished in my life.

Acknowledgements reflect the views of the author and are not endorsed by committee members or Oklahoma State University.

Name: VENKATA RAMANA MURTHY JONNADA

Date of Degree: JULY, 2016

Title of Study: DEVELOPMENT AND APPLICATIONS OF NOVEL MONOLITHIC STATIONARY PHASES FOR LIQUID PHASE SEPARATIONS

Major Field: CHEMISTRY

Abstract: This dissertation aims at developing novel monolithic stationary phases for HPLC, in which three different materials were fabricated for different modes of separation, such as hydrophilic liquid interaction chromatography (HILIC), bio-affinity and reversed-phase chromatography (RPC). Firstly, for HILIC based separations, zwitterionic monolithic columns were prepared by the functionalization of glycidyl methacrylate based monoliths with various glycine moieties. The applications of this monolithic column were demonstrated in the separation of nucleobases and some highly polar drugs, e.g., catecholamine derivatives. This was followed by the introduction of monolithic micro columns that were prepared in 1mm i.d. stainless steel tubing. It involved the *in situ* co-polymerization of *N*-acryloxysuccinimide (NAS) and ethylene glycol dimethacrylate (EDMA) in toluene as the porogen. Through its surface *N*-hydroxysuccinimide functional groups, the NAS-EDMA monolith allowed the immobilization of n-alkyl amine ligands or protein ligands *via* the reaction between the primary amines of the ligands and the NAS-EDMA forming stable amide linkages. The utility of NAS-EDMA monolith was assessed in two different immobilizations of proteins. In one immobilization process, 4 different lectins with different affinity to glycoconjugates were immobilized onto the NAS-EDMA monolith, and the 4 resulting lectin columns were arranged in tandem to capture sub-glycoproteomes from healthy and breast cancer sera. In a second approach, a micro-immobilized enzyme reactor consisting of NAS-EDMA monolith with immobilized trypsin was prepared. This enzyme reactor was coupled on line with an octadecyl silica column and its performance was tested with the tryptic map of cytochrome C. In addition, the NAS-EDMA monolith with covalently attached n-octadecyl chains proved useful in RPC protein separations by micro-HPLC. In the aim of furthering the progress of RPC monoliths, a novel organic monolithic column with surface bound naphthyl ligands was prepared and its applications in RPC were investigated. The monolithic column was prepared by *in situ* co-polymerization of 2-naphthyl methacrylate and trimethylolpropane trimethacrylate and its usefulness was demonstrated in the separation of both small and large molecules. Furthermore, 3 cm short column was prepared for the fast separation of proteins by ultra-steep linear gradients. Finally, oil and meat samples were analyzed for their fatty acid content by a novel fluorescent derivatization strategy, and the separation of the derivatized fatty acids was achieved on both in-house synthesized naphthyl functionalized monolithic column and commercially available silica columns.

TABLE OF CONTENTS

LIST OF TABLES

LIST OF FIGURES

FIGURE PAGE

LIST OF SYMBOLS AND ABBREVIATIONS

6-AQ	6-Aminoquinoline
ABs	Alkylbenzenes
ACN	Acetonitrile
AHA	6-Azidohexanoic acid
AIBN	2,2'Azobis(isobutyronitrile)
AM	Acrylamide
AOD	3-Methylacrylol-3-oxapropyl-3-(*N*,*N*-dioctadecylcarbomyl)-propionate
ATRP	Atom transfer radical polymerization
AZT	3'-Azido-3'-deoxythymidine
BIGDMA	Bisphenol A glycerolate dimethacrylate
BMA	Butyl methacrylate
BSA	Bovine serum albumin
BVPE	1,2-bis(p-vinylphenyl) ethane
CEC	Capilary electrochromatography
CLC	Capillary liquid chromatography
Con A	Concanavalin A
Cyt C	Cytochrome C
DCC	N, N`-dicyclohexyl carbodiimide

DEPs	Differentially expressed proteins
DiEDMA	Dioxyethylene dimethacrylate
DoDDMA	1,12-dodecanediol imethacrylate
EDMA	Ethylene glycol dimethacrylate
FA	Fatty acid
FDR	False discovery rate
GCMA	Glycerol carbonate methacrylate
GG	Glycylglycine
GGG	Glycylglycylglycine
GMA	Glycidyl methacrylate
GMM	Glyceryl monomethacrylate
GNPs	Gold nanoparticles
GO	Graphene oxide
H	Theoretical plate height
HETP	Height equivalent to theoretical plates
HILIC	Hydrophilic interaction liquid chromatography
HPLC	High performance liquid chromatography
i.d.	Internal diameter
IMER	Immobilized enzyme reactor
k	Retention factor
L	Length of the column
LAC	Lectin affinity chromatography
LCA	*Lens culinaris* agglutinin

LFQ	Label free quantification
LMA	Lauryl methacrylate
MAA	Methacrylic acid
MA-L-Phe-OMe	*N*-methacryloyl-L-phenylalanine methyl ester
MBA	*N,N'*-methylenebisacrylamide
MEDSA	*N*,*N*-dimethyl-*N*-metacryloxyethyl-*N*-(3-sulfopropyl)ammonium betaine
Me-α-Man	Methyl-α-D-mannopyranoside
MS	Mass spectrometry
MWCNT	Multi walled carbon nanotubes
N	Theoretical plate number
NA	Nitroalkane
NAHAM	*N*-acryloyltris(hydroxymethyl)aminomethane
NAPM	2-Naphthylmethacrylate
NAS	N-acryloxysuccinimide
NASM	NAS monolith
NASM-OD	NASM-octadecyl
NIPAAm	N-isopropylacrylamide
NMM	Naphthyl methacrylate monolithic
NPC	Normal phase chromatography
NVP	*N*-vinyl-2-pyrrolidinone
o.d.	Outer diameter
ODS	Octadecyl silane
PAHs	Polyaromatic hydrocarbons

PCB-HEM	[6,6]-Phenyl-C_{61}-butyric acid 2-hydroxyethyl methacrylate
PDA	1,4-Bis(acryloyl)piperazine
PEDAS	Pentaerythritol diacrylate
PEG	Polyethylene glycol
PEGDA	Poly(ethyleneglycol) diacrylate
PEI	Polyethyleneimine
PETA	Pentaerythritol tetraacrylate
PMA	Propargyl methacrylate
PTM	Post translational modifications
RCA	*Ricinus communis* I agglutinin
RPC	Reversed phase chromatography
RRT	Relative retention times
SLAC	Serial lectin affinity chromatography
SMA	Stearyl methacrylate
SNA	*Sambucus nigra* agglutinin
SPE	*N*,*N*-dimethyl-*N*-methacryloxyethyl-*N*-(3-sulfopropyl)ammonium betaine
t_0	Retention time of the unretained solute
TCEP	Tris(2-carboxylethyl)phosphine
TEA	Triethylamine
TeEDMA	Tetraethyleneglycol dimethacryl
TMPTA	Trimethylolpropane triacrylate
TOH	Tocopherol

TPTM	Trimethylolpropane tris(3-mercaptopropionate)
t_R	Retention time
TRIM	Trimethylolpropane trimethacrylate
Tris	Tris(hydroxymethyl)aminomethane
u	Linear flow velocity
VPBA	4-vinylphenyl boronic acid
W_i	Peak width at inflection point
α	Selectivity factor
β-CD	β-cyclodextrin
σ	Standard deviation

CHAPTER I

BACKGROUND, RATIONALE AND SCOPE OF THIS INVESTIGATION

Introduction

High performance liquid chromatography (HPLC) is the most used analytical technique for the separation and quantification of complex mixtures of compounds. Various fields such as pharmaceutical, food, forensic and environmental industries frequently depend on HPLC for analyzing numerous samples in their chain of manufacturing activities including raw material analysis, monitoring of the reactions and purity assay of the finished products [1]. The number of samples to be analyzed per day to meet the production line are ever increasing and regularly becoming one of the deciding factors in determining the cost of the manufacturing. This makes chromatography an important tool in the industrial setup. So, chromatographers are often in search for a fast, reliable and efficient methods for throughput analysis with no compromise in resolution. The chromatographic column in which the separation of analytes occurs can be regarded as the heart of HPLC. These HPLC columns are predominantly made of functionalized

** Some of the contents of this chapter have been published in Electrophoresis 2015. 36(1): p. 76-100.*

silica particles and are often regarded as “packed columns” and these packed columns suffer from some limitations such as bed settling, high backpressure at column inlet and instability at high pH. Monolithic HPLC columns represent a new category of column chemistry, which is made of a single piece of polymeric rod with bimodal porous structure consisting of macropores and mesopores [2-4]. These monolithic columns have distinctive features, which distinguish them from packed columns in that they are devoid of inter-particular spaces with reduced backpressures and no bed settling at column inlet. The preparation of monolithic columns is convenient, economical and can be easily modified with a variety of surface functionalities. Moreover, monolithic columns made from organic backbone are resistant to varying the mobile phase pH, which makes them very robust. More significantly, the monolithic column technology finds its advantages in the preparation of micro and nanoscale chromatographic columns where packing of silica particles is challenging to accomplish. Specially, after hyphenation of LC to mass spectrometry (MS) has become the most sensitive and efficient analytical methodology in the analysis of small and large biomolecules. In this task, micro and nano scale chromatographic columns have become significant tools in recent times [5].

This dissertation aims at the development of novel stationary phases with diverse functionalities for various modes of separation strategies in liquid chromatography. Thus, this chapter provides the background and basics of the chromatographic parameters that are relevant to this study and also provides a detailed update of the recent progress in monolithic column chemistry pertaining to HPLC over the last five years, which are relevant to this dissertation.

Three different modes of separation in liquid chromatography, *viz*., hydrophilic interaction liquid chromatography (HILIC), affinity chromatography and reversed phase chromatography (RPC) are explored with novel organic monolithic stationary phases. In chapter II, the preparation of highly polar stationary phases with surface bound glycylglycylglycine (GGG) along with its applications in HILIC based separations will be discussed which will be followed by chapter III, where the preparation of poly (N-acryloxy succinimide (NAS)-co-ethylene glycol dimethacrylate (EDMA)) monolith will be discussed along with its use as a precursor monolith for grafting octadecyl surface ligands for RPC. Later, chapter IV comprises the methodology to further exploit the potentials of the NAS monolithic (NASM) precursor to immobilize proteins on its surface followed by demonstrating its applications in bio-affinity chromatography. To broaden the scope of monolithic columns in HPLC, an RPC based naphthyl functionalized organic monolithic (NMM) column and its characterization will be discussed in chapter V. Thereafter, chapter VI comprises of a newly designed fluorescent derivatization strategy for fatty acids and their analysis in complex food samples.

Chromatographic parameters relevant to this dissertation

Some of the chromatographic parameters that are relevant to this dissertation are illustrated by means of a sketchy chromatogram shown in Figure 1, where t_0 is the retention time of unretained solute or simply the column dead time. This corresponds to the so-called inert tracer, which is assumed not to interact with the stationary phase, and therefore travels with the mobile phase flow velocity and elutes at time t_0. In this dissertation, thiourea and toluene were used as the t_0 markers for hydrophobic and

hydrophilic stationary phases, respectively. On the other hand, the retained sample emerges after the t_0 marker at time t_R (see Figure 1), which is the solute' retention time. It is defined as the time elapsed between the sample introduction and the appearance of the peak apex at the end of the column.

Retention factor (k): Solute retention is measured by the dimensionless quantity called retention factor (k), which is a distribution ratio for the amount of solute in the stationary phase to that in the mobile phase. It is calculated from the chromatogram as follows

$$k = \frac{t_R - t_0}{t_0} \qquad \text{I}$$

The difference in the retention time of the solute (t_R) from that of the inert tracer (t_0) gives the time spent by the solute in the stationary phase $t_R` = t_R - t_0$.

Selectivity factor (α) or retention ratio: The selectivity factor is calculated by the ratio of the retention factors of two adjacent peaks on the chromatogram and is given by

$$\alpha = \frac{k_2}{k_1} \quad (\text{Where } k_2 > k_1) \qquad \text{II}$$

Plate height (H) and plate number (N): In the plate theory, a chromatographic column is viewed as a series of contiguous discrete sections called theoretical plates. The movement of the solute through the column is thought of as the stepwise transfer of the solute from plate to plate while moving down the column. Thus, the number of theoretical plates or plate number (N) is used to measure the efficiency of the column, which is defined as the

square of the ratio of the retention time of the analyte to the standard deviation (σ) of its peak as shown in equation III.

$$N = \left(\frac{t_R}{\sigma}\right)^2 \qquad \text{III}$$

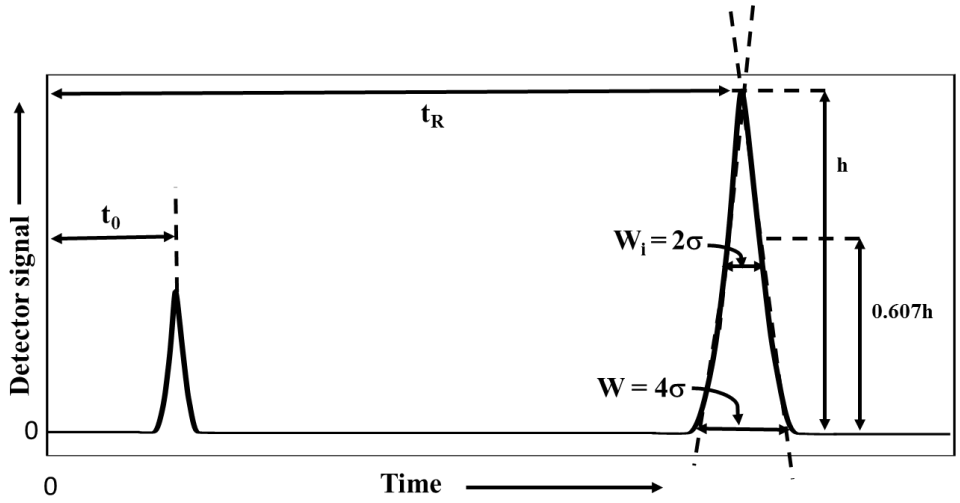

Figure 1. *Sketchy chromatogram for illustrating some essential chromatographic parameters.*

In this dissertation σ is estimated from the peak width at inflection point W_i, (See Figure 1) at exactly 0.607 h, where h is the peak height.

$$N = 16\left(\frac{t_R}{W}\right)^2 = 4\left(\frac{t_R}{W_i}\right)^2 \qquad \text{IV}$$

Since the retention time and peak width have the same units, N is a dimensionless quantity. The height of each plate or height equivalent to theoretical plates (HETP) is obtained from the length of the column (L) and the plate number (N) and is calculated according to equation V. Generally, this HETP is used to assess the efficiency of the chromatographic column.

$$H = \frac{L}{N} \qquad \text{V}$$

van Deemter equation*:* The van Deemter equation describes the relationship between the HETP and the linear flow velocity (u) of the mobile phase. It consists of three different terms as follows

$$H = A + \frac{B}{u} + Cu \qquad \text{VI}$$

The velocity independent term A represents the contribution to zone broadening by eddy diffusion. The second term is that of longitudinal molecular diffusion and is inversely proportional to the linear flow velocity (u), while the C term signifies the contribution of resistance to mass transfer in both the stationary and mobile phases (see Figure 2). Plot of H versus u or the so-called van Deemter plot shows the dependence of column efficiency on mobile phase flow velocity where one can see the major contributor to band broadening at low u values is longitudinal molecular diffusion while at high u values mass transfer resistance is the main contributor to band broadening. In between, there is a minimum plate height H_{min} corresponding to optimum u (u_{opt}) where maximum plate count is obtained.

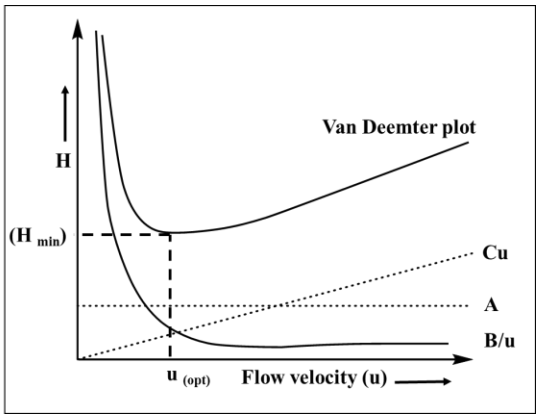

Figure 2. *van Deemter plot.*

Overview of current trends in monolithic HPLC column chemistry

In the following section, an overview about the various monolith column chemistries introduced over the last five years is presented. This section focuses mainly on nonpolar and polar functionalized monolithic stationary phases and their use in RPC and HILIC based separations, respectively. Therefore, the following section is divided into two main sub-sections: (I) Nonpolar based monolithic stationary phases for RPC separations and (II) polar functionalized monolithic stationary phases for HILIC based separations.

Nonpolar organic monolithic stationary phases for RPC separations

There are two main strategies adopted in the fabrication of nonpolar organic monolithic columns: (I) Functionalization by direct copolymerization and (II) post polymerization modification with various functionalities. The second strategy is adopted when significant portion of the functional ligands remain concealed in the polymer network. Both of the adopted strategies involve judicious choice of the functional monomer, cross-linker and porogenic mixture. In recent times, a number of monoliths were introduced for various modes of HPLC. These monoliths are designed to withstand the high flow velocity usually encountered in HPLC. As such the monolith should have a good mechanical stability and not compress under high pressure.

Nonpolar monolithic columns prepared by direct copolymerization of monomers. In order to obtain a generalization about the effect of alkyl chain length and shape of the

functional monomer on the structural features of the monolith, Urban et al. used different alkyl methacrylate monomers with butyl, cyclohexyl, 2-ethyl hexyl, lauryl, and stearyl functional groups in the polymerization mixture with EDMA as the crosslinker. 1-Propanol and 1,4-butanediol were chosen as the porogens in all cases [6]. The polymerization was performed in 0.32 mm i.d. fused capillary columns. Alkyl benzenes (ABs) and standard proteins were used as test solutes, and the standard parameters such column permeability, methylene and phenyl selectivity were assessed. The highest permeability was observed for butyl methacrylate monolith and the least for the lauryl methacrylate while the other three monoliths showed similar permeability. Lauryl and cyclohexyl methacrylate provided marginally better separations for the tested standard proteins by gradient elution in HPLC.

Triallyl isocyanurate [7] was used as a functional monomer along with trimethylolpropane triacrylate (TMPTA) as the crosslinker to prepare a monolith using atom transfer radical polymerization (ATRP) with CCl_4 as an initiator and $FeCl_2$ as a catalyst. The monolith was prepared both in stainless steel columns (5 cm x 4.6 mm i.d.) and in fused-silica capillaries (100 mm x 150 μm i.d.) for their applications in HPLC and capillary liquid chromatography (CLC), respectively. The composition of the porogens and the polymerization temperature by ATRP process were further optimized to get the desired mechanical characters and the monoliths were characterized by using FT-IR and SEM imaging. The backpressures obtained at the column inlet showed a fairly linear relationship with the linear velocity of the mobile phase. Separation of some aromatic compounds was demonstrated in both columns of analytical and capillary format.

Recently, a novel monolithic column with double C-18 chains was introduced by Duan *et al*. [8] for RPC whereby the functional monomer 3-methylacrylol-3-oxapropyl-3-(*N*,*N*-dioctadecylcarbomyl)-propionate (AOD) was co-polymerized with the crosslinker EDMA. Fused-silica capillary columns with 100 µm i.d. were used in the preparation of the monolithic column for µHPLC. A binary porogenic mixture of 2-methyl-1-propanol and 1, 4-butanediol was used. This column showed good permeabilities with ACN, MeOH and water. Alkylphenones were used as test solutes and the methylene selectivity was observed to be as 1.68, which was similar to 1.70 obtained with the poly (stearyl methacrylate (SMA)-co-EDMA) monolithic column. 16 poly aromatic hydrocarbons were separated on the poly (AOD-co-EDMA) monolithic column by using gradient elution. Again tocopherol (TOH) was used to test this column, and a complete separation of α-, β-, γ-, and δ- TOH isomers was obtained in in less than 30 min. Baseline separation was achieved for three different standard proteins in less than 8 min in reversed phase gradient elution.

A set of eight different crosslinkers were evaluated in the preparation of a series of reversed-phase monolithic capillary columns for use in nano LC and their effect on the separation efficiency was systematically investigated [9]. The eight different dimethacrylate crosslinking monomers were copolymerized with lauryl methacrylate (LMA) as the functional monomer in the presence of the porogens 1,4-butanediol and 1-propanol using a thermally initiated free radical polymerization. Fused silica capillary columns of 320 µm i.d. were used. The crosslinkers used have repeated methylene and oxymethylene units, including EDMA, tetramethylene dimethacrylate, hexamethylene dimethacrylate, dioxyethylene dimethacrylate, trioxyethylene dimethacrylate,

tetraoxyethylene dimethacrylate, pentaerythritol dimethacrylate, and bisphenol A dimethacrylate. Four standard proteins, namely insulin from bovine serum pancreas, cytochrome C, bovine serum albumin and β-lactoglobulin were separated on the three monolithic columns by gradient elution in nano LC method. The separation improved from the EDMA based column to the tetramethylene dimethacrylate based column and baseline separation was achieved in less than 4 min for the hexamethylene dimethacrylate based monolith. On the other hand, the monoliths made with the crosslinkers of repetitive oxymethylene groups showed very poor efficiency for the separation of proteins.

In a very recent work, Liu et al. [10] introduced a monolithic column for HPLC by the free-radical co-polymerization of a mixture of two functional monomers, TMPTA along with N-isopropylacrylamide (NIPAAm) and the crosslinker EDMA. The polymerization process yielded a highly crosslinked poly (TMPTA-co-NIPAAm-co-EDMA) monolith in a 50 mm x 4.6 mm i.d. stainless steel column. Flow rates of up to 7 mL/min were achieved indicating good mechanical stability and permeability of the column. Furthermore, separation of benzene, biphenyl and phenanthrene was demonstrated on the column by isocratic elution. In another work from the same laboratory, Bai et al. [11] used the TMPTA along with EDMA to produce a dense network of nonpolar monolith in a 50 mm x 4.6 mm i.d. stainless steel column and used it for the RPC separations of small aromatic molecules.

1,6-Hexanediol ethoxylate diacrylate, a new crosslinker was reported by Lin et al. [12] for making nonpolar monoliths for RPC separations in capillaries. The suitability of this new crosslinker was studied with three alkyl methacrylate functional monomers, namely butyl methacrylate (BMA), LMA and SMA. The co-polymerization was achieved

in the presence of the porogenic mixture of 1-propanol and 1,4-butanediol. *In situ* thermally initiated free radical polymerization was performed in 250-µm i.d. fused silica capillaries. The permeabilities, porosities and the separation efficiencies of the 18 different monoliths were compared of which the 1,6-hexanediol ethoxylate diacrylate based alkyl methacrylate monoliths was found to have the highest column efficiencies of up to 14,800 plates/m for uracil and separation of mixture of eight phenyl urea herbicides samples.

In a strategy to increase the surface area of the monolith, Li et al. [13] used the approach of solely using crosslinking monomers to produce nonpolar monoliths a concept that was originally introduced by El Rassi and coworkers [14, 15]. Bisphenol A dimethacrylate, bisphenol A ethoxylate diacrylate and pentaerythritol diacrylate monostearate were used to produce nonpolar monolithic capillary columns (75 µm i.d.) for RPC of small molecules. ABs and alkylparabens were used as test solutes in both gradient and isocratic nano LC. Baseline separations were achieved for ABs and alkylparabens when used with poly(bisphenol A ethoxylate diacrylate), poly(bisphenol A dimethacrylate) and poly(pentaerythritol diacrylate monostearate) monolithic columns in gradient elution. The poly (bisphenol A ethoxylate diacrylate) yielded an average plate number of 30,000 plates/m, whereas the poly (bisphenol A dimethacrylate) and the poly (pentaerythritol diacrylate monostearate) exhibited a maximum of around 61,000 plates/m and 21,000 plates/m, respectively. These columns showed good permeabilities and highly repeatable results. This may be due to the single monomer approach in the synthesis of the monoliths, which involves lesser variables in the synthesis.

In a more recent work from the same laboratory, Lui et al. [16] further exploited the above concept of using single crosslinking monomers to produce highly crosslinked polymeric monoliths for RPC in 75 μm i.d. fused-silica capillary columns. Alkanediol methacrylates monomers, namely, 1,4-butanediol dimethacrylate, 1,5-pentanediol dimethacrylate, 1,6-hexanediol dimethacrylate, 1,10-decanediol dimethacrylate, 1,12-dodecanediol dimethacrylate, 1,3-butanediol dimethacrylate, and neopentyl glycol dimethacrylate were used in this study. Dodecanol and methanol were selected as the porogens for the synthesis of the monoliths. The columns showed good mechanical stability, permeability and reproducibility. ABs and parabens were separated using gradient elution and baseline separations were achieved in both cases. The plate numbers for all the monolithic columns were observed between 14,000 and 35,000 plates/m.

In a further report, the same group demonstrated the use of highly crosslinking polymers made from various dimethacrylate of C6 functional groups namely, 1,6-hexanediol dimethacrylate, cyclohexanediol dimethacrylate and 1,4-phenylene diacrylate in the separation of small molecules (e.g., ABs) by RPC using the nano LC format. The 1,6-hexanediol dimethacrylate column exhibited the highest efficiency (86,000 plates/m) with the least permeability. Single monomer approach might be the reason for the repeatability of the monolith fabrication [17]. Isocratic elution of ABs was performed at an optimum flow rate of 300 nL/min on the capillary columns made with monolith from these monomers. Whereas the1,6-hexanediol dimethacrylate and the 1,4-cyclohexanediol dimethacrylate-based monoliths offered baseline resolution for the ABs investigated, the 1,4-phenylene diacrylate based monolith showed very poor resolution.

Liu et al. have synthesized new monolithic RPC stationary phases for CLC based on single multi-acrylate/methacrylate containing monomers [i.e., 1,12-dodecanediol imethacrylate (1,12-DoDDMA), trimethylolpropane trimethacrylate (TRIM) and pentaerythritol tetraacrylate (PETA)] using organotellurium-mediated living radical polymerization, which was expected to produce more efficient monolithic columns than conventional free radical polymerization [18]. Rigid structural monoliths were obtained using all of the monomers, and all monolithic columns could be used to separate ABs. As poly(PETA) has a C5 functional group it showed less retention and selectivity than poly(1,12-DoDDMA) and poly(TRIM), which contain more hydrophobic C12 and C6 functionalities respectively.

The same research group has prepared a high efficient monolith by single crosslinker polymerization of poly(ethyleneglycol) diacrylate (PEGDA) monomers for RPC of small molecules [19]. This monolithic column was successfully used to separate low molecular weight compounds such as hydroxyl benzoic acids, phenols, alkyl parabens and phenyl urea herbicides. The retention mechanism was found to follow typical reversed phase behavior with additional hydrogen bonding interactions, making the column suitable for separation of polar compounds, which are otherwise poorly retained on C-18 columns.

Lately, photo initiated thiol-acrylate polymerization was exploited for the preparation of monolithic columns, in which the acrylate are not only homopolymerized, but also coupled with thiol containing monomers offering a simple way to fabricate various porous polymer monoliths. In this regard, Wang et al. have developed a simple approach for rapid preparation of polymeric monolithic columns in UV-transparent fused-silica capillaries *via* photo initiated thiol-acrylate polymerization of pentaerythritol

diacrylate (PEDAS) and trimethylolpropane tris(3-mercaptopropionate) (TPTM) within 10 min, in which the acrylate homopolymerized and copolymerized with thiol simultaneously [20]. The chromatographic properties of poly(PEDAS-*co*-TPTM) monolith was evaluated by micro-LC separation of ABs, phenols and basic compounds under RPC conditions. Beside the separation of these small molecules, the separation of complex sample, a tryptic digest of four proteins (BSA, myoglobin, ovalbumin and α-casein), was also performed on of poly(PEDAS-*co*-TPTM) monolith by micro-LC-MS/MS indicating that this monolith may have a potential in proteomics analysis.

Nonpolar monolithic columns prepared by incorporating nanoparticles. Some nonpolar nano-entities such as C_{60} fullerenes and carbon nanotubes have been incorporated into monolithic columns either by physical adsorption or by covalent attachment to the surface of the monolith. The covalent incorporation of nanoparticles was addressed in a recent investigation by Chambers et al. [21] who reported porous monoliths functionalized through copolymerization of a C60 fullerene-containing methacrylate monomer for the separations of small molecules in a CLC format. The monoliths consisted of poly(glycidyl methacrylate (GMA)-co-EDMA) and poly(BMA-co-EDMA) capillary columns, which incorporated the new monomer [6,6]-phenyl-C_{61}-butyric acid 2-hydroxyethyl methacrylate (PCB-HEM). Both reported monoliths showed added advantages in the separation of ABs. Upon the addition of PCB-HEM, the plate number for benzene increased to 72,000 plates/m. When compared to the parent monolith, the addition of PCB-HEM to poly(BMA-co-EDMA) monolith, yielded enhanced retention toward AB and showed an efficiency for benzene exceeding 110,000 plates/m.

Along the same lines, another monolithic column was prepared in a 50.0 mm x 4.6 mm i.d. stainless steel tubing through the copolymerization of 3-(trimethoxysilyl) propylmethacrylate modified graphene oxide (GO) with GMA and EDMA. The GO monolithic column thus prepared was evaluated in the RPC separation of small molecules such as some steroids and aniline compounds [22]. The rationale behind using GO is that these carbonaceous nanoparticles have a unique structure and excellent physiochemical and mechanical characteristic features, including the high surface area and the π-π stacking ability. In fact, a methacrylic acid (MAA)-co-EDMA based monolithic column with incorporated GO was introduced for the CEC of polyaromatic hydrocarbons *via* π-π interactions [23].

Using physical entrapment, Chambers et al. reported the use of entrapped carbon nanotubes in poly(GMA-co-EDMA) monoliths for CLC in order to improve the retention abilities of the monolith towards small molecules [24]. The entrapment of the multi walled carbon nanotubes (MWCNT) in the methacrylate monoliths significantly improved the column efficiency to 35,000 plates/m, when compared to the parent GMA-EDMA monolith, which was on the order of 1800 plates/m.

In a different recent investigation, Aqel et al. reported the incorporation of MWCNT by physical entrapment in benzyl methacrylate-co-EDMA monolithic columns for CLC [25]. Capillaries of 0.32 mm i.d. were used for making the monolithic columns. Alkylphenones and phenols, which were chosen as the test solutes showed significant improvement in separation efficiencies when going from the parent monolith to the one with incorporated MWCNT.

Mayadunne and El Rassi [26] reported the incorporation by physical entrapment of MWCNT into monolithic columns for the separations of small and large molecules in HPLC. An octadecyl monolithic column based on the *in situ* polymerization of octadecyl acrylate and TRIM was optimized for use in HPLC separations of small and large solutes (e.g., proteins). To further modulate the retention and separation of proteins, small amounts of carbon nanotubes were incorporated into the octadecyl monolith column. This carbon nanotube "coated" monolith proved useful in the HPLC separation of a wide range of small solutes including enantiomers. The authors claimed that nonpolar and π-π interactions were responsible for solute retention on the monolith with incorporated carbon nanotubes.

Nonpolar monolithic columns prepared by post polymerization modification with various functionalities. In a post polymerization kind of approach, the GMA-EDMA monolith, which was used to entrap MWCNT [24], was functionalized with ammonia, and then shortened carbon nanotubes, bearing carboxyl functionalities, were attached *via* electrostatic interactions with the amine functionalities of the monolith. Six ABs were separated on this new MWCNT modified monolithic columns exhibiting an efficiency of 44,000 plates/m [24] when using THF as the organic modifier in the hydro-organic mobile phase.

Very recently, Poupart et al. have prepared in capillary reactive polymer monoliths from glycerol carbonate methacrylate (GCMA) functional monomers and EDMA crosslinker followed by further functionalization with different ligands [27]. Cyclic carbonates can undergo ring opening in the presence of nucleophilic compounds

such as primary amines for further easy and straightforward functionalization of the as-obtained porous matrix with organic compounds of interest. A successive radical photo-triggered thiol-ene "click" addition allowed for the efficient grafting of 1-octane thiol or mercaptobutyric acid onto the alkene functionalized monolith. Four ABs were baseline separated on C8-grafted GCMA-based monolith under RPC conditions showing the potential of such functional GCMA-based monoliths.

From the above overview of the literature, one can quickly realize that the field of monolithic columns of improved chemistries is still evolving, and the need for better columns is currently an active theme of research. This dissertation is aimed at furthering the development of the field of RPC monoliths for HPLC separations.

Polar organic monolithic columns for HILIC based separations.

The use of polar organic stationary phases for HILIC based separations was discovered in early 1990s [28] and its usage has been extensively increased over the last ten years. They are highly advantageous in the separation of highly polar compounds, which is very difficult to achieve in RPC separations. The details of HILIC based stationary phases is discussed in detailed in the introduction of chapter II. As discussed in the preceding sections, HILIC stationary phases also are further sub-classified based on their preparation by (i) direct co-polymerization and (ii) functionalization by post polymerization modification.

HILIC stationary phases by direct copolymerization of monomers. Staňková et al. [29] have studied the effect of crosslinkers on the performance of polar monolithic

columns intended for use in HILIC applications. They have synthesized seven different polymethacrylate monolithic capillary columns using *N*,*N*-dimethyl-*N*-metacryloxyethyl-*N*-(3-sulfopropyl)ammonium betaine (MEDSA) functional monomer and various crosslinking monomers differing in polarity and size including EDMA, tetramethylene dimethacrylate, hexamethylene dimethacylate, dioxyethylene dimethacrylate (DiEDMA), PETA, bisphenol A dimethacrylate and bisphenol A glycerolate dimethacrylate (BIGDMA). The zwitterionic monolithic columns prepared with polar crosslinkers show dual RPC-HILIC separation mechanisms, depending on the sample properties, and on the mobile phase composition. The separations of some highly polar compounds and phenolic acids were demonstrated.

Jandera et al. have prepared 0.53 and 0.32 mm i.d. micro columns by the *in situ* copolymerization of zwitterionic sulfobetaine functional monomer MEDSA with BIGDMA and DiEDMA crosslinker in the presence of 1-propanol, 1,4-butanediol, and water as the porogens [30]. The HILIC analysis of a mixture of antioxidants containing 32 phenolic acids and flavonoids on the 0.53 mm i.d. monolithic column under gradient conditions was demonstrated.

A novel poly(*N*-acryloyltris(hydroxymethyl)aminomethane (NAHAM)-co-PETA) monolith has been prepared by Chen et al. and its usefulness investigated in CLC [31]. The polymer monolith was synthesized by the *in situ* copolymerization of the functional monomer NAHAM and the crosslinker PETA in the presence of polyethylene glycol (PEG) in dimethyl sulfoxide as the porogens. Efficient separation of five nucleosides, seven benzoic acids and five anilines were achieved on this monolithic column. In addition, an online coupling of solid phase micro-extraction with CLC was developed by

using the poly(NAHAM-co-PETA) monolith, which was successfully applied for the rapid and sensitive determination of four nucleosides in urine samples.

Chen et al. have studied the effect of hydrophilic and hydrophobic porogenic systems on the porous properties of the poly (MAA-co-EDMA) monolith and its separation efficiencies in HILIC in CLC format. Baseline separation was achieved for five nucleosides along with the separation of aniline and benzoic acid derivatives. Retention patterns of aniline and benzoic acid solutes exhibited a typical hydrophilic interaction with the anionic monolith. Moreover, electrostatic repulsion experienced by the acidic solutes revealed the presence of ion exchange type of interactions in the column. The poly(MAA-co-EDMA) monolith column was used to separate the tryptic digest of bovine serum albumin (BSA) [32]

Lin et al. have reported a novel polymer monolith with three modes of interactions including reversed phase, hydrophilic and cation-exchange interactions in CLC. This monolith was prepared by the *in situ* copolymerization of GMA and 4-vinylphenyl boronic acid (VPBA) functional monomers with the EDMA crosslinker [33]. VPBA was chosen as one of the monomers to prepare the mixed mode monolith because it was believed that monoliths containing hydrophilic/ionizable $B(OH)_2$ groups would afford more flexible adjustment of selectivity in terms of hydrophobic and hydrophilic as well as cation-exchange interactions. The column performance was assessed by the separation of series of amides and anilines. Poly(GMA-co-VPBA-co-EDMA) monolith was used to separate alkaloids and proteins successfully due to its RPC and HILIC mixed mode retention behavior.

Yuan et al. have used the highly polar monomer *N*,*N*-dimethyl-*N*-acryloyloxyethyl-*N*-(3-sulfopropyl)ammonium betaine (SPE) and the hydrophilic crosslinker *N,N'*-methylenebisacrylamide (MBA) for the preparation of a HILIC monolith to be used in micro-HPLC [34]. Simultaneously, they have prepared another novel monolithic column containing SPE as the functional monomer and EDMA as the crosslinker. The polarity and separation efficiency of poly(SPE-co-MBA) monolith column was compared with that of the poly(SPE-co-EDMA) monolithic column. The authors have reported that the poly(SPE-co-MBA) monolith yields better overall separation efficiencies, and greater polarity than the poly (SPE-co-EDMA) monolith and finally, the optimized poly(SPE-co-MBA) monolith was successfully applied to the separation of a series of polar compounds, such as phenols, bases, benzoic acid derivatives and peptides. It was also suitable for the separation of highly polar compounds, such as allantoin and urea and their determination in cosmetic products.

In another report, Chen et al. have described a porous monolith for HILIC applications using SPE as the functional monomer and PEGDA, which is a relatively hydrophilic crosslinker in a binary porogenic system comprising isopropanol and decanol [35]. This monolith showed typical HILIC retention mechanism when the content of ACN in the mobile phase was higher than 60%. Since SPE contains both positive and negative charges, the poly(SPE-co-PEGDA) monolith may exhibit ionic interactions with charged compounds in addition to hydrophilic interactions. As expected, varying the organic solvent concentration, pH and salt concentration of the mobile phase largely affected the selectivity, resolution and peak shapes. The poly(SPE-co-PEGDA) monolith was successfully used to separate amides, phenols and benzoic acid derivatives.

Another zwitterionic monolith has been reported by Foo et al. [36] which was prepared in a 200 µm i.d. fused capillary tubes by the co-polymerization of the zwitterionic functional monomer SPE and the crosslinker 1,2-bis(p-vinylphenyl) ethane (BVPE) in the presence of porogens toluene and methanol. The chromatographic properties of the optimized poly (SPE-co-BVPE) monolithic column were evaluated with test mixtures containing both basic and neutral compounds in the HILIC mode using a gradient elution. This poly(SPE-co-BVPE) monolith was successfully applied for the rapid and high resolution separation of low molecular weight compounds such as pyrimidines and purines producing sharp and symmetrical peaks using HILIC gradient separation mode.

HILIC has been used for glycoprotein/peptide enrichment due to low bias to different types of glycopeptides, mild and convenient operational conditions and good compatibility with LC-MS analysis. In this regard, amide functionalized hydrophilic monolith was synthesized in 100 µm i.d. capillary columns by the *in situ* photo-polymerization of *N*-vinyl-2-pyrrolidinone (NVP), acrylamide (AM) and MBA in a UV transparent capillary, and successfully applied for HILIC based enrichment of N-linked glycopeptides [37]. For the preparation of hydrophilic monolith, AM and MBA were respectively selected as the functional monomer and the crosslinker. The NVP was used as the stabilizer monomer to prevent structural damages to the monolith under high mobile phase flow velocities. The prepared monolith was successfully applied to the N-glycosylation profiling of HeLa cells and human serum samples showing the suitability of the HILIC column in large scale glycoproteomics analysis.

Guo et al. have prepared a derivatized β-cyclodextrin (β-CD) functionalized monolithic columns by a "one-step" strategy using click chemistry for HIILIC based separations [38]. First, the intended derivatized β-CD functional monomers were synthesized by a click reaction between propargyl methacrylate and mono-6-azido-β-CD and sulfonation or methylation was carried out. Finally, monolithic columns were prepared in 100 μm i.d. capillary column through a one-step *in situ* copolymerization of the derivatized β-CD functional monomer and ethylene glycol dimethacrylate (EDMA) crosslinker. DMSO was used as a porogen in the polymerization mixture to facilitate dissolvation of polar monomer with non-polar crosslinker while methanol was used as the microporogen. Polar solutes such as nucleosides, small peptides and some other polar solutes were well separated under HILIC conditions.

In the same way, Li et al. have reported versatile method to prepare hydrophilic interaction/ weak anion exchange/ reversed phase trimodal polymer monoliths by one step copolymerization of amino-acid based monomers and MBA crosslinker [39]. First amino acid containing monomer namely, *N*-methacryloyl-L-phenylalanine methyl ester (MA-L-Phe-OMe) was synthesized through the acrylation reaction between L-phenylalanine methyl ester hydrochloride and methacryloyl chloride. Then poly(MA-L-Phe-OMe-*co*-MBA) monolith was synthesized within a stainless steel column (50 × 4.6 mm i.d.) by the *in situ* copolymerization of functional monomer (MA-L-Phe-OMe) and the crosslinker MBA in the presence of dodecanol and DMSO as porogens. In the poly(MA-L-Phe-OMe-*co*-MBA) monolith, MA-L-Phe-OMe has hydrophobic aromatic ring and MBA has more hydrophilic amide groups. Therefore, this amino acid based monolithic column shows HILIC/RP mixed mode behavior and separation of

hydrophobic polycyclic aromatic hydrocarbons and hydrophilic nucleobases/nucleosides could be achieved in a single column by just altering the ACN content in the mobile phase.

Recently, Yu et al. have developed a simple, time saving synthetic procedure by combining free radical polymerization and azide-alkyne cycloaddition "click" reaction for the one-pot synthesis of poly(6-azidohexanoic acid (AHA)-*co*-propargyl methacrylate (PMA)-*co*-EDMA) polymer monolithic column for CLC carrying without using any post modification [40]. Here a binary porogenic solvent containing DMSO and 1- dodecanol was chosen. Mixtures of nucleobases/nucleosides, polar amides and phenolic compounds were successfully separated on poly(AHA-*co*-PMA-*co*-EDMA) under HILIC conditions. Similarly a mixture of polycyclic aromatic hydrocarbons was separated on the same column under RPC conditions.

The same research group followed a similar "one-pot" approach for the preparation of poly(3'-azido-3'-deoxythymidine(AZT)-*co*- PMA-*co*-PETA) monolith by combining free radical polymerization with click chemistry [41]. Owing its unique chemical structure containing the hydrophilic/ionizable nucleoside group and the azido group, AZT is regarded as an ideal functional monomer to make polar monoliths for mixed mode chromatography. A mixture of polar amides was successfully separated on poly(AZT-*co*-PMA-*co*-PETA) under HILIC conditions. Similarly a mixture of ABs was separated on the same column under RPC conditions. Hydrophilic partitioning/cation exchange interaction was also evaluated by the separation of five benzoic acid derivatives which was possible due to the electrostatic interactions between poly(AZT-*co*-PMA-*co*-PETA) monolith and charged analytes due to the existence of multiple ionizable moieties.

In order to investigate the effect of the crosslinker on the separation performance of polar zwitterionic sulfoalkylbetaine-type monolithic columns, three crosslinkers, i.e. 1,4-bis(acryloyl)piperazine (PDA), EDMA and MBA, were copolymerized with the hydrophilic monomer SPE [42]. Results showed that the hydrophilicity of poly(SPE-*co*-MBA) and poly(SPE-*co*-PDA) was significantly higher than that of poly(SPE-*co*-EDMA) and the hydrophilicities are in accordance with the polarity order of the crosslinkers. Finally, the separation of four benzoic acid derivatives was demonstrated in 100 μm i.d. capillary for its applications in CLC.

HILIC stationary phases by post polymerization modification. Yongqin and coworkers have prepared a porous polymer monolith with zwitterionic functionalities *via* the "thio-ene" click chemistry for CLC [43]. The popular poly(GMA-co-EDMA) monolith was used for this purpose. The epoxy groups of the generic GMA-EDMA monolith were reacted first with cystamine followed by snipping the disulfide bond using tris(2-carboxylethyl)phosphine (TCEP) that liberates the desired thiol groups. Most of the cystamine reacts through both amine functionalities to deliver a more substantial degree of functionalization. Then, the thiol-containing monolith was clicked with the zwitterionic SPE functional monomer. This reaction yielded a monolith with a hydrophilic surface chemistry suitable for separation in HILIC. This monolith was successfully used to separate six peptides by performing gradient elution with decreasing percentage of acetonitrile in the mobile phase. Four nucleosides were also selectively separated on this HILIC monolith with high separation efficiencies.

Lv and coworkers have developed a novel approach to porous polymer hypercrosslinked monoliths to obtain large surface area with zwitterionic functionalities through the attachment of gold nanoparticles (GNPs) in a layered architecture [44]. The generic poly(4-methylstyrene-co-vinylbenzyl chloride-co-divinylbenzene) monolith was prepared in a capillary and hypercrosslinked *via* a Friedel-Crafts alkylation forming a plethora of mesopores within the monolith. Then, the free radical bromination was used to bind cysteine on to the surface of the monolith. Then, GNPs were attached to this thiol containing monolithic surface. In order to prepare HILIC monolithic column, these GNPs were further modified with cysteine and polyethyleneimine (PEI). When comparing the two monoliths, the attachment of PEI produced a column exhibiting better performance than those modified with cysteine alone mainly because of the formation of a dense hydrophilic polymer layer on the surface of the GNPs. Finally, the authors have prepared monolithic columns with layered architecture by embedding a second layer of nanoparticles after modification with PEI, which served as a spacer enabling construction of a dual layer of GNPs that were then functionalized with cysteine. This dual layered monolith was successfully used for the separation of nucleosides and peptides with higher separation efficiency and resolution.

Škeříková and Urban have used a two-step surface modification of poly(styrene-co-vinylbenzyl chloride-co-divinylbenzene) monolithic stationary phase, including hypercrosslinking and thermally initiated surface grafting of [2-(methacryloyloxy)ethyl] dimethyl(3-sulfopropyl)ammonium hydroxide [45]. The prepared monolith column provided a dual retention mechanism, combining RPC and HILIC. The authors have demonstrated the separation of uracil thiourea and some phenolic acids.

Moreover, Currivan et al. have proposed a novel two step polymerization pathway as an alternative method to introduce smaller pores to the monolith surface possibly with increased surface area for high efficient separation of smaller polar molecules [46]. First a poly(LMA-*co*-tetraethyleneglycol dimethacryl (TeEDMA)) polymer scaffold monolithic column was prepared in the presence of 1,4-butanediol and 1-propanol as porogens. Then, it was used without further modification as a support for the second monolithic layer poly(MEDSA-*co*-BIGDMA) with zwitterionic functionalities. The separation of nucleobases and nucleosides, phenolic acids and flavones were achieved on the two-step zwitterionic polymer monolith under HILIC conditions. This novel two-step polymerization method has shown promising possibilities in the fabrication of polymer hybrid materials, and manipulation of porosity by means of secondary polymerization.

Furthermore, Liang et al. have modified poly(GMA-*co*-PEGDA) monolith with GNPs, with advantages of enhanced reactive sites, facile modification and good hydrophilicity [47]. Variable functional modification of GNPs with cysteine and PNGase were carried out for developing stationary phases capable of HILIC-based enrichment and on-line deglycosylation of glycopeptides, respectively. During glycopeptides elution, the same matrix functionalized with PNGase F was directly coupled with such a HILIC column to achieve the on-line deglycosylation without buffer exchange and pH adjustments. Due to the high hydrophilicity of cysteine functionalized monolith, the enrichment selectivity has been improved. The developed columns were successfully used to analyze the glycoproteome of human plasma.

Terborg et al. have used a similar approach to prepare porous polymer monolithic columns with GNPs for the separation of proteins [48]. In this report, the open surface of

GNPs was then functionalized using alkanethiols, mercaptoalkanoic acids, and amine containing thiols to obtain monolithic capillary columns suitable for separations using RP, cation exchange and anion exchange mechanisms. Columns modified with mercaptooctanoic acid were tested for the separation of proteins under typical ion exchange chromatography mode using increasing salt gradient in aqueous mobile phase and good separation of three proteins (ribonuclease A, cytochrome C and lysozyme) was achieved.

Although significant progress has been made in HILIC monolithic materials on the CLC scale, monolithic columns of analytical size in stainless steel tubing are scarce for HPLC separations at the mL/min flow rate for larger scale fractionation. This dissertation addresses this need by developing and evaluating zwitterionic monoliths in 4.6 mm i.d. stainless steel tubing.

Rationale and significance of the investigation

Due to their distinct advantages, polymeric monolithic stationary phases can serve as efficient alternative column materials for HPLC, a separation technique that is primarily dominated by silica-based packed particle columns. Currently, monolithic columns are mainly applied for the separation of large molecules and are not quite employed for the separation of small molecules [49]. This dissertation aims at developing monolithic stationary phases for HPLC in stainless steel columns with 4.6 mm and 1 mm i.d. for analytical and semi micro scale chromatography, respectively. The motivation for the current research is to furthering the development of monolithic HPLC columns by

introducing monolithic stationary phases specially designed for the separations of small and large molecules with unique selectivity.

The significance for this investigation lies in the materials that were developed for various modes of HPLC such as HILIC, bio-affinity and RPC. For HILIC based separations, a highly polar functional stationary phase was developed with surface functionalized GGG prepared by the post polymerization functionalization of poly (GMA-co-EDMA) monolith. Followed by this polar monolith, poly (NAS-co-EDMA) narrow-bore functionalized columns were made with surface functionalized succinimide groups. This NAS-based monolith (NASM) was explored in the immobilization of n-alkyl amine ligands or protein ligands *via* reaction with the primary amines forming stable amide linkages. By following this approach, octadecylamine, trypsin and lectins were immobilized and their applications were explored in RPC, enzyme reactors and lectin affinity chromatography (LAC), respectively. The LAC was further used to capture glycoproteins from human serum to identify differentially expressed protein in breast cancer serum with respect to that of disease free serum. This was followed by the fabrication of a π electron rich napthyl functionalized monolithic column for its applications in RPC. Separations of small and large molecules were achieved on that column. Finally, an actual application of these stationary phases was explored in food samples where oil and meat samples were analyzed for their fatty acid content by a novel fluorescent derivatization strategy and the separation of the food samples was achieved on both in-house synthesized monolithic column and commercially available silica columns for the completeness of the analysis of fatty acids.

Conclusions

This chapter has introduced the readers to the content of the dissertation and some basic chromatographic concepts that are relevant to the study. Subsequently, trends in monolithic column chemistries for the last 5 years for use in HPLC were overviewed, and that revealed the rationale for furthering the development of the field, which was finally capped by the significance of the investigations reported in this dissertation.

References

1. Fekete, S., I. Kohler, S. Rudaz, and D. Guillarme, *Importance of instrumentation for fast liquid chromatography in pharmaceutical analysis.* J. Pharm. Biomed. Anal., 2014. **87**: p. 105-119.
2. Guiochon, G., *Monolithic columns in high-performance liquid chromatography.* J. Chromatogr. A, 2007. **1168**(1–2): p. 101-168.
3. Hjertén, S., J.-L. Liao, and R. Zhang, *High-performance liquid chromatography on continuous polymer beds.* J. Chromatogr. A, 1989. **473**(0): p. 273-275.
4. Svec, F. and J.M.J. Frechet, *Continuous rods of macroporous polymer as high-performance liquid chromatography separation media.* Anal. Chem., 1992. **64**(7): p. 820-822.
5. Wu, R.a., L. Hu, F. Wang, M. Ye, and H. Zou, *Recent development of monolithic stationary phases with emphasis on microscale chromatographic separation.* J. Chromatogr. A, 2008. **1184**(1–2): p. 369-392.
6. Urban, J., P. Jandera, and P. Langmaier, *Effects of functional monomers on retention behavior of small and large molecules in monolithic capillary columns at isocratic and gradient conditions.* J. Sep. Sci., 2011. **34**(16-17): p. 2054-2062.
7. Zhong, J., M. Hao, R. Li, L. Bai, and G. Yang, *Preparation and characterization of poly(triallyl isocyanurate -co- trimethylolpropane triacrylate) monolith and its applications in the separation of small molecules by liquid chromatography.* J. Chromatogr. A, 2014. **1333**: p. 79-86.
8. Duan, Q., C. Liu, Z. Liu, Z. Zhou, W. Chen, Q. Wang, J. Crommen, and Z. Jiang, *Preparation and evaluation of a novel monolithic column containing double*

octadecyl chains for reverse-phase micro high performance liquid chromatography. J. Chromatogr. A, 2014. **1345**: p. 174-181.

9. Jandera, P., M. Staňková, V. Škeříková, and J. Urban, *Cross-linker effects on the separation efficiency on (poly)methacrylate capillary monolithic columns. Part I. Reversed-phase liquid chromatography.* J. Chromatogr. A, 2013. **1274**: p. 97-106.
10. Liu, H., X. Bai, D. Wei, and G. Yang, *High-performance liquid chromatography separation of small molecules on a porous poly (trimethylol propane triacrylate-co-N-isopropylacrylamide-co-ethylene dimethacrylate) monolithic column.* J. Chromatogr. A, 2014. **1324**: p. 128-134.
11. Bai, X., H. Liu, D. Wei, and G. Yang, *Preparation of a novel porous poly (trimethylol propane triacrylate-co-ethylene dimethacrylate) monolithic column for highly efficient HPLC separations of small molecules.* Talanta, 2014. **119**: p. 479-484.
12. Lin, S.-L., Y.-R. Wu, T.-Y. Lin, and M.-R. Fuh, *Preparation and evaluation of 1,6-hexanediol ethoxylate diacrylate-based alkyl methacrylate monolithic capillary column for separating small molecules.* J. Chromatogr. A, 2013. **1298**: p. 35-43.
13. Li, Y., H.D. Tolley, and M.L. Lee, *Preparation of monoliths from single crosslinking monomers for reversed-phase capillary chromatography of small molecules.* J. Chromatogr. A, 2011. **1218**(10): p. 1399-1408.
14. Okanda, F.M. and Z. El Rassi, *Capillary electrochromatography with monolithic stationary phases. 4. Preparation of neutral stearyl – acrylate monoliths and their evaluation in capillary electrochromatography of neutral and charged small*

species as well as peptides and proteins. Electrophoresis, 2005. **26**(10): p. 1988-1995.

15. Bedair, M. and Z. El Rassi, *Capillary electrochromatography with monolithic stationary phases: II. Preparation of cationic stearyl-acrylate monoliths and their electrochromatographic characterization.* J. Chromatogr. A, 2003. **1013**(1–2): p. 35-45.
16. Liu, K., H.D. Tolley, and M.L. Lee, *Highly crosslinked polymeric monoliths for reversed-phase capillary liquid chromatography of small molecules.* J. Chromatogr. A, 2012. **1227**: p. 96-104.
17. Liu, K., H.D. Tolley, J.S. Lawson, and M.L. Lee, *Highly crosslinked polymeric monoliths with various C6 functional groups for reversed-phase capillary liquid chromatography of small molecules.* J. Chromatogr. A, 2013. **1321**: p. 80-87.
18. Liu, K., P. Aggarwal, H.D. Tolley, J.S. Lawson, and M.L. Lee, *Fabrication of highly cross-linked reversed-phase monolithic columns via living radical polymerization.* J. Chromatogr. A, 2014. **1367**: p. 90-98.
19. Aggarwal, P., J.S. Lawson, H.D. Tolley, and M.L. Lee, *High efficiency polyethylene glycol diacrylate monoliths for reversed-phase capillary liquid chromatography of small molecules.* J. Chromatogr. A, 2014. **1364**: p. 96-106.
20. Wang, H., J. Ou, J. Bai, Z. Liu, Y. Yao, L. Chen, X. Peng, and H. Zou, *Improving permeability and chromatographic performance of poly(pentaerythritol diacrylate monostearate) monolithic column via photo-induced thiol-acrylate polymerization.* J. Chromatogr. A, 2016. **1436**: p. 100-108.

21. Chambers, S.D., T.W. Holcombe, F. Svec, and J.M.J. Fréchet, *Porous Polymer Monoliths Functionalized through Copolymerization of a C60 Fullerene-Containing Methacrylate Monomer for Highly Efficient Separations of Small Molecules.* Anal. Chem., 2011. **83**(24): p. 9478-9484.

22. Li, Y., L. Qi, and H. Ma, *Preparation of porous polymer monolithic column using functionalized graphene oxide as a functional crosslinker for high performance liquid chromatography separation of small molecules.* Analyst, 2013. **138**(18): p. 5470-5478.

23. Wang, M.-M. and X.-P. Yan, *Fabrication of Graphene Oxide Nanosheets Incorporated Monolithic Column via One-Step Room Temperature Polymerization for Capillary Electrochromatography.* Anal. Chem., 2012. **84**(1): p. 39-44.

24. Chambers, S.D., F. Svec, and J.M.J. Fréchet, *Incorporation of carbon nanotubes in porous polymer monolithic capillary columns to enhance the chromatographic separation of small molecules.* J. Chromatogr. A, 2011. **1218**(18): p. 2546-2552.

25. Aqel, A., K. Yusuf, Z.A. Al-Othman, A.Y. Badjah-Hadj-Ahmed, and A.A. Alwarthan, *Effect of multi-walled carbon nanotubes incorporation into benzyl methacrylate monolithic columns in capillary liquid chromatography.* Analyst, 2012. **137**(18): p. 4309-4317.

26. Mayadunne, E. and Z. El Rassi, *Facile preparation of octadecyl monoliths with incorporated carbon nanotubes and neutral monoliths with coated carbon nanotubes stationary phases for HPLC of small and large molecules by hydrophobic and π–π interactions.* Talanta, 2014. **129**: p. 565-574.

27. Poupart, R., D.N. El Houda, D. Chellapermal, M. Guerrouache, B. Carbonnier, and B. Le Droumaguet, *Novel in-capillary polymeric monoliths arising from glycerol carbonate methacrylate for flow-through catalytic and chromatographic applications.* RSC Advances, 2016. **6**(17): p. 13614-13617.

28. Alpert, A.J., *Hydrophilic-interaction chromatography for the separation of peptides, nucleic acids and other polar compounds.* J. Chromatogr. A, 1990. **499**: p. 177-196.

29. Staňková, M., P. Jandera, V. Škeříková, and J. Urban, *Cross-linker effects on the separation efficiency on (poly)methacrylate capillary monolithic columns. Part II. Aqueous normal-phase liquid chromatography.* J. Chromatogr. A, 2013. **1289**: p. 47-57.

30. Jandera, P., M. Staňková, and T. Hájek, *New zwitterionic polymethacrylate monolithic columns for one- and two-dimensional microliquid chromatography.* J. Sep. Sci., 2013. **36**(15): p. 2430-2440.

31. Chen, M.-L., S.-S. Wei, B.-F. Yuan, and Y.-Q. Feng, *Preparation of methacrylate-based monolith for capillary hydrophilic interaction chromatography and its application in determination of nucleosides in urine.* J. Chromatogr. A, 2012. **1228**: p. 183-192.

32. Chen, M.-L., L.-M. Li, B.-F. Yuan, Q. Ma, and Y.-Q. Feng, *Preparation and characterization of methacrylate-based monolith for capillary hydrophilic interaction chromatography.* J. Chromatogr. A, 2012. **1230**: p. 54-60.

33. Lin, Z., H. Huang, X. Sun, Y. Lin, L. Zhang, and G. Chen, *Monolithic column based on a poly(glycidyl methacrylate-co-4-vinylphenylboronic acid-co-ethylene*

dimethacrylate) copolymer for capillary liquid chromatography of small molecules and proteins. J. Chromatogr. A, 2012. **1246**: p. 90-97.

34. Yuan, G., Y. Peng, Z. Liu, J. Hong, Y. Xiao, J. Guo, N.W. Smith, J. Crommen, and Z. Jiang, *A facile and efficient strategy to enhance hydrophilicity of zwitterionic sulfoalkylbetaine type monoliths.* J. Chromatogr. A, 2013. **1301**: p. 88-97.

35. Chen, X., H.D. Tolley, and M.L. Lee, *Preparation of zwitterionic polymeric monolithic columns for hydrophilic interaction capillary liquid chromatography.* J. Sep. Sci., 2011. **34**(16-17): p. 2088-2096.

36. Foo, H.C., J. Heaton, N.W. Smith, and S. Stanley, *Monolithic poly (SPE-co-BVPE) capillary columns as a novel hydrophilic interaction liquid chromatography stationary phase for the separation of polar analytes.* Talanta, 2012. **100**: p. 344-348.

37. Jiang, H., H. Yuan, Y. Qu, Y. Liang, B. Jiang, Q. Wu, N. Deng, Z. Liang, L. Zhang, and Y. Zhang, *Preparation of hydrophilic monolithic capillary column by in situ photo-polymerization of N-vinyl-2-pyrrolidinone and acrylamide for highly selective and sensitive enrichment of N-linked glycopeptides.* Talanta, 2016. **146**: p. 225-230.

38. Guo, J., Q. Zhang, Z. Yao, X. Zhao, D. Ran, J. Crommen, and Z. Jiang, *One-step strategy for the synthesis of a derivatized cyclodextrin-based monolithic column.* J. Sep. Sci., 2014. **37**(14): p. 1720-1727.

39. Li, N., Y. Shen, L. Qi, Z. Li, J. Qiao, and Y. Chen, *Preparation of an amino acid-based polymer monolith for trimodal liquid chromatography.* RSC Advances, 2015. **5**(75): p. 61436-61439.

40. Yu, R., W. Hu, G. Lin, Q. Xiao, J. Zheng, and Z. Lin, *One-pot synthesis of polymer monolithic column by combination of free radical polymerization and azide–alkyne cycloaddition "click" reaction and its application in capillary liquid chromatography.* RSC Advances, 2015. **5**(13): p. 9828-9836.

41. Lin, Z., R. Yu, W. Hu, J. Zheng, P. Tong, H. Zhao, and Z. Cai, *Preparation of a poly (3'-azido-3'-deoxythymidine-co-propargyl methacrylate-co-pentaerythritol triacrylate) monolithic column by in situ polymerization and a click reaction for capillary liquid chromatography of small molecules and proteins.* Analyst, 2015. **140**(13): p. 4626-4635.

42. Liu, C., W. Chen, G. Yuan, Y. Xiao, J. Crommen, S. Xu, and Z. Jiang, *Influence of the crosslinker type on the chromatographic properties of hydrophilic sulfoalkylbetaine-type monolithic columns.* J. Chromatogr. A, 2014. **1373**: p. 73-80.

43. Lv, Y., Z. Lin, and F. Svec, *"Thiol–ene" click chemistry: a facile and versatile route for the functionalization of porous polymer monoliths.* Analyst, 2012. **137**(18): p. 4114-4118.

44. Lv, Y., Z. Lin, and F. Svec, *Hypercrosslinked Large Surface Area Porous Polymer Monoliths for Hydrophilic Interaction Liquid Chromatography of Small Molecules Featuring Zwitterionic Functionalities Attached to Gold Nanoparticles Held in Layered Structure.* Anal. Chem., 2012. **84**(20): p. 8457-8460.

45. Škeříková, V. and J. Urban, *Highly stable surface modification of hypercrosslinked monolithic capillary columns and their application in hydrophilic interaction chromatography.* J. Sep. Sci., 2013. **36**(17): p. 2806-2812.

46. Currivan, S., J.M. Macak, and P. Jandera, *Polymethacrylate monolithic columns for hydrophilic interaction liquid chromatography prepared using a secondary surface polymerization.* J. Chromatogr. A, 2015. **1402**: p. 82-93.

47. Liang, Y., C. Wu, Q. Zhao, Q. Wu, B. Jiang, Y. Weng, Z. Liang, L. Zhang, and Y. Zhang, *Gold nanoparticles immobilized hydrophilic monoliths with variable functional modification for highly selective enrichment and on-line deglycosylation of glycopeptides.* Anal. Chim. Acta, 2015. **900**: p. 83-89.

48. Terborg, L., J.C. Masini, M. Lin, K. Lipponen, M.-L. Riekolla, and F. Svec, *Porous polymer monolithic columns with gold nanoparticles as an intermediate ligand for the separation of proteins in reverse phase-ion exchange mixed mode.* Journal of Advanced Research, 2015. **6**(3): p. 441-448.

49. Svec, F., *Quest for organic polymer-based monolithic columns affording enhanced efficiency in high performance liquid chromatography separations of small molecules in isocratic mode.* J. Chromatogr. A, 2012. **1228**(0): p. 250-262.

CHAPTER II

ZWITTERIONIC MONOLITHIC HPLC COLUMNS BASED ON GLYCYL MOIETIES FOR HYDROPHILIC INTERACTION LIQUID CHROMATOGRAPHY

INTRODUCTION

Hydrophilic interaction liquid chromatography (HILIC) gained prominence in the last decade, since it addresses mainly the areas where the normal- or the reversed-phase chromatography (NPC or RPC) were unsuccessful. It is based on the partition of the analyte between the adsorbed hydration layer on the surface of the stationary phase and the bulk organic-rich mobile phase. Hence, in this class of chromatography the aqueous component of the hydro-organic mobile phase acts as a strong component, which is exactly, opposite to the conventional RPC and therefore this technique can be described as the inverse of RPC. Polar stationary phases are well known for a long time and are used for a variety of applications where the adsorbed water layers are used to take up the analytes [1]. It was not until 1990 the term HILIC [2] was coined and this was followed by many excellent reviews explaining the HILIC backgrounds and the details regarding the retention mechanism [1, 3]. In the last decade, the popularity of HILIC has increased tremendously since the need for the analysis of more polar analytes was in great demand such as polar drugs, carbohydrates, and clinically significant areas of proteomics and

glycomics where highly polar solutes were often needed to be analyzed. HILIC also found its advantage in samples pertaining to pharmaceutical and food industries [3]. Another advantage of HILIC is that it can be readily hyphenated with a mass spectrometer, due to the high ACN concentrations in the mobile phase. Many commercial columns have become available in the last decade and they are the subject of interest for both academic researchers and column manufacturers [1, 4]. Unlike RPC, in HILIC the retention of the analytes can be altered in a very narrow aqueous range of 3-40% in the majority of cases where a minimum of 3% of the aqueous component is needed to form the adsorbed water layer on the stationary phase and the increasing water content of the hydro-organic mobile phase will elute the analytes faster. Here, highly polar solutes are retained in the aqueous layer by a variety of interactions such as the hydrophilic partitioning of the solute between the aqueous layer and the hydro-organic mobile phase, hydrogen bonding between the polar solutes and the stationary phase and finally the electrostatic interactions between the ionized solutes and the stationary phase [5]. Therefore, it can be stated that unlike RPC, the HILIC retention mechanism is quite complex with a mixture of interactions as just mentioned. When it comes to the stationary phases in HILIC, a wide variety of polar functionalities are available which can be chosen based on the combination of interactions that exist between the analytes and the stationary phase.

Of all the polar stationary phases' available, zwitterionic stationary phases are quite a new class with their popularity increasing rapidly [6]. Zwitterionic phases carry both positive and negative groups in a stoichiometric ratio, so that the net surface charge is zero. These surface charges form a stable water layer on the stationary phase surface,

which offers mild electrostatic interactions with charged solutes. This provides added advantage in the separation of polar and charged compounds. These zwitterionic moieties were coated on the surface of the stationary phases by either dynamic coating or by covalent bonding [7, 8]. For HILIC based applications covalent attachment of the zwitterionic phases would give more stable stationary phases, since it involves the use of high organic content in the mobile phase. Zwitterionic phases such as sulfoalkylbetaine and phosphorylcholine groups which are incorporated into polymeric functionalities are the most popular species and are used for a variety of applications with a range of polar neutral and charged species [1, 9, 10]. Recently, numerous silica based columns with surface bound zwitterion functionalities such as lysine [11], glycosyl phenyl glycine [12], glutathione [13], ammonium propanesulfonate [14], imidazolium [15], cysteine [16], diphenylphosphonium propylsulfonate [17] have been published for their applications in HILIC based separations along with many other commercially available columns [1, 5].

On the other hand, monolithic columns are becoming increasingly popular due to their distinct characteristic advantage over their silica counterparts with a variety of advantages, which include the ability to covalently graft the surface with a variety of functionalities, stability at higher pH, reduced flow resistance and no inlet bed settling. Many reviews have been published recently addressing the current trends in monolithic columns [18, 19]. The rising popularity of HILIC coincides with that of monolithic polymeric stationary phases, which offer a surface that can be specifically grafted with a variety of polar functional groups for attaining the proper selectivity that can facilitate the separation and retention of polar compounds. Our lab has recently developed a variety of robust HPLC monolithic columns for a range of applications [20, 21]. The current study

is aimed at making a diol monolith using different combinations of glyceryl monomethacrylate (GMM) and glycidyl methacrylate (GMA) with the cross-linkers ethylene glycol dimethacrylate (EDMA) and trimethylolpropane trimethacrylate (TRIM) with well-designed pore structure and functionalize the surface with the amino acid glycine and its di- and tripeptide which are glycylglycine (GG) and glycylglycylglycine (GGG), respectively. The functionalization can be carried out by oxidizing the diol by the periodate chemistry which is then followed by the attachment of glycine by reductive amination on the surface of the monolith. Glycine is bound to the surface and this offers a zwitterionic ligand on the surface with zero net charge coming from stoichiometric ratios of negatively charged carboxylate ion and positively charged secondary ammonium ion. The carboxylate group at the distal end might introduce partial electrostatic interactions with the charged solutes. GG and GGG functionalization not only offers the advantage of the zwitterion, but also the amide functionalities (i.e., the peptide bonds) offer additional polarity to the stationary phase which is known to be less prone to irreversible adsorption with good reproducibility and stability [22]. Using nucleobases and nucleosides as test solute probes, these HPLC columns have been characterized for HILIC mode separations. Finally, highly polar basic pharmaceutical drugs have been separated in gradient elution.

Experimental

Reagents and materials

All the HPLC column end fittings were obtained from Crawford Fitting Co., (Solon, OH, USA). Stainless steel tubing with 4.6 mm i.d. was purchased from Alltech Associates (Deerfield, IL, USA) and was cut accordingly to the desired length. The monomers and porogens used in the current study, namely glycidyl monomethacrylate

(GMA), ethylene glycol methacrylate (EDMA), trimethylolpropane trimethacrylate (TRIM) and the porogens cyclohexanol, dodecanol were from Sigma-Aldrich (Milwaukee, WI, USA) and glycerol monomethacrylate (GMM) was from Monomer-Polymer and Dajac Labs (Trevose, PA, USA). HPLC grade acetonitrile (ACN) and isopropyl alcohol (IPA) were purchased from Pharmco-Aaper (Brookfield, CT, USA). Sulfuric acid, glacial acetic acid (reagent grade, ACS), ammonium acetate (NH_4Ac) and citric acid monohydrate (certified ACS grade) were from Fischer Scientific (Fair Lawn, NJ, USA). Sodium (meta)periodate, glycine (G), glycylglycine (GG) and glycylglycylglycine (GGG) were purchased from Sigma (St. Louis, MO, USA). Sodium cyanoborohydride ($NaCNBH_3$) was purchased from Acros Organics (Morris Plains, NJ, USA). Nucleobases and nucleosides such as adenine, cytosine, uracil, thymine, guanosine, cytidine, inosine, adenosine and uridine were purchased from CN biosciences, Inc. (La Jolla, CA, USA). Highly basic compounds such as octopamine, tyramine, synephrine, phenylpropalamine (PPA), ephedrine, propranolol and epinephrine that were used for the chromatographic evaluation are of analytical grade and were purchased from Sigma (St. Louis, MO, USA).

Instrumentation and procedures

All HPLC separations were performed on a Waters Alliance 2690 separations module (Milford, MA, USA), equipped with an in-line degasser, a quaternary solvent pump, an auto sampler and a thermostated column compartment. Detection was performed using a PDA detector (W2996). The sample and the column compartments were maintained at ambient temperature for all the chromatographic separations.

For carrying out post polymerization reactions on the column, an HPLC solvent delivery system Model 590 from Waters Associates (Milford, MA, USA) and a Rheodyne high pressure injection valve (Rohnert Park, CA, USA) fitted with an injection loop of 2.8 mL volume was used to pass the reagents onto the column at high pressures. For column packing, a constant pressure pump from Shandon Southern Products Ltd. (Cheshire, UK) was used. Polymerization reactions were carried out in a water bath Model Isotemp 105 from Fisher Scientific (Pittsburgh, PA, USA). All the buffers, reagents and water were filtered through a 0.45 µm membrane filter (Millipore, Bedford, USA) and thoroughly degassed before passing into the column. The data acquisitions were carried out using Empower 2 (Build 2154) software (Waters chromatography) and the chromatographic data were processed by OriginPro v8.5.1 (Origin Lab Corp., Northampton, MA, USA). Stock solutions of 1 mg/mL of each solute were dissolved in ACN and diluted to the desired concentrations in the mobile phase yielding adequate detector response. The buffer concentrations that are mentioned throughout this chapter are with respect to the aqueous part only unless otherwise mentioned.

In situ polymerization

The constituents of the reaction mixture were added according to their corresponding weights as mentioned in Table 1 to a clean glass vial. The total weight of the polymerization mixture was approximately 4.7 g. The contents were vigorously shaken and 1% (w/w) of AIBN with respect to the monomer and crosslinker was added to the mixture, which was then thoroughly degassed by sonication for 15 min for degassing. The contents were transferred into a stainless steel column (25 cm x 4.6 mm i.d.) with

fittings at both column ends, which were sealed with end plugs. Thereafter, the polymerization was allowed to proceed at an appropriate temperature for a given time in a water bath. For the polymerization temperature and time refer to Table 1. After polymerization, the end plugs were removed and the column was washed with ACN thoroughly to remove the porogens and unreacted monomers leaving the porous monolithic matrix behind, which was referred to as the "mold". Then the column was equilibrated with IPA and using the same solvent, a packing pressure of 8000 psi was used to transfer this mold into a 15 cm long column consisting of two sections of 10 cm × 4.6 mm i.d. connected with a ¼ in union to a 5 cm × 4.6 mm i.d. The high-pressure packing ensures a tightly packed column void of free spaces and serves as a test to demonstrate the sustainability of the column with high pressures that are generally associated with HPLC separations (see Figure 1). The extra 5 cm x 4.6 mm i.d. was added to the 10 cm x 4.6 mm i.d. HPLC column to account for any size reduction in the monolith due to the periodate oxidation and subsequent post polymerization modifications of the base monolith and also to ensure that the 10 cm column was fully formed without any void.

Post polymerization modification

All the reactions were performed on the (10 + 5) cm x 4.6 mm i.d. HPLC column connected with end fittings and the reagent were injected into the HPLC column at high pressure by using a solvent delivery system which was connected to an injector with an injection loop of 2.8 mL volume. Prior to hydrolyzing the surface epoxide groups

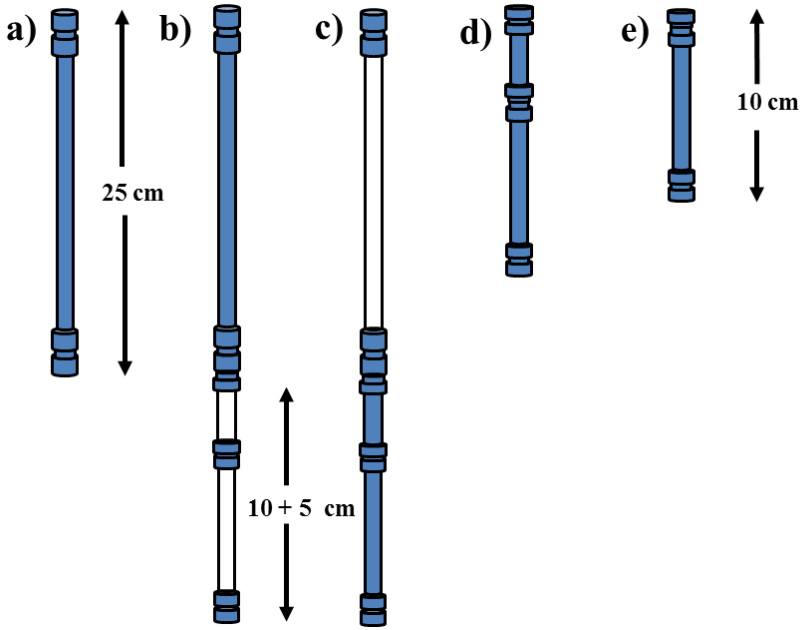

Figure 1. *Monolithic column preparation process used in this dissertation. In situ polymerization of monomers along with the porogens was carried out in a 25 cm x 4.6 mm i.d. stainless steel column (a), which was connected with two sections of empty 10 and 5 cm x 4.6 mm i.d. columns by means of ¼ in union (b). The formed monolith from the 25 cm was pushed into the 10 + 5 cm column by means of high pressure (c). The post polymerization modification was performed on the 10+5 cm connected columns and finally the 10 cm column was detached (e) and was used for further study.*

TABLE 1

COMPOSITIONS OF MONOMERS AND POROGENS USED IN THE PREPARATION OF THE VARIOUS HPLC MONOLITHIC COLUMNS

Column Series	Column Name	GMM	GMA	EDMA	TRIM	Cyclohexanol	Dodecanol	Water	Polymerization temperature/ time	Modification	Comments
I	GMT-1	12.6	-	-	17.4	53.8	13.7	2.5	60°C/12 h	NA	Low permeability
	GMT-2	13.5	-	-	16.5	53.8	13.7	2.5	60°C/12 h	NA	
	GMT-3	14.7	-	-	15.3	53.8	13.7	2.5	60°C/12 h	NA	
II	GME-4	29.8	-	13.4	-	30.4	26.4	-	55°C/15 h	GG	Highly permeable and stable
	GME-5	29.8	-	13.4	-	35.8	21.0	-	55°C/15 h	GG	
	GME-6	29.8	-	13.4	-	40.5	16.3	-	55°C/15 h	GG	
III	GAE-7	-	26.0	14.0	-	40.0	20.0	-	50°C/24 h	NA	Unstable at high flow rates
	GAE-8	-	24.0	16.0	-	40.0	20.0	-	50°C/24 h	NA	
	GAE-9	-	24.0	16.0	-	50.0	10.0	-	50°C/24 h	NA	Impermeable
IV	GAE-10	-	18.0	12.0	-	59.5	10.5	-	50°C/24 h	GGG	Permeable and stable monolith
	GAE-11	-	16.0	14.0	-	59.5	10.5	-	50°C/24 h	GGG	
	GAE-12	-	15.0	15.0	-	59.5	10.5	-	50°C/24 h	GGG	
	GAE-13	-	15.0	15.0	-	57.0	13.0	-	50°C/24 h	GGG	

Column Series	Column Name	GMM	GMA	EDMA	TRIM	Cyclohexanol	Dodecanol	Water	Polymerization temperature/ time	Modification	Comments
V	GAT-14	-	18.9	-	6.1	63.8	11.2	-	60°C/12 h	GGG	Unstable
	GAT-15	-	20.3	-	6.7	62.1	10.9	-	60°C/12 h	GGG	
VI	GAT-16	-	13.5	-	16.5	53.8	13.7	2.5	60°C/12 h	GGG	Stable and low permeability
	GAT-17	-	15.0	-	15.0	53.8	13.7	2.5	60°C/12 h	GGG	
	GAT-18	-	16.5	-	13.5	53.8	13.7	2.5	60°C/12 h	GGG	Stable and good permeability

* 1 % AIBN (w/w) with respect to monomers was added as an initiator and its weight was not included in the percentage calculations, NA: Not Applied

originating from GMA functional monomer of the precursor monolith, two column volumes of 1.0 M H_2SO_4 were passed through the precursor monolithic column. The ends of the column were sealed and heated in a water bath at 70 ˚C for 3 h. This acid wash step was not needed for the monoliths based on GMM functional monomer where the monolithic surface already has diol groups. The columns were then thoroughly flushed with water until all the acid was removed from the column. This was followed by equilibration of the column with one to two column volumes of 50 mM $NaIO_4$ at a flow rate of 0.1 mL/min to oxidize the ethylene glycol on the surface of the monolith to aldehyde. This was followed by flushing the column with water to remove the unreacted $NaIO_4$ and then by equilibration with one column volume of 20 mM citric acid solution. Now, to facilitate the reductive amination, the column was filled with a solution of 100 mM of either G or GG or GGG prepared in 20 mM citric acid solution for one column volume at a flow rate of 0.1 mL/min. Then, 20 mM citric acid solution containing 50 mM $NaCNBH_3$ and 100 mM G or GG or GGG was passed through the column for one column volume at a flow rate of 0.01 mL/min. The column was equilibrated by ACN thoroughly for about 20-30 column volumes with water until all the unreacted reagents were removed from the column. Finally, the 10 cm x 4.6 mm i.d. part of the column was separated from the ¼ in union and was fitted with end fittings, and then equilibrated with ACN before use.

Results and discussion

Monolith fabrication

Figure 2 depicts the structures of the monomers GMM and GMA along with the crosslinker TRIM and EDMA, which were used in the current study. The goal was to

produce a monolith with good permeability for use in HPLC at a relatively high flow velocity, which was then followed by a post polymerization modification of the monolith surface with GGG zwitterionic ligands. This approach of surface modification is shown in Figure 3.

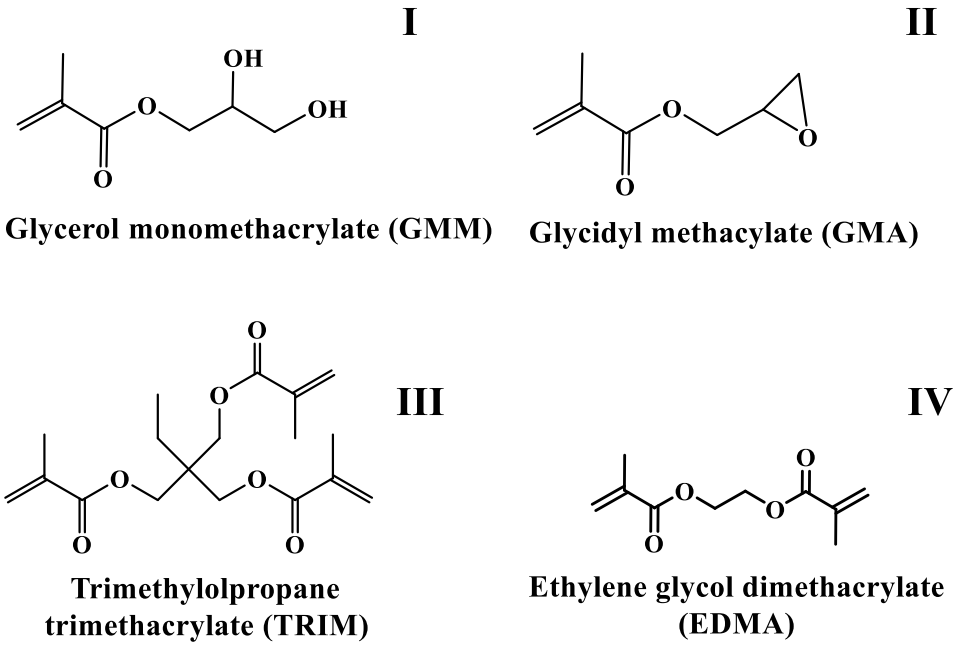

Figure 2. *Monomers (I and II) and crosslinkers (III and IV) used in the study.*

As discussed in the previous sections, the primary step was to start with a diol surface, which was realized on the surface of the monolith by using either of the two functional monomers GMM or GMA. EDMA and TRIM were chosen as the crosslinkers with 1-dodecanol, cyclohexanol and water as the porogens. The polymerization time and temperature and time are listed in Table 1. A different series of monoliths was made where the concentrations of the functional monomers and the crosslinker were systematically altered to arrive at the perfectly tailored precursor monolith for HPLC. The formed monolith was primarily tested for its permeability and later for its stability at

high pressures. The constant pressure pump (see previous sections) served as a “litmus test” for this purpose. The corresponding components were altered accordingly until a monolith of the desired characteristics was obtained, and subsequently used in the post polymerization modification. Finally, the performance of the column was tested for its application in HILIC chromatography. This was done by testing the column with a non-polar solute such as toluene for indicating the dead time (t_0) of the column and another neutral polar solute such as uracil to assess the degree of column hydrophilicity using an organic rich mobile phase consisting of 95:5 ACN:water (v/v). Monolithic column series I (see Table 1) was prepared in an attempt to make a diol monolith from the GMM functional monomer using TRIM as the crosslinker with a ternary porogen mixture consisting of dodecanol, cyclohexanol and water [20]. This series gave impermeable monoliths even before the periodate modification, which indicates that the porogen was not suitable for use with the polar GMM functional monomer. Thereafter, GMM/EDMA columns were made according to a recent publication [21] from our laboratory which showed high permeability and was followed by the post polymerization modification. The column showed very high permeability and stability. However, upon testing the column with functionalized GG moieties under HILIC conditions using uracil as the test solute, very broad peaks were observed (chromatogram not shown). This might be due to the formation of mesopores. A further decrease in the macroporogen, dodecanol (columns GME-4 to GME-6) did not improve the peak shape. These results indicate that GMM, which is a polar monomer, was not suitable in forming a suitable stable monolith for HPLC. Instead, a relatively nonpolar functional monomer GMA was used and column series III was made which generated highly unstable

monoliths (columns GAE-7 to GAE-9) with high backpressures. Later, different columns were made with decreased dodecanol, which were designated as series IV (columns

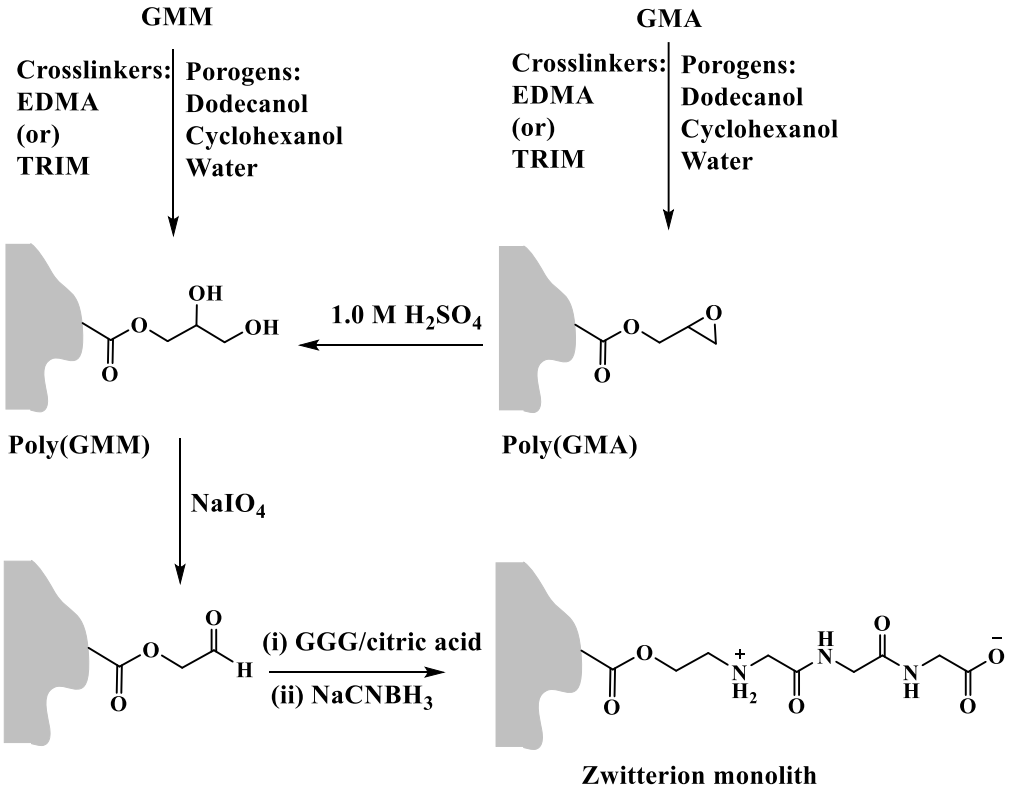

Figure 3. *Schematic representation of the preparation of zwitterionic GGG functionalized monolith.*

GAE-10 to GAE13). These showed excellent permeability and stability at high flow rates, which were then functionalized with GGG ligands. The column showed retention for uracil. A fine-tuning of the crosslinker (column GAE-8) or the dodecanol (column GAE-9) did not improve the peak shape of the retained uracil. Again, TRIM was used as a crosslinker for GMA functional monomer and column series V was made. This series proved highly unstable after the periodate modifications. Finally, monolithic columns (series VI) mimicking the compositions from our previous publication [20] which gave

excellent monolith structure (visual observation) with limited permeability for column GAT-16 and column GAT-17 after the post polymerization reactions. Then, the ratio of the functional monomer was increased with respect to the crosslinker to get the best permeability. Here, TRIM composition with respect to the functional monomer was reduced to increase the permeability. The column GAT-19 gave excellent peak shape for uracil. Of all the prepared chromatographic columns, only columns GME-4, GAE-12 and GAT-18, which refer to GMM/EDMA-GG, GMA/EDMA-GGG and GMA/TRIM-GGG monolithic columns, respectively, were chromatographically evaluated in detail in the following sections.

Optimizing the post polymerization modification conditions

The three main reactions in the post polymerization reaction include the periodate oxidation of the diol groups to form the aldehyde groups which was followed by the nucleophilic addition of the amino group of the glycine/glycyl residue to form an imine (Schiff's base) (see Figure 3 for the reactions) and finally the reduction of imine to amine in the presence of sodium cyanoborohydride ($NaCNBH_3$) resulting in the formation of covalently attached glycine/glycyl to the surface of the monolith. The concentration of $NaIO_4$ was maintained at 50 mM and care was taken not to over react the monolith with periodate, since it might alter the nature of the pore size if it is treated for a prolonged period of time [23]. Citric acid (20 mM, pKa=3.13) was used as the catalyst in the reductive amination step, since the formation of the Schiff's base is generally acid catalyzed [24, 25]. Finally, a study was performed to assess the effect of the amount of G, GG or GGG offered in the final step. Two different GMA/EDMA columns were made

with different concentrations of GG offered on to the surface of the monolith; one with 10 mM GG and the other with 100 mM GG along with 20 mM citric acid solution. The retention of uracil was evaluated on the GG columns thus obtained to reveal the effect of the amount of GG bound on the surface of the monolith. The k value of uracil increased from 2.86 to 3.15 with the increase in the GG concentration from 10 to 100 mM indicating an increased amount of GG surface coverage. So, the concentration of G/GG/GGG was maintained at 100 mM in the column preparation throughout this study.

Chromatographic evaluation of GMM/EDMA column modified with GG

Unmodified and GG modified GMM/EDMA columns were evaluated in HILIC based separation of some polar solutes using a mobile phase composed of 95% (v/v) ACN and 5% of 20 mM NH_4Ac, pH 6.0, at 1.00 mL/min flow rate. Toluene, which was used as the t_0 marker was observed to elute at 1.13 and 0.97 min, for GMM/EDMA unmodified and GG modified columns using100 mM GG in 20 mM citric acid , respectively. The k values of the solutes tested on the two columns are listed in Table 2. These results show a clear decrease in solute retention when going from the unmodified GMM/EDMA column to the GG modified GMM/EDMA column. The k values of uracil and thiourea decreased from 2.03 to 1.31 and from 2.41 to 2.22, respectively, when going from the unmodified column to the GG modified column. Owing to its possession of a ribose moiety in its molecule, the nucleoside uridine was more retained than uracil but its k value decreased from 4.10 to 3.55 when going from unmodified to GG modified

TABLE 2

RETENTION FACTOR K OBTAINED ON THE GMM/EDMA MONOLITH FUNCTIONALIZED WITH GG

Solute	GMM/EDMA	GMM/EDMA-GG
	k	
Thiourea	2.03	1.31
Uracil	2.41	2.22
Uridine	4.10	3.55
Cytidine	6.05	1.83

Mobile phase conditions:
95:5/ACN:NH4Ac, 20 mM, pH 6.0

GMM/EDMA columns. Also, GG functionalization significantly affected the retention of the charged solute cytidine, whose k value decreased by more than 3-fold (from 6.05 to 1.83) when compared to that obtained on the unmodified GMM/EDMA column. This may have resulted from the periodate oxidation of the GMM/EDMA monolith by eventually affecting the morphology of the monolith and in turn the surface density of active aldehyde sites for the subsequent GG functionalization by reductive amination. These results did not favor the further exploitation of GMM/EDMA precursor column.

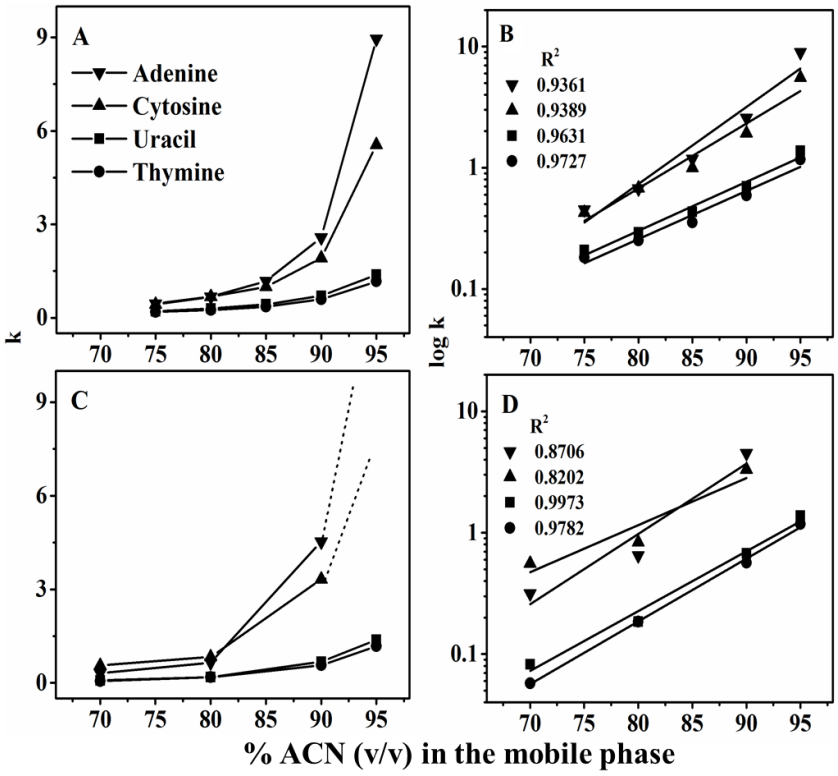

Figure 4. *Plots of k in (A) and log k in (B) for GMA/TRIM-GGG column and k in (C) and log k in (D) for GMA/EDMA-GGG column for nucleobases. Mobile phase conditions: various %ACN in 20 mM NH_4Ac buffer, pH 6.0; flow rate, 1.0 mL/min; UV detection, 254 nm.*

TABLE 3

RETENTION FACTOR K OBTAINED ON THE GMA MONOLITH FUNCTIONALIZED WITH GGG USING EDMA AND TRIM AS THE CROSSLINKERS

	GMA/EDMA-GGG		GMA/TRIM-GGG	
Solute	Mobile phase-1	Mobile phase-2	Mobile phase-1	Mobile phase-2
Uracil	1.40	0.72	1.38	0.70
Thiourea	0.97	0.58	1.29	0.74
Thymine	1.20	0.60	1.17	0.59
Adenine	NE	3.42	5.55	1.92
Adenosine	1.17	0.36	3.56	1.20
Uridine	0.63	0.22	1.78	0.71
Ionosine	2.58	0.66	4.86	1.42
Cytosine	NE	4.66	8.95	2.58
Guanosine	NE	0.97	11.19	2.44
Cytidine	NE	1.00	8.44	2.12

NE: Not Eluted
Mobile phase-1: 95:5/ACN:buffer. Buffer: 20 mM NH_4Ac, pH 6.0.
Mobile phase-2: 90:10/ACN:buffer. Buffer: as in mobile phase-1

Chromatographic evaluation of GMA/EDMA and GMA/TRIM columns modified with GGG

The chromatographic evaluation was performed on GGG functionalized column with a hydro-organic mobile phase whose aqueous component was NH_4Ac at pH 6.0, which corresponds to the pI value of GGG where it exists as a zwitterion with zero net charge. To study the HILIC properties of the GGG column, nucleobases and nucleosides were chosen as the test solutes and their retention behavior and peak shape were studied mainly at 95% (v/v) and 90% (v/v) ACN concentrations in NH_4Ac buffer whose plain concentration is 20 mM (see Table 3). The results are discussed in the following sections.

Effect of crosslinker. After the in-depth trials in developing the monolithic matrix in the previous sections, the retention behaviors of various solutes were carefully studied on the GGG functionalized GMA/TRIM and GMA/EDMA columns. Toluene and thiourea were used as the neutral test solutes to evaluate the HILIC property of the column. On both GMA/EDMA-GGG and GMA/TRIM-GGG column, toluene being non-polar solutes served as the t_0 marker (eluted at around 1.19 min) and thiourea being neutral polar retained with k values of 0.97 and 1.29, respectively, on EDMA and TRIM based GMA columns. Clearly, the retention is greater on the GGG column made with TRIM as the crosslinker, which is an obvious indication of more porous structure of the TRIM-based monolith. On the other hand, the neutral polar solute, uracil, retained similarly on both GMA/EDMA-GGG and GMA/TRIM-GGG columns with k values of 1.40, See Table 3 for the k values. However, Figure 6 shows the peak shape of uracil obtained on both columns, which indicate the better mass transfer of uracil on TRIM

based column than on the EDMA based column. This might be due to the more uniform pore structure of TRIM over EDMA based GMA polymers. On the other hand, EDMA based GMA monoliths gave broad peaks due to their strong interactions with some solutes, which resulted in broad peaks. This was quite evident with the retention of polar amino substituted compounds such as adenine and cytosine where they were bound irreversibly to

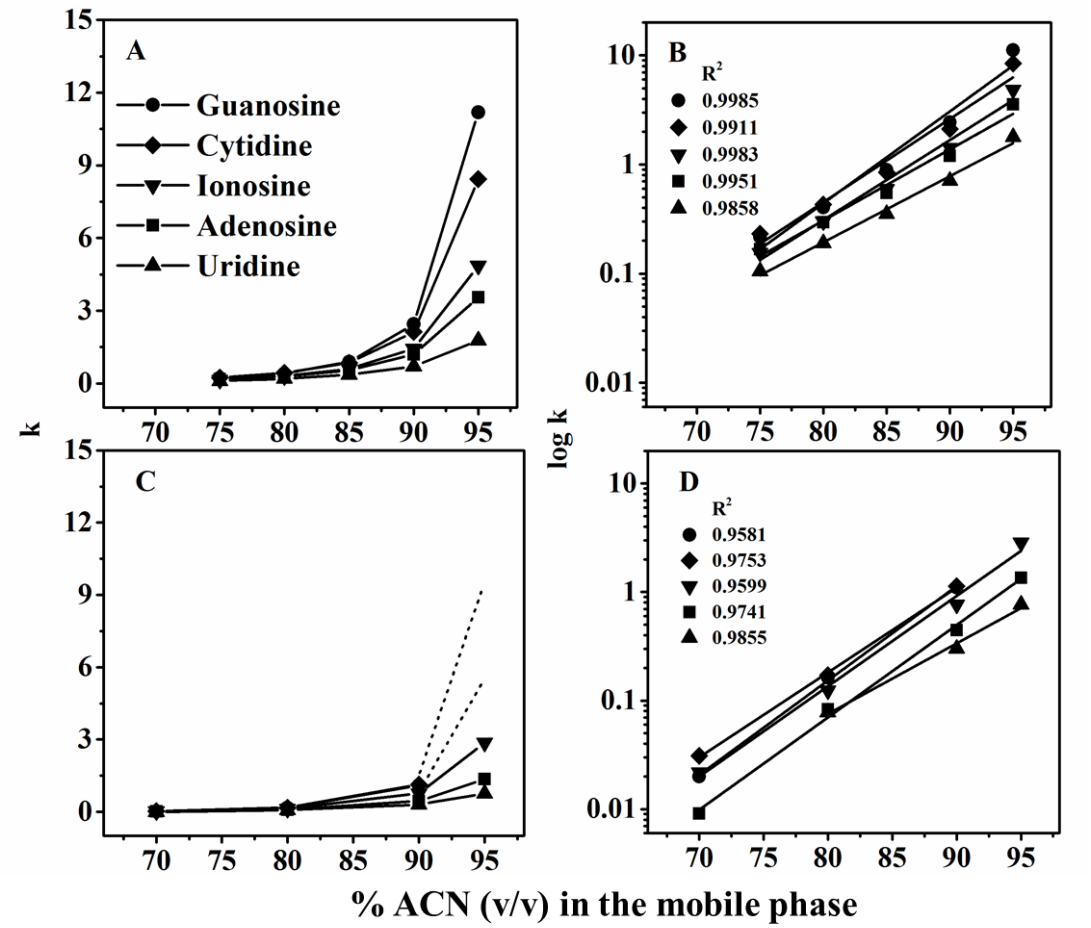

Figure 5. *Plots of k in (A) and log k in (B) for GMA/TRIM-GGG column and k in (C) and log k in (D) for GMA/EDMA-GGG column for nucleosides. Other chromatographic conditions as in Figure 4.*

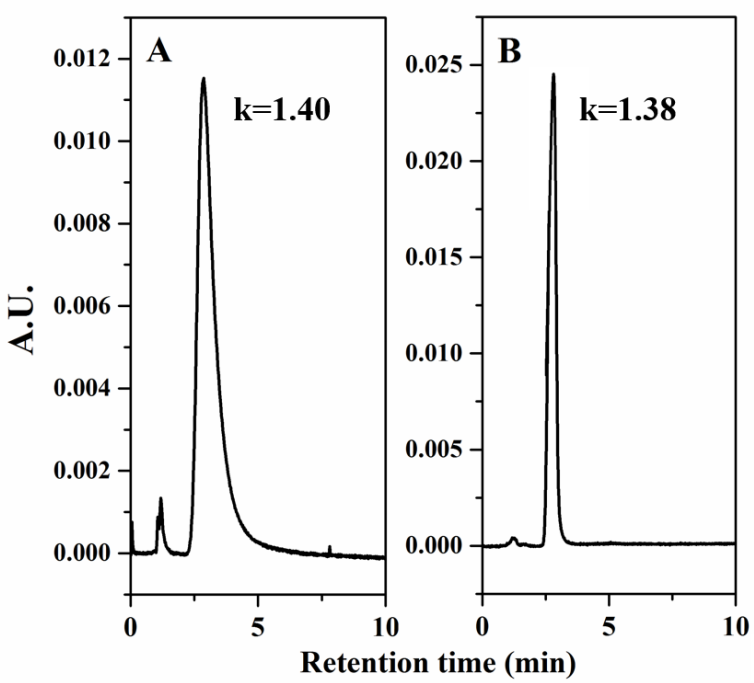

Figure 6. *Chromatograms showing the retention of uracil on A) GMA/EDMA GGG and B) GMA/TRIM GGG columns. Mobile phase conditions: 95:5, ACN:20 mM NH_4Ac buffer, pH 6.0; flow rate, 1.0 mL/min; UV detection, 254 nm.*

GMM/EDMA-GGG columns at 95% (v/v) ACN mobile phase runs (see Figure 4). Cytosine being amino substituted was also retained irreversibly on GMA/EDMA based columns and showed a high retention with a k value of 8.95 for GMA/TRIM columns. The separation of nucleobases is shown for a GMA/TRIM-GGG column in Figure 7. As per the nature of the HILIC separations, the retention of the nucleobases should increase with increasing the concentration of ACN. Figure 4 clearly demonstrates the increase in their retention with the increase in ACN concentration in the mobile phase. The retention pattern of uracil and thymine are almost the same for both columns and thymine being more non-polar than uracil was eluted first. Their retention is mainly due to hydrophilic partitioning. However, the retention of amino substituted nucleobases such as adenine

and cytosine is due to the combination of hydrophilic partitioning, hydrogen bonding and electrostatic interactions which produce a characteristic broad peak. They are retained at higher than 85% (v/v) ACN concentration on both columns but the retention

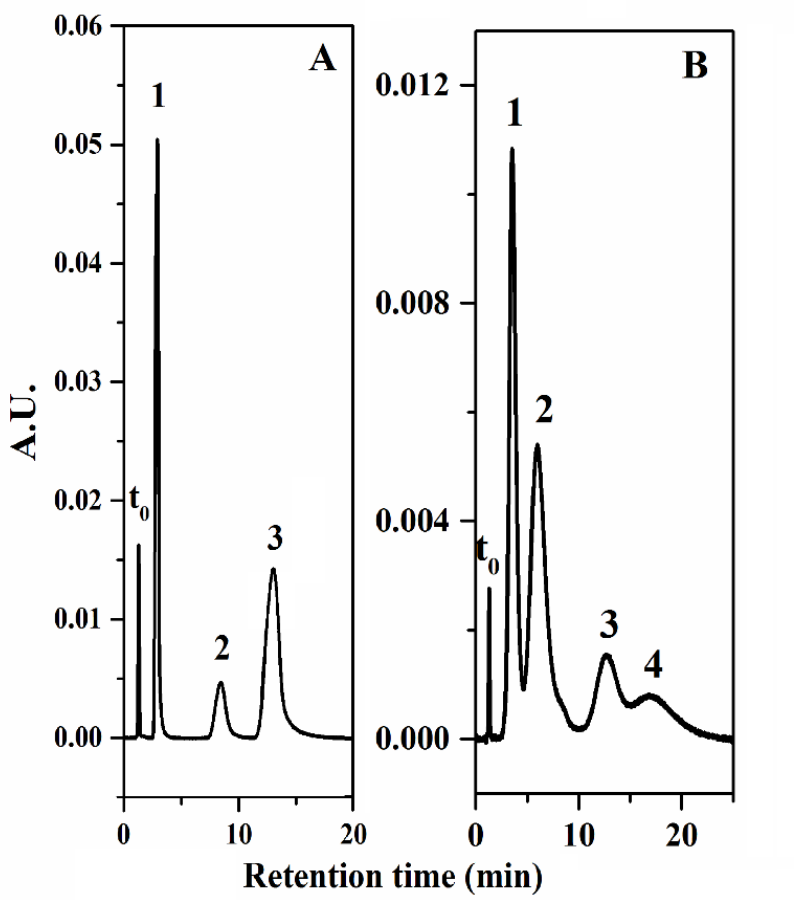

Figure 7. *Chromatogram showing the retention of A) nucleobases B) nucleosides on GMA/TRIM-GGG column. Mobile phase conditions: 95/5, ACN/20mM NH_4Ac buffer, pH 6.0; flow rate, 1.0 mL/min; UV detection, 254 nm. Solutes A): t_0, toluene; 1, uracil; 2, adenine; 3, cytosine. B) t_0, toluene; 1, uridine; 2, adenosine; 3, cytidine; 4, guanosine.*

drastically increased in the case of GMA/EDMA based columns at 90% ACN and could not be eluted at 95% (v/v) ACN in the mobile phase (see Figure 5). When log k was

plotted against %ACN, the R^2 values for the EDMA and TRIM based column were in the range 0.8706-0.9782 and 0.9361-0.9727, respectively. Nucleosides, on the other hand, are more retained than nucleobases due to the extra hydrophilicity added by the attached ribosyl moiety. As nucleobases, nucleosides were also irreversibly retained at 95% (v/v) ACN on the GMA/EDMA-GGG column, guanosine and cytidine were not eluted whereas uridine, adenosine and inosine eluted. However, in the case of GMA/TRIM-GGG all the solutes eluted and their separation is shown in Figure 7. The elution order is uridine followed by adenosine, which was followed by the retention of cytidine and guanosine. The dependence of the k values with the percentage of ACN in the mobile phase was studied and the values are reported in Figures 5A and 5B. The TRIM based columns showed a gradual increase in solute retention starting from 80% (v/v) ACN in the mobile phase. On the other hand, the EDMA based monolith gave a broad peak for all the nucleosides with retention observed at 90% (v/v) ACN. At 95% (v/v) ACN concentration uridine, adenosine and inosine were eluted leaving cytidine and guanosine not eluted. These results clearly indicated the superiority of GMA/TRIM functionalized GGG monolith in terms of both retention and peak shape, which was therefore used for further evaluation.

Reproducibility of GGG. The reproducibility of analysis on GGG column was conducted using uracil and adenine as two typical solutes. The k values were measured from run-to-run (n =6) for the two solutes, which yielded %RSD of 0.54 and 0.71 for uracil and adenine, respectively. Furthermore, the column-to-column reproducibility was evaluated (n =2) using the same two solutes, which gave %RSD values of 3.66 and 5.69

for uracil and adenine, respectively, for two different columns fabricated independently on two different days. These results indicate a good reproducibility of the monolith as well as for the post polymerization modification strategy adopted in the current study.

Comparison of G and GGG functionalized columns. The GMA/TRIM was modified with both G and GGG and was compared with the unmodified blank column for the retention of nucleobases and nucleosides. The GMA/TRIM column where the epoxide rings were opened up by hydrolysis with a solution of 1.0 M H_2SO_4, was used as the unmodified column for this section. Apart from having the zwitterion characteristics, GGG imparted the precursor column with additional hydrophilicity arising from the amide linkages. The amide groups are known for their "soft" adsorption characteristics [22] and are less prone to irreversible adsorption. The k values of nucleobases and nucleosides observed for the unmodified, G and GGG modified columns with a mobile phase consisting of 95 % (v/v) ACN and 5% (v/v) of 20 mM NH_4Ac buffer are listed in Table 4. The values clearly demonstrate the enhanced HILIC characteristics of the modified columns compared to the unmodified column. Uracil, which has a k value of 0.96 on the unmodified column, exhibited increased k values of 1.15 and 1.25 on G and GGG modified columns, respectively, at 95% v/v ACN in the hydro-organic mobile

TABLE 4

RETENTION FACTOR K OF NUCLEOBASES AND NUCLEOSIDES OBTAINED ON G AND GGG FUNCTIONALIZATED GMA/TRIM COLUMN

Solute	Blank	G	GGG
Toluene	0.00	0.00	0.00
Uracil	0.96	1.15	1.25
Adenine	NE	5.18	5.46
Cytosine	NE	8.39	9.10
Uridine	1.39	1.65	1.70
Adenosine	7.40	3.26	3.59
Cytidine	7.40	8.77	8.72
Guanosine	7.40	11.92	12.20

Mobile phase conditions: 95:5/ACN:NH4Ac, 20 mM, pH 6.0

phase. On the unmodified column, adenine and cytosine were irreversibly bound and were not eluted. On the other hand, G and GGG modified columns yielded close k values for adenine and cytosine with the GGG column exhibiting slightly higher k values than the G column. Coming to the selectivity (α) values, the G and GGG columns showed α values of 4.15 and 4.37 between uracil and adenine, respectively. The selectivity between adenine and cytosine was found to be 1.62 and 1.66 for G and GGG modified GMA/ TRIM columns, respectively. When it comes to nucleosides, G and GGG modified columns showed α values of 1.98 and 2.11 between uridine and adenosine, respectively. On the other hand, the α values for the solute pair adenosine and cytidine were found to be 2.69 and 2.42 for G and GGG columns, respectively. Similarly, cytidine and guanosine showed α values of 1.36 and 1.40 for G and GGG modified columns, respectively. These results indicate that both G and GGG modified columns show similar α values, whereas in the case of the unmodified column, the nucleosides co-eluted with a k value of 7.40 with no selectivity.

Effect of mobile phase pH on the retention of nucleobases and nucleosides. One main advantage of having an organic stationary phase is its remarkable stability even at alkaline pH. This provides an unrestricted testing of solute retention at different pHs on the GMA/TRIM-GGG column. In this regard, the retention of thiourea, nucleobases and nucleosides was studied at various pHs while keeping the ACN concentration constant at 90% (v/v) (see Figure 8). The retention of neutral polar solutes such as thiourea and uracil is not affected by the change in mobile phase pH. This is due to the fact that their retention is mainly based on the hydrophilic partitioning between the stagnant aqueous

layer and the mobile bulk hydro-organic layer. Uridine, because of its ribose sugar moiety showed higher retention than uracil. But again, the pH change in the mobile phase did not affect its retention because it is a neutral solute. On the other hand, owing to the presence of the amine group in their structures, adenine and cytosine showed significant variations in their k values with when changing mobile phase pH as shown in Figure 7. At very low pH (1.57), adenine, cytosine and cytidine were unretained whereas adenosine showed a relatively high k value (~ 6.1) at 90% (v/v) ACN. The basic solutes, which are positively charged at acidic pH are partitioned more in the stagnant aqueous layer, and therefore, show high retention. With the increase in the mobile phase pH, the net charge on the

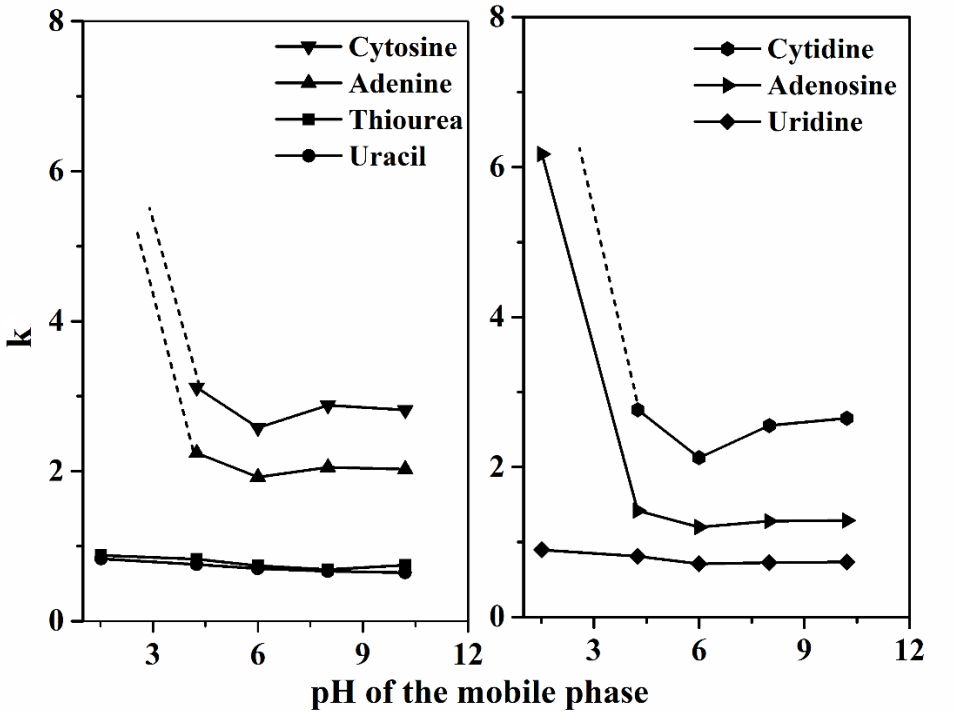

Figure 8. *Plots of k values of nucleobases and nucleosides vs. mobile phase pH. Column, GMA/TRIM-GGG; mobile phase: 90:10 ACN:NH_4Ac buffer prepared at different pH; flow rate, 1.00 mL/min; UV detection, 254 nm.*

surface of the column slowly tends towards zero and also the solutes predominantly exist with neutral charge where the most practical retention was observed. At pHs above 6.0, the retention of thiourea, uracil and uridine remained unaltered while a slight increase in the retention of charged solutes was observed, which can be attributed to the increased electrostatic interactions due to the negatively charged surface carboxylate ions. Though the basic solutes exist as neutral at alkaline pH, the stationary phase is now negatively

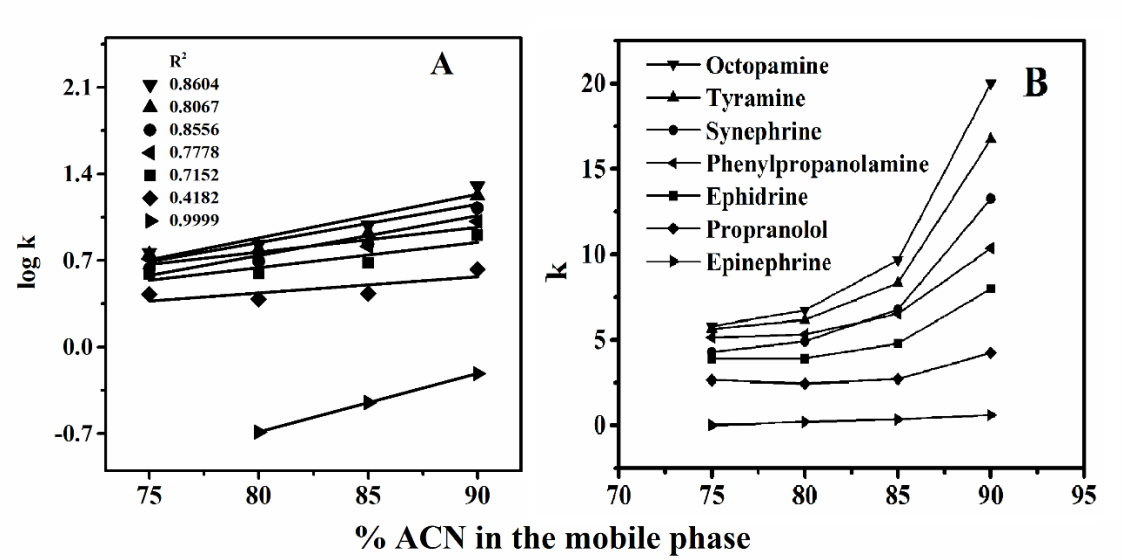

Figure 9. *Plots of log k in (A) and k in (B) of some highly polar compounds versus % ACN in the mobile phase. Column: GMA/TRIM-GGG column. Mobile phase conditions: various % (v/v) ACN and % (v/v) of 20 mM NH_4Ac, pH 6.0; flow rate, 1.0 mL/min; UV detection, 280 nm.*

charged with carboxylate ions on the surface of the monolith. This charge on the surface may lead to a thicker stagnant aqueous layer, which would result in higher retention of the basic solutes. Figure 8 shows the plots of the k values versus the pH of the mobile phase. In the case of zwitterionic stationary phases, as the surface of the stationary phase

is charged with both positive and negative charges, the pH of the mobile phase affects its net charge, which significantly alters the retention nature of the stationary phase.

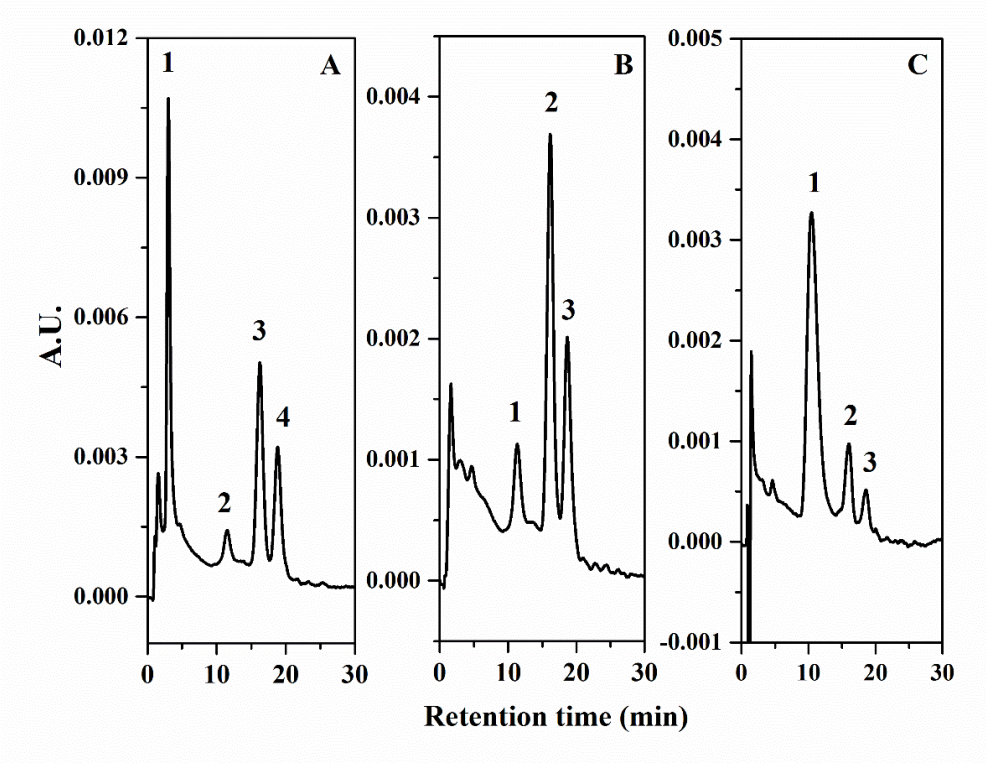

Figure 10. *Gradient elution of some clinically significant drugs. Mobile phase conditions: Solvent A: 96 % (v/v) ACN and solvent B: 75 % (v/v) ACN, both were prepared in 20 mM NH_4Ac buffer, pH 6.0; gradient conditions, 0-100% B in 30 min; flow rate, 1.0 mL/min; UV detection, 280 nm. Solutes in A: 1, epinephrine; 2, ephedrine; 3, metanephrine; 4, normetanephrine; solutes in B: 1, ephedrine; 2, synephrine; 3, normetanephrine; solutes in C: 1, propranolol; 2, metanephrine; 3, normetanephrine.*

Retention of basic polar compounds. The GMA/TRIM-GGG column showed favorable retention towards small basic drugs as shown in Figure 9A and B. This might be due to the surface carboxylic groups of the GMA/TRIM-GGG column, which are

negatively charged, thus exhibiting some electrostatic interactions with the positively charged amine groups of the basic drug solutes, such as synephrine, ephedrine, epinephrine, normetanephrine, metanephrine, octopamine, phenylpropanolamine and propranolol. As can be seen in Figure 9B, their retention increased with increasing the % ACN in the mobile phase, and more significantly after 85% (v/v) ACN in the mobile phase. The optimum separation for all the solutes was realized at 90% (v/v) ACN. Figure 9A depicts the dependence of log k versus the %ACN in the mobile phase, which shows poor linearity (R^2 values from 0.4182-0.9999) indicating the complexity of HILIC separations. By taking into account the nature of the dependence of the retention of the various solutes on the %ACN in the mobile phase (see Figure 9A), a shallow linear gradient of 4-25% (v/v) in aqueous content in the mobile phase for 30 min was applied for the separation as shown in Figure 10A, B and C. For all the gradient runs, a 15 min equilibration time was maintained at a flow rate of 1.0 mL/min. This was needed for the complete regeneration of the initial water layer on the surface of the monolith, which is an essential criterion for HILIC separations.

Conclusions

A novel organic monolithic zwitterionic HPLC column was prepared and its application in HILIC based separation was demonstrated. It is a GGG functionalized GMA/TRIM column, which was optimized from testing various columns with exhaustive trails until a robust column with the desired permeability and stability was obtained. This column was characterized by analyzing the retention of small polar solutes, nucleobases and nucleosides. The zwitterionic stationary phase was further characterized by studying

the dependence of solute retention on the mobile phase pH. The results indicate that the column is seamlessly suitable for the retention of polar basic solutes and shallow linear gradient elution resulted in the separation of clinically significant pharmaceutical drugs.

References

1. Hemström, P. and K. Irgum, *Hydrophilic interaction chromatography.* J. Sep. Sci., 2006. **29**(12): p. 1784-1821.
2. Alpert, A.J., *Hydrophilic-interaction chromatography for the separation of peptides, nucleic acids and other polar compounds.* J. Chromatogr. A, 1990. **499**: p. 177-196.
3. Jandera, P., *Stationary and mobile phases in hydrophilic interaction chromatography: a review.* Anal. Chim. Acta, 2011. **692**(1–2): p. 1-25.
4. Guo, Y. and S. Gaiki, *Retention and selectivity of stationary phases for hydrophilic interaction chromatography.* J. Chromatogr. A, 2011. **1218**(35): p. 5920-5938.
5. McCalley, D.V., *Study of the selectivity, retention mechanisms and performance of alternative silica-based stationary phases for separation of ionised solutes in hydrophilic interaction chromatography.* J. Chromatogr. A, 2010. **1217**(20): p. 3408-3417.
6. Nesterenko, E.P., P.N. Nesterenko, and B. Paull, *Zwitterionic ion-exchangers in ion chromatography: A review of recent developments.* Anal. Chim. Acta, 2009. **652**(1–2): p. 3-21.
7. Hu, W. and P.R. Haddad, *Electrostatic ion chromatography.* TrAC Trends Anal. Chem., 1998. **17**(2): p. 73-79.
8. Jiang, W. and K. Irgum, *Synthesis and Evaluation of Polymer-Based Zwitterionic Stationary Phases for Separation of Ionic Species.* Anal. Chem., 2001. **73**(9): p. 1993-2003.

9. Jiang, W., G. Fischer, Y. Girmay, and K. Irgum, *Zwitterionic stationary phase with covalently bonded phosphorylcholine type polymer grafts and its applicability to separation of peptides in the hydrophilic interaction liquid chromatography mode.* J. Chromatogr. A, 2006. **1127**(1–2): p. 82-91.

10. Yuan, G., Y. Peng, Z. Liu, J. Hong, Y. Xiao, J. Guo, N.W. Smith, J. Crommen, and Z. Jiang, *A facile and efficient strategy to enhance hydrophilicity of zwitterionic sulfoalkylbetaine type monoliths.* J. Chromatogr. A, 2013. **1301**: p. 88-97.

11. Guo, H., R. Liu, J. Yang, B. Yang, X. Liang, and C. Chu, *A novel click lysine zwitterionic stationary phase for hydrophilic interaction liquid chromatography*. J. Chromatogr. A, 2012. **1223**: p. 47-52.

12. Huang, H., H. Guo, M. Xue, Y. Liu, J. Yang, X. Liang, and C. Chu, *Click novel glycosyl amino acid hydrophilic interaction chromatography stationary phase and its application in enrichment of glycopeptides.* Talanta, 2011. **85**(3): p. 1642-1647.

13. Shen, A., X. Li, X. Dong, J. Wei, Z. Guo, and X. Liang, *Glutathione-based zwitterionic stationary phase for hydrophilic interaction/cation-exchange mixed-mode chromatography*. J. Chromatogr. A, 2013. **1314**: p. 63-69.

14. Jiang, W. and K. Irgum, *Tentacle-Type Zwitterionic Stationary Phase Prepared by Surface-Initiated Graft Polymerization of 3-[N,N-Dimethyl-N-(Methacryloyloxyethyl)- ammonium] Propanesulfonate through Peroxide Groups Tethered on Porous Silica.* Anal. Chem., 2002. **74**(18): p. 4682-4687.

15. Qiao, L., A. Dou, X. Shi, H. Li, Y. Shan, X. Lu, and G. Xu, *Development and evaluation of new imidazolium-based zwitterionic stationary phases for hydrophilic interaction chromatography.* J. Chromatogr. A, 2013. **1286**: p. 137-145.

16. Shen, A., Z. Guo, X. Cai, X. Xue, and X. Liang, *Preparation and chromatographic evaluation of a cysteine-bonded zwitterionic hydrophilic interaction liquid chromatography stationary phase.* J. Chromatogr. A, 2012. **1228**: p. 175-182.

17. Qiu, H., E. Wanigasekara, Y. Zhang, T. Tran, and D.W. Armstrong, *Development and evaluation of new zwitterionic Hydrophilic interaction liquid chromatography stationary phases based on 3-P,P-diphenylphosphonium-propylsulfonate.* J. Chromatogr. A, 2011. **1218**(44): p. 8075-8082.

18. Guiochon, G., *Monolithic columns in high-performance liquid chromatography.* J. Chromatogr. A, 2007. **1168**(1–2): p. 101-168.

19. Jonnada, M., R. Rathnasekara, and Z. El Rassi, *Recent advances in nonpolar and polar organic monoliths for HPLC and CEC.* Electrophoresis, 2015. **36**(1): p. 76-100.

20. Jonnada, M. and Z. El Rassi, *Robust naphthyl methacrylate monolithic column for high performance liquid chromatography of a wide range of solutes.* J. Chromatogr. A, 2015. **1409**: p. 166-172.

21. Aydoğan, C. and Z. El Rassi, *Monolithic stationary phases with incorporated fumed silica nanoparticles. Part I. Polymethacrylate-based monolithic column*

with incorporated bare fumed silica nanoparticles for hydrophilic interaction liquid chromatography. J. Chromatogr. A, 2016. **1445**: p. 55-61.

22. Ikegami, T., K. Tomomatsu, H. Takubo, K. Horie, and N. Tanaka, *Separation efficiencies in hydrophilic interaction chromatography*. J. Chromatogr. A, 2008. **1184**(1–2): p. 474-503.

23. Kornyšova, O., R. Jarmalavičienė, and A. Maruška, *A simplified synthesis of polymeric nonparticulate stationary phases with macrocyclic antibiotic as chiral selector for capillary electrochromatography.* Electrophoresis, 2004. **25**(16): p. 2825-2829.

24. Evangelista, R.A., F.-T.A. Chen, and A. Guttman, *Reductive amination of N-linked oligosaccharides using organic acid catalysts.* J. Chromatogr. A, 1996. **745**(1–2): p. 273-280.

25. Evangelista, R.A., A. Guttman, and F.T.A. Chen, *Acid-catalyzed reductive amination of aldoses with 8-aminopyrene-1, 3, 6-trisulfonate.* Electrophoresis, 1996. **17**(2): p. 347-351.

CHAPTER III

PREPARATION OF N-ACRYLOXYSUCCIMIDE-CO-ETHYLENE GLYCOL DIMETHACRYLATE AND ITS POST-POLYMERIZATION MODIFICATION WITH OCTADECYL LIGANDS FOR USE IN HPLC

Introduction

Organic monolithic HPLC columns are becoming increasingly popular for their distinctive advantages of (i) easy *in situ* preparation in columns or separation channels of different dimensions, and (ii) tunable flow characteristics by adjusting the monomers to porogens ratio [1-3]. Monolithic columns with narrow inner diameter tubing represent a new trend in HPLC, which can be termed as "micro-scale HPLC" [4]. They have characteristic of low dead volume and separation efficiencies comparable to that of conventional HPLC columns within their typical flow rates. The low flow rates facilitate the cutting down on the consumption of mobile phase and stationary phase, which is the main attractive feature of micro-scale HPLC. However, micro-scale HPLC systems which run with micro-bore columns with diameters of 200-500 μm i.d. require specialized instrumentation, pumps and flow cells. Therefore, there exist an intermediate class to bridge the gap between the two, which can be termed as semi-micro column with 1-2 mm i.d. and separations can be performed on a standard HPLC system with minor

changes in the tubing (e.g., injection loop volume) to decrease the pre-column dead volume [4]. The main advantage of these semi micro columns is that they consume far less solvent than the conventional HPLC columns having 4.6 mm i.d. thus leading to a reduction in the cost of analysis. Apart from this cost reduction, these narrow bore columns provide their users with many other advantages such as convenience of direct coupling with mass spectrometry, high resolution by using long columns and easy control of column temperature [5]. Also, the low consumption of stationary phase allows the packing of the narrow bore columns with various valuable materials and therefore reduces the cost of the columns.

Semi-micro columns have usually 1-2 mm i.d. and this idea of miniaturizing the HPLC column dates back to the early history of HPLC in the mid-seventies [6, 7]. However, lack of efficient packing methods have hindered the rise in using narrow bore columns which were soon substituted by ¼" columns (4.6 mm i.d.). But with the advent of polymeric based monolithic columns, the difficulties which arise from the packing of narrow bore columns with particles was eliminated, since the column material is formed by *in situ* polymerization.

The functional monomer *N*-acryloxysuccinimide (NAS) is well known for its reactivity towards primary amines and its application in capillary electrochromatography (CEC) was explored in the covalent attachment of aliphatic amines to the NAS functionalized monolithic surface [8]. In the current study, NAS and ethylene glycol dimethacrylate (EDMA) were polymerized by thermally initiated *in situ* polymerization in 1 mm i.d. stainless steel columns. Octadecylamine was functionalized onto the surface of the NAS monolith and its application was demonstrated in reversed phase

chromatography (RPC). Nonpolar solutes such alkylbenzenes (ABs) and polyaromatic hydrocarbons (PAHs) were used as the test solutes. Also, standard proteins were separated by gradient elution. All the separations were carried out with minimal consumption of solvent and stationary phase materials.

Experimental

Instrumentation

All HPLC separations were performed on a Waters Alliance 2690 HPLC separations module (Milford, MA, USA), equipped with an in-line degasser, a quaternary solvent pump, an auto sampler and a thermostated column compartment. The data acquisition was carried out using Empower 2 (Build 2154) software (Waters, Milford, MA, USA). Detection was performed on a PDA detector model W2990. A syringe pump was obtained from Cole-Parmer (Vernon Hills, IL, USA) and was used in the post polymerization reactions of the column surface to pump the reagents into the NAS column at appropriate flow rates. The sample and the column compartments were maintained at ambient temperature. Chromatographic data were processed by OriginPro v8.5.1 from Origin Lab Corp (Northampton, MA, USA). Stock solutions of 1 mg/mL of each solute were prepared in ACN and diluted to the desired concentrations in the mobile phase yielding adequate detector response. Water was filtered through a 0.45 µm membrane (Millipore, Bedford, USA) before use.

Reagents and materials

The narrow bore columns with 1/16” o.d. and 1 mm i.d. were fitted with /16” ferrules and 1/16” column end fittings. The stainless steel tubing and the associated fittings were purchased from Alltech Associates (Deerfield, IL, USA) while the retaining nano frits were purchased from Valco Instruments Co. Inc. (Houston, TX, USA). The functional monomer used in the current study, *N*-acryloxysuccinimide (NAS) was obtained from Acros Organics (Morris Plains, NJ, USA), the crosslinker ethylene glycol methacrylate (EDMA), the initiator 2,2’azobis(isobutyronitrile) (AIBN) and the porogen toluene were purchased from Aldrich (Milwaukee, WI, USA). HPLC grade acetonitrile (ACN) was acquired from Pharmco-Aaper (Brookfield, CT, USA) and ethanolamine from Kodak Eastman, (Rochester, NY, USA). All the non-polar solutes including the ABs, PAHs were procured from Sigma (St Louis, MO, USA). Standard proteins that are used in the current study such as equine heart cytochrome C, chicken egg white lysozyme, chicken egg white conalbumin, bovine milk β-lactoglobulin and human serum albumin were purchased from Sigma (St Louis, MO, USA).

Preparation of NAS-co-EDMA monolith in narrow bore columns

The base monolithic precursor poly (NAS-co-EDMA) referred to as NASM was polymerized by *in situ* polymerization in a stainless steel column (25 cm x 1 mm i.d.) according to the following procedure. The 25 cm column bearing end fittings was filled with the polymerization reaction mixture that was prepared by weighing the contents into a clean glass vial corresponding to a total weight of 0.5 g consisting of 18.0% (w/w) NAS as the functional monomer, 15.8% (w/w) EDMA as the crosslinker and 66.2% (w/w)

toluene as the porogen. A 1% (w/w) of the initiator AIBN with respect to the monomers was added to the reaction mixture. The weight of AIBN was not taken into account while calculating the percentages of the reaction mixture. The reaction mixture was shaken gently to dissolve the NAS and mildly degassed by a low power sonicator. The polymerization mixture was then transferred to the column with a syringe fitted with an appropriate connection to the column. In this filling process, the column was kept vertical and the mixture was introduced into the column against gravity to ensure proper filling of the column without any air bubbles. Thereafter, the column was sealed at both ends, and the polymerization was carried out at 50 ˚C in a water bath for 15 h. After polymerization, the column was flushed with ACN to remove the porogens and the unreacted monomers. This was followed by equilibrating the column with one to two column volumes of toluene before proceeding to the post polymerization reaction. Figure 1 shown below gives us an estimate of the dimensions of the narrow-bore column used in the current study.

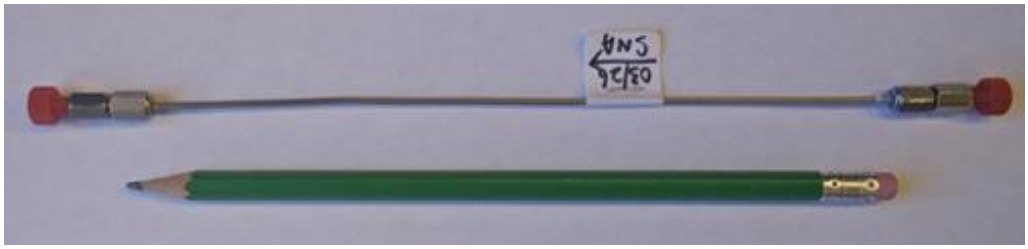

Figure 1. *Picture of the narrow bore HPLC column with dimensions, 25 cm x 1 mm i.d.*

Post polymerization modification of NAS with octadecyl ligands

After the base monolith was made, it was further modified with octadecylamine to form the NASM-OD. The concentration of octadecylamine solution prepared in toluene was 0.04 g/mL, which was flushed through the column for about two column volumes. The octadecylamine concentration was maintained in large excess in order to ensure high surface coverage of the NAS monolith with octadecyl ligands. Then, the column was washed with methanol to remove the unreacted octadecylamine and toluene. This was followed by scavenging the unreacted succinimide functions of the NASM by passing a 10% (v/v) methylamine solution prepared in methanol through the column. For this reaction, refer to Figure 2. As the columns used in the current chapter were narrow-bore columns (1 mm i.d.), preparation and transfer of "mold" was not possible as in the case of 4.6 mm i.d. columns, and consequently a different methodology was adopted. The formed void at the inlet of the column was removed by cutting the column up to the position where there was monolith and a new ferrule was inserted at different position with column end fittings. Care was taken while cutting the column, which might form a restriction. A 3.5 cm void was observed at the inlet of the column, which was cut yielding a column of 21.5 cm total length. This shortened column was then flushed with ACN before use.

Preparation of NASM functionalized with octadecyl ligands for HPLC

The NAS monolith (NASM) prepared as mentioned above was intended to have high mechanical stability to suit the HPLC running conditions. That is, the monolith should withstand high pressures, which are usually encountered in HPLC at relatively high flow velocities. This was done by increasing the percentage of the crosslinker EDMA with respect to the functional monomer NAS. The previously reported NASM

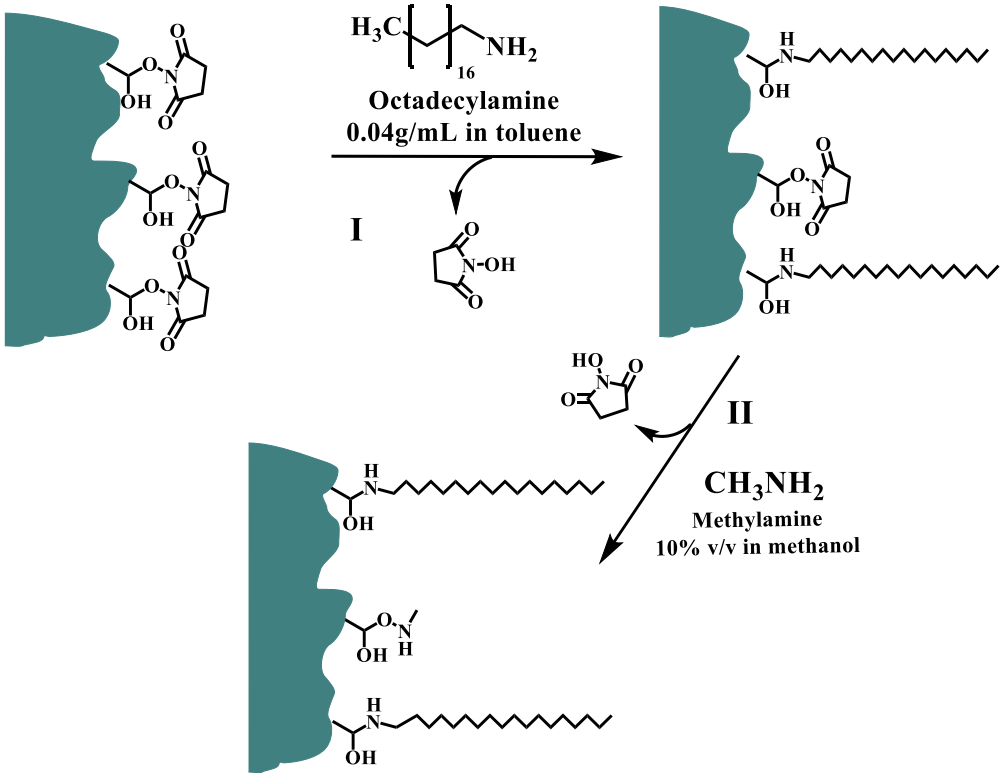

Figure 2. *Post polymerization modification of NAS monolith (NASM) with octadecyl ligands. I) Reaction of the surface succinimide groups of the base monolith with octadecylamine. II) Scavenging of the unreacted succinimide groups with methylamine.*

TABLE 1

K VALUES OBSERVED FOR THE DIFFERENT NASM-OD COLUMNS OBTAINED WITH DIFFERENT MODIFICATION SOLVENTS

	0.04 g/mL octadecylamine in toluene	0.04 g/mL octadecylamine in 1,4-dioxane	0.04 g/mL octadecylamine in THF
Toluene	1.27	1.27	1.24
Ethylbenzene	1.51	1.48	1.24
Propylbenzene	2.05	2.03	1.70
Butylbenzene	2.79	2.77	2.41

Conditions: Mobile phase, water:ACN 47.5:52.5 (v/v); flow rate, 0.1 mL/min; column, 21.5 cm x 1 mm i.d.

was prepared for use in capillary electrochromatography (CEC) [8], where the monolith does not encounter high backpressure and moreover, the monolith needs to be covalently bound to the wall of the capillary to avoid its moving out from the column. In the previously reported work, the ratio of NAS to EDMA was designed to suit the needs of CEC applications. In the current work, the percentage of EDMA was increased to improve the mechanical stability of the monolith to withstand the high pressures that are encountered in HPLC. The total percentage of monomers was 33.8% (w/w) with the ratio of NAS to EDMA being maintained at 1.33 and the single porogen toluene was used which corresponds to the remaining 66.2% (w/w). Under these fabrication conditions, the monolith thus obtained was mechanically durable and it was found to be stable after many consecutive injections. For carrying out the post polymerization reactions different solvents were studied to select the best for obtaining the maximum surface coverage with octadecyl groups. The results are tabulated in Table 1. Three solvents namely toluene, dioxane and THF were explored for this purpose and the retention of four ABs were estimated. From the k values, the column modified with toluene and 1,4 dioxane gave similar results while the one made in toluene yielded a better peak shape. The column modified with THF gave lower retention and the peaks of toluene and ethylbenzene co-eluted. Thus, toluene was the chosen solvent for the rest of this investigation.

Chromatographic evaluation of NASM-OD column

Conventional HPLC instrumentation was used without any modifications for testing the 1 mm i.d. column. The flow rates were typically in the range 0.05-0.3 mL/min and only 5-30% of the total solvent normally used in conventional HPLC was consumed.

The narrow bore NASM-OD column was evaluated in the RPC mode with hydro-organic mobile phases consisting of water and ACN in various ratios.

Alkylbenzenes. Alkylbenzenes (ABs) are commonly used test solutes to study the RPC behavior of nonpolar columns. Figure 3A shows the retention behavior of ABs from toluene to butyl benzene with varying ACN concentration in the mobile phase in the range of 35-52.5% (v/v) ACN, and the retention factor (k) decreased logarithmically in a linear fashion which is indicative of RPC behavior. The magnitude of the slopes increased from 0.032 to 0.048 when going from toluene to butylbenzene indicating

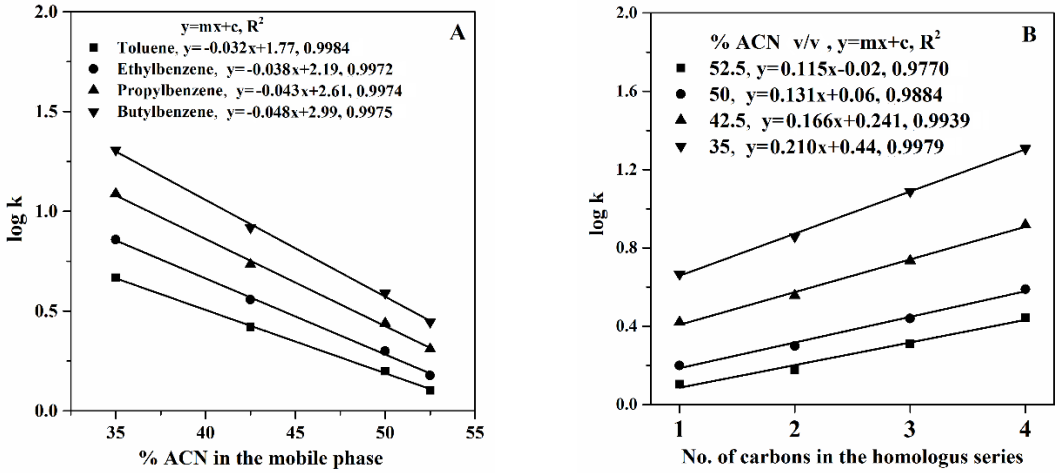

Figure 3. *Plots of log k of the ABs homologues series vs. % ACN (v/v) in the mobile phase (A) and log k vs. carbon number of the homologous series at different ACN concentration in the mobile phase (B). Column, NASM-OD, 22.5 cm x 1 mm i.d.; flow rate, 0.1 mL/min; detection, 214 nm.*

the increase in the extent of interaction with increased solute size or solute hydrophobicity. The R^2 values are in the range 0.9972-0.9984. Linear curves were

obtained when plotting log k against the number of carbon in the ABs homologues series as shown in Figure 3B. The slopes of the lines correspond to the log of methylene selectivity (log α_{CH2}). The methylene group selectivity values were calculated by applying the antilog to the obtained values for the slopes of the linear plots. The α_{CH2}values increased from 1.30 to 1.62 when the % (v/v) of ACN decreased from 52.5 to 35. The R^2 values also increased from 0.9770 to 0.9979.

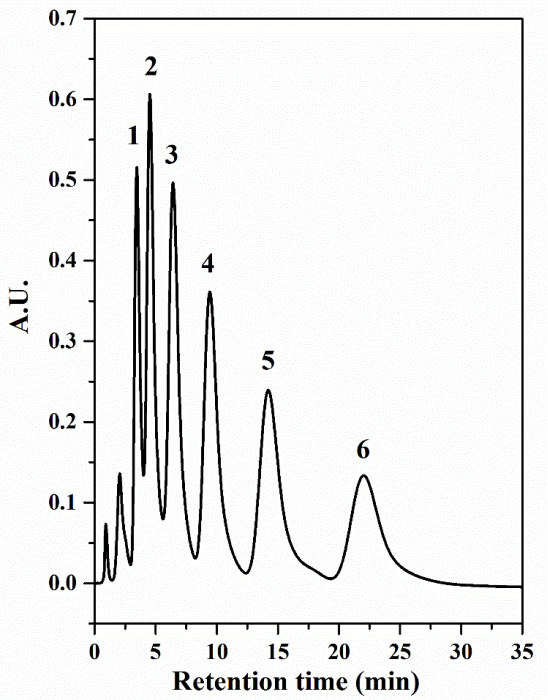

Figure 4. *Separation of ABs on NASM-OD column; dimensions, 21.5 cm x 1 mm i.d.; flow rate, 0.1 mL/min; mobile phase, water:ACN 45:55 (v/v). Peaks, 1) toluene, 2) ethylbenzene, 3) propylbenzene, 4) butylbenzene, 5) pentylbenzene, 6) hexylbenzene; UV detection at 214 nm.*

The chromatogram for the separation of six alkyl benzenes is shown in Figure 4. A flow rate of 0.1 mL/min was employed for pumping the hydro-organic mobile phase containing 55% (v/v) ACN. Other ligands such as benzylamine and naphthylamine were

bound to the NASM surface, which generate benzyl and napthyl surfaces, respectively. Similar to the NASM-OD column, these surfaces are known to exhibit reversed phase behavior. In fact, when testing the benzyl and the naphthyl columns with ABs, the columns showed similar retention behavior as that of octadecyl column, but with poor resolution and broad peaks (chromatograms not shown). These results indicate the superior reversed phase nature and surface coverage of the NASM-OD column.

Polyaromatic hydrocarbons. The retention ability of NASM-OD column was tested with some PAHs. A column length of 21.5 cm was used in this study, and a relatively elevated flow rate of 0.3 mL/min was used. Figure 5 shows the separation of 1-nitronaphthalene, fluorene, phenanthrene and pyrene. Pyrene, being the most nonpolar with four benzene rings fused together, eluted last.

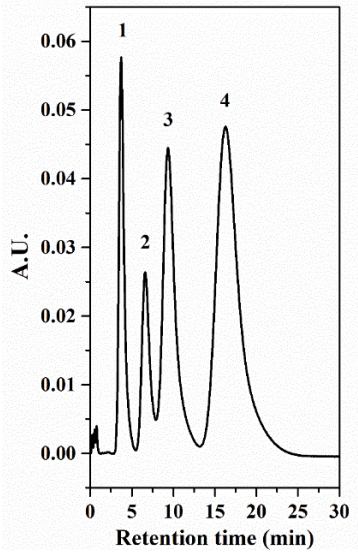

Figure 5. *Separation of PAHs obtained on NASM-OD column; dimensions, 21.5 cm x 1 mm i.d.; flow rate, 0.3 mL/min; mobile phase, water:ACN (60:40, v/v); UV detection at 254nm. Peaks, 1) 1-nitronaphthalene; 2) fluorene; 3) phenanthrene; 4) pyrene.*

Reproducibility of data obtained on the NASM-OD column. The reproducibility of analysis on the NASM-OD column was performed using the AB test solutes. The k values were measured from run-to-run (n = 4) for the four ABs, which yielded %RSD values of 1.27, 1.69, 1.80 and 2.52, for toluene, ethylbenzene, propylbenzene and butylbenzene, respectively. Similarly, the column-to-column reproducibility was evaluated (n = 2) using the same AB test solutes, which gave %RSD values of 0.86, 6.26, 6.76 and 5.91 for toluene, ethylbenzene, propylbenzene and butylbenzene, respectively. For all of the above reproducibility studies, 50% (v/v) ACN was used as the mobile phase at a flow rate of 0.1 mL/min.

Separation of proteins. Polymer based monolithic columns are well suited to high separation efficiency of proteins owing to the absence of micropores in the monolithic structure [3]. NASM-OD column was tested in the separation of standard proteins using linear gradient elution at increasing % ACN concentration in the mobile phase. Trifluoroacetic acid was used as an additive in the aqueous and ACN mobile phase. A flow rate of 0.1 mL/min was used with a slow gradient of 0-100% eluting mobile phase in 30 min. A mixture of six standard proteins consisting of ribonuclease A (M_r, 13.7 kDa; pI, 9.6), cytochrome C (M_r, 14.4 kDa; pI, 10.0), lysozyme (M_r, 14.3 kDa; pI, 9.3), conalbumin (M_r, 75.0 kDa; pI, 6.6), β-lactoglobulin A (M_r, 18.4kDa; pI, 5.1) and human serum albumin (M_r, 66.0 kDa; pI, 4.7) was readily separated in 30 min, and the chromatogram is shown Figure 6.

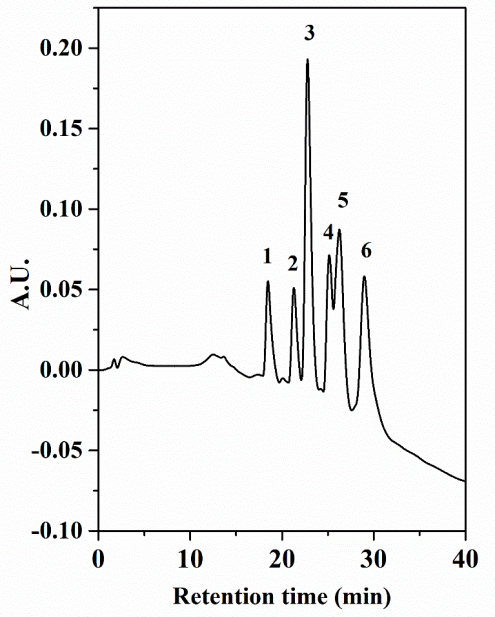

Figure 6. *Chromatogram of six standard proteins obtained on NASM-OD column. Column, 21.5 cm x 1 mm i.d.; mobile phase A, 0.1% (v/v) TFA in water:ACN, 95: 5 (v/v); mobile phase B, 0.1% (v/v) TFA in water:ACN, 5:95 (v/v); linear gradient from 0-100 %B in 30 min; flow rate, 0.1 mL/min; detection at 214 nm. Solutes: 1, ribonuclease A; 2) cytochrome C; 3) lysozyme; 4) conalbumin; 5) β-lactoglobulin; 6) human serum albumin.*

Conclusions

A narrow bore HPLC column was developed by the co-polymerization of NAS and EDMA, which was further functionalized with octadecyl ligands for its applications in RPC. The column was tested for its RPC behavior with ABs and PAHs and demonstrated good chromatographic utilities at very low flow rates of 0.1-0.3 mL/min, consuming much less solvent than the regular analytical scale HPLC column. The separation of six standard proteins was also demonstrated using linear gradient elution of

increasing ACN concentration in the mobile phase. This column was made by *in situ* polymerization in stainless steel tubing with 1 mm i.d. and it represents a class referred to as semi-micro column, which do not require any additional instrumentation and can be used on a conventional HPLC system without any additional instrumentation. The cost of the analysis is greatly reduced by consuming less mobile phase and stationary phase material. It satisfies the growing need of cost cutting strategies employed in various industries.

References

1. Guiochon, G., *Monolithic columns in high-performance liquid chromatography.* J. Chromatogr. A, 2007. **1168**(1–2): p. 101-168.
2. Jonnada, M., R. Rathnasekara, and Z. El Rassi, *Recent advances in nonpolar and polar organic monoliths for HPLC and CEC.* Electrophoresis, 2015. **36**(1): p. 76-100.
3. Zhang, J., S.-L. Wu, J. Kim, and B.L. Karger, *Ultratrace liquid chromatography/mass spectrometry analysis of large peptides with post-translational modifications using narrow-bore poly(styrene-divinylbenzene) monolithic columns and extended range proteomic analysis.* J. Chromatogr. A, 2007. **1154**(1–2): p. 295-307.
4. Takeuchi, T., *Modern aspects of micro-bore column HPLC.* Fresenius J. Anal. Chem., 1990. **337**(6): p. 631-637.
5. Nischang, I., F. Svec, and J.M.J. Fréchet, *Downscaling Limits and Confinement Effects in the Miniaturization of Porous Polymer Monoliths in Narrow Bore Capillaries.* Anal. Chem., 2009. **81**(17): p. 7390-7396.
6. Scott, R.P.W. and P. Kucera, *Mode of operation and performance characteristics of microbore columns for use in liquid chromatography.* J. Chromatogr. A, 1979. **169**: p. 51-72.
7. Ishii, D., K. Asai, K. Hibi, T. Jonokuchi, and M. Nagaya, *A study of micro-high-performance liquid chromatography.* J. Chromatogr. A, 1977. **144**(2): p. 157-168.

8. Guerrouache, M., B. Carbonnier, C. Vidal-Madjar, and M.-C. Millot, *In situ functionalization of N-acryloxysuccinimide-based monolith for reversed-phase electrochromatography.* J. Chromatogr. A, 2007. **1149**(2): p. 368-376.

CHAPTER IV

N-ACRYLOXYSUCCINIMIDE-CO-ETHYLENE GLYCOL DIMETHACRYLATE WITH SURFACE IMMOBILIZED TRYPSIN AND LECTINS FOR MINIATURIZED ENZYME REACTORS AND LECTINAFFINITY CHROMATOGRAPHY RESPECTIVELY

Introduction

Post translational modifications (PTM) of proteins, mainly glycosylation, play an important role especially in disclosing information relevant to various cellular malfunctions. Protein glycosylation is about more than 50% of total PTMs and carries important information pertaining to many cellular activities such as immune recognition, protein-protein interactions and various other cellular activities [1]. The study of glycosylation is of major importance in the field of biomedical research for the identification of biomarkers for the early detection and diagnosis of various diseases, especially cancers. Breast cancer is the most diagnosed cancer among women in The United States [2]. Identification of dependable biomarkers for the early diagnosis of breast cancer is the core interest of many researchers. Of all the biological fluids present in the human body, blood (serum and plasma) serves as the main source for a wealth of information for research. Blood plasma is often very complex and challenging due to its

broad dynamic concentration range of proteins. The top eight proteins make up about 85% of the total proteins present in the serum. These high abundant proteins mask the detection of the low abundant glycoproteins, which might be potential cancer protein biomarkers. The patterns of these glycoproteins carry significant information regarding the progress of the disease. With the recent significant advances in the field of mass spectrometry (MS) the need for various sample preparation, depletion, and enrichment techniques for the identification of the low abundance glycoproteins has increased. An enrichment technique for the pre-concentration, purification and differentiation of the glycoproteins from cancerous serum with respect to the disease free serum is the best method in identifying protein biomarkers for diseases [3, 4].

Lectins are proteins of non-immune origin and are known to have an affinity towards particular glycoconjugates thus serving as specific reagents for glycoprotein enrichment from biological fluids in order to identify differentially expressed glycoproteins [5, 6]. The glycans that are attached to the proteins are generally very complex and there is no single lectin that covers all the glycoproteome. So, in general an efficient approach called serial lectin affinity chromatography (SLAC) was applied in this investigation [1, 7]. Using SLAC, whereby a series of lectin columns with different carbohydrate binding specificities are connected in tandem was used to capture different glycoproteins from human serum. In this process, the serum is usually passed through the serial lectin columns. By this kind of approach, the heterogeneity of the glycoproteome can be obtained and the pattern of the glycoproteome can be studied which can be a major source of information for the further confirmation of biomarkers.

In this chapter, the SLAC setup has a total of 4 immobilized lectin columns, namely concanavalin A (Con A), *Lens culinaris* agglutinin (LCA), *Ricinus communis* I agglutinin (RCA) and *Sambucus nigra* agglutinin (SNA). For their structures refer to

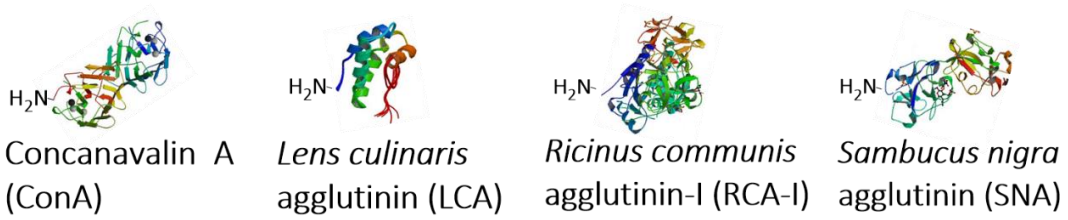

Figure 1. *Lectins used in the current study (structure from http://www.rcsb.org/pdb)*

Figure 1. Each lectin is known to have its own binding specificity. LCA is known to interact with α-mannosyl residues on *N*-glycans, but the *N*-acetyl glucosamine at the reducing terminal should be substituted with a fucose at its C-6 hydroxyl. RCA interacts specifically with the non-reducing terminals of the outer chain structures of the *N*-glycans. On the other hand, SNA shows specificities towards sialic acid containing glycans. The high mannose and hybrid type glycans which have an affinity towards Con A are shown in Figure 2A and B and can be described as the mannome and hybridome, respectively. The glycan chains with core fucosylation (Figure 2C) are known to have affinity towards LCA and sialoglycoproteins represented in Figure 2D are known to bind to SNA. Finally, RCA generally binds to glycoproteins bearing branched *N*-glycans such as bi-, tri-, and tetraantennary complex type glycans shown in Figure 2E, 2F and 2G, respectively. So, all the branched glycoproteins that are captured by RCA can be categorized as the 'branched glycome'. The haptenic sugar for LCA and Con A is the

methyl-α-D-mannopyranoside (Me-α-Man) and that for RCA and SNA is lactose. In SLAC, the order of lectin column determines the range of glycoproteins that are bound to

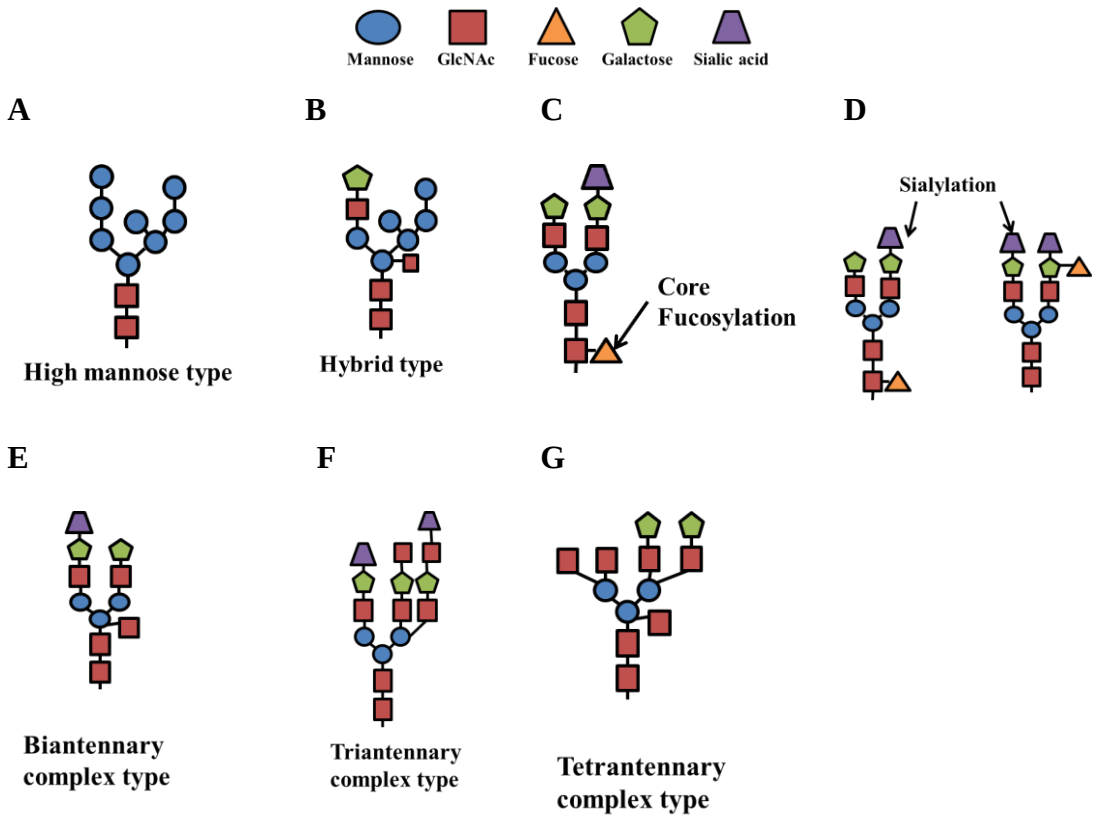

Figure 2. *Sugar binding specificities of: Con A, high mannose (A) and hybrid type (B); LCA, core-fucosylated N-glycans (C); SNA, sialic acids bound to galactose in α(1,2) linkages (D); RCA-I, biantennary (E), triantennary (F) and tetrantennary (G) complex type glycans.*

each lectin column. Based on the above-mentioned complementary specificities of the different lectins, the following strategy was adopted, according to which, two different chromatographic setups, namely A and B were used. In setup A, three lectin columns were connected in tandem in the order LCA → Con A → RCA and used for the

extraction of glycoproteins. In setup B, only the SNA column was used to capture the bound sialoglycoproteins. In setup A, the LCA column is the first in the series to capture the bi and triantennary glycosylated proteins with fucosylated inner core and this is followed by Con A for the capture of mannose and hybrid type glycans. Then, RCA will bind to the remaining branched glycoproteins with or without core fucosylation. Thus, in the currently designed SLAC, the three lectin columns, LCA → Con A → RCA with complimentary specificities captured the glycoproteins with the broadest glycosylation possible in both cancer and healthy sera. The SNA column in setup B capture exclusively proteins with (α-2,6) linked sialic acids (sialylated glycoproteins). The rationale behind using SNA in setup B is in the fact that the sialylation takes place in almost all kinds of glycans where it will capture all sialic acid containing glycoproteins.

With the beginning of MS analysis becoming an indispensable tool for proteomics research and in the analysis of biological samples, the need for small reactors has increased. These reactors can handle very small sample volumes, have a potential to be directly connected to MS to reduce the operator intervention and increase high throughput. In MS, protein analysis generally involves enzymatic digestion where sample volumes are in the range of microliters. This proteolysis of the parent protein is the essential step in the ladder of analysis carried out in MS analysis protocols. So, there is a need for a special device for tryptic digestion such as the so-called immobilized enzyme reactor (IMER) with surface immobilized trypsin, which offers many distinct advantages compared to the in-solution digestion. This reactor completes the digestion in minutes compared to an in-solution protocol, which takes up to 24 h. The immobilized enzyme in IMER is generally stable to harsh environments such as pH, temperature and organic

solvents. Moreover, enzyme autolysis is another major constraint in the case of in-solution digestion. Besides all these, IMER generally offers high turnover numbers compared to in-solution digestion. Currently, many publications have emerged which reported IMER made from beads, nanoparticles, membranes and other monolithic materials [8-10].

In this chapter, a narrow bore HPLC column with monolithic material prepared from the copolymerization of *N*-acryloxysuccinimide (NAS) and ethylene glycol dimethacrylate (EDMA) was constructed in a 1 mm i.d. stainless steel column. This monolithic material with surface succinimide groups readily binds with primary amines of the lysine residues of the proteins to form stable amide bonds. This type of bio-conjugation reaction between *N*-hydroxysuccinimide and amine is well known and was exploited for a long time [11, 12]. The functional monomer *N*-acryloxysuccinimide was previously used in the preparation of hydrophilic gels where proteins were covalently immobilized onto the surface of solid gel for various applications [13, 14]. Monoliths made with co-polymerized NAS and EDMA were previously reported for CEC for various applications in HILIC [15], RPC [16, 17] and chiral [18] formats. The NAS-co-EDMA monolith, which was optimized for narrow bore HPLC in Chapter III, was bound with lectins and trypsin for SLAC and trypsin IMER, respectively.

Experimental

Reagents and materials

The 1/16” o.d. narrow bore columns with dimensions 25 cm x 1 mm i.d., were fitted with 1/16” ferrules and 1/16” column end fittings, which were purchased from

Alltech Associates (Deerfield, IL, USA). The micro retaining frits with 0.5µm porosity and thickness of 0.75 mm were purchased from Valco Instruments Co. Inc. (Houston, TX, USA). Octadecyl silica (ODS) UltraSphere™ column packed with 5-µm average particle diameter, and having the dimensions 4.5 cm x 4.6 mm i.d. was obtained from Beckman Coulter Inc. (Brea, CA, USA). The functional monomer used in the current study, *N*-acryloxysuccinimide (NAS) was obtained from Acros Organics (Morris Plains, NJ, USA), the crosslinker ethylene glycol methacrylate (EDMA), the initiator 2,2'-azobis(isobutyronitrile) (AIBN) and the porogen toluene were purchased from Aldrich (Milwaukee, WI, USA). HPLC grade acetonitrile (ACN) was acquired from Pharmco-Aaper (Brookfield, CT, USA) and ethanolamine from Kodak Eastman (Rochester, NY, USA). Sodium chloride, calcium chloride dihydrate, manganese chloride hexahydrate, sodium phosphate monobasic monohydrate, sodium phosphate dibasic anhydrous and magnesium chloride were obtained from Fisher Scientific (Fair Lawn, NJ, USA). Tris(hydroxymethyl)aminomethane (Tris), *N*-acetyl-D-glucosamine were procured from Aldrich (Milwaukee, WI, USA). For conducting in-solution trypsin digestion, urea, dithiothreitol, iodoacetamide, sodium azide, trifluoroacetic acid (TFA), ammonium bicarbonate, and standard proteins (e.g., horse skeletal muscle myoglobin, equine heart cytochrome C (Cyt C), human IgG and transferrin) were purchased from Sigma (St Louis, MO, USA). The eluting sugars used in LAC, namely methyl-α-D-mannopyranoside (Me-α-Man) and lactose were purchased from Aldrich (Milwaukee, WI, USA). The four lectins, which are concanavalin A (Con A) from jack bean seeds, *Lens culinaris* agglutinin (LCA) from lentil seeds, *Ricinuss communis* I agglutinin (RCA) from castor bean seeds and *Sambucus nigra* agglutinin (SNA) from elderberry bark were

acquired from Vector Laboratories (Burlingame, CA, USA). Pooled breast cancer serum from six donors (stages, 2, 3 and 4) and pooled disease free human serum from six donors (same age group and race as the cancer serum) were purchased from Bioreclamation (Jericho, NY, USA).

Instrumentation and procedures

All HPLC separations were performed on a Waters Alliance 2690 HPLC separations module (Milford, MA, USA), equipped with an in-line degasser, a quaternary pump, an auto sampler and a thermostated column compartment. The data acquisition were carried out by using Empower 2 (Build 2154) software (Waters, Milford, MA, USA). The sample and the column compartments were maintained at ambient temperature. Detection was carried out on a PDA detector model W2990. The syringe pump, which was used to pump the reagents into the column at appropriate flow rates, was obtained from Cole-Parmer (Vernon Hills, IL, USA). A Rheodyne high-pressure injection valve (Rohnert Park, CA, USA) was used to by-pass the flow of the mobile phase into the enzyme reactor. Chromatographic data were processed by OriginPro v8.5.1 from Origin Lab Corp. (Northampton, MA, USA). Stock solutions of 1 mg/mL of each solute were dissolved in binding mobile phase and diluted to the desired concentrations in the mobile phase yielding adequate detector response. Water was filtered through a 0.45 μm membrane (Millipore, Bedford, USA) before use.

In-situ polymerization of NAS monolith (NASM)

As previously described in Chapter III, the base monolithic precursor poly (NAS-co-EDMA) (NASM) was prepared by *in situ* polymerization in a stainless steel column (25 cm x 1 mm i.d.) according to the following procedure. Briefly, the 25 cm column bearing end fittings was filled with the polymerization reaction mixture that was prepared by weighing the contents into a clean glass vial corresponding to a total weight of 0.5 g consisting of 18.0% (w/w) NAS as the functional monomer, 15.8% (w/w) EDMA as the crosslinker and 66.2 % (w/w) toluene as the porogen. The initiator AIBN 1% (w/w) with respect to the monomers, was added to the reaction mixture. The weight of AIBN was not taken into account while calculating the various percentages of the reaction mixture. The reaction mixture was shaken gently to dissolve the NAS and mildly degassed in a low power sonicator. The contents were then transferred to the column with a syringe fitted with an appropriate connection to the column. While passing the content, care was taken that all the fittings were properly sealed with no leaks. While injecting the reaction mixture, the column was vertical and the contents were injected against gravity to ensure proper filling of the column without any air bubbles. After filling with the reaction mixture, the column end fittings were sealed and the polymerization was carried out at 50 ˚C in a water bath for 15 h. After polymerization, the column was flushed with ACN to remove the porogens and the unreacted monomers. This was followed by equilibrating the column with one to two column volumes of toluene before proceeding to the post polymerization reaction.

Immobilization of proteins on NASM

All the post polymerization reactions were performed on the column by injecting the content into the column by means of a syringe pump. The 1 mm i.d. narrow-bore column HPLC, which was filled with NASM according to the above procedure described in the preceding section, was washed with water and 5 mM phosphate buffer for a brief period of time (1 to 2 column volumes), and then with 1 mL of a 10 mg/mL protein solution (trypsin/lectin) prepared in 20 mM phosphate buffer was injected for a period of 4 h. The lectin solutions were added with their corresponding hapten sugars in addition to the above-mentioned buffer. The lectins Con A and LCA were prepared with the above buffer with additional 0.1 M Me-α-Man and 1mM solutions of $CaCl_2$, $MgCl_2$ and $MnCl_2$. The lectin RCA and SNA were prepared with their hapten sugar lactose at 0.1 M concentration in the solution. Through its surface *N*-hydroxysuccinimide functional groups, proteins were immobilized *via* reaction with the primary amines provided by the side chain of lysine residues forming stable amide linkages. This is a straightforward approach, which involves no additional reagents. The residual succinimide groups of the column were then scavenged with 0.1 M ethanolamine/acetic acid buffer, pH 9.0. The reaction scheme is presented in Figure 3. As some of the proteins are heat sensitive, the entire setup was placed in a cold room, which was previously maintained at 4 ˚C. The columns thus prepared were stored in the binding buffer containing 0.02% NaN_3 while not in use.

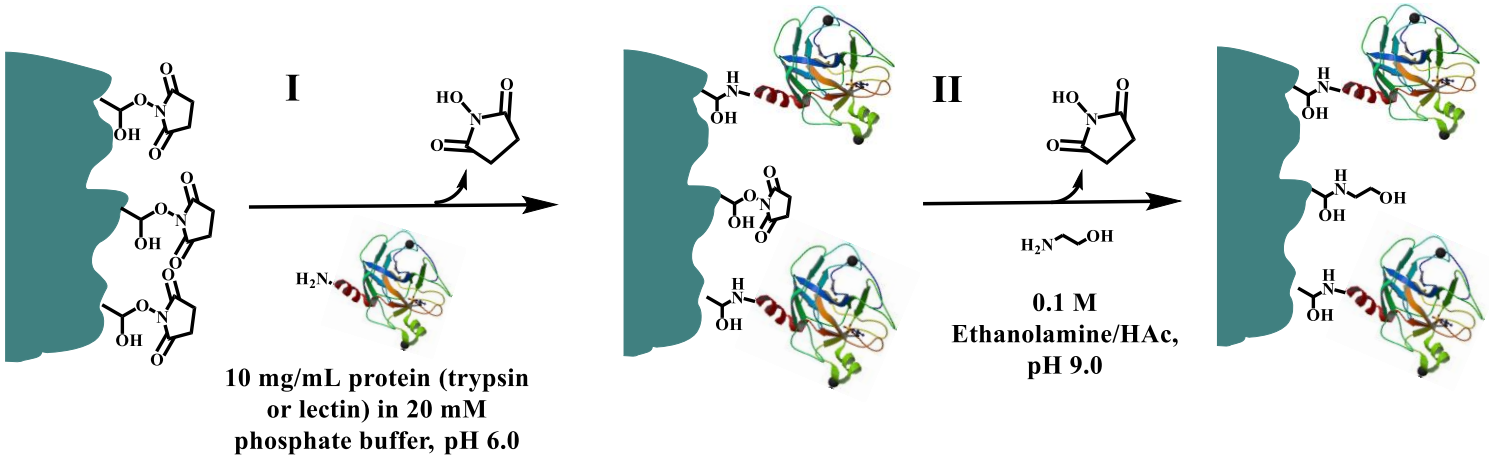

Figure 3. *Post polymerization of NASM with protein (e.g., trypsin/lectin) whereby it is illustrated in (I) the reaction of the amine group of the protein with the succinimide on the monolith surface forming stable amide linkages and in (II) the scavenging of the unreacted succinimide groups with ethanolamine.*

Online digestion of cytochrome C using NASM-trypsin immobilized enzyme reactor (IMER)

The chromatographic set-up for the on-line digestion of proteins using trypsin IMER is depicted in Figure 4. Two 2-way valves were connected before and after the IMER as shown in the figure. The valve before the IMER is used to regulate the flow of mobile phase in/out of the IMER and the one situated after IMER is connected to a 200-µL loop, which was used to collect the digest. The second valve is then connected to an RPC column for the online generation of the peptide map. The three solvent channels in the HPLC system were equilibrated with three solvents, namely, solvent A comprised of 25 mM $NH_4(HCO_3)$, pH 8.0, for the digestion of the proteins and solvents B and C containing 0.1% (v/v) TFA in 95:5 water:ACN and 95:5 ACN:water, respectively, for the gradient elution of the peptide map on the RPC column. The arrow in Figure 4 is to indicate the direction of the solvent flow. The protein to be digested, which was cytochrome C (Cyt C) was injected in appropriate amounts into the trypsin IMER. The digestion flow rate was 10 µL/min and it was carried out for about 20 min. The digest was collected in the 200-µL loop of valve II. Then, valve I was switched to the inject position and the gradient elution using solvents B and C started by-passing the IMER.

In solution digestion of cytochrome C

Cytochrome C was dissolved in approximately 100 µL of 6.0 M urea in a 1.5 mL plastic centrifuge tube. To this solution, 5 µL of reducing agent (200 mM dithioerythritol

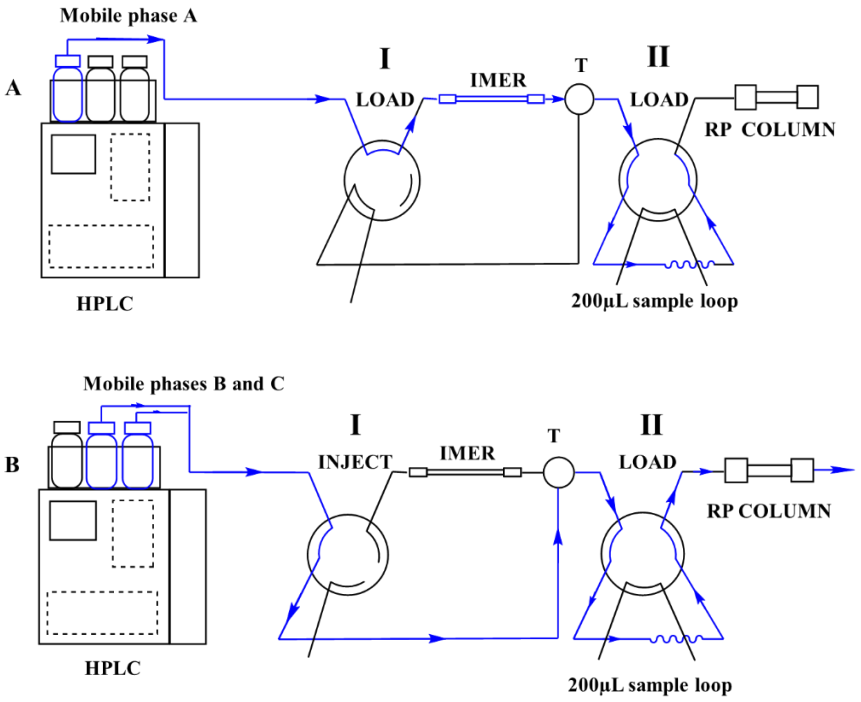

Figure 4. *Chromatographic set-up for the online digestion of proteins by NASM-trypsin IMER and RPC peptide mapping. A) For allowing digestion mobile phase to pass through the IMER, both switching valves are in load position, thus permitting the digestion of Cyt C and simultaneously the digest is collected in the 200 µL loop. B) The valve before the IMER is changed to inject position to by-pass the mobile phase from the IMER and facilitate the subsequent injection of the collected digest in the 200 µL loop into the RPC column to generate the peptide map. The arrows indicate the path of the mobile phase through the setup. Chromatographic conditions for online digestion: injection volume, 5µL; flow rate, 10 µL/min; digestion mobile phase (Solvent A), 25mM $NH_4(HCO)_3$, pH 8.0; digestion time, 20 min. Chromatographic conditions for peptide mapping: solvent B consists of 0.1% (v/v) TFA in 5% ACN; solvent C is made of 0.1% (v/v) TFA in 50% ACN; gradient conditions: two consecutive linear gradients from 0 to 60 %C in 20 min and then to 100% C in 5 min; flow rate, 1.0 mL/min.*

in 25 mM ammonium bicarbonate) were added, gently vortexed and incubated for 1 h at 37 ˚C in an oven. This was followed by the addition of 20 µl of alkylating reagent (200 mM iodoacetamide in 25 mM ammonium bicarbonate) and alkylation was carried out for 1 h at room temperature in the dark. Then, 20 µL of reducing reagent were added to consume any leftover of the alkylating reagent, which can in turn alkylate trypsin. This solution was diluted with 900 µL of 25 mM ammonium bicarbonate and the enzyme trypsin in the ratio of 1:30 to the approximate weight of protein was added to allow protein digestion overnight at 37 ˚C.

Fractionation of human serum glycoproteins by lectin affinity chromatography

A total of four lectin columns were prepared based on the procedures described in the preceding sections. They were NASM immobilized with LCA, Con A, RCA and SNA. Two different lectin column setups were used in the fractionation of human serum. In setup A, three different columns were arranged in tandem in the order of LCA → Con A → RCA to ensure the capture of the targeted glycoproteins. In setup B, only the column with immobilized SNA was used to capture the sialoglycoproteins (refer to Figure 5). The columns were equilibrated with the binding mobile phase consisting of 20 mM TrisHCl buffer containing 100 mM NaCl, 1 mM $MgCl_2$, 1 mM $MnCl_2$ and 1 mM $CaCl_2$, pH 7.4. In all experiments, serum was used in 1:3 dilution ratio and a total of 20 µL were injected into the lectin columns in both setups A and B. The unbound serum proteins were washed away with the binding mobile phase at a flow rate of 0.1 mL/min. The columns were washed sufficiently with the binding mobile phase for 1 h to remove proteins that were bound nonspecifically to the lectin columns. Then, the columns were

disassembled and each column was eluted with the eluting mobile phase containing its respective hapten sugar to elute out the bound glycoproteins. The bound glycoproteins on the LCA and RCA were eluted using 0.1 M Me-α-Man, and those bound to RCA and SNA were eluted with 0.1 M lactose (see the results and discussion for the detailed description of the experiments). The columns were again equilibrated with 10-20 column volumes of the binding mobile phase before injecting the next serum sample. This cycle was repeated 7 times and the fractions from the respective lectin columns were pooled into one vial and were concentrated by using a SpeedVac from Savant Instruments, Inc. (Holbrook, NY) and stored at -20 ˚C until conducting MS analysis.

Digestion of protein fractions by trypsin

For solution digests, the dried protein fractions were dissolved in 50 μL of solution containing 8 M urea, 100 mM Tris/HCl pH 8.5, 5 mM tris (2-carboxyethyl) phosphine and reduced at room temperature for 20 min. After incubation, 5 μL of 200 mM iodoacetamide was added, and the alkylation was allowed to proceed for 15 min in the dark at room temperature. The sample was then brought up to a total volume of 200 μL with 100 mM Tris/HCl, and digested with 4.0 μg/mL trypsin overnight at 37 ˚C. Digested samples were acidified with 1% (v/v) formic acid by adding 2 μL of formic acid to each of the 200 μL protein samples, and then purified by RPC using C18 affinity media (OMIX tips from Agilent Technologies, Santa Clara, CA, USA), and analyzed by MS.

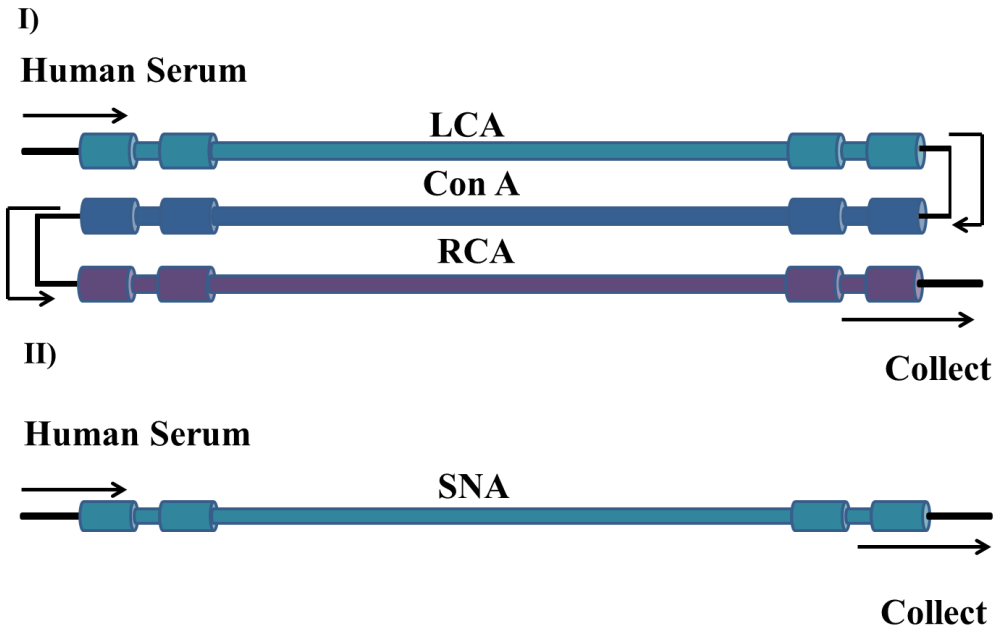

Figure 5. *Lectin affinity chromatography used for the capturing and enrichment of glycoproteins from human breast cancer and disease free sera. Two chromatographic setups are illustrated: I) Setup A, tandem lectin columns in the order of LCA → Con A → RCA. II) Setup B, SNA column.*

LC-MS/MS methodology

Samples were analyzed on a hybrid LTQ-Orbitrap mass spectrometer from Thermo Fisher Scientific, (Waltham, MA, USA) coupled to a New Objectives PV-550 nanoelectrospray ion source and an Eksigent NanoULC chromatography system. For chromatography, peptides were injected onto 5 cm pre-column packed in house with 3 µm Magic C18 AQ beads using vented column configuration, followed by analytical separation on a New Objective 40 cm × 75 µm ID fused silica column with an integral fused silica emitter, packed in house with 3 µm Magic C18 AQ beads. Peptides were eluted using a 5-40% ACN/0.1% formic acid gradient performed over 110 min at a flow rate of 250 nL/min.

During elution, samples were analyzed using Big Six methodology, consisting of one full-range FT-MS scan (nominal resolution of 60,000 FWHM, 300 to 2000 *m/z*) and six data-dependent MS/MS scans performed in the linear ion trap. MS/MS settings used a trigger threshold of 8,000 counts, monoisotopic precursor selection, and rejection of parent ions that had unassigned charge states, were previously identified as contaminants on blank gradient runs, or that had been previously selected for MS/MS (dynamic exclusion at 150% of the observed chromatographic peak width).

LC-MS/MS data analysis

Mascot search engine. Centroided ion masses were extracted using the extract_msn.exe utility from Bioworks 3.3.1. All MS/MS samples were analyzed using Mascot v2.2.04 from Matrix Science (London, UK). Mascot was set up to search the

UniProt_Human_plus_040813 database assuming the digestion enzyme trypsin. Mascot was searched with a fragment ion mass tolerance of 0.60 Da and a parent ion tolerance of 5-10 ppm. Gln->pyro-Glu of the N-terminus, oxidation of methionine, formyl of the N-terminus, acetyl of the N-terminus and acrylamide adducts of cysteine were specified in Mascot as a variable modification.

Scaffold (version Scaffold_4) from Proteome Software (Portland, OR, USA) was used to validate MS/MS-based peptide and protein identifications. Peptide identifications were accepted if they could be established at ≥ 95% probability as specified by the Peptide Prophet algorithm. Protein identifications were considered if they could be established at ≥ 99% probability and contained at least 2 unique identified peptides. Protein probabilities were assigned by the Protein Prophet algorithm. Proteins that contained similar peptides and could not be differentiated based on MS/MS analysis alone were grouped to satisfy the principles of parsimony. The search was performed against a decoy or reversed database and the false rate discovery was calculated using the count of decoy database identifications. The false rate discovery was 0% for protein and peptide identifications.

Label free quantification (LFQ). The MS/MS raw files from LTQ Orbitrap were analyzed with MaxQuant (v1.5.3.30) using default settings for the Andromeda search engine. The identification was done using a 1% false discovery rate (FDR) against Uniprot databases (downloaded from http://www.uniprot.org/) and were used together with the contaminant databases that contained sequences of common contaminants. Trypsin/P was selected as the digestive enzyme with other settings including two

potential missed cleavages, parent ion tolerance of 20 ppm, fragment ion tolerance of 0.5 Da and carbamidomethyl (C) was set as a fixed modification.

Filtering and further bioinformatics analysis of the MaxQuant/Andromeda workflow output and the analysis of the abundance of the identified proteins were performed with the Perseus (v1.5.2.6) module (available at the MaxQuant suite). Reversed hits and potential contaminants were deleted from the MaxQuant result table. Relative protein quantitation of cancer to disease free serum was done by applying a binary logarithm to the ratio of the LFQ peak intensities of cancer vs disease free serum. Total non-normalized protein intensities were corrected for the number of measurable tryptic peptides (intensity-based absolute quantification intensity), and after taking the binary logarithm were used for plotting the y-axis in a protein ratio versus abundance plot. Both the Q-Q plots and the scatter plots were plotted in OriginPro v8.5.1.

Results and discussion

On-line digestion of a standard protein using trypsin IMER and its comparison with in-solution digestion

The NASM narrow bore column format (1 mm i.d.) with surface immobilized trypsin was exploited in the proteolytic digestion of a typical standard protein, namely Cytochrome C (Cyt C). Monoliths in general which are known to have interconnected networks (macropores) with small microglobules (mesopores) [19, 20] should in principle provide the perfect media for fast mass transfer and in turn immobilized enzymatic sites, e.g., immobilized trypsin, should result in an effective proteolytic digestion of a given protein. For demonstrating the digestion efficiency of the trypsin-

IMER under investigation, Cyt C of M_r 12.4 kDa was chosen for assessing the online enzymatic digestion of protein. Cyt C contains 104 amino acids with 20 trypsin cleavage sites (http://web.expasy.org/peptide_cutter/). To perform the on-line digestion, Cyt C was dissolved in an appropriate amount in the digestion mobile phase which was 25 mM $NH_4(HCO_3)$, pH 8.0. The IMER was equilibrated with the digestion mobile phase, which was connected between the two 2-way valves. For the instrumental set-up refer to Figure 4. The first valve was kept in the "load" position to direct the digestion mobile phase into the IMER and then to reach the 200µL loop which was connected to the

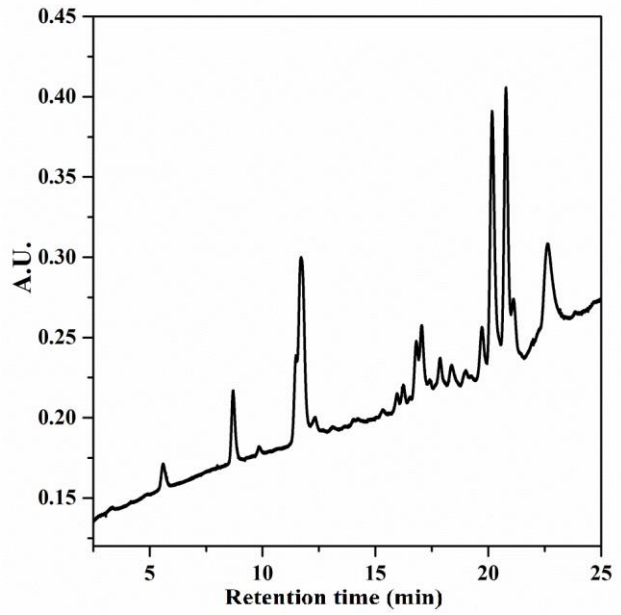

Figure 6. *IMER digestion of Cyt C. Conditions: Mobile phase for digestion, 25 mM $NH_4(HCO_3)$, pH 8.0; injection volume, 5 µL (4.0 mg/mL); flow rate, 10 µL/min; time 20 min. For peptide mapping by RPC, mobile phase B, 0.1 % (v/v) TFA in 95:5 water:ACN; mobile phase C, 0.1 % (v/v) TFA in 50:50 water:ACN; two consecutive linear gradients from 0 to 60 %C in 20 min and then to 100 %C in 5 min; flow rate, 1.0 mL/min, UV detection at 214 nm.*

second valve. At this point the RPC column, which was previously equilibrated with the mobile phase B consisting of 0.05% TFA in 95:5 (v/v) water:ACN was connected. Cyt C was injected into the IMER and the digestion was carried out at a flow rate of 10 µL/min for about 20 min. The online integration of IMER with the RPC column demonstrates the minimum operator intervention and a straightforward workflow. After the completion of the digestion, the first valve was switched to the "inject" position, which by-passed the IMER from the RPC mobile phase. Now, a gradient program was applied with the following two solvents: B consisting of 0.1% (v/v) TFA in 95:5 (v/v) water:ACN and C composed of 0.1% (v/v) TFA in 50:50 (v/v) water:ACN. For more details about the mobile phase compositions and the flow of the mobile phases (indicated by an arrow), refer to Figure 4. The gradient flow was by-passed from the IMER to prevent the immobilized trypsin from coming in contact with ACN. The peptide map thus obtained is represented in Figure 6. A two-step gradient covering 0-60% of C in 20 min and 60-100% of % C in 5 min was applied at a flow rate of 1.0 mL/min. To evaluate the digestion efficiency of the IMER, an off-line digestion with trypsin in-solution was performed and the obtained peptide map was compared to that generated from the trypsin IMER. The in-solution digestion was performed according to the standard protocol as described above in the experimental section. The chromatograms obtained with undigested Cyt C, and digested Cyt C by IMER and in-solution are presented in Figures 7 A, B and C, respectively. From the 20 cleavage sites available for trypsin on Cyt C, 21 peptides were generated of which 15 peptide fragments contained 2 or more amino acids. When the peptide maps generated by IMER and in-solution digestion were carefully

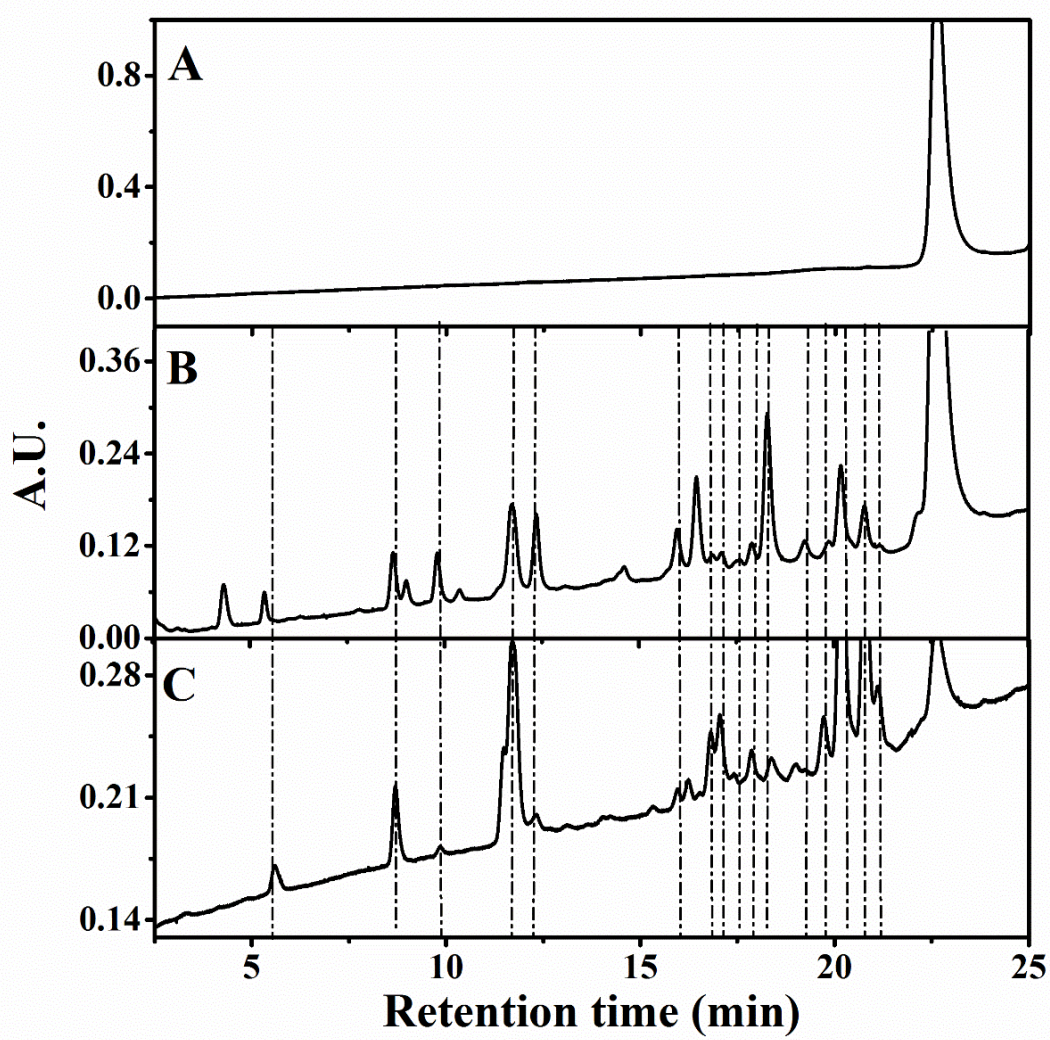

Figure 7. *Comparison of peptide maps obtained by online and in-solution digestion of Cyt C, A) Cyt C undigested; injection volume, 20 µL (1 mg/min), B) Cyt C in-solution digestion; injection volume, 20 µL (1 mg/min), C) Cyt C on-line digestion by single pass µIMER for 20 min; injection volume, 5 µl (4.0 mg/mL); For other chromatographic conditions refer to Figure 6)*

inspected, the number of peaks that were common to both maps has been found to be 15 peaks which are indicated by dotted lines in Figure 7 and the unique peaks that were generated (other than the common peaks) might be due to the non-specific cleavages. The

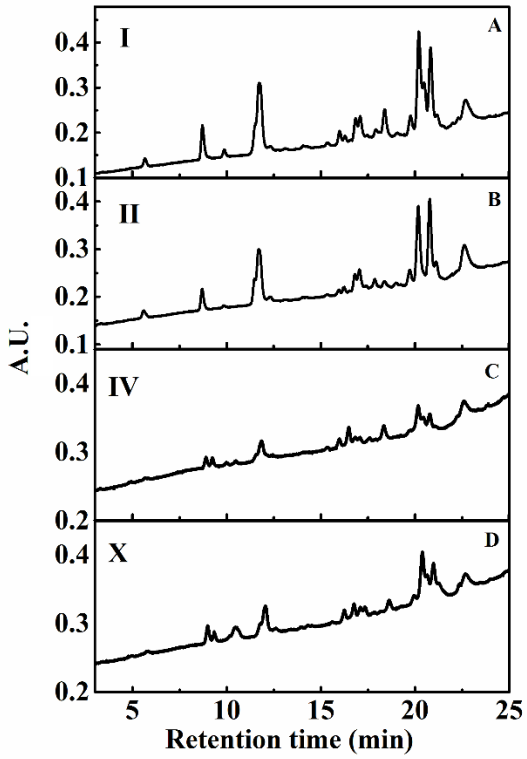

Figure 8. *Peptides maps showing the repeatability and reusability of the trypsin IMER. Amount of Cyt C injected (A) 30 µL (2. mg/mL), (B) 5 µL (4. mg/mL), (C) and (D) 1 µL (2. mg/mL); For mobile phase for digestion and peptide mapping refer to Figure 6. The reusability was demonstrated by using one IMER for over X digestions spanning over 6 days, where column was stored with digestion buffer with 0.02% NaN_3 at 4 °C.*

peptide map obtained from in-solution digestion generated more non-specific cleavages (see Figure 7B) than the one obtained from online digestion by the IMER (see Figure 7C). This can be attributed to the digestion time of the protein with the trypsin, which is 20 min in IMER to one day for in-solution digestion. Also, the immobilized enzyme is known to be more tolerant to the denaturing agents that are added to the proteins [21].

To test the repeatability and the reusability of the trypsin IMER, the on-line digestion was repeated ten times for a span of 6 days. After each digestion the IMER was equilibrated with 0.02% NaN_3 in the digestion buffer and stored at 4 ˚C until the next digestion. Figure 8 shows the repeatability and the reusability study of the IMER, which clearly demonstrates that the activity of the enzyme trypsin is intact and can be used for many more digestions. Different concentrations of the Cyt C were injected to test the sensitivity of the IMER and the peptides that were generated at different concentration ranges of injected Cyt C, and the results are shown in Figure 8. The peptide maps in Figures 8A and B were generated from different injection volumes of Cyt C, namely, 30 µL (0.66 mg Cyt C/mL) and 5µl (4.0 mg Cyt C /mL), respectively. The profiles of the eluted peptides were similar in both chromatograms. In the case of the peptide maps shown in Figure 8(C) and (D), a dilute concentration of 1 µL (2.0 mg Cyt C/mL) was used. For all the peptide maps, the calculated peak areas of the undigested Cyt C peaks were less than 5%, which indicates that the prepared narrow bore IMERs provided high digestion efficiency at various injected concentrations of the protein under investigation.

Evaluation of NASM columns with immobilized lectins

The lectins, namely LCA, Con A, RCA and SNA under investigation were immobilized onto the monolithic support according to the experimental procedure described in the preceding sections. In the immobilization process of lectins onto the surface of the monolith, their corresponding sugars were added to the reaction solution in order to preserve the sugar-binding site of the lectin. The pore size of the NASM column

onto which the lectins were immobilized seems to accommodate large biomolecules such as the used lectins.

The lectin columns, namely, Con A, LCA, RCA and SNA thus prepared were evaluated for their nonspecific and specific binding towards proteins. Different standard glycoproteins and non-glycoproteins were used in these assessments. The nonspecific binding nature of all the lectin columns was tested with myoglobin, which is a known standard non-glycoprotein. All the columns showed no binding towards myoglobin, which was eluted at t_0 (chromatograms not shown). The Con A column, which is known to have an affinity towards high-mannose type glycans retained the fraction of ribonuclease B (refer to Figure 9) that is rich in high mannose glycans. On the other hand, a small fraction of ovalbumin was retained on the Con A column indicating that this fraction has surface bound hybrid type glycans (see Figure 9B). In the Con A column, 0.1 M Me-α-Man hapten sugar was used in the eluting mobile phase to displace the bound glycoproteins. For the binding and eluting mobile phases, refer to the respective figure legends. When human IgG was injected on the NASM-LCA column, a portion of the injected IgG showed affinity toward immobilized LCA, which was eluted with 0.1 M Me-α-Man (see Figure 10A). The NASM-RCA showed similar behaviors when tested with human transferrin whereby some of the glycoproteins were bound to the lectin and eluted upon applying the eluting mobile phase consisting of 0.1 M lactose (see Figure 10B). Finally, the NASM-SNA column was tested with human IgG, which showed affinity towards a fraction of the injected sample that was eluted by using 0.1 M lactose in the eluting mobile phase as shown in Figure 11.

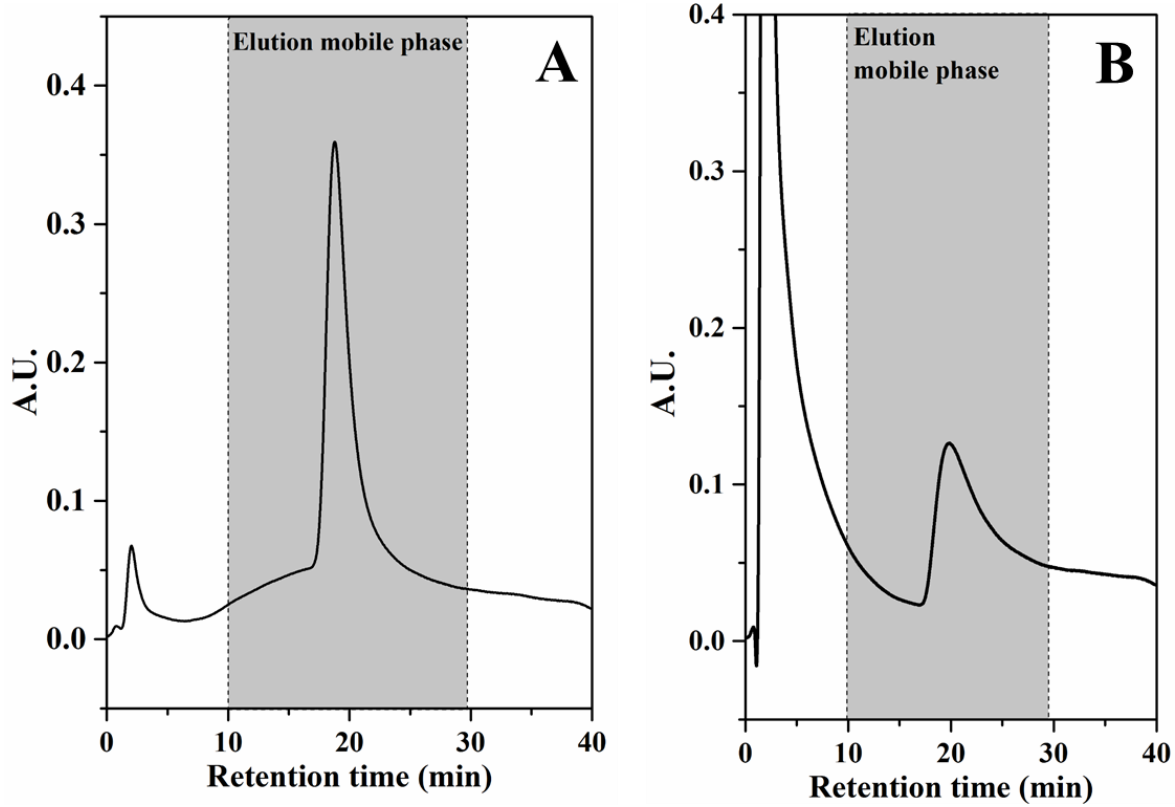

Figure 9. *Chromatograms of ribonuclease B (A) and ovalbumin (B) obtained on the NASM-Con A column (21.5 cm x 1 mm i.d.). Binding mobile phase, 20 mM Tris HCl buffer, pH 7.4, containing 100 mM NaCl and 1mM Ca^{2+}, Mg^{2+} and Mn^{2+}; eluting mobile phase, 0.1 M Me-α-Man in the binding mobile phase; flow rate, 0.1 mL/min; wavelength, 214 nm, elution mobile phase is indicated by the gray region.*

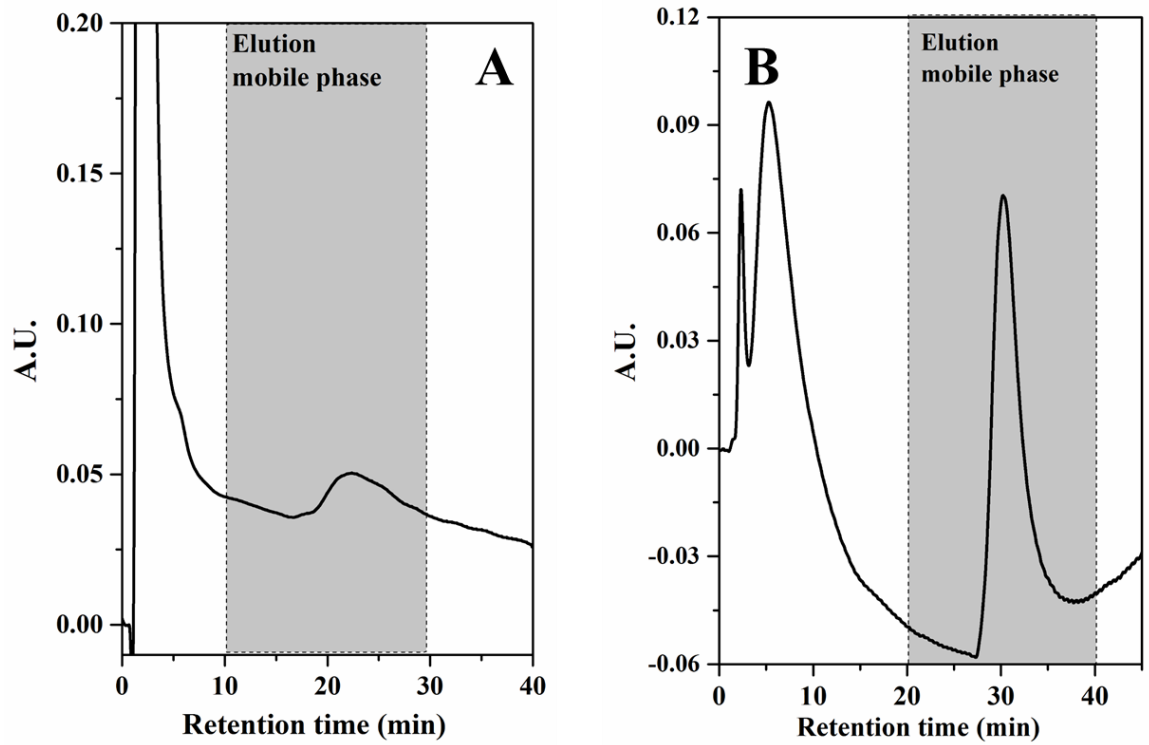

Figure 10. *(A) Chromatogram of IgG obtained on NASM-LCA (21.5 cm x 1 mm i.d.). Binding mobile phase, 20 mM Tris HCl buffer, pH 7.4, containing 100 mM NaCl and 1mM Ca^{2+}, Mg^{2+} and Mn^{2+}; eluting mobile phase, 0.1 M Me-α-Man in the binding mobile phase; flow rate, 0.1 mL/min; wavelength, 280 nm. (B). Chromatogram of human transferrin obtained on NASM-RCA (25.0 cm x 1 mm i.d.). Binding mobile phase, 20 mM Tris HCl buffer, pH 7.4, containing 100 mM NaCl; eluting mobile phase, 0.1 M Lactose in the binding mobile phase; flow rate, 0.1 mL/min; wavelength, 214 nm, elution mobile phase is indicated by the gray region.*

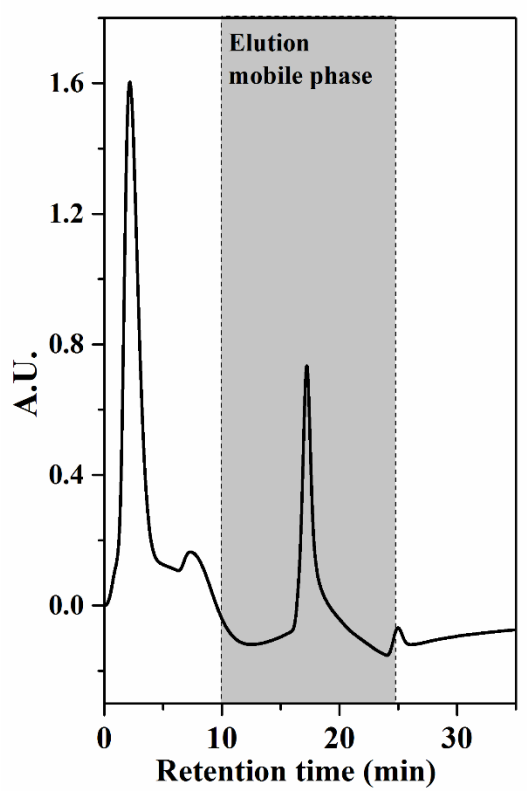

Figure 11. *Chromatogram of IgG obtained on NASM-SNA (21.5 cm x 1 mm i.d.). Binding mobile phase, 20 mM Tris HCl buffer, pH 7.4 , containing 100 mM NaCl and 1 mM Ca^{2+}, Mg^{2+} and Mn^{2+}; eluting mobile phase, 0.1 M Lactose + 0.1 % acetic acid in the binding mobile phase; flow rate, 0.1 mL/min; wavelength, 280 nm, elution mobile phase is indicated by the gray region*

On-line capturing of serum glycoproteins from breast cancer and disease free sera

The glycoproteins from the cancerous serum and disease free serum were captured using the setups A and B as described in the experimental section. Figures 12 and 13 represent the chromatograms obtained for the breast cancer serum by setups A and B, respectively. The unbound fractions are shown in Figure 12 A, and 13A, where a large portion of the proteins was eluted out from the column, which was sufficiently equilibrated and run with the binding mobile phase to ensure that proteins were not bound *via* nonspecific interactions. Then, the columns were disassembled and the specifically bound glycoproteins were eluted out from each column by passing the eluting mobile phase containing their respective hapten sugars. The glycoproteins eluted from LCA, Con A, RCA and SNA are shown in Figure 12B, C and D and in Figure ***13***B, respectively, which correspond to the breast cancer serum. The intensity of the eluted glycoprotein peaks from the LCA and SNA columns were lower than those eluted from Con A and RCA. This may be attributed to the difference in the range of glycoprotein recognitions of each corresponding lectin. Similarly, disease free serum was subjected to glycoprotein extraction by chromatographic setups A and B and their unbound serum fractions are shown in Figure 14A and 15A, respectively, while glycoproteins from the disease free serum that eluted from LCA, Con A, RCA and SNA are shown in Figure 14B, C, D and 15B, respectively. The pooled fractions from each lectin column were concentrated along with the eluted sugars and the protein pellets thus obtained were subjected to trypsin digestion followed by MS analysis. As the intensity of the glycoprotein fractions obtained from the SNA column for both breast cancer and healthy sera were lower than

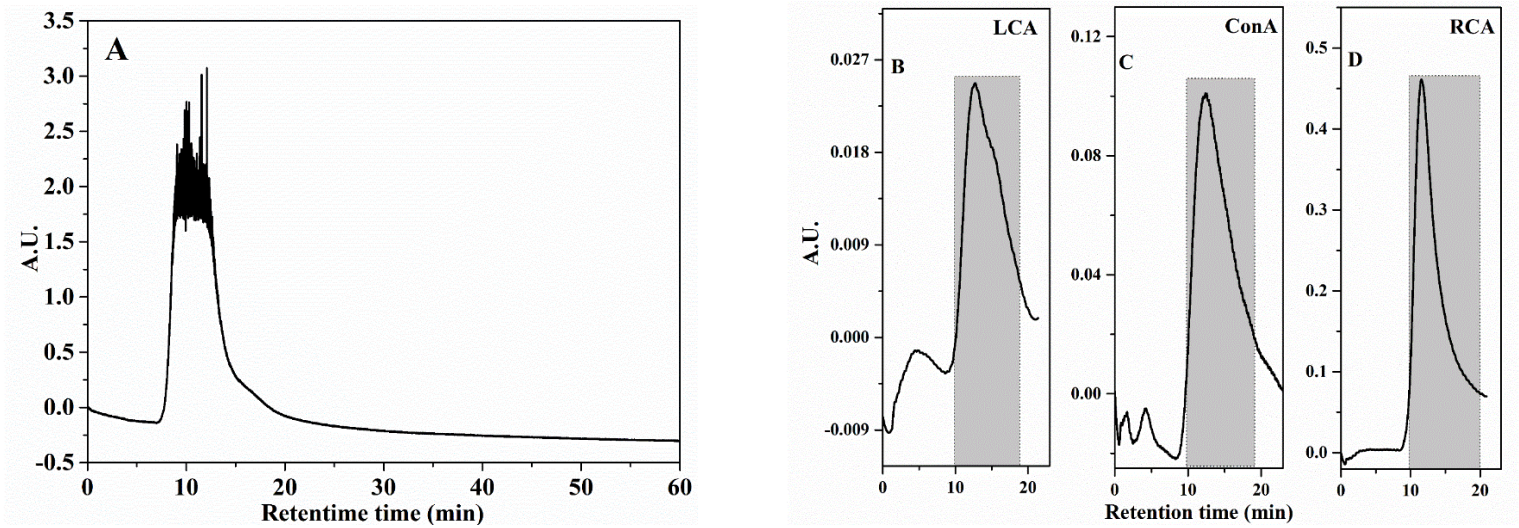

Figure 12. *Chromatograms showing the capturing of glycoproteins from the breast cancer serum. A) Unbound serum proteins from the tandem lectin columns shown in Figure 5(I)). After passing the binding mobile phase, the lectin columns were disassembled and eluted with their respective hapten sugars to displace the bound proteins. Chromatograms B, C and D are from the lectin columns LCA, Con A and RCA, respectively. The gray regions indicate the collected fractions.*

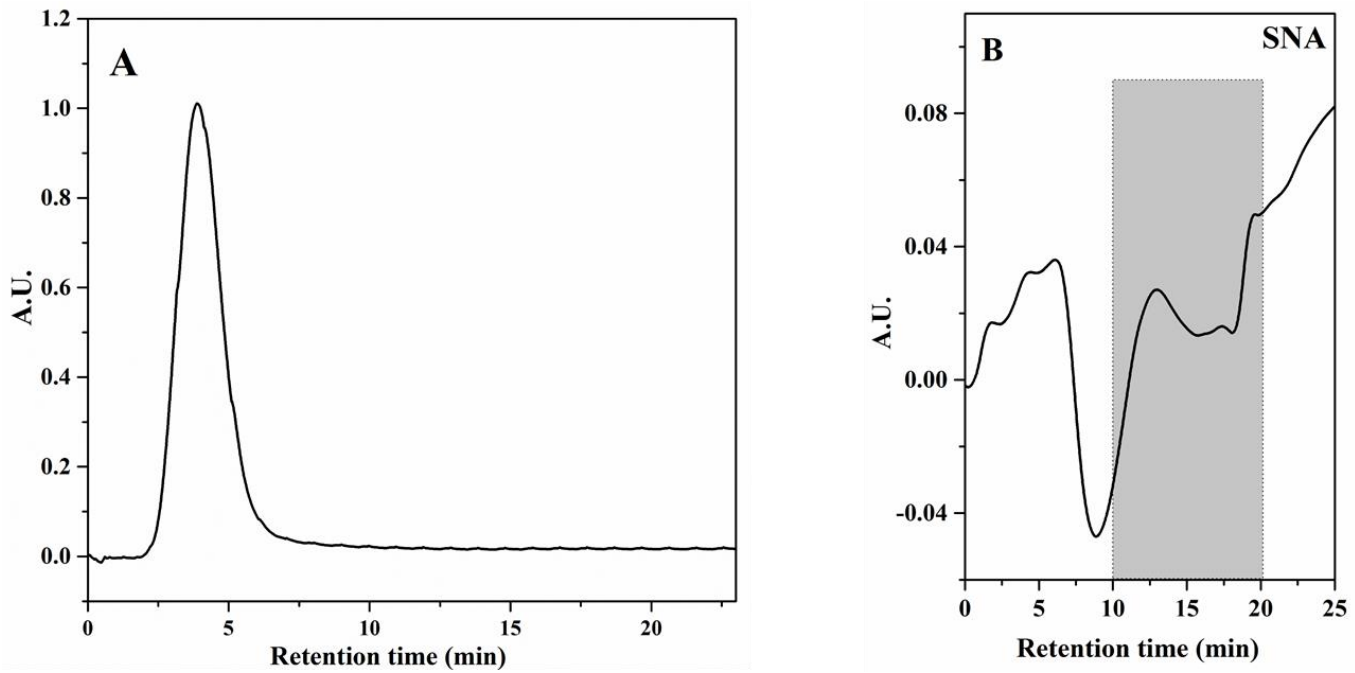

Figure 13. *Chromatograms showing the capturing of glycoproteins from the breast cancer serum on the SNA column. A) Unbound serum proteins from the lectin column shown in Figure 5(II)). After passing the binding mobile phase, the lectin column was eluted with its hapten sugar consisting of 0.1 M lactose to displace the bound proteins. The eluted glycoproteins are shown in chromatogram B. The gray region indicates the collected fraction.*

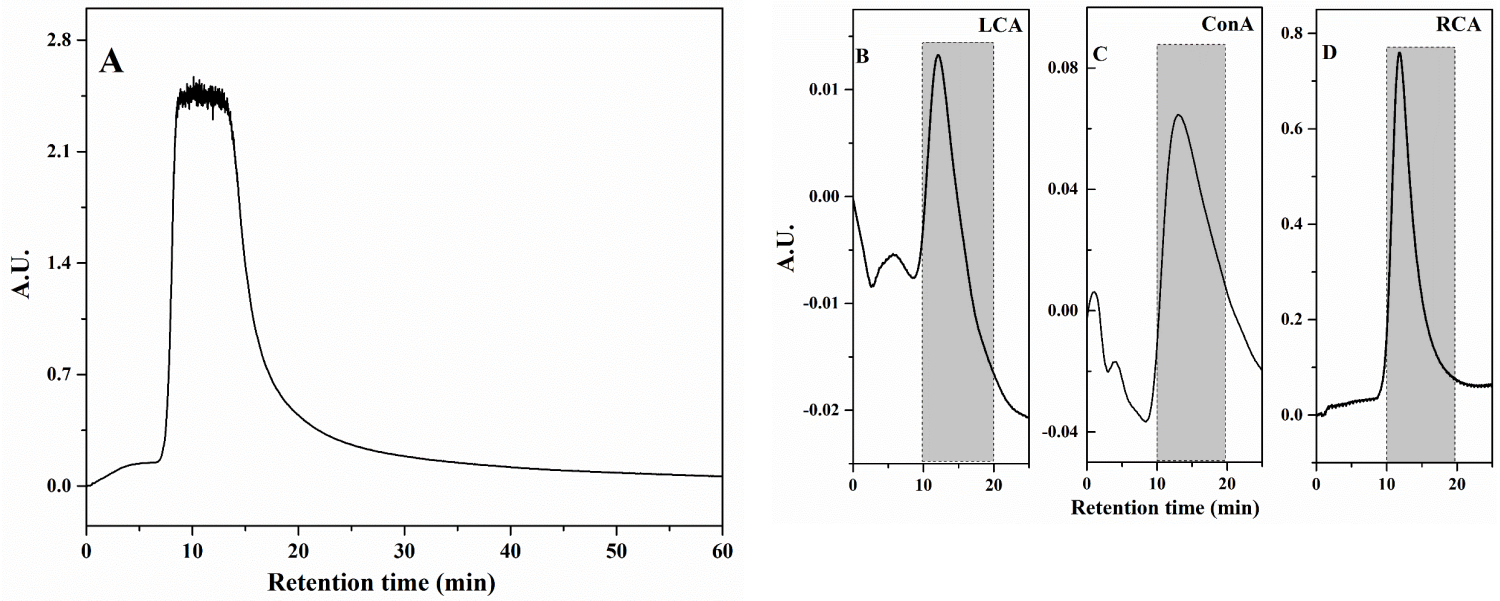

Figure 14. *Chromatograms showing the capturing of glycoproteins from the disease free serum. A) Unbound serum proteins from the tandem lectin columns shown in Figure 5(I)). After passing the binding mobile phase, the lectin columns were disassembled and eluted with their respective hapten sugars to displace the bound proteins. The chromatograms B, C and D are from the lectin columns LCA, Con A and RCA, respectively. The gray regions indicate the collected fractions.*

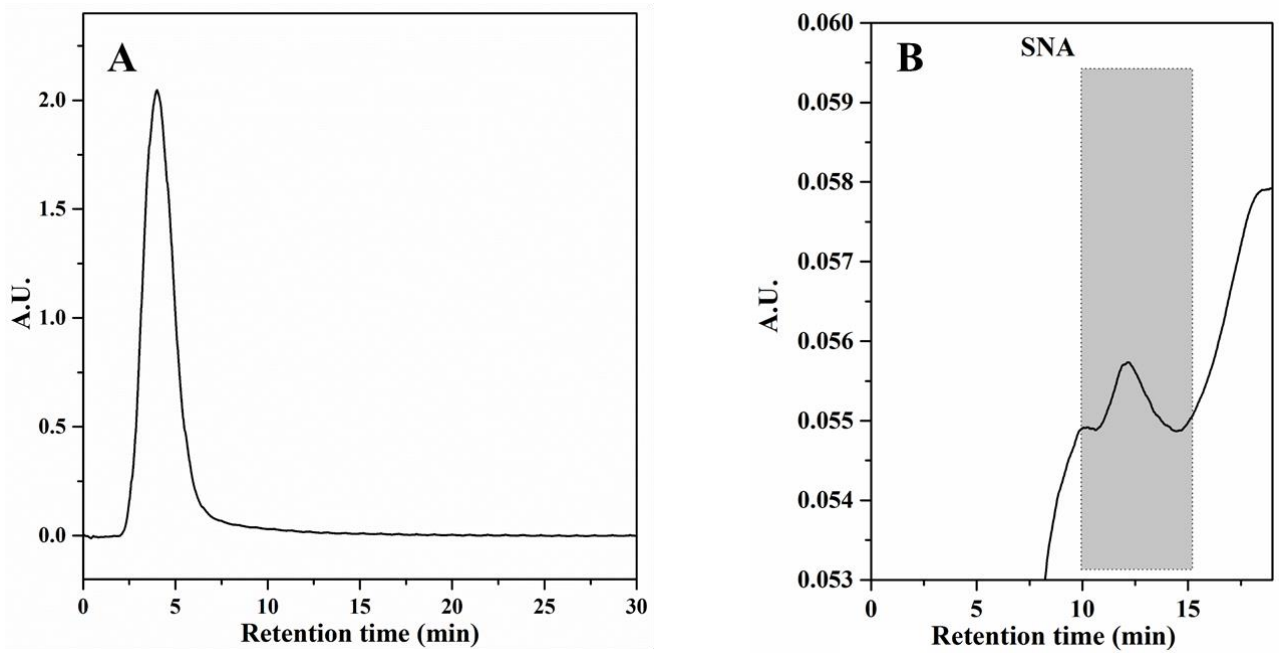

Figure 15. *Chromatograms showing the capturing of glycoproteins from the disease free serum on the SNA column. A) Unbound serum proteins from the lectin column shown in Figure 5(II)). After passing the binding mobile phase, the lectin column was eluted with its hapten sugar consisting of 0.1 M lactose to displace the bound proteins. The eluted glycoproteins are shown in chromatogram B. The gray region indicates the collected fraction.*

those from other columns, the protein fractions were purified by reversed phase extraction on a C4 column to remove the sugars and the dissolved salts.

LC-MS/MS analysis of the lectin enriched fractions from cancer and disease free sera

The proteins captured by each lectin column were subjected to LC-MS/MS analysis as described in the experimental section (see LC-MS/MS methodology and the data analysis sections). Only proteins that exhibit protein and peptide identification probability of at least 99.9% and 95%, respectively, and containing at least three unique peptides were considered (see Table 1 for the total list of identified proteins). A total of 76 non-redundant proteins in both cancer and disease free sera were identified. The LCA column captured a total of 59 and 33 proteins from cancer and healthy sera, respectively, of which 33 proteins are common to both sera. This indicates that no unique proteins were detected in the disease free serum in the case of LCA column captured proteins. These results may signal the absence of core fucosylated glycoproteins that are unique to the disease free serum. Similarly, a total of 69 proteins were identified for both cancer and healthy sera in the Con A column captured fraction, of which 65 proteins are common to both the cancer and healthy sera, which represent the total mannome and the hybridome of both types of sera. Since, mannome and hybridome generally do not represent any cancerous activity, they are equally expressed in both cancer and healthy sera. For the RCA column a total of 69 and 74 proteins were identified for cancer and healthy sera, respectively, with 68 proteins being common for both sera and these represent the total glycoproteins with branched glycome. Finally, SNA column captured a total of 22 and 36 proteins from cancer and healthy sera, respectively, with 21 proteins

being common for both cancer and healthy sera, which represent the total sialoglycoprotein components of both sera.

Likewise, the raw data from the MS analysis were analyzed by the MaxQuant bioinformatics tool (see experimental) and the LFQ peak areas were calculated for the proteins captured by each lectin column and their binary logarithms are listed in Table 2. A total of 64 proteins were identified for all the lectin columns of which 46 proteins were non-redundant proteins. A total of 9 fucosylated proteins are identified in the LCA column captured fraction by using the LFQ approach. Literature search indicated that all of these proteins were previously reported as core fucosylated [22-24], expect for the Ig kappa chain C region, which is a non-glycoprotein. These results indicate the validity of the LFQ approach in the identification of proteins. The Con A column captured 30 proteins which covers the mannome and hybridome of the serum glycoproteins in both the cancer and disease free serum. The 'branched glycome', which was captured by the RCA column consisted of 29 glycoproteins. Finally, the SNA column captured 3 proteins which represent the sialoglycoproteins in both cancer and disease free sera. Data on fucosylation, core fucosylation and sialylation of each protein are reported in Table 2, which were obtained from previously reported publications [22-29].

The variations in the data generated by Mascot and MaxQuant proteomic software for each lectin column were evaluated and the Venn diagrams representing the corresponding proteins observed in the two-different software are shown in Figure 16. For the LCA column, the Ig mu chain C region is the only protein, which is uniquely identified by MaxQuant and the remaining 8 proteins were common for both Mascot and MaxQuant searches. For the Con A column, 21 proteins are commonly identified in both

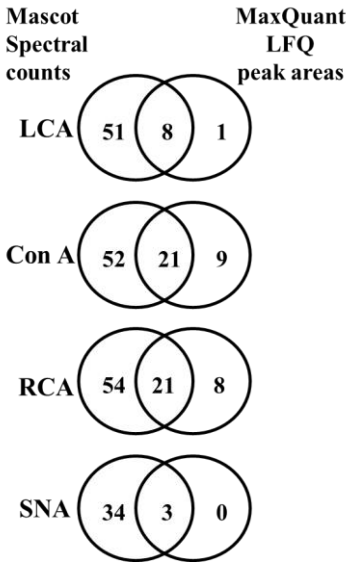

Figure 16. *Comparison of total proteins observed using Mascot and MaxQuant proteomic software.*

Mascot and MaxQuant searches, and 52 and 9 proteins are uniquely identified by Mascot and MaxQuant searches, respectively. Of all the proteins that are uniquely identified by MaxQuant, the majority of glycoproteins are found to contain either core fucosylated or fucosylated glycans. This indicates the enhanced quality of data obtained from MaxQuant. In the case of the RCA column, 21 proteins were identified by both searches and 54 and 8 proteins are uniquely identified by Mascot and MaxQuant searches, respectively. Finally, for the SNA column, no unique glycoproteins were observed using MaxQuant proteomic software, but Mascot search engine generated about 34 proteins and 3 proteins common for both the Mascot and MaxQuant programs. Though the MaxQuant generated fewer proteins when compared to Mascot proteomic software, the majority of proteins generated by MaxQuant were observed to be glycoproteins which had fucosylated, core fucosylated or sialylated glycans (see Table 2).

TABLE 1

LIST OF PROTEINS IDENTIFIED IN THE LECTIN BOUND FRACTIONS AND THEIR SPECTRAL COUNTS

#	*Identified proteins*	*Accession number*	*Mol. Wt.*	*Average spectral counts for breast cancer serum proteins*				*Average spectral counts for disease free serum proteins*			
				LCA	*Con A*	*RCA*	*SNA*	*LCA*	*Con A*	*RCA*	*SNA*
1	Afamin	AFAM_HUMAN	69 kDa	0	1	6	0	0	2	6	0
2	Alpha-1-acid glycoprotein 1	A1AG1_HUMAN	24 kDa	0	0	12	0	0	0	7	0
3	Alpha-1-acid glycoprotein 2	A1AG2_HUMAN	24 kDa	0	0	8	0	0	0	3	0
4	Alpha-1-antichymotrypsin	AACT_HUMAN (+1)	48 kDa	0	1	8	0	0	4	7	0
5	Alpha-1-antitrypsin	A1AT_HUMAN	47 kDa	3	11	20	0	0	11	26	2
6	Alpha-1B-glycoprotein	A1BG_HUMAN	54 kDa	0	5	7	0	0	2	3	0
7	Alpha-2-macroglobulin	A2MG_HUMAN	163 kDa	45	106	67	0	14	80	72	8
8	Alpha-S1-casein	CASA1_BOVIN	25 kDa	0	0	0	0	0	0	8	0
9	Angiotensinogen	ANGT_HUMAN	53 kDa	0	2	5	0	0	1	5	0
10	Antithrombin-III	|ANT3_HUMAN (+1)	53 kDa	0	2	9	0	0	2	10	0
11	Apolipoprotein A-I *	APOA1_HUMAN	31 kDa	8	10	13	0	0	6	15	0
12	Apolipoprotein B-100	APOB_HUMAN	516 kDa	48	22	8	0	2	55	9	0
13	Beta-2-glycoprotein 1	APOH_HUMAN	38 kDa	5	16	6	0	1	8	1	0

#	*Identified proteins*	*Accession number*	*Mol. Wt.*	*Average spectral counts for breast cancer serum proteins*				*Average spectral counts for disease free serum proteins*			
				LCA	*Con A*	*RCA*	*SNA*	*LCA*	*Con A*	*RCA*	*SNA*
14	Carboxypeptidase N subunit 2	CPN2_HUMAN	61 kDa	0	0	4	0	0	0	6	0
15	Cationic trypsin, Alpha-trypsin chain 1	TRY1_BOVIN	26 kDa	2	0	0	0	0	0	0	2
16	CD5 antigen-like	CD5L_HUMAN	38 kDa	7	5	5	0	1	6	5	0
17	Ceruloplasmin	CERU_HUMAN	122 kDa	0	2	35	0	0	2	24	0
18	Coagulation factor XII	FA12_HUMAN	68 kDa	0	4	0	0	0	5	0	0
19	Complement C1s subcomponent	C1S_HUMAN	77 kDa	2	2	1	0	0	2	5	0
20	Complement C3	CO3_HUMAN	187 kDa	12	120	3	0	0	102	10	9
21	Complement C4-A	CO4A_HUMAN	193 kDa	17	39	5	0	1	37	5	1
22	Complement component C6	CO6_HUMAN	105 kDa	0	7	0	0	0	2	0	0
23	Complement component C8 alpha chain	CO8A_HUMAN	65 kDa	2	2	0	0	0	6	0	0
24	Complement factor B	B4E1Z4_HUMAN	141 kDa	8	32	14	0	0	35	17	0
25	Complement factor H	CFAH_HUMAN	139 kDa	28	25	1	0	1	19	0	0
26	Complement factor I	CFAI_HUMAN (+2)	66 kDa	0	10	2	0	0	6	6	0

#	*Identified proteins*	*Accession number*	*Mol. Wt.*	*Average spectral counts for breast cancer serum proteins*				*Average spectral counts for disease free serum proteins*			
				LCA	*Con A*	*RCA*	*SNA*	*LCA*	*Con A*	*RCA*	*SNA*
27	Cytochrome c	CYC_HORSE	12 kDa	0	0	0	47	0	0	0	15
28	Dermcidin	DCD_HUMAN	11 kDa	3	1	0	8	2	2	5	10
29	Desmoglein-1	DSG1_HUMAN	114 kDa	3	0	0	4	0	0	6	1
30	Desmoplakin	DESP_HUMAN	332 kDa	31	6	2	14	0	1	30	3
31	Ficolin-3	FCN3_HUMAN	33 kDa	6	0	0	0	4	3	0	0
32	Filaggrin *	FILA_HUMAN	435 kDa	1	0	0	3	0	0	2	4
33	Haptoglobin	HPT_HUMAN (+1)	45 kDa	11	47	63	0	3	32	61	0
34	Hemoglobin subunit alpha	HBA_HUMAN (+1)	15 kDa	0	3	14	0	0	0	6	0
35	Hemoglobin subunit beta	HBB_HUMAN (+1)	16 kDa	0	11	18	0	0	0	5	0
36	Hemopexin	HEMO_HUMAN	52 kDa	4	24	34	0	1	22	37	0
37	Heparin cofactor 2	HEP2_HUMAN	57 kDa	0	4	4	0	0	1	5	0
38	Hornerin	HORN_HUMAN	282 kDa	18	4	6	40	1	0	19	30
39	Ig alpha-1 chain C region	IGHA1_HUMAN	38 kDa	15	12	14	0	8	10	14	0

#	*Identified proteins*	*Accession number*	*Mol. Wt.*	*Average spectral counts for breast cancer serum proteins*				*Average spectral counts for disease free serum proteins*			
				LCA	*Con A*	*RCA*	*SNA*	*LCA*	*Con A*	*RCA*	*SNA*
40	Ig gamma-1 chain C region	IGHG1_HUMAN	36 kDa	14	10	14	0	6	8	18	4
41	Ig gamma-3 chain C region	IGHG3_HUMAN	41 kDa	10	10	9	0	6	11	10	3
42	Ig kappa chain C region	IGKC_HUMAN	12 kDa	9	7	11	0	3	5	12	6
43	Immunoglobulin lambda-like polypeptide 5	IGLL5_HUMAN	23 kDa	8	6	10	0	2	5	10	4
44	Inter-alpha-trypsin inhibitor heavy chain H1	ITIH1_HUMAN (+1)	101 kDa	2	12	8	0	0	10	5	0
45	Inter-alpha-trypsin inhibitor heavy chain H2	ITIH2_HUMAN (+1)	106 kDa	0	9	17	0	0	7	5	0
46	Isoform 10 of Fibronectin	FINC_HUMAN (+9)	240 kDa	5	28	4	0	0	10	1	0
47	Isoform 2 of Attractin	ATRN_HUMAN (+1)	141 kDa	0	6	3	0	0	6	6	0
48	Isoform 2 of Clusterin	CLUS_HUMAN	58 kDa	0	5	21	0	0	7	20	0
49	Isoform 2 of Ig mu chain C region	IGHM_HUMAN (+1)	52 kDa	26	24	23	0	10	23	23	6
50	Isoform 2 of Inter-alpha-trypsin inhibitor heavy chain H4	ITIH4_HUMAN (+4)	101 kDa	0	9	13	0	0	4	13	0
51	Isoform LMW of Kininogen-1	KNG1_HUMAN	48 kDa	1	1	17	0	0	3	10	0
52	Keratin, type I cytoskeletal 10	K1C10_HUMAN (+1)	59 kDa	50	38	31	57	23	21	43	39

#	*Identified proteins*	*Accession number*	*Mol. Wt.*	*Average spectral counts for breast cancer serum proteins*				*Average spectral counts for disease free serum proteins*			
				LCA	*Con A*	*RCA*	*SNA*	*LCA*	*Con A*	*RCA*	*SNA*
53	Keratin, type I cytoskeletal 14	K1C14_HUMAN	52 kDa	38	23	18	36	16	14	31	19
54	Keratin, type I cytoskeletal 16	K1C16_HUMAN	51 kDa	39	25	13	36	14	10	26	21
55	Keratin, type I cytoskeletal 17	K1C17_HUMAN	48 kDa	33	13	12	18	6	5	25	9
56	Keratin, type I cytoskeletal 9	K1C9_HUMAN (+1)	62 kDa	42	36	37	77	23	25	62	61
57	Keratin, type II cytoskeletal 1	K2C1_HUMAN (+1)	66 kDa	62	56	48	103	39	40	66	79
58	Keratin, type II cytoskeletal 2 epidermal	K22E_HUMAN (+1)	65 kDa	45	45	42	74	28	31	47	52
59	Keratin, type II cytoskeletal 5	K2C5_HUMAN	62 kDa	44	24	18	58	16	21	36	31
60	Keratin, type II cytoskeletal 6C	K2C6C_HUMAN	60 kDa	48	26	16	48	11	15	37	27
61	Keratin, type II cytoskeletal 78	K2C78_HUMAN	57 kDa	1	2	1	5	2	2	3	1
62	Keratinocyte proline-rich protein	KPRP_HUMAN	64 kDa	4	3	0	1	1	0	2	2
63	Leucine-rich alpha-2-glycoprotein	A2GL_HUMAN	38 kDa	0	0	7	0	0	0	2	0
64	Lysozyme C	LYSC_CHICK	16 kDa	0	0	0	0	0	0	2	6
65	Plasma kallikrein heavy chain (Fragment)	H0YAC1_HUMAN	77 kDa	8	6	0	0	0	8	0	0

#	*Identified proteins*	*Accession number*	*Mol. Wt.*	*Average spectral counts for breast cancer serum proteins*				*Average spectral counts for disease free serum proteins*			
				LCA	*Con A*	*RCA*	*SNA*	*LCA*	*Con A*	*RCA*	*SNA*
66	Plasma protease C1 inhibitor	IC1_HUMAN (+2)	55 kDa	6	7	3	0	2	4	3	0
67	Pregnancy zone protein	PZP_HUMAN	164 kDa	5	29	18	0	2	26	19	2
68	Protein AMBP	AMBP_HUMAN	39 kDa	2	2	6	0	0	2	4	0
69	Prothrombin	THRB_HUMAN	70 kDa	1	5	5	0	0	5	4	0
70	Serotransferrin	TRFE_HUMAN (+1)	77 kDa	6	23	21	0	2	19	14	4
71	Serum albumin*	ALBU_BOVIN	69 kDa	6	4	7	54	3	7	5	22
72	Serum albumin*	ALBU_HUMAN (+1)	69 kDa	41	40	48	13	23	55	60	7
73	Suprabasin	SBSN_HUMAN	61 kDa	3	0	0	5	0	0	10	9
74	Trypsin	TRYP_PIG	24 kDa	16	7	11	12	6	8	6	18
75	Vitronectin	VTNC_HUMAN	54 kDa	0	0	7	0	0	2	4	0
76	Zinc-alpha-2-glycoprotein	ZA2G_HUMAN	34 kDa	0	2	9	0	0	1	1	0

TABLE 2

TOTAL NUMBER OF PROTEINS IDENTIFIED IN EACH LECTIN COLUMN BASED ON LFQ PEAK AREAS

#	*Protein names*	*Protein ID*	*Gene names*	*Log2(ratio) Cancer: Healthy*	*Log2 (Intensity)*	*Log2(LFQ intensity Breast cancer)*	*Log2(LFQ intensity disease free serum)*	*Log 2 (Ratio) Cancer: Healthy, Significance B*
	LCA							
1	Serotransferrin (CF, S)	A5A6I6	TF	-1.521	19.995	19.343	20.864	0.070
2	Ig gamma-1 chain C region (CF)	P01857	IGHG1	-0.524	26.945	26.651	27.175	0.317
3	Plasma protease C1 inhibitor (CF)	P05155-2	SERPING1	-0.388	23.075	22.575	22.963	0.374
4	Ig kappa chain C region *	P01834	IGKC	0.444	24.504	24.292	23.848	0.830
5	Ig alpha-1 chain C region (CF)	P01876	IGHA1	1.092	26.573	26.814	25.722	0.583
6	Ig mu chain C region (CF, F)	P01871	IGHM		27.047	26.840	25.545	0.401
7	Alpha-2-macroglobulin (CF, S)	P01023	A2M	1.361	26.074	25.855	24.494	0.350
8	Apolipoprotein B-100 (CF, F)	P04114	APOB	1.407	23.538	23.491	22.084	0.317
9	Complement factor H (CF, F, S)	P08603	CFH	2.962	24.936	24.881	21.920	0.001
	ConA							
12	Apolipoprotein B-100 (CF, F)	P04114	APOB	-1.852	25.432	24.081	25.933	0.002
13	Complement C2 (CF)	Q8SQ75	C2	-1.218	22.130	21.234	22.452	0.055
14	Complement C4-B (F)	P0C0L5	C4B;C4A	-1.101	26.626	25.721	26.822	0.090
15	Ig gamma-3 chain C region (F, S)	P01860	IGHG3	-0.826	27.107	24.666	25.492	0.240
16	Plasma kallikrein	P03952	KLKB1	-0.784	25.365	21.049	21.833	0.274
17	Apolipoprotein A-I (F,S)	P0DJG0	APOA1	-0.734	24.483	22.774	23.509	0.317
18	Attractin (CF)	O75882-3	ATRN	-0.687	29.441	20.780	21.466	0.363
19	Complement factor B (F)	P00751	CFB	-0.686	21.409	25.357	26.043	0.364

#	*Protein names*	*Protein ID*	*Gene names*	*Log2(ratio) Cancer: Healthy*	*Log2 (Intensity)*	*Log2(LFQ intensity Breast cancer)*	*Log2(LFQ intensity Disease free serum)*	*Log 2 (Ratio) Cancer: Healthy, Significance B*
20	Alpha-2-macroglobulin (CF, S)	P01023	A2M	-0.617	25.966	30.273	30.890	0.437
21	Complement factor H (CF, F, S)	P08603	CFH	-0.586	21.011	24.814	25.400	0.472
22	Clusterin (CF, S)	P10909-4	CLU	-0.571	25.452	21.703	22.274	0.490
23	Ig lambda-3 chain C regions *	P0CG06	IGLC3	-0.380	29.854	24.118	24.498	0.742
24	Plasma protease C1 inhibitor (CF)	P05155-2	SERPING1	-0.350	24.659	22.389	22.739	0.786
25	Pregnancy zone protein (CF,S)	P20742	PZP	-0.321	22.862	23.749	24.071	0.828
26	Alpha-1-antitrypsin (CF,F,S)	P01009	SERPINA1	-0.306	21.212	24.761	25.066	0.851
27	Serotransferrin (CF,S)	P02787	TF	-0.207	24.622	24.826	25.033	1.000
28	Ig gamma-1 chain C region (CF)	P01857	IGHG1	-0.200	23.662	24.279	24.480	0.994
29	Complement factor I	P05156	CFI	-0.151	25.138	23.312	23.463	0.950
30	Prothrombin (CF, F)	P00734	F2	-0.023	24.187	21.006	21.029	0.837
31	Inter-alpha-trypsin inhibitor heavy chain H2 (CF, S)	P19823	ITIH2	0.030	22.891	22.545	22.515	0.791
32	Complement C3(F, S)	P01024	C3	0.107	22.716	29.629	29.522	0.725
33	CD5 antigen-like (O)	O43866	CD5L	0.208	22.208	22.533	22.325	0.642
34	Complement component C6 (F)	P61134	C6	0.441	27.740	20.826	20.385	0.468
35	Ig mu chain C region (CF, F)	P01871	IGHM	0.461	30.837	27.678	27.216	0.454
36	Haptoglobin (CF)	P00738	HP;HPR	0.621	25.586	29.379	28.758	0.353
37	Ig alpha-1 chain C region (CF)	P01876	IGHA1	0.685	23.471	25.539	24.855	0.317
38	Ig kappa chain C region*	P01834	IGKC	0.747	21.702	24.601	23.853	0.285
39	Hemopexin (CF)	P02790	HPX	0.870	23.303	27.123	26.253	0.227
40	Beta-2-glycoprotein 1 (CF)	Q95LB0	APOH	1.212	25.681	25.799	24.587	0.112
41	Fibronectin (CF, F, S)	P02751-10	FN1	2.370	24.471	24.712	22.342	0.004

#	Protein names	Protein ID	Gene names	Log2(ratio) Cancer: Healthy	Log2 (Intensity)	Log2(LFQ intensity Breast cancer)	Log2(LFQ intensity Disease free serum)	Log 2 (Ratio) Cancer: Healthy, Significance B
RCA								
44	Serum paraoxonase/arylesterase 1 (F)	P27169	PON1	-0.913	24.272	21.582	22.495	0.010
45	Alpha-1-antitrypsin (CF, F, S)	P01009	SERPINA1	-0.850	29.339	26.863	27.713	0.014
46	Carboxypeptidase N subunit 2	P22792	CPN2	-0.664	24.670	22.270	22.934	0.035
47	Apolipoprotein A-I (F, S)	P0DJG0	APOA1	-0.618	27.074	24.586	25.204	0.044
48	Clusterin (CF, S)	P10909-4	CLU	-0.191	28.435	26.442	26.633	0.235
49	Alpha-2-macroglobulin (CF, S)	P01023	A2M	-0.095	31.036	29.047	29.142	0.317
50	Alpha-1-antichymotrypsin (F)	P01011	SERPINA3	-0.084	26.153	24.136	24.220	0.328
51	Ig gamma-1 chain C region (CF)	P01857	IGHG1	-0.061	29.278	27.337	27.398	0.350
52	Hemopexin (CF)	P02790	HPX	0.003	30.797	28.953	28.950	0.419
53	Inter-alpha-trypsin inhibitor heavy chain H4 (F)	Q14624-4	ITIH4	0.059	25.290	23.285	23.226	0.484
54	Pregnancy zone protein (CF, S)	P20742	PZP	0.084	25.781	23.907	23.824	0.514
55	Ig lambda-3 chain C regions	P0CG06	IGLC3	0.185	28.375	26.805	26.620	0.649
56	Apolipoprotein A-II (F)	P0DJD2	APOA2	0.260	25.600	23.945	23.686	0.757
57	Antithrombin-III (S)	Q5R5A3	SERPINC1	0.286	25.009	23.099	22.813	0.797
58	Ig alpha-1 chain C region (CF)	P01876	IGHA1	0.306	29.662	27.853	27.547	0.827
59	Complement factor B (F)	P00751	CFB	0.345	25.244	23.477	23.132	0.886
60	Haptoglobin (CF)	P00738	HP	0.418	34.067	32.271	31.852	1.000
61	Ceruloplasmin (CF, F)	P00450	CP	0.539	27.811	26.452	25.913	0.918
62	Ig kappa chain C region (O)	P01834	IGKC	0.800	28.945	27.601	26.801	0.743
63	Vitronectin (CF, F, S)	P04004	VTN	0.859	23.133	21.749	20.891	0.705

#	*Protein names*	*Protein ID*	*Gene names*	*Log2(ratio) Cancer: Healthy*	*Log2 (Intensity)*	*Log2(LFQ intensity Breast cancer)*	*Log2(LFQ intensity Disease free serum)*	*Log 2 (Ratio) Cancer: Healthy, Significance B*
64	Serotransferrin (CF, S)	P02787	TF	0.920	26.570	25.331	24.411	0.666
65	Immunoglobulin lambda-like polypeptide 5	B9A064	IGLL5	1.196	28.008	27.050	25.854	0.504
66	CD5 antigen-like (O)	O43866	CD5L	1.268	24.527	23.475	22.207	0.466
67	Immunoglobulin J chain (CF)	P01591	IGJ	1.277	25.744	24.597	23.321	0.461
68	Ig mu chain C region (CF, F)	P01871	IGHM	1.278	29.298	28.045	26.767	0.460
69	Afamin (CF, F)	P43652	AFM	1.583	23.117	21.991	20.408	0.317
70	Leucine-rich alpha-2-glycoprotein(S)	P02750	LRG1	1.597	23.616	22.676	21.079	0.311
71	Alpha-1-acid glycoprotein 1	P02763	ORM1	2.839	28.172	27.769	24.930	0.038
72	Hemoglobin subunit alpha (O)	P69907	HBA1	4.008	25.711	25.540	21.531	0.002
73	Hemoglobin subunit beta (O)	P68873	HBB	4.177	27.492	27.319	23.142	0.001
SNA								
76	Dermcidin	P81605	DCD	-2.139	26.621	28.760	27.926	0.317
77	Suprabasin	Q6UWP8	SBSN	-2.603	22.843	25.445	24.402	0.001
78	Desmoplakin (N)	P15924	DSP;Dsp	0.877	24.536	23.659	24.905	0.317

(CF: Core fucosylated, F: Fucosylated, S: Sialylated, , N, O: a candidate for N-liked or O-linked glycoprotein, respectively)

Differentially expressed proteins in breast cancer serum

For the identification of differentially expressed proteins (DEPs), Q-Q plots were used whereby the normalized MS spectral counts of the proteins found in the cancer serum were plotted against the normalized MS spectral counts of the same protein in the disease free serum. The proteins that were more than two standard deviations away from being the same were considered as DEPs. In selecting the proteins identified by MS, the data were evaluated by the t-test and a p-value < 0.05 was set as the limit for all the identified proteins. The scatterplots obtained for all the proteins captured by the four-lectin columns with their standard deviation limit markers are shown in Figure 17. The difference in the distribution pattern and the number of DEPs varied from column to column due to the differences in the lectin recognition patterns. The DEPs identified for each lectin column i.e., LCA, Con A, RCA and SNA are listed in Tables 3, 4, 5 and 6, respectively.

A total of 23 DEPs were captured by the LCA column, which is known to bind with core fucosylated glycoproteins. Among these 23 DEPs 12 were found to be up regulated and 11 were found to be down regulated. Based on the previously published results by other labs and compiled in Refs [22-30], the proteins with core fucosylated glycans and fucosylated glycans are tabulated in Table 3, which shows that the majority of the DEPs identified in the LCA column fraction are core fucosylated, thus further confirming the specificity of the LCA column. Some non-glycoproteins were also found to bind to the LCA column and this might be due to the protein-protein interactions. Similarly, the glycoproteins that were bound to the Con A column, which constitute the mannome and the hybridome are listed in Table 4. A total of 16 DEPs were identified of

which 10 were up regulated and 6 were down regulated in breast cancer serum with respect to the disease free serum. The number of DEPs detected in the Con A column captured glycoproteins was lower than that captured by the LCA column. This may be due to the fact that the mannome and the hybridome, which are specific to the Con A column and typically not indicative of any cancerous activity in the cell. On the other hand, LCA bound core fucosylated proteins were more representative of cancerous activity in the cellular processes. A total of 26 DEPs were identified for the RCA column of which 15 were up regulated and 11 were down regulated in breast cancer serum with respect to the disease free serum (see Table 5). In the same way, the DEPs identified in the SNA column captured proteins (listed in Table 6), one can find a total of 19 DEPs of which 5 were up regulated and 14 were down regulated in breast cancer serum compared to the disease free serum.

Similarly, the LFQ peak areas obtained from MaxQuant were used in assessing DEPs. The binary logarithm of the ratio of LFQ peak areas obtained for the cancer versus the disease free serum was calculated and was plotted against summed peptide intensities. The scatter plots are shown in Figure 18. The proteins that exhibit log 2 (cancer/healthy) ratio values greater than +1 and less than -1 are considered as DEPs. A log 2 value of +1 indicates a two-fold increase in the LFQ peak area ratio whereas a value of -1 indicates two fold decrease in the ratio. The corresponding DEPs obtained for individual lectin column are listed in Table 7. A total of 5 up regulated and 1 down regulated proteins were identified in cancer serum with respect to disease free serum using the LCA column

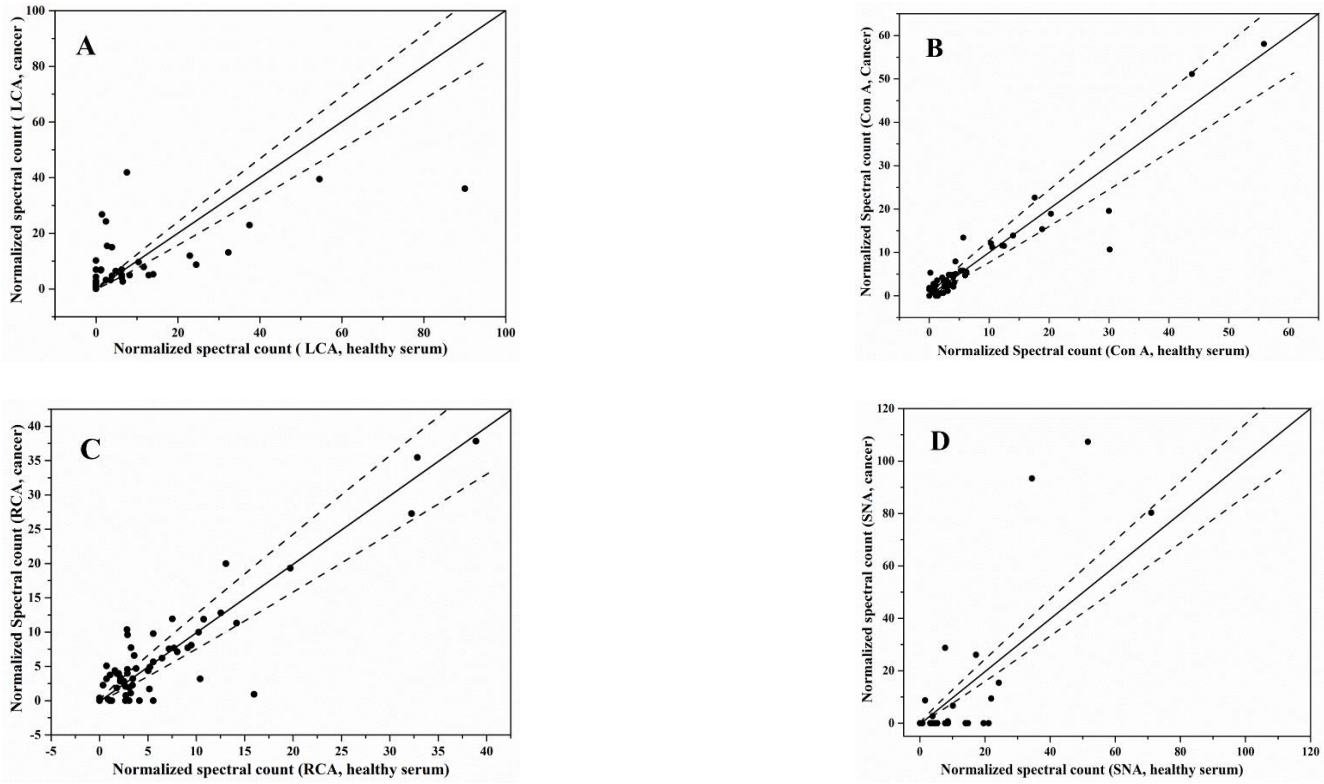

Figure 17. *Representative Q-Q scatterplots for the identification of DEPs, which are plotted as dots outside the dotted lines that mark the boundaries of two standard deviations away from being the same in both categories. The dotted lines delimit the upper and lower error bars. The Q-Q plots for the collected fractions from the LCA, the Con A, the RCA and the SNA columns are shown in plots A, B, C and D, respectively.*

TABLE 3

DEPS OBTAINED FROM THE Q-Q PLOTS OF PROTIENS IDENTIFIED IN THE LCA COLUMN FRACTIONS

#	*Up regulated proteins*	*Down regulated proteins*
1	Alpha-1-antitrypsin (CF, F)	Alpha-2-macroglobulin (CF)
2	Apolipoprotein A-I (F)	Dermcidin
3	Apolipoprotein B-100 (CF, F)	Ficolin-3 (CF, F)
4	Complement C3 (F)	Ig alpha-1 chain C region (CF)
5	Complement C4-A (CF, F)	Ig gamma-1 chain C region (CF)
6	Complement factor B (F)	Ig gamma-3 chain C region (F)
7	Complement factor H (CF, F)	Ig kappa chain C region *
8	Desmoplakin	Isoform 2 of Ig mu chain C region
9	Filaggrin	Pregnancy zone protein (CF)
10	Hornerin	Serotransferrin (CF)
11	Isoform 10 of Fibronectin (F)	Serum albumin *
12	Plasma kallikrein heavy chain (Fragment)	

(CF: core fucosylated, F: fucosylated, *: nonglycoprotein)

TABLE 4

DEPS OBTAINED FROM THE Q-Q PLOTS OF PROTIENS IDENTIFIED IN THE CON A COLUMN FRACTIONS

#	*Up regulated proteins*	*Down regulated proteins*
1	Beta-2-glycoprotein 1	Alpha-1-antichymotrypsin
2	Complement component C6	Alpha-1B-glycoprotein
3	Complement factor I	Apolipoprotein B-100
4	Desmoplakin	Complement component C8 alpha chain
5	Haptoglobin	Ficolin-3
6	Hemoglobin subunit alpha	Serum albumin*
7	Hemoglobin subunit beta	
8	Hornerin	
9	Isoform 10 of Fibronectin	
10	Isoform 2 of Inter-alpha-trypsin inhibitor heavy chain H4	

(*: nonglycoprotein)

TABLE 5

DEPS OBTAINED FROM THE Q-Q PLOTS OF PROTIENS IDENTIFIED IN THE RCA COLUMN FRACTIONS

#	*Up regulated proteins*	*Down regulated proteins*
1	Alpha-1-acid glycoprotein 1	Alpha-S1-casein
2	Alpha-1-acid glycoprotein 2	Complement C1s subcomponent
3	Beta-2-glycoprotein 1	Complement C3
4	Ceruloplasmin	Complement factor I
5	Hemoglobin subunit alpha	Dermcidin
6	Hemoglobin subunit beta	Desmoglein-1
7	Inter-alpha-trypsin inhibitor heavy chain H1	Desmoplakin
8	Inter-alpha-trypsin inhibitor heavy chain H2	Filaggrin
9	Isoform 10 of Fibronectin	Hornerin
10	Isoform LMW of Kininogen-1	Lysozyme C
11	Leucine-rich alpha-2-glycoprotein	Suprabasin
12	Protein AMBP	
13	Serotransferrin	
14	Vitronectin	
15	Zinc-alpha-2-glycoprotein	

TABLE 6

DEPS OBTAINED FROM THE Q-Q PLOTS OF PROTIENS IDENTIFIED IN THE SNA COLUMN FRACTIONS

#	*Up regulated proteins*	*Down regulated proteins*
1	Cytochrome c	Alpha-2-macroglobulin (S)
2	Desmoglein-1 (S)	Cationic trypsin
3	Desmoplakin	Complement C3 (S)
4	Hornerin	Complement C4-A
5	Serum albumin*	Dermicidin
6		Filaggrin
7		Ig gamma-1 chain C region
8		Immunoglobulin lambda-like polypeptide 5 *
9		Isoform 2 of Ig mu chain C region (S)
10		Keratinocyte proline-rich protein
11		Lysozyme C
12		Pregnancy zone protein (S)
13		Serotransferrin (S)
14		Suprabasin

(S): Sialylated *: Non glycoprotein

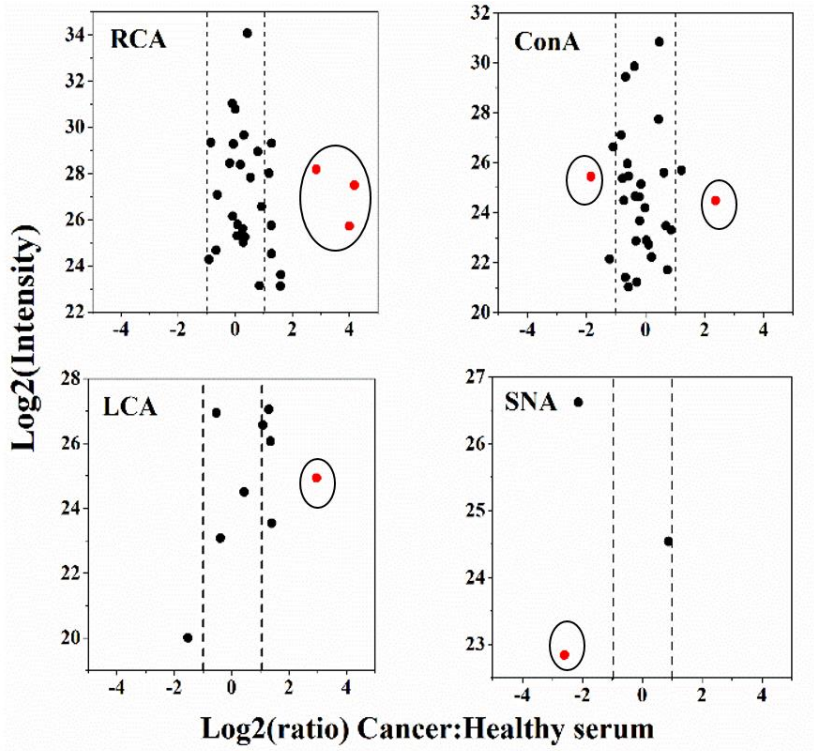

Figure 18. *LFQ of protein ratios plotted against summed peptide intensities. The dotted line delimits the boundaries of log2 values equal to '+1' and '-1', which correspond to a two-fold increase and a two-fold decrease in the LFQ intensities, respectively. The data points encircled are the ones that have 'Significance B' values <0.05.*

TABLE 7

DEPS IDENTIFIED IN DIFFERENT LECTIN COLUMNS BASED ON LFQ PEAK AREAS

	Protein ID	Gene name	Log2(ratio) Cancer:Healthy	Log 2 (ratio) Cancer:Healthy, Significance B
LCA				
Down regulated proteins				
Serotransferrin (CF, S)	A5A6I6	TF	-1.52104	0.0702881
Up regulated proteins				
Ig alpha-1 chain C region (CF)	P01876	IGHA1	1.09168	0.582814
Ig mu chain C region (CF, F)	P01871	IGHM	1.29438	0.401433
Alpha-2-macroglobulin (CF, S)	P01023	A2M	1.36115	0.350035
Apolipoprotein B-100 (CF, F)	P04114	APOB	1.40695	0.317311
Complement factor H (CF, F, S) §	P08603	CFH	2.96169	0.00126979
ConA				
Down regulated proteins				
Apolipoprotein B-100 (CF, F) §	P04114	APOB	-1.85209	0.00182143
Complement C2 (CF)	Q8SQ75	C2	-1.21827	0.055266
Complement C4-B (F)	P0C0L5	C4B;C4A	-1.10096	0.090175
Up regulated proteins				
Beta-2-glycoprotein 1 (CF)	Q95LB0	APOH	1.21218	0.111537
Fibronectin (CF, F, S) §	P02751-10	FN1	2.36989	0.00385701

	Protein ID	Gene name	Log2(ratio) Cancer:Healthy	Log 2 (Ratio) Cancer:Healthy, Significance B
RCA				
Up regulated proteins				
Immunoglobulin lambda-like polypeptide 5	B9A064	IGLL5	1.19591	0.504288
CD5 antigen-like (O)	O43866	CD5L	1.26768	0.465761
Immunoglobulin J chain (CF)	P01591	IGJ	1.27672	0.46103
Ig mu chain C region (CF, F)	P01871	IGHM	1.27825	0.460231
Afamin (CF, F)	P43652	AFM	1.58278	0.317311
Leucine-rich alpha-2-glycoprotein(S)	P02750	LRG1	1.59731	0.311311
Alpha-1-acid glycoprotein 1(CF,F) §	P02763	ORM1	2.83878	0.0376495
Hemoglobin subunit alpha (O) §	P69907	HBA1	4.00836	0.0020487
Hemoglobin subunit beta (O) §	P68873	HBB	4.17709	0.00124664
SNA				
Down regulated proteins				
Suprabasin §	Q6UWP8	SBSN	-2.60251	0.00139459
Dermcidin	P81605	DCD	-2.13931	0.317311

(CF: Core fucosylated, F: Fucosylated, S: Sialylated, O: a candidate for O-linked glycoprotein, §: DEPs that are having 'Significance B' values < 0.05)

captured proteins. For the Con A column, 3 down-regulated and 2 up-regulated proteins in the cancer with respect to the healthy serum were identified. Also, for the RCA column a total of 9 up regulated proteins in the cancer with respect to the disease free serum were observed. For the SNA column, a total of 2 down-regulated proteins in cancer with respect to disease free serum were observed. In addition significance B values were calculated, according to which the DEP complement factor H was observed to have a significance value less than 0.05 in the LCA column. For the Con A column, apolipoprotein B-100 and fibronectin and for the RCA column alpha-1-acid glycoprotein 1 and hemoglobin subunit alpha and beta were found to have significance B values of less than 0.05. Suprabasin was the only protein in SNA column whose statistical significance was less than 0.05. Similarly, the DEPs identified by the two search engines were compared using Venn diagrams and are presented in Figure 19. For the LCA column, only the protein Ig mu chain C region was identified as differentially expressed in breast cancer serum with respect to the disease free serum by the MaxQuant proteomic software. Mascot on other hand uniquely identified 18 proteins, and 5 proteins were identified by both Mascot and MaxQuant.

Correspondingly, the MaxQuant uniquely identified three proteins: complement C-2, complement C4-B and fibronectin. Apolipoprotein B-100 and beta-2-glycoprotein 1 were identified by both Mascot and MaxQuant and 14 other proteins were uniquely identified by Mascot in the Con A column. Likewise, for the RCA column 23 and 6 DEPs were identified uniquely by Mascot and MaxQuant searches, respectively, and 3 DEPs were identified by both Mascot and MaxQuant searches. Finally, for the SNA column, no unique proteins are observed in the MaxQuant searches whereas Mascot uniquely

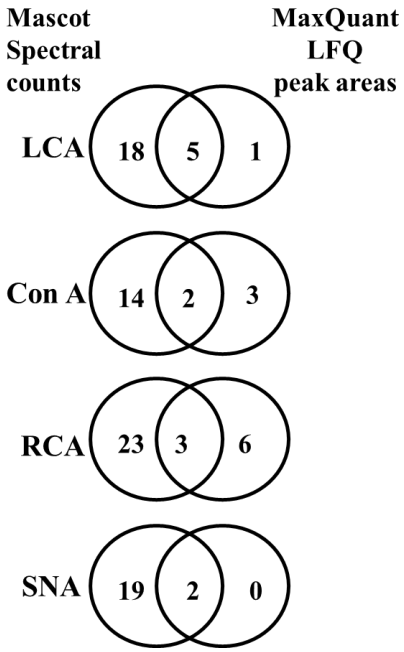

Figure 19. *Comparison of DEPs identified using both Mascot and MaxQuant proteomic software.*

identified 19 DEPs, and 2 DEPs were identified by both proteomic software. Table 7 shows the total DEPs observed by using MaxQuant proteomic. Furthermore, common keratin protein contaminants are effectively removed in MaxQuant proteomic software.

DEPs that are unique to each lectin column

After assessing the total number of DEPs that are both up- and down-regulated in each of the lectin column protein fractions, the DEPs that are unique to each lectin are listed in Table 8. Apolipoprotein A-I and alpha-1-antitrypsin, which were previously reported as biomarkers for breast and lung cancers were captured by the LCA column [31]. In the same way, core fucosylated glycoproteins complement factor H, complement factor B, the Ig alpha-1 chain C region and fucosylated Ig gamma-3 chain C region were captured by LCA column and are unique to that lectin column. Likewise, the Con A

column uniquely captured alpha-1-antichymotrypsin, alpha-1B-glycoprotein and haptoglobin, which were previously reported protein biomarkers for breast cancer [32, 33]. Isoform 2 of inter-alpha-trypsin inhibitor heavy chain H4, which is a fucosylated protein was also uniquely captured by the Con A column. When it comes to unique DEPs captured by the RCA column, the core fucosylated glycoproteins such as ceruloplasmin, inter-alpha-trypsin inhibitor heavy chain H1, inter-alpha-trypsin inhibitor heavy chain H2 and the fucosylated complement C1s subcomponent were identified. Among these DEPs, ceruloplasmin was previously reported as a protein biomarker for prostate, lung and hepatocellular carcinoma [31]. Apart from these proteins AMBP and vitronectin were also observed as unique DEPs for the RCA column [34], which are also biomarkers for the breast cancer serum. When it comes to the unique proteins captured by the SNA column, only four proteins were identified, namely cytochrome C, cationic trypsin, immunoglobulin lambda-like polypeptide 5 and keratinocyte proline-rich protein. This might be due to the fact that the majority of glycoproteins are sialylated and were already captured in the other lectin columns.

In the same way, by using the LFQ peak area approach, the uniquely identified glycoproteins in each lectin column are listed in Table 9. The unique DEPs observed for the LCA column were alpha-2-macroglobulin, complement factor H, Ig alpha-1 chain C region, and serotransferrin, all of which were previously reported as core fucosylated [22, 26]. Of these proteins, complement factor H and Ig alpha-1 chain C region are common for both Q-Q plots of MS spectral counts and LFQ peak area ratio approaches. The

TABLE 8

DEPS OBTAINED FROM THE Q-Q PLOTS THAT ARE EXPRESSED UNIQUELY IN EACH LECTIN COLUMN

LCA	*ConA*	*RCA*	*SNA*
Apolipoprotein A-I (F) (breast & lung cancer)	Alpha-1-antichymotrypsin (breast cancer)	Alpha-1-acid glycoprotein 1	Cytochrome C
Alpha-1-antitrypsin (CF, F) (HCC, breast & lung cancer)	Alpha-1B-glycoprotein (breast cancer)	Alpha-1-acid glycoprotein 2	Cationic trypsin
Complement factor H (CF, F)	Complement component C6	Alpha-S1-casein	Immunoglobulin lambda-like polypeptide 5 *
Complement factor B (F)	Complement component C8 alpha chain	Ceruloplasmin (CF, F) (prostate & lung cancer, HCC)	Keratinocyte proline-rich protein
Ig alpha-1 chain C region (CF)	Haptoglobin (CF) (breast cancer)	Complement C1s subcomponent (F)	
Ig gamma-3 chain C region (F)	Isoform 2 of Inter-alpha-trypsin inhibitor heavy chain H4 (F)	Inter-alpha-trypsin inhibitor heavy chain H1 (CF)	
Ig kappa chain C region *		Inter-alpha-trypsin inhibitor heavy chain H2 (CF)	
Plasma kallikrein heavy chain (Fragment)		Isoform LMW of Kininogen-1	
		Leucine-rich alpha-2-glycoprotein	
		Protein AMBP (lung & breast cancer)	
		Vitronectin (breast cancer)	
		Zinc-alpha-2-glycoprotein	

(CF: core fucosylated, F: fucosylated, *: nonglycoprotein)

TABLE 9

DEPS THAT ARE UNIQUE TO EACH LECTINS BASED ON LFQ PEAK AREAS

LCA	*ConA*	*RCA*	*SNA*
Alpha-2-macroglobulin (CF, S)	Beta-2-glycoprotein 1 (CF)	Afamin (CF, F)	Dermcidin
Complement factor H (CF, F, S)	Complement C2 (CF)	Alpha-1-acid glycoprotein 1	Suprabasin
Ig alpha-1 chain C region (CF)	Complement C4-B (F)	CD5 antigen-like (O)	
Serotransferrin (CF, S)	Fibronectin (CF, F, S)	Hemoglobin subunit alpha	
		Hemoglobin subunit beta	
		Immunoglobulin J chain (CF)	
		Immunoglobulin lambda-like polypeptide 5	
		Leucine-rich alpha-2-glycoprotein(S)	

(CF: Core fucosylated, F: Fucosylated, S: Sialylated, , O: a candidate for O-linked glycoprotein)

Con A column uniquely captured beta-2-glycoprotein 1, complement C2, complement C4-B and fibronectin. Both Q-Q plots and LFQ peak area methods revealed unique proteins captured by Con A column and no common proteins. Likewise, 8 proteins were characterized as unique among all the proteins captured by the RCA column. Of these, hemoglobin subunit alpha and beta were previously reported protein biomarkers for ovarian, head and neck cancer [35, 36]. These hemoglobin subunit alpha and beta were differentially expressed in both the Con A and RCA columns using Q-Q plots based on MS/MS spectral counts. Core fucosylated afamin and immunolgobin J chain and sialylated leucine-rich alpha-2-glycoprotein were also uniquely captured by the RCA column. By using the LFQ peak area ratio method only two proteins, namely, dermicidin and suprabasin were unique in the SNA captured glycoproteins.

DEPs that are common to two or more lectin columns

Several DEPs were identified in two or more lectin columns in both Q-Q plots based on MS/MS spectral counts and LFQ peak areas. For the Q-Q plots, desmoplakin, which was previously reported as a protein biomarker for breast cancer [37] and hornein were differentially expressed in all the lectin columns. Complement C3, dermicidin, filaggrin, isoform 10 of fibronectin and serotransferrin were differentially expressed in three or more columns. Of these DEPs, complement C3 and serotransferrin are protein biomarkers for hepatocellular carcinoma and breast cancer [38], respectively. The DEPs in two or more lectin columns are listed in Table 10. Of all these proteins, beta-2-glycoprotein 1, hemoglobin subunit alpha and pregnancy zone protein were previously reported as biomarkers for breast cancer [33]. Alpha-2-macroglobulin and complement factor I which are potential biomarkers for hepatocellular carcinoma [38] were also

TABLE 10

DEPS COMMON TO TWO OR MORE LECTIN COLUMNS

DEPs	*LCA*	*Con A*	*RCA*	*SNA*
Alpha-2-macroglobulin (CF, S) (prostate & lung cancer, HCC)	✓			✓
Apolipoprotein B-100 (CF, F)	✓	✓		
Beta-2-glycoprotein 1 (breast cancer)		✓	✓	
Complement C3 (F, S) (HCC)	✓		✓	✓
Complement C4-A (CF, F)	✓			✓
Complement factor I (HCC)		✓	✓	
Dermcidin	✓		✓	✓
Desmoglein-1 (S, CF)			✓	✓
Desmoplakin (breast cancer)	✓	✓	✓	✓
Ficolin-3 (CF, F)	✓	✓		
Filaggrin	✓		✓	✓
Hemoglobin subunit alpha (breast cancer)		✓	✓	
Hemoglobin subunit beta		✓	✓	
Hornerin	✓	✓	✓	✓
Ig gamma-1 chain C region (CF)	✓			✓
Isoform 10 of Fibronectin (F)	✓	✓	✓	
Isoform 2 of Ig mu chain C region (S)	✓			✓
Lysozyme C			✓	✓
Pregnancy zone protein (CF, S) (breast cancer)	✓			✓
Serotransferrin (CF, S) (HCC, breast cancer)	✓		✓	✓
Serum albumin*	✓	✓		✓
Suprabasin	▪	▪	✓	✓

(CF, Core fucosylated; F, Fucosylated; S, Sialylated; *, Non-glycoprotein; HCC, hepatocellular carcinoma)

TABLE 11

DEPS THAT ARE COMMON TO TWO LECTINS BASED ON LFQ PEAK AREAS

	LCA	*ConA*	*RCA*
Apolipoprotein B-100 (CF, F)	✓	✓	
Ig mu chain C region (CF, F)	✓		✓

captured by multiple lectin columns. Table 10 demonstrates that 15 DEPs were identified for the SNA column of which, alpha-2-macroglobulin, complement C3, desmoglein-1, isoform 2 of Ig mu chain C region, pregnancy zone protein and serotransferrin were previously reported as sialylated glycoproteins [29]. By using the LFQ peak area ratio method, apolipoprotein B-100 was differentially expressed in both the LCA and Con A columns and Ig mu chain C region were differentially expressed in the LCA and RCA columns. The data also suggests that, in LFQ peak area ratio method the majority of proteins are differentially expressed uniquely in one lectin column.

Conclusions

The monolith prepared by the copolymerization of NAS and EDMA was developed in a narrow-bore HPLC columns and its applications in trypsin IMER and bio-affinity chromatography were demonstrated. Firstly, a trypsin IMER was prepared and the digestion of the standard protein Cyt C was demonstrated by means of an online setup with zero operator intervention. The greatest advantage of the designed trypsin IMER is

that it can perform enzyme digestion in shorter times, in the range of minutes with improved digestion efficiencies, compared to in-solution digestion protocols, which take up to one day. The digestion volumes handled by this narrow bore monolithic HPLC column are in the span that are generally handled by MS and therefore they have a potential to be directly coupled with MS. Secondly, the narrow-bore HPLC columns were bound with lectins and their applications in LAC were demonstrated where a novel strategy was established by using these lectin columns to capture the widest range of glycoproteins possible from blood serum. The differentially expressed glycoproteins from pooled samples, which were made from the sera of patients diagnosed with various stages of breast cancer were identified with respect to the disease free serum. The strategy that was demonstrated involved an efficient approach to capture the serum glycoproteins without depleting the high abundance proteins by using the SLAC of narrow bore HPLC columns. The extracted glycoproteins were analyzed by MS, and the obtained data were processed in two different proteomics software, namely, Mascot and MaxQuant. This strategy can be described as a ‘gel free’ and ‘label free’ approach, which has many advantages such as high sensitivity, potential to be automated and avoidance of expensive isotope labels. By using this strategy, glycoproteins from a large pool of serum samples of patients belonging to various stages of cancer, age, gender and race can be extracted and studied for further validation of biomarkers.

References

1. Jmeian, Y. and Z. El Rassi, *Multicolumn Separation Platform for Simultaneous Depletion and Prefractionation Prior to 2-DE for Facilitating In-Depth Serum Proteomics Profiling.* J. Proteome Res., 2009. **8**(10): p. 4592-4603.
2. *http://www.breastcancer.org/symptoms/understand_bc/statistics.*
3. Selvaraju, S. and Z. El Rassi, *Tandem lectin affinity chromatography monolithic columns with surface immobilised concanavalin A, wheat germ agglutinin and Ricinus communis agglutinin-I for capturing sub-glycoproteomics from breast cancer and disease-free human sera.* J. Sep. Sci., 2012. **35**(14): p. 1785-1795.
4. Selvaraju, S. and Z.E. Rassi, *Targeting human serum fucome by an integrated liquid-phase multicolumn platform operating in "cascade" to facilitate comparative mass spectrometric analysis of disease-free and breast cancer sera.* Proteomics, 2013. **13**(10-11): p. 1701-1713.
5. Fanayan, S., M. Hincapie, and W.S. Hancock, *Using lectins to harvest the plasma/serum glycoproteome.* Electrophoresis, 2012. **33**(12): p. 1746-1754.
6. Bedair, M. and Z. El Rassi, *Affinity chromatography with monolithic capillary columns: I. Polymethacrylate monoliths with immobilized mannan for the separation of mannose-binding proteins by capillary electrochromatography and nano-scale liquid chromatography.* J. Chromatogr. A, 2004. **1044**(1–2): p. 177-186.
7. Jung, K. and W. Cho, *Serial Affinity Chromatography as a Selection Tool in Glycoproteomics.* Anal. Chem., 2013. **85**(15): p. 7125-7132.

8. Marangoni, R., R. Chiarini, G. Iannone, and M. Salerno, *DigesTip: A new device for a rapid and efficient in-solution protein digestion.* Proteomics, 2008. **8**(11): p. 2165-2167.

9. Li, Y., X. Xu, C. Deng, P. Yang, and X. Zhang, *Immobilization of Trypsin on Superparamagnetic Nanoparticles for Rapid and Effective Proteolysis.* J. Proteome Res., 2007. **6**(9): p. 3849-3855.

10. Gao, J., J. Xu, L.E. Locascio, and C.S. Lee, *Integrated Microfluidic System Enabling Protein Digestion, Peptide Separation, and Protein Identification.* Anal. Chem., 2001. **73**(11): p. 2648-2655.

11. Hermanson, G.T., *Bioconjugate techniques*. 2013: Academic press.

12. Lomant, A.J. and G. Fairbanks, *Chemical probes of extended biological structures: Synthesis and properties of the cleavable protein cross-linking reagent [35S]dithiobis(succinimidyl propionate).* J. Mol. Biol., 1976. **104**(1): p. 243-261.

13. Chen, J.P. and A.S. Huffman, *Polymer-protein conjugates.* Biomaterials, 1990. **11**(9): p. 631-634.

14. Wang, C., M. Gao, P. Zhang, and X. Zhang, *Efficient Proteolysis of Glycoprotein Using a Hydrophilic Immobilized Enzyme Reactor Coupled with MALDI-QIT-TOF-MS Detection and μHPLC Analysis.* Chromatographia, 2014. **77**(5): p. 413-418.

15. Guerrouache, M., A. Pantazaki, M.-C. Millot, and B. Carbonnier, *Zwitterionic polymeric monoliths for HILIC/RP mixed mode for CEC separation applications.* J. Sep. Sci., 2010. **33**(6-7): p. 787-792.

16. Guerrouache, M., B. Carbonnier, C. Vidal-Madjar, and M.-C. Millot, *In situ functionalization of N-acryloxysuccinimide-based monolith for reversed-phase electrochromatography.* J. Chromatogr. A, 2007. **1149**(2): p. 368-376.

17. Carbonnier, B., M. Guerrouache, R. Denoyel, and M.-C. Millot, *CEC separation of aromatic compounds and proteins on hexylamine-functionalized N-acryloxysuccinimide monoliths.* J. Sep. Sci., 2007. **30**(17): p. 3000-3010.

18. Guerrouache, M., M.-C. Millot, and B. Carbonnier, *Functionalization of Macroporous Organic Polymer Monolith Based on Succinimide Ester Reactivity for Chiral Capillary Chromatography: A Cyclodextrin Click Approach.* Macromol. Rapid Commun., 2009. **30**(2): p. 109-113.

19. Guiochon, G., *Monolithic columns in high-performance liquid chromatography.* J. Chromatogr. A, 2007. **1168**(1–2): p. 101-168.

20. Jonnada, M., R. Rathnasekara, and Z. El Rassi, *Recent advances in nonpolar and polar organic monoliths for HPLC and CEC.* Electrophoresis, 2015. **36**(1): p. 76-100.

21. Puvanakrishnan, R. and S.M. Bose, *Properties of trypsin immobilized on sand.* Biotechnol. Bioeng., 1980. **22**(11): p. 2449-2454.

22. Jia, W., Z. Lu, Y. Fu, H.-P. Wang, L.-H. Wang, H. Chi, Z.-F. Yuan, Z.-B. Zheng, L.-N. Song, and H.-H. Han, *A strategy for precise and large scale identification of core fucosylated glycoproteins.* Mol. Cell. Proteomics, 2009. **8**(5): p. 913-923.

23. Comunale, M.A., M. Wang, J. Hafner, J. Krakover, L. Rodemich, B. Kopenhaver, R.E. Long, O. Junaidi, A.M.D. Bisceglie, T.M. Block, and A.S. Mehta,

Identification and Development of Fucosylated Glycoproteins as Biomarkers of Primary Hepatocellular Carcinoma. J. Proteome Res., 2009. **8**(2): p. 595-602.

24. Tan, Z., H. Yin, S. Nie, Z. Lin, J. Zhu, M.T. Ruffin, M.A. Anderson, D.M. Simeone, and D.M. Lubman, *Large-Scale Identification of Core-Fucosylated Glycopeptide Sites in Pancreatic Cancer Serum Using Mass Spectrometry.* J. Proteome Res., 2015. **14**(4): p. 1968-1978.

25. Kolarich, D., A. Weber, P.L. Turecek, H.-P. Schwarz, and F. Altmann, *Comprehensive glyco-proteomic analysis of human α1-antitrypsin and its charge isoforms.* Proteomics, 2006. **6**(11): p. 3369-3380.

26. Treuheit, M.J., C.E. Costello, and H.B. Halsall, *Analysis of the five glycosylation sites of human α1-acid glycoprotein.* Biochem. J, 1992. **283**(1): p. 105-112.

27. Senshu, T., S. Kan, H. Ogawa, M. Manabe, and H. Asaga, *Preferential Deimination of Keratin K1 and Filaggrin during the Terminal Differentiation of Human Epidermis.* Biochem. Biophys. Res. Commun., 1996. **225**(3): p. 712-719.

28. Mann, B., M. Madera, I. Klouckova, Y. Mechref, L.E. Dobrolecki, R.J. Hickey, Z.T. Hammoud, and M.V. Novotny, *A quantitative investigation of fucosylated serum glycoproteins with application to esophageal adenocarcinoma.* Electrophoresis, 2010. **31**(11): p. 1833-1841.

29. Cho, W., K. Jung, and F.E. Regnier, *Sialylated Lewis x Antigen Bearing Glycoproteins in Human Plasma.* J. Proteome Res., 2010. **9**(11): p. 5960-5968.

30. Karenga, S. and Z. El Rassi, *A novel, neutral hydroxylated octadecyl acrylate monolith with fast electroosmotic flow velocity and its application to the*

separation of various solutes including peptides and proteins in the absence of electrostatic interactions. Electrophoresis, 2010. **31**(19): p. 3192-3199.

31. Maciel, C.M., M. Junqueira, M.E.M. Paschoal, M.T. Kawamura, R.L.M. Duarte, M.d.G.d.C. Carvalho, and G.B. Domont, *Differential proteomic serum pattern of low molecular weight proteins expressed by adenocarcinoma lung cancer patients.* J. Exp. Ther. Oncol., 2005. **5**(1).

32. Huang, H.-L., T. Stasyk, S. Morandell, H. Dieplinger, G. Falkensammer, A. Griesmacher, M. Mogg, M. Schreiber, I. Feuerstein, C.W. Huck, G. Stecher, G.K. Bonn, and L.A. Huber, *Biomarker discovery in breast cancer serum using 2-D differential gel electrophoresis/ MALDI-TOF/TOF and data validation by routine clinical assays.* Electrophoresis, 2006. **27**(8): p. 1641-1650.

33. Abd Hamid, U.M., L. Royle, R. Saldova, C.M. Radcliffe, D.J. Harvey, S.J. Storr, M. Pardo, R. Antrobus, C.J. Chapman, N. Zitzmann, J.F. Robertson, R.A. Dwek, and P.M. Rudd, *A strategy to reveal potential glycan markers from serum glycoproteins associated with breast cancer progression.* Glycobiology, 2008. **18**(12): p. 1105-1118.

34. Kadowaki, M., T. Sangai, T. Nagashima, M. Sakakibara, H. Yoshitomi, S. Takano, K. Sogawa, H. Umemura, K. Fushimi, Y. Nakatani, F. Nomura, and M. Miyazaki, *Identification of vitronectin as a novel serum marker for early breast cancer detection using a new proteomic approach.* J. Cancer Res. Clin. Oncol., 2011. **137**(7): p. 1105-1115.

35. Woong-Shick, A., P. Sung-Pil, B. Su-Mi, L. Joon-Mo, N. Sung-Eun, N. Gye-Hyun, C. Young-Lae, C. Ho-Sun, J. Heung-Jae, K. Chong-Kook, K. Young-Wan,

H. Byoung-Don, and J. Hyun-Sun, *Identification of hemoglobin-α and -β subunits as potential serum biomarkers for the diagnosis and prognosis of ovarian cancer.* Cancer Sci., 2005. **96**(3): p. 197-201.

36. Roesch-Ely, M., M. Nees, S. Karsai, A. Ruess, R. Bogumil, U. Warnken, M. Schnolzer, A. Dietz, P.K. Plinkert, C. Hofele, and F.X. Bosch, *Proteomic analysis reveals successive aberrations in protein expression from healthy mucosa to invasive head and neck cancer.* Oncogene, 2006. **26**(1): p. 54-64.

37. Sommers, C.L., S.W. Byers, E.W. Thompson, J.A. Torri, and E.P. Gelmann, *Differentiation state and invasiveness of human breast cancer cell lines.* Breast Cancer Res. Treat., 1994. **31**(2): p. 325-335.

38. Comunale, M.A., M. Lowman, R.E. Long, J. Krakover, R. Philip, S. Seeholzer, A.A. Evans, H.-W.L. Hann, T.M. Block, and A.S. Mehta, *Proteomic Analysis of Serum Associated Fucosylated Glycoproteins in the Development of Primary Hepatocellular Carcinoma.* J. Proteome Res., 2006. **5**(2): p. 308-315.

CHAPTER V

ROBUST NAPHTHYL METHACRYLATE MONOLITHIC COLUMN FOR HIGH PERFORMANCE LIQUID CHROMATOGRAPHY OF A WIDE RANGE OF SOLUTES

Introduction

Since its early stages of development, high performance reversed-phase chromatography (RPC) using nonpolar stationary phases has been practiced primarily with surface bound n-alkyl chain ligands and predominantly with n-octadecyl (i.e., C18) bound surfaces [1]. In a search for different selectivity stationary phases, other nonpolar sorbents were introduced and in particular surfaces bearing, among other things, aromatic ligands, e.g., phenyl, naphthyl, anthryl, pyrenyl [2-5] and pentafluorophenyl [6]. These aromatic surfaces offer additional $\pi - \pi$ interactions apart from their hydrophobicity [7-9]. This combined feature of stationary phases with surface bound aromatic ligands has been exploited in the separation of various kinds of aromatic compounds [2, 10-12]. Pi-pi interactions are based on the fact that aromatic stationary phases are π-electron rich

* *The contents of this chapter have been published* in *J. Chromatogr. A, 2015. 1409: p. 166-172.*

(i.e., soft Lewis bases) [13], which can then associate with solutes that are relatively π-electron deficient (i.e., soft Lewis acids) such as aromatic compounds with electron withdrawing substituents (i.e., deactivating substituents) thus leading to π – π interactions that are considered as a type of electron donor – electron acceptor interactions between the stationary phase and the solutes [9].

Monolithic columns are currently witnessing increased use in liquid phase separation techniques (for recent reviews, see [14, 15]) due to their distinctive characteristic features, including relatively high permeability, rapid solute mass transfer through the network of mesopores that are interconnected with large flow through pores and the readily tailor made surface chemistry (for a recent review, see [16]). Despite the major progress made in monolithic columns for liquid phase separations, organic monolithic columns with phenyl ligands for HPLC separations have been mostly based on the traditional poly(styrene-co-divinylbenzene) monolith [17-20] and its variants such as poly(*p*-methylstyrene-co-1,2-bis(*p*-vinylphenyl)ethane) [21], poly(phenyl acrylate-co-1,4-phenylene diacrylate) [22] and poly(styrene-divinylbenzene-methacrylic acid) [23]. Therefore, it is the aim of this research report to further the development of monolithic columns with aromatic ligands by optimizing a recently developed naphthyl monolithic (NMM) column with surface bound naphthyl ligands, which was introduced by Karenga and El Rassi for CEC separations of aromatic compounds *via* π-π and hydrophobic interactions [7]. This NMM monolith is derived from the co-polymerization of 2-naphthylmethacrylate (NAPM) as the functional monomer and trimethylolpropane trimethacrylate (TRIM) as the crosslinker. As will be discussed below, the basic composition of the polymerization mixture was altered and tailored to suit HPLC use.

Experimental

Instrumentation and procedures

HPLC experiments were performed on an in-house assembled instrument consisting of a quaternary solvent delivery system Model Q-grad pump from Lab Alliance (State College, PA, USA), a Model Spectromonitor 3100 UV-VIS variable wavelength detector from Milton Roy, LDC Division (Riviera Beach, FL, USA), and a Rheodyne high pressure injection valve Model 7010 from IDEX Health & Science LLC (Rohnert Park, CA, USA) equipped with a 20 µL injection loop. The chromatograms were occasionally recorded with a C-R5A integrator from Shimadzu (Kyoto, Japan). Otherwise, data collection was made by a Clarity Chromatography Station v3.0.06.589 (Data Apex, Prague, The Czech Republic) and the chromatographic data were processed by OriginPro v8.5.1 from Origin Lab Corp., (Northampton, MA, USA). During the experiment, the entire HPLC system including the pump, injector, column and detector was kept at ambient temperature. The UV detector was set at 214 nm, and a constant flow rate was maintained at 1.00 mL/min, unless otherwise mentioned. The number of theoretical plates of a column (N) was calculated based on peak width at inflection point.

An HPLC solvent delivery system Model M-45 from Waters Associates (Milford, MA, USA) was used to wash the monolithic column from porogens and unreacted monomers. A constant pressure pump from Shandon Southern Products Ltd (Cheshire, UK) was used to transfer the monolithic mold at high pressures into the HPLC column. Water bath Model Isotemp 105 from Fischer Scientific (Pittsburgh, PA, USA) was used to carry out the polymerization reactions at specified temperatures.

Standard solutions of various compounds were prepared within the concentration range of 2.0-5.0 µg/L and were stored in a lab refrigerator at 4˚C. Protein samples were prepared in the concentration range of 0.02-0.05 mg/mL. Water was thoroughly filtered through a 0.45 µm membrane (Millipore, Bedford, MA, USA) before use to remove micro-particulates.

Reagents and materials

Stainless steel tubing of 4.6 mm i.d. was obtained from Alltech Associates (Deerfield, IL, USA). Columns were made with Swagelok end fittings purchased from Crawford Fitting Co., (Solon, OH, USA). An octadecyl silica (ODS) UltraSphere™ column, 5-µm average particle diameter, 4.5 cm x 4.6 mm i.d. was obtained from Beckman Coulter (Brea, CA, USA). Methacryloyl chloride, 2-naphthol, diethyl ether (analytical grade), triethylamine (TEA), 1-dodecanol, 2,2'-azobis(isobutyronitrile) (AIBN), TRIM, cyclohexanol, alkylbenzenes (ABs), chlorophenols, aniline, benzene, toluene, their derivative compounds and all other test standard solutes were purchased from Sigma-Aldrich (Milwaukee, WI, USA). Nitrobenzene, ethyl acetate (HPLC grade) and chloroform (GR grade) were obtained from Fisher Scientific (Fair Lawn, NJ, USA). Benzaldehyde was obtained from Mallinckrodt (St. Louis, MO, USA). Acetonitrile (HPLC grade), methanol (analytical grade), isopropyl alcohol (IPA) and hexanes (GR grade) were obtained from Pharmco-Aaper (Brookfield, CT, USA). Standard proteins such as bovine milk β-lactoglobulin A, horse skeletal muscle myoglobin, equine heart cytochrome C, chicken egg white lysozyme, bovine pancreas ribonuclease A and α-chymotrypsinogen A were obtained from Sigma (St. Louis, MO, USA).

Preparation of monolith

Monomer synthesis. The monomer NAPM was synthesized according to a previously published procedure (see Figure 1) [24] and characterized by ^{1}H NMR and ^{13}C NMR. Firstly in a 500 mL round bottom flask 10 g of 2-naphthol (69.4 mmol) was dissolved in 150 mL of diethyl ether, 14.5 mL of TEA (104.0 mmol) was added and constantly stirred by a magnetic stirrer. To this solution, 8.0 mL of methacrylol chloride (81.9 mmol) dissolved in 100 mL of diethyl ether was added drop-wise for about 1 h *via* dropping funnel while the reaction is kept at 0˚C, the mixture was continuously stirred for another 24 h at room temperature. The resulting precipitate was filtered off and the solvent was evaporated *in vacuo* to get a white colored powder. This powder was again dissolved in small amount of chloroform and purified by column chromatography on a silica gel of bed dimensions 50 cm x 3 cm, using 10% (v/v) ethyl acetate in hexanes as the mobile phase. The obtained fractions were concentrated *in vacuo* and the white solid thus obtained showed a peak purity of 98.12 % (*m/z* 212.2) as analyzed by GC-MS. This purified white solid was characterized by ^{1}H and ^{13}C NMR. In the ^{1}H NMR (400 MHz, chloroform-*d*), the following signals characteristic of the product NAPM were observed: δ 7.90 – 7.83 (m, 2H), 7.83 – 7.79 (m, 1H), 7.60 (d, *J* = 2.1 Hz, 1H), 7.49 (dtd, *J* = 12.7, 6.8, 3.4 Hz, 2H), 7.28 (d, *J* = 2.3 Hz, 1H), 6.41 (s, 1H), 5.80 (s, 1H), 2.11 (s, 3H). The

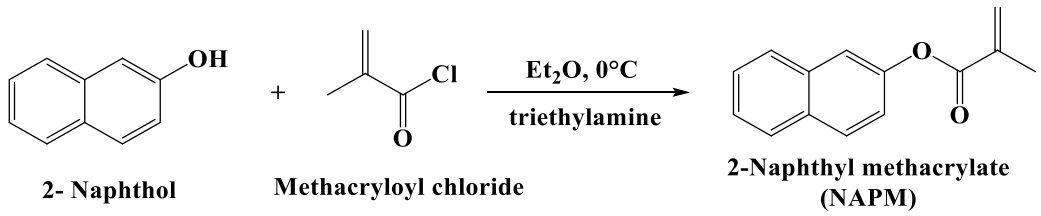

Figure 1. *Synthesis of the functional monomer 2-naphthyl methacrylate (NAPM)*

^{13}C NMR (chloroform-*d*) produced the following unique signals for the NAPM product: δ 166.26, 148.77, 136.12, 127.97, 127.56, 125.86, 121.40, 118.76, 18.66.

In situ polymerization. The reaction mixture for the NMM column was prepared as follows: The reactants were weighed into clean glass vials with 4.7 g of total polymeric solution comprising 13.46% w/w NAPM as the functional monomer, 16.50% w/w TRIM as the crosslinker, the porogenic solvents cyclohexanol, 1-dodecanol and water in the proportions of 53.87% w/w, 13.64% w/w and 2.53% w/w, respectively (see Figure 2). The mixture was gently shaken in a water bath at 40˚C to facilitate the dissolution of the NAPM, vigorously mixed in a vortex mixture and sonicated for about 20 min. Thereafter, the polymerization mixture was introduced into a stainless steel column (250 mm x 4.6 mm i.d.) with fittings at both column ends, which were then sealed with end plugs. Thereafter, the polymerization was allowed to proceed at 60˚C for 12 h in a water bath. The end plugs were removed and the column was washed with acetonitrile to remove any traces of unreacted monomers and the porogenic solvents. The column was equilibrated with IPA, and then, using the same solvent a packing pressure of 8000 psi was used to transfer this 'mold' into a 100 mm x 4.6 mm i.d. stainless steel column. Usually, upon monolith formation a contraction may take place at both ends of the mold, and most often at the column inlet end. The high-pressure transfer to a shorter column will result in a total filling of the shorter column thus removing any column contraction or voids, which were formed during the polymerization process in the 'mold' column by making the transferred portion of the monolith to the shorter column tightly

"compressed" and void free. Thereafter, the column was conditioned for 1 h with acetonitrile prior to the chromatographic tests.

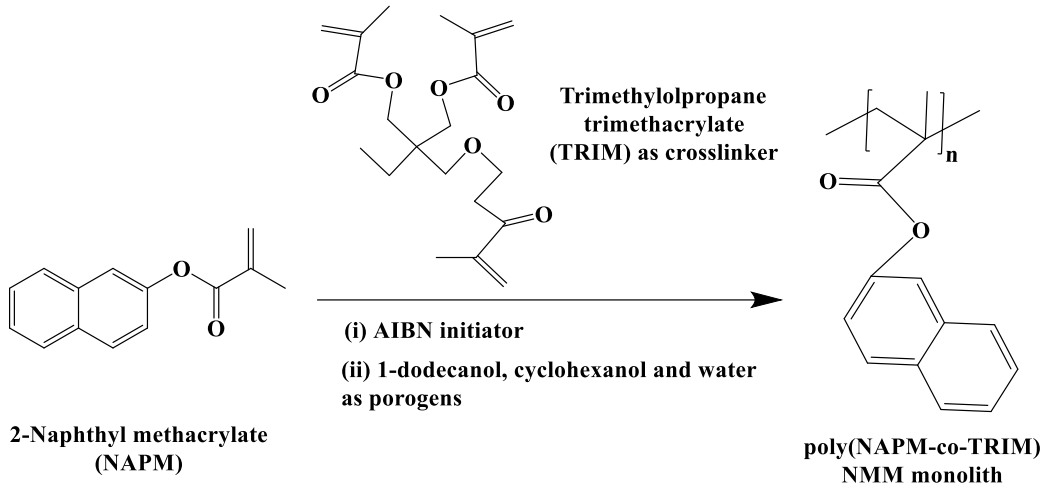

Figure 2.*Preparation of poly (NAPM-co-TRIM) monolith (NMM) by in situ polymerization*

Results and discussion

Mechanical stability, reproducibility and separation efficiency

The NMM column described in this article is an optimized version of the one reported earlier for CEC separations by Karenga and El Rassi [7] for use in HPLC. The composition of the monolith has to be altered in order to suit HPLC conditions, which involve a relatively high linear pumped flow velocity as opposed to electroosmotic flow in CEC. That is, optimal column composition for CEC separations may not be the best suited for HPLC. In fact, using the optimal monolith composition for CEC yielded HPLC columns with low permeability. While the monomer to porogen ratio was the same

30:70 w/w in both cases, the NAPM and TRIM content of the monomers has to be changed from 50:50 (w/w) in CEC to 44.9-wt% NAPM and 55.1-wt% TRIM in HPLC. Also, the porogen content of cyclohexanol and 1-dodecanol had to be adjusted from 75.7-wt% and 20.7-wt%, respectively, in CEC to 76.9-wt% and 19.5-wt%, respectively, in HPLC. The water content in both cases was kept constant at 3.6-wt%.

As any other newly introduced HPLC column, the mechanical stability of the NMM column is a primary prerequisite for justifying its further use. Generally, the mechanical stability of a polymeric monolithic stationary phase is evaluated by measuring the pressure drop across the column with commonly used solvents at different flow rates. As shown in Figure 3, a linear relationship ($R^2 > 0.99$) between flow rate and the resulting backpressure is obtained for pure ACN and MeOH as well as with 60:40 (v/v) ACN:H_2O and 70:30 (v/v) MeOH:H_2O. This is a clear indication of good mechanical stability for the NMM column. The much higher backpressure observed with mixtures of MeOH:H_2O than with equivalent mixtures of ACN:H_2O can be attributed to the much higher viscosity of the hydro-organic eluents in the former case than in the later case. For pure solvents, the viscosity of ACN and MeOH is 0.38 cP and 0.58 cP, respectively, while for the mixtures of MeOH:H_2O at 70:30 (v/v) and for ACN:H_2O at 60:40 (v/v) used in Figure 3, the respective viscosities are 1.60 cP and 0.94 cP.

Reproducibility of the NMM column was investigated in terms of percent relative standard deviation (% RSD) of k values for three test solutes, including indole (k_{av} = 0.65), toluene (k_{av} = 2.21) and pentylbenzene (k_{av} = 6.57) using a mobile phase composition of 70:30 (v/v) ACN:H_2O at a flow rate of 1 mL/min. The % RSD for the k values from run-to-run (n = 6) were 0.23, 0.53 and 0.60 for indole, toluene and

pentylbenzene, respectively. These % RSD, which are less than 1% indicate that the column is suitable for the routine analysis with remarkable precision. Finally

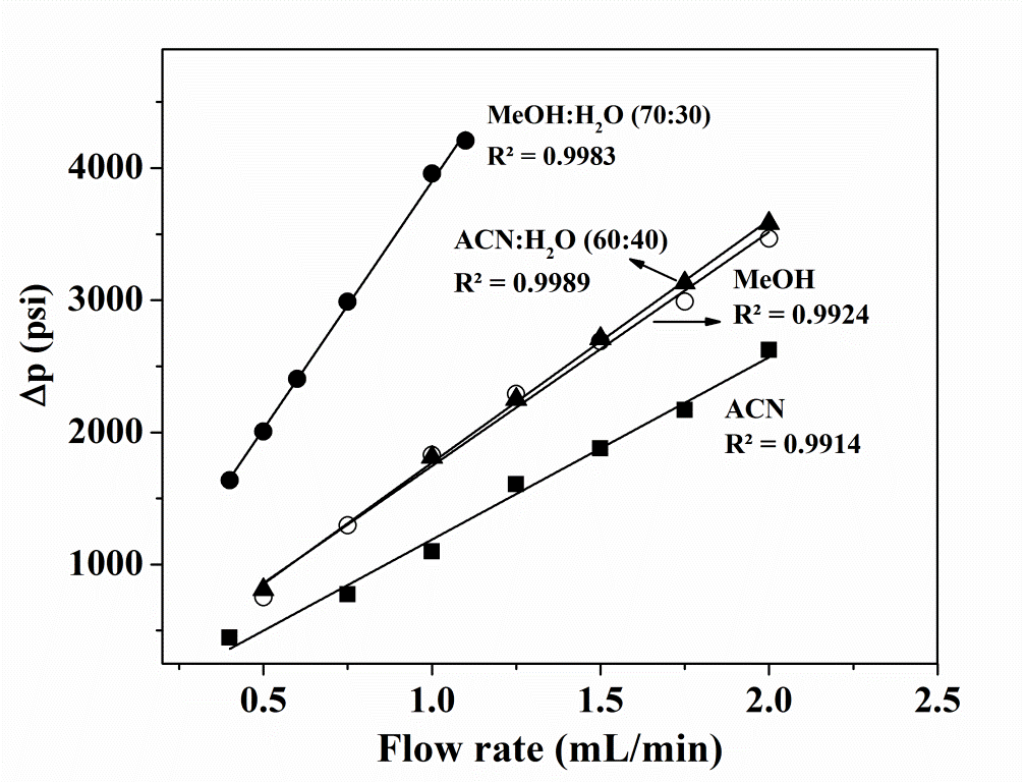

Figure 3. *Column backpressure (Δp) versus mobile phase flow rates obtained on NMM column (10 cm x 4.6 mm i.d.) for ACN, MeOH, ACN:H2O (60:40 v/v) and MeOH:H2O (70:30 v/v).*

the robustness of the column was investigated by comparing column-to-column reproducibility on NMM column preparations on different days and from two different batches of NAPM monomer, which were independently synthesized in the lab. A total of 45 different runs were performed on 5 independently fabricated columns from two batches of the NAPM monomer and the k values of the previous analytes were estimated under otherwise the same mobile phase composition. A % RSD values of 3.50, 3.24 and

1.97 were observed for indole, toluene and pentylbenzene, respectively. These % RSD, which are in the range of ~ 2 - 3.5% indicate excellent reproducible results between columns and batches prepared on different days as well as from day-to-day runs. In short, the above reproducibility results indicate that the monolithic column is capable of both short term and long term repeatability.

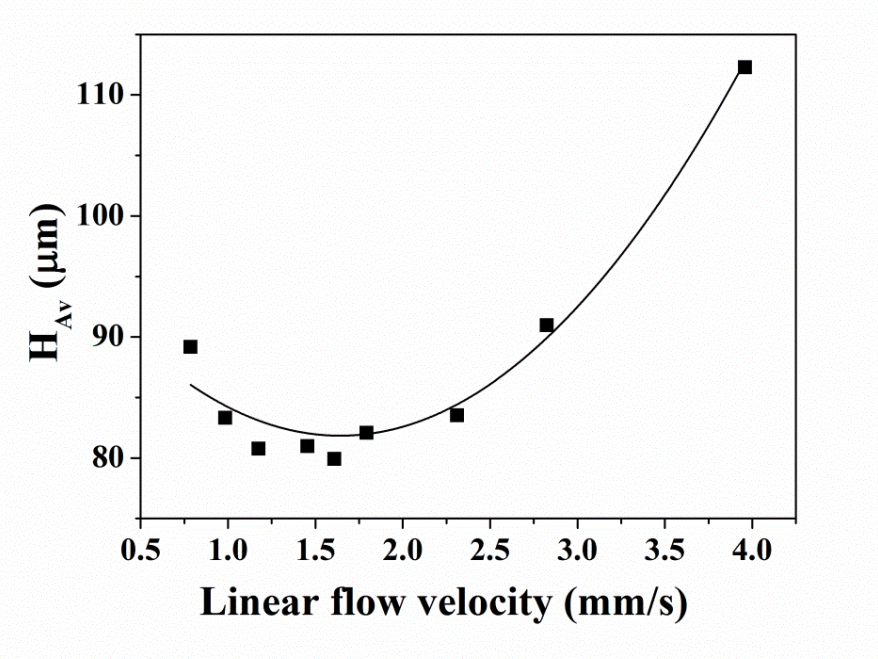

Figure 4. *van Deemter plot obtained on NMM column (10 cm x 4.6 mm i.d.). Solutes, ABs (C1-C7); mobile phase, ACN:H_2O (77:23 v/v).*

A plot of plate height (H) versus the mobile phase linear flow velocity, the so-called van Deemter plot, is typically used to gauge the separation efficiency of a given column. Figure 4 shows a typical van Deemter plot for the average H of seven alkyl

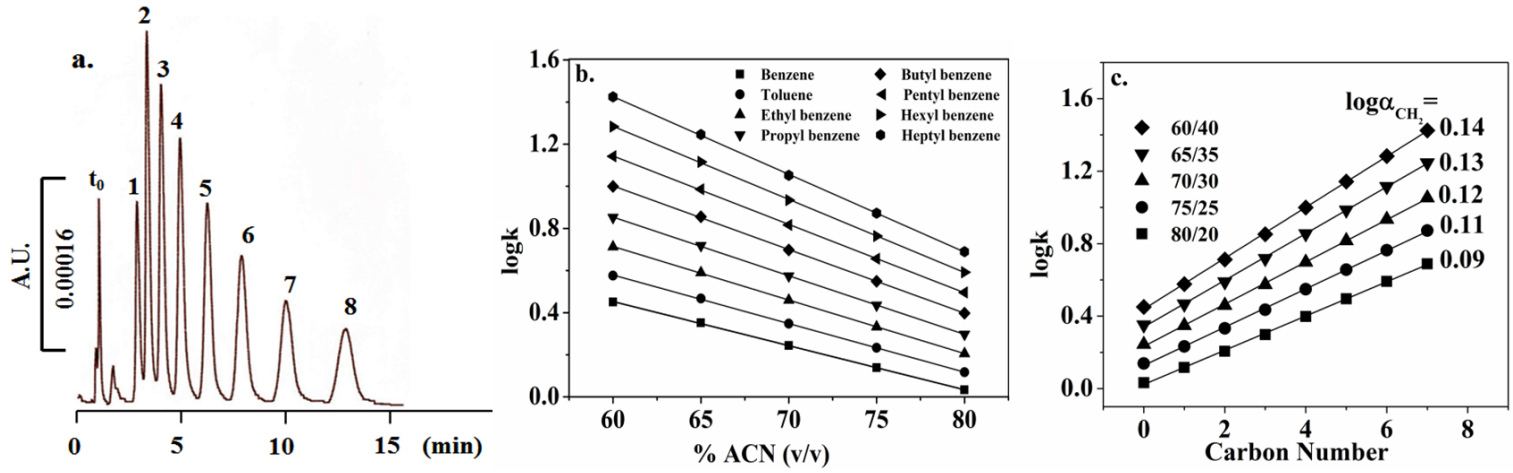

Figure 5. *Chromatogram of benzene and ABs (a), plot of log k of ABs versus % ACN in mobile phase (b) and plot of log k of ABs versus carbon number in the ABs homologous series at various ACN:H_2O in the mobile phase. Column, NMM, 10 cm x 4.6 mm i.d.; mobile phase, ACN:H_2O (65:35 v/v) in (a); flow rate, 1.00 mL/min, UV detection at 214 nm. Peaks in (a): t_0, thiourea; 1, benzene; 2, toluene; 3, ethylbenzene; 4, propylbenzene; 5, butylbenzene; 6, pentylbenzene; 7, hexylbenezene; 8, heptylbenzene.*

benzenes (ABs) (C1-C7). The H values were obtained under isocratic elution using ACN:H_2O at 77:23 (v/v) as the mobile phase, which yielded the following k values for the homologs: toluene (k = 1.72), ethylbenzene (k = 2.12), propylbenzene (k = 2.63), butylbenzene (k = 3.31), amylbenzene (k = 4.19), hexyl benzene (k = 5.29), and heptylbenzene (k = 6.67). As shown in Figure 4, the ABs showed an H_{min} averaging ~82 μm over a wide linear flow velocity extending from 0.9 to 2.3 mm/sec. This constancy in efficiency allows the use of the column over a relatively wide range of flow rates to achieve analyse at varying speeds.

Retention of some model small solutes

Model homologous series of varying hydrophobic characters. ABs are widely considered as model nonpolar solutes widely used for gauging the retention behavior of a given reversed phase column. Eight ABs homologs were chromatographed on the NMM column (see Figure 5a) with an average plate count of 12,800/m. Figure 5b displays the linear relationship for log k of the ABs vs. %ACN (v/v) in the mobile phase, which is a typical RPC behavior of a nonpolar monolithic column such as the NMM column under investigation. R^2 values of greater than 0.9998 were obtained for all the ABs tested. Moreover, the hydrophobicity of the stationary phase can be conveniently characterized by the logarithmic methylene group selectivity (log α_{CH2}) [1], which is calculated from the slope of log k against the carbon number of the AB homologous series Figure 5c). A slope ranging from 0.09-0.14 was observed for mobile phases with %ACN varying from 80-60%. These studies show a typical reversed phase mechanism, which is similar to that observed on normal C-18 columns.

In another set of experiments slightly more polar homologous solutes than ABs, namely nitroalkanes (NAs) were analyzed. NAs are smaller in size when compared to ABs and are more polar homologs with a nitro group and less π electron density (2π electrons). Being small and slightly more polar than ABs, the NAs (C1-C6) were separated much faster in less than 7 min (chromatogram not shown) as compared to 14 min for ABs (see Figure 5a) under otherwise the same elution conditions, with an average plate count of 9,500 plates/m.

Other model solutes – Evidence of π-π interactions. Polynuclear aromatic hydrocarbons such as the surface naphthyl ligands of the NMM columns are known as efficient donors of π-electrons. Therefore, the NMM column is considered to have an electron donating ability towards solutes with electron accepting ability, and consequently might establish strong electron donor-acceptor complexes with these solutes. In order to illustrate the presence of a dual retention mechanism consisting of hydrophobic and π-π interactions with the NMM stationary phase, four test mixtures consisting of aromatic solutes, including aniline derivatives, benzene derivatives, phenol derivatives and toluene derivatives with different electron donating/electron withdrawing functional groups were separated on the NMM column, see below.

Electron-donating substituents on a benzene ring make the ring more π-donating than the benzene itself and are called activating groups [25]. Oppositely, electron-withdrawing substituents on a benzene ring make the ring more π-accepting than benzene itself and are considered as deactivating groups. Typical examples of strongly activating groups are $–NH_2$, –NHR, $–NR_2$, –OH and O^-; moderately activating substituents are

–NHCOR, –OCH_3 and –OR; weakly activating substituents are –CH_3, –

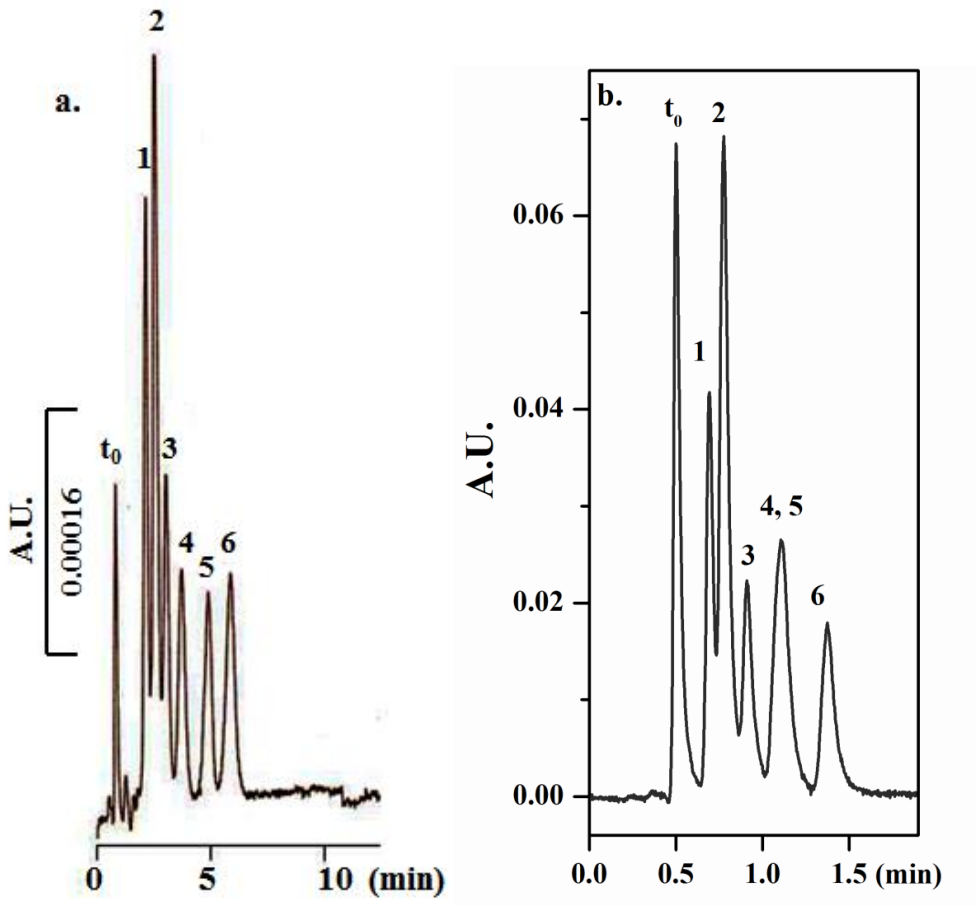

Figure 6. *Chromatograms of aniline and aniline derivatives obtained on NMM column (10 cm x 4.6 mm i.d.) in (a) and ODS column (4.5 cm x 4.6 mm i.d.) in (b). Conditions: mobile phase, ACN:H_2O (55:45 v/v); flow rate, 1 mL/min; UV detection at 214 nm. Peaks: t_0, thiourea; 1, aniline; 2, 3-methylaniline; 3, 4-ethylaniline; 4, 4-isopropylaniline; 5, N-methylaniline; 6, N, N-dimethylaniline.*

C_2H_5, and –C_6H_5. Examples of weakly deactivating groups are –F, –Cl, –Br and –I; moderately deactivating substituents are –CN, –SO_3H, –COOH, –COOR, –CHO, and –COR; strongly deactivating groups are –NO_2, –NR_3^+, –CF_3 and –CCl_3 [25]. Aromatic

species with electron donating substituents are expected to establish weaker π-π interactions with the NMM column than their aromatic solute counterparts with electron withdrawing substituents. In other words, the first class of solutes would interact mostly by hydrophobic interactions and to a lesser extent by π-π interactions while the second group of solutes would establish stronger π-π interactions in addition to hydrophobic interactions with the NMM column.

Aniline derivatives. Some alkyl-substituted anilines were chromatographed on the NMM column and for the sake of comparison on a commercial ODS column too (see Figs. 4a and 4b). These anilines derivatives are slightly more polar solutes than the preceding homologous solutes, requiring a mobile phase richer in water content to bring about their retention and separation. Under the conditions stated in Figure 6a, the plate count was about 11,000 plates/m. As can be seen in Figure 6a, adding an alkyl moiety to the aniline ring increased the solute retention proportionally to the size of the alkyl groups (weakly activating substituents); that is the aniline substituted with isopropyl is more retained than those substituted with ethyl or methyl group. This retention behavior parallels that obtained on the ODS column (compare Figure 6a to 6b). Also, adding methyl groups to the amino group resulted in higher retention of the solute. Despite the fact that the –NHR, $–NR_2$ groups are strong activating substituents of the benzene ring and the majority of interactions with the NMM column are based on the hydrophobicity of the solute, the level of π-π interactions seem to be significant. In fact, when comparing the retention pattern of the aniline solutes on the NMM column to that on the ODS column (compare Figure 6a to 6b) one can notice the full resolution of 4-isopropylaniline from *N*-methylaniline on the NMM column and their co-elution on the ODS column

despite the fact that the plate count of the ODS column was about 32,000 plates/m (3 times higher than that of the NMM column) indicating the presence of additional π-π interactions on the NMM column.

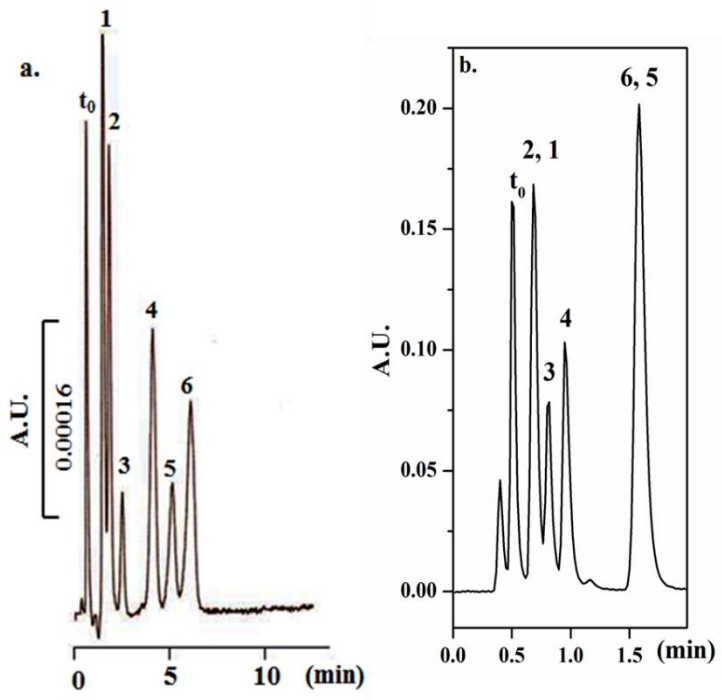

Figure 7. *Chromatograms of benzene derivatives obtained on (a) an NMM column (10 cm x 4.6 mm i.d.) and (b) an ODS column (4.5 cm x 4.6 mm i.d.). Conditions as in Figure 6. Peaks: t_0, thiourea; 1, phenol; 2, aniline; 3, cyanobenzene, 4, nitrobenzene; 5, toluene; 6, chlorobenzene*

Benzene derivatives. A series of experiments were conducted in which mono substituted aromatic compounds were analyzed with 55:45 (v/v) ACN:H_2O as mobile phase and the order of elution was found to be phenol (k = 1.03), aniline (k = 1.44), cyanobenzene (k =2.21), nitrobenzene (k = 4.23), toluene (k = 5.42) and chlorobenzene (k = 6.67) with an average plate count of 12,700 plates/m, see Figure 7a. This order of elution was not conserved on the ODS column. Another major difference was that the

retention and selectivity on the ODS column were lower and some of the peaks co-eluted. In fact, the k values were 0.42, 0.36, 0.58, 0.89, 2.10 and 2.01 for phenol, aniline, cyanobenzene, nitrobenzene, toluene and chlorobenzene, respectively. Note the insufficient selectivity between the aniline/phenol pair and chlorobenzene/toluene pair on the ODS column. While aniline is more polar than phenol and eluted first on the ODS column, the $-NH_2$ substituent seems to be less activating than the –OH substituent thus inducing stronger π-π interactions with the NMM column, which explains the higher retention of aniline than phenol on the NMM column (compare Figs 5a and 5b). Since –Cl is a deactivating substituent while $-CH_3$ is an activating substituent, it follows then that chlorobenzene is more retained and well resolved from toluene on the NMM column than on the ODS column. Despite the fact that the separation efficiency on the ODS column is about 2.5 fold higher than the NMM column (31,500 vs. 12,700 plates/m) the additional π-π interactions allowed improved selectivity and consequently a better spacing (i.e., resolution) between the peaks.

Phenol derivatives. To further gain insight into the retention behavior of aromatic solutes on the NMM column, the effects of activating OH substituent and deactivating Cl substituent were examined by chromatographing a series of phenol derivatives on the NMM and ODS columns. As expected, while phenol and catechol eluted on both columns in the order of decreasing polarity (i.e., catechol eluting first followed by phenol), the chlorophenols markedly exhibited π-π interactions with the NMM column in the sense that the retention increased proportionally with the number of chlorine substituents, see Figure 8. The k values for catechol, phenol, 2-chlorophenol, 3,4,5-

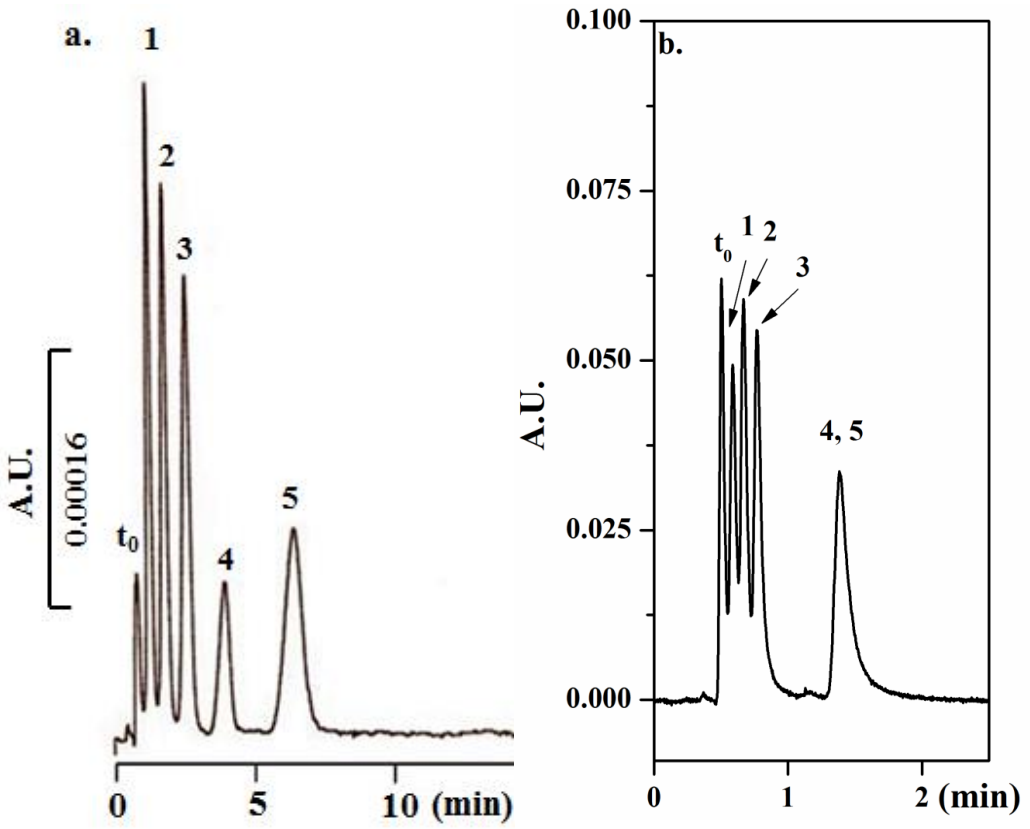

Figure 8. *Chromatograms of phenol and phenol derivatives obtained on (a) an NMM column (10 cm x 4.6 mm i.d.) and (b) an ODS column (4.5 cm x 4.6 mm i.d.) in (b). Conditions as in Figure 6. Peaks: t_0, thiourea; 1, catechol; 2, phenol; 3, 2-chlorophenol; 4, 3,4,5- trichlorophenol; 5, 2,3,4,5,6-pentachlorophenol.*

trichlorophenol and 2,3,4,5,6-pentachlorophenol were 0.42, 1.01, 1.83, 3.20 and 5.76, respectively, on the NMM column versus 0.24, 0.38, 0.58, 1.77 and 1.89, respectively, on the ODS column. Despite the average plate number was 2.5 times greater on the ODS column (20,650 plates/m on the ODS column vs. 8,300 plates/m on the NMM column) the much lower selectivity of the ODS column did not allow resolution of the

3,4,5-trichlorophenol and 2,3,4,5,6-pentachlorophenol solute pair, whereas on the NMM column this pair of solutes was very well resolved.

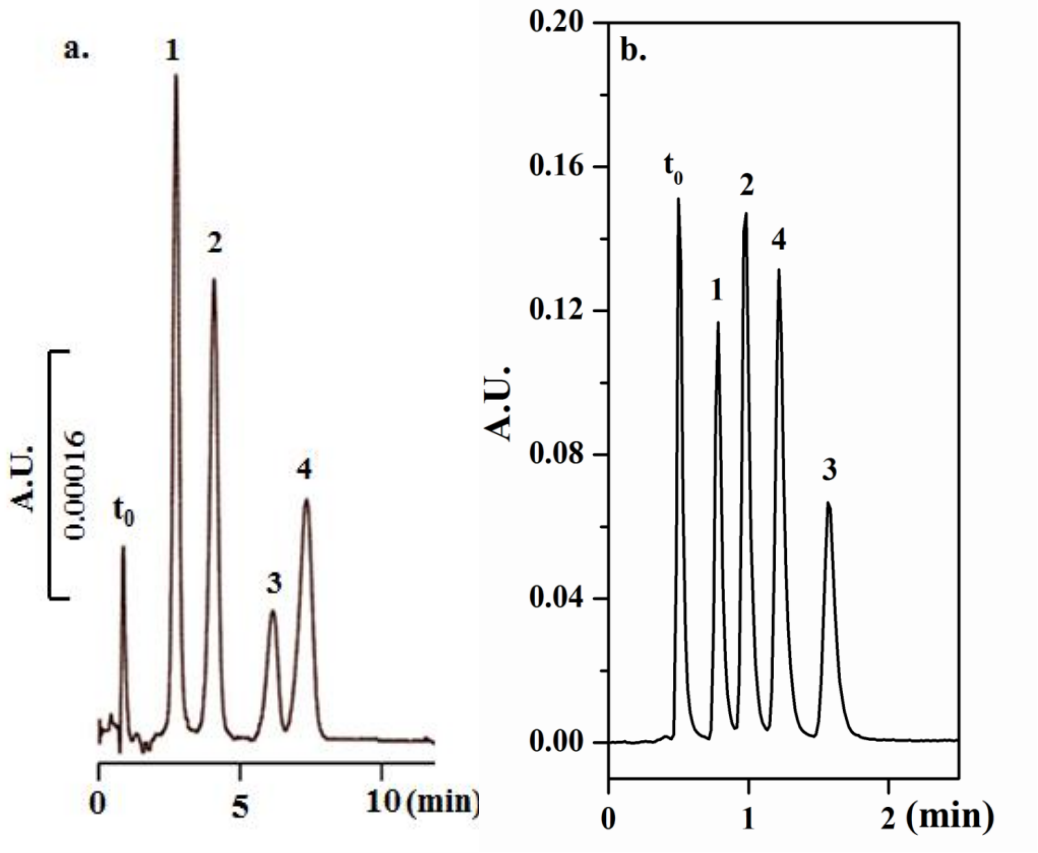

Figure 9. *Chromatograms of toluene and toluene derivatives obtained on (a) an NMM column (10 cm x 4.6 mm i.d.) and (b) an ODS column (4.5 cm x 4.6 mm i.d.) in (b). Conditions as in Figure 6. Peaks: t_0, thiourea; 1, m-toluidine; 2, m-tolualdehyde; 3, toluene; 4, m-nitrotoluene*

Toluene derivatives. In the aim of furthering the understanding of retention of aromatic solutes on the NMM column, a series of *meta*-substituted toluene compounds were analyzed on the NMM column. Figure 9 shows the order of elution, which is *m*-toluidine (k=1.82), *m*-tolualdehyde (k = 3.17), toluene (k = 5.59), *m*-nitrotoluene (k = 6.93). The average plate count is around 9,500 plates/m. This elution order reflects solute

polarity and its tendency of establishing π-π interactions with the NMM column. Besides being a polar group, $–NH_2$ in *m*-toluidine is also an activating substituent, thus explaining the weaker interaction of *m*-toluidine with the NMM column. In tolualdehyde, the –CHO is a moderately deactivating substituent and it is also less polar than $–NH_2$, thus providing more retention for tolualdehyde with respect to m-toluidine. Although toluene is more nonpolar than nitrotoluene, the presence of the strongly deactivating $–NO_2$ group in nitrotoluene makes this solute interact were strongly with the NMM column than toluene and it elutes last. This retention pattern is quite different from what was obtained on the ODS column. In fact, on the ODS column, the elution order of toluene and *m*-nitrotoluene was inverted with the former solute retained longer than the latter solute. The k values of *m*-toluidine *m*-tolualdehyde, toluene and *m*-nitrotoluene on the ODS column were 0.54, 0.94, 2.10 and 1.48, respectively.

Separation of proteins

The NMM column also proved useful in protein separation. In fact, 6 standard proteins including 5 basic and one quasi-neutral of differing molecular weights (M_r) and isoelectric points (pI) were readily separated under mild elution conditions using linear gradient elution at increasing ACN concentration in the mobile phase. The 6 proteins were ribonuclease A (M_r =13.7 kDa; pI = 9.6), cytochrome C (M_r = 14.4 kDa; pI =10.0-10.5), lysozyme (Mr = 14.3 kDa; pI = 9.3), β lactoglobulin A (M_r = 18.4 kDa; pI = 5.1), myoglobin (M_r = 17.5 kDa; pI = 6.88 and 7.33) and α chymotrypsinogen A (M_r = 25.67

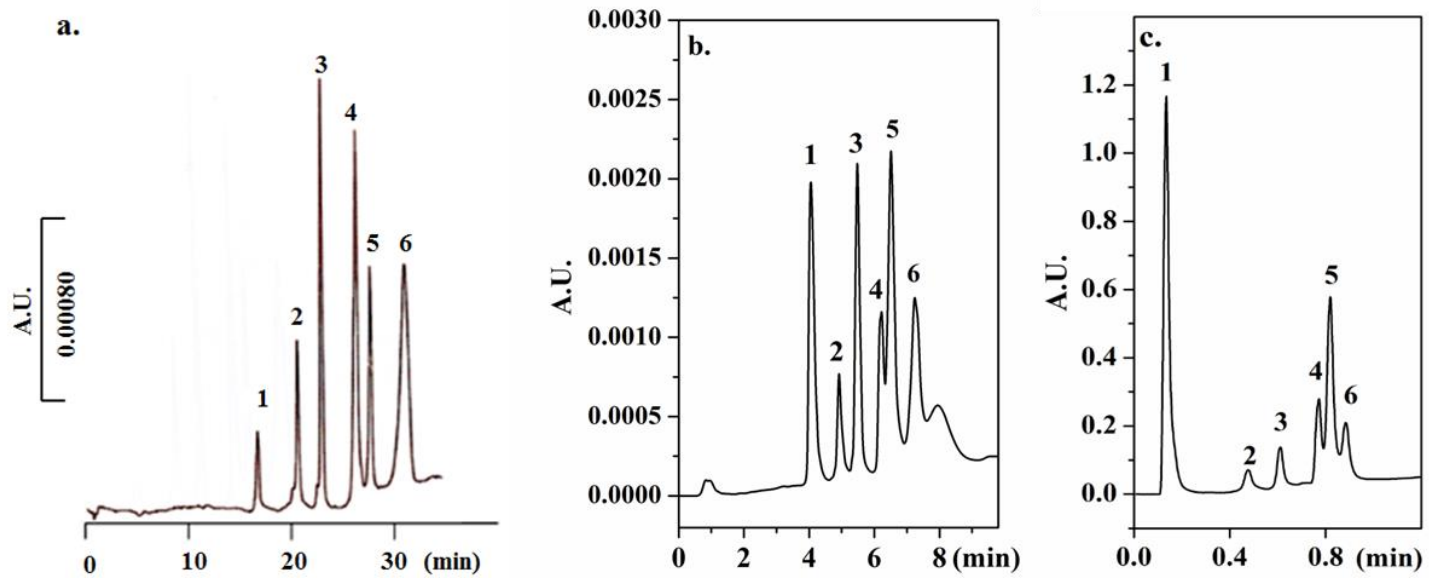

Figure 10. *Chromatograms of six standard proteins obtained on NMM column using shallow (a), steep (b) and ultra-steep (c) linear gradient elution at increasing ACN concentration in the mobile phase. Conditions: column dimensions, 10 cm x 4.6 mm i.d. in (a) and (b) and 3 cm x 4.6 mm i.d. in (c); flow rates, 1.00 mL/min in (a) and (b), 3.00 mL/min in c; mobile phase A, 5% v/v ACN in water at 0.05% v/v TFA; mobile phase B, 95% v/v ACN in water at 0.05% v/v TFA; UV detection at 214 nm. Gradient elution: 5-60% B in 30 in (a); 10-80% B in 10 min in (b); 15-60% B in 1 min. Peaks: 1, ribonuclease A; 2, cytochrome C; 3, lysozyme; 4, β-lactoglobulin A; 5, myoglobin; 6, α-chymotrypsinogen A.*

kDa; pI = 8.97). Figure 10 shows the separations under shallow and steep linear gradients at 1.0 mL/min using a 10 cm column by running the gradient either in 30 min or in 10 min, respectively. By shortening the column to 3.0 cm, a fast gradient of 1 min at a flow rate 3.0 mL/min could be achieved leading to fast separation in less than 1 min (see Figure 10c).

Conclusions

The NMM column with its hydrophobic surface and π-electron rich naphthyl ligands exhibited sufficient retention and selectivity toward various probe solutes, namely ABs, toluene, phenol and aniline derivatives. In addition, the NMM column proved useful in the separation of various standard proteins using linear gradient elution at increasing ACN concentration in the mobile phase at different rates including shallow, steep and ultra-steep rates, thus allowing protein separations at various speeds. Six standard proteins were readily separated on the NMM column using shallow (30 min at 1.0 mL/min), steep (10 min at 1.0 mL/min) and ultra-steep (1 min at 3.0 mL/min) linear gradient elution at increasing ACN concentration in the mobile phase using a 10 cm x 4.6 mm i.d. column in case of shallow and steep linear gradients and a 3 cm x 4.6 mm i.d. column for ultra-steep linear gradient. The column was mechanically highly stable at high mobile phase flow velocity with virtually “zero” compressibility over a long period of daily use with a wide range of mobile phase composition. These promising results make organic monolithic columns based on NAPM-TRIM co-polymer efficient and complimentary HPLC separation media to the existing traditional HPLC separation media.

References

1. Melander, W.R. and C. Horváth, *Reversed-phase chromatography,* in *High Performance Liquid Chromatography, Advances and Perspectives*, C. Horváth, Editor. 1980, Academic Press: New York. p. 113-319.
2. Euerby, M.R., P. Petersson, W. Campbell, and W. Roe, *Chromatographic classification and comparison of commercially available reversed-phase liquid chromatographic columns containing phenyl moieties using principal component analysis.* J. Chromatogr. A, 2007. **1154**(1–2): p. 138-151.
3. Goss, J.D., *Improved liquid chromatography of salicylic acid and some related compounds on a phenyl column.* J. Chromatogr. A, 1998. **828**(1-2): p. 267-271.
4. Große-Rhode, C., H.G. Kicinski, and A. Kettrup, *Comparison of two anthryl-modified silica stationary phases for the HPLC separation of PAHs and nitro-PAHs.* Chromatographia, 1990. **29**(9-10): p. 489-494.
5. Kimata, K., T. Hirose, K. Moriuchi, K. Hosoya, T. Araki, and N. Tanaka, *High-Capacity Stationary Phases Containing Heavy-Atoms for Hplc Separation of Fullerenes.* Anal. Chem., 1995. **67**(15): p. 2556-2561.
6. Gonzalez-Ruiz, V., A.I. Olives, and M.A. Martin, *Challenging cor-shell stationary phases with the separation of closely related anti-cancer compounds: performance studies and application to drug quantitation with multi-well plate clean-up.* J. Chromatogr. A, 2014. **1364**: p. 83-95.
7. Karenga, S. and Z. El Rassi, *Naphthyl methacrylate-based monolithic column for RP-CEC via hydrophobic and π-interactions.* Electrophoresis, 2010. **31**: p. 991-1002.

8. Karenga, S. and Z. El Rassi, *Naphthyl methacrylate-phenylene diacrylate-based monolithic column for reversed-phase capillary electrochromatography via hydrophobic and π interactions (pages 3200–3206).* Electrophoresis, 2010. **31**: p. 3200-3206.

9. Nondek, L., *Liquid chromatography on chemically bonded electron donors and acceptors.* J. Chromatogr. A, 1986. **373**(0): p. 61-80.

10. Brindle, R. and A. Klaus, *Stationary phases with chemically bonded fluorene ligands: A new approach for environmental analysis of pi-electron containing solutes.* J. Chromatogr. A, 1997. **757**(1-2): p. 3-20.

11. Reubsaet, J.L.E. and R. Vieskar, *Characterisation of pi-pi interactions which determine retention of aromatic compounds in reversed-phase liquid chromatography.* J. Chromatogr. A, 1999. **841**(2): p. 147-154.

12. Tanaka, N., Y. Tokuda, K. Iwaguchi, and M. Araki, *Effect of stationary phase structure on retention and selectivity in reversed-phase liquid chromatography.* J. Chromatogr. A, 1982. **239**(0): p. 761-772.

13. March, J., *Advanced organic chemistry: reactions, mechanisms, and structure*. 1985, New York: Wiley.

14. Jandera, P., *Advances in the development of organic polymer monolithic columns and their applications in food analysis—A review.* J. Chromatogr. A, 2013. **1313**(0): p. 37-53.

15. Jonnada, M., R. Rathnasekara, and Z. El Rassi, *Recent advances in nonpolar and polar organic monoliths for HPLC and CEC.* Electrophoresis 2015. **36**: p. 76-100.

16. Guiochon, G., *Monolithic columns in high-performance liquid chromatography.* J. Chromatogr. A, 2007. **1168**(1–2): p. 101-168.

17. Wang, Q.C., F. Svec, and J.M.J. Fréchet, *Macroporous polymeric stationary-phase rod as continuoius separation medium for rversed-phase chromatography.* Anal. Chem. , 1993. **65**: p. 2243-2248.

18. Oefner, P.J. and C.G. Huber, *A decade of high-resolution liquid chromatography of nucleic acids on styrene-divinylbenzene copolymers.* J. Chromatogr. B, 2002. **782**: p. 27-55.

19. Nischang, I., *On the chromatographic efficiency of analytical scale column format porous polymer monoliths: interplay of morphology and nanoscale gel porosity.* J. Chromatogr. A, 2012. **1236**: p. 152-163.

20. Vaast, A., H. Terryn, F. Svec, and S. Eeltink, *Nanostructured porous polymer monolithic columns for capillary liquid chromatography of peptides.* J. Chromatogr. A, 2014. **1374**: p. 171-179.

21. Trojer, L., S.H. Lubbad, C.P. Bisjak, and G.K. Bonn, *Monolithic poly(p-methylstyrene-co-1,2-bis(p-vinylphenyl)ethane) capillary columns as novel styrene stationary phases for biopolymer separation.* J. Chrom. A, 2006. **1117**(1): p. 56-66.

22. Bisjak, C.P., S.H. Lubbad, L. Trojer, and G.K. Bonn, *Novel monolithic poly(phenyl acrylate-co-1,4-phenylene diacrylate) capillary columns for biopolymer chromatography* J. Chromatogr. A, 2007. **1147**: p. 46-52.

23. Svobodova, A., T. Krizek, J. Sirc, P. Salek, E. Tesarova, P. Coufal, and K. Stulik, *Monolithic columns based on a poly(styrene-divinylbenzene-methacryluc acid)*

copolymer for capillary liquid chromatography of small organic molecules J. Chromatogr. A, 2011. **1218**: p. 1544-1547.

24. Tian, F., N. Cheng, N. Nouvel, J. Geng, and O.A. Scherman, *Site-Selective Immobilization of Colloids on Au Substrates via a Noncovalent Supramolecular "Handcuff".* Langmuir, 2010. **26**(8): p. 5323-5328.

25. Graham Solomons, T.W. and C.B. Fryhle, in *Organic Chemistry*. 2008, John Wiley & Sons, Inc. p. 650 - 653.

CHAPTER VI

REVERSED-PHASE CHROMATOGRAPHY METHOD DEVELOPMENT AND SELECTIVE PRE-COLUMN DERIVATIZATION STRATEGIES FOR THE ANALYSIS OF FATTY ACIDS IN OILS AND OTHER FOOD SAMPLES

Introduction

Fatty acids (FAs) are dispersed extensively in nature with a wide structural variety and serve as an important nutritional source for the living organisms through oxidation. FAs are found in various food samples that originate from plants and animals. The concentration range of these FAs is generally very broad and it varies from high abundance to very low trace levels. The study of the distribution of these FAs has high physiological and biological significance. FAs are the key quality indicators in food samples in recent times [1, 2]. Their assessment in various food samples at different stages of production, storage and marketing generally determines the price of the food product. A rapid, sensitive and reliable method for the detection of FAs, which can be applied to their quantification in complex food sample matrices, is always highly desirable.

Recently, with the increase in the public awareness, the knowledge of the FAs with increased structural details is needed, especially the knowledge of trans FAs. It is well known that different trans-FA isomers have their own biological significance [3]. However, the health benefits of the components of *trans*-FA [4], especially vaccenic acid (18:1 *trans*-11) which is present in the ruminant fats needs to be addressed in many food samples such as meat and milk. Vaccenic acid (18:1 *trans*-11) has a promising effect in the human FA metabolic pathway, since its occurrence is connected with a reduced threat of diabetes and heart failure [5]. Vaccenic acid in the FA metabolism serves as a major precursor for conjugated linoleic acids, which have been in recent times subject to major interest due to their benefits to human health [3, 6].

FAs generally lack chromophores in their structures and cannot be detected directly in LC. Therefore, GC and GC-MS have been widely used in their micro-scale analysis [7, 8]. However, GC suffers from many disadvantages and predominantly fails in the analysis of long chain FAs and heat labile compounds. Also, sample preparation techniques involved in the GC protocol are very laborious and generally involve the elimination of all potential non-volatile interferences from the sample, such as salts and proteins. In the case of HPLC, the analysis can be carried out at room temperature, which removes the risk of the decomposition of heat sensitive compounds, and the complex food samples can be analyzed by simple extraction protocols. HPLC also has an advantage of hyphenating with various types of detectors such as UV-VIS [9], evaporative light scattering detector [10], fluorescence [1, 7, 11-14] and MS detection [15]. Furthermore, HPLC separations can always be scaled up to a preparative format.

Generally, FAs show very little absorptivity in the ultraviolet region. Therefore, the efficient derivatization of the FAs with suitable reagents is essential for the detection of trace of FAs in complex food matrices. Apart from boosting their detectability, derivatization of FAs has many advantages such as reduced peak tailing and decreasing the polarity of FAs, which is advantageous especially in reversed phase chromatography (RPC). Therefore, derivatization of FAs with labelling agents is often adopted, especially fluorescence detection is implemented for its increased sensitivity [15] and low background in complex sample matrices. Many fluorescent tags were reported previously for the detection of FAs [7, 16-19]. In the current study, we report the highly sensitive detection of FAs by the extremely selective coupling of FAs with 6-aminoquinoline (6AQ) in the presence of *N, N*`-dicyclohexylcarbodiimide (DCC). The derivatizing agent 6AQ used in the current study showed excellent fluorescent properties with a straightforward reaction set up and the reaction was carried out at room temperature with minimal sample preparations.

This chapter can be divided into two sections. In the first, an fluorescent detection of FAs and their RPC separations were established on the in-house made naphthyl based organic monolithic column. This section reports on the FAs separation and detection on the novel monolithic column, which is followed by the separation of FAs in food samples and their quantification in oils. Secondly, the derivatized FAs were separated on commercially available silica based columns for more detailed insight of ultra-trace FAs in meat samples, especially vaccenic acid, which was successfully separated from oleic acid.

Experimental

Reagents and materials

Analytical grade FA standards, namely, enanthic acid (7:0), caprylic acid (8:0), capric acid (10:0), lauric acid (12:0), myristic acid (14:0), palmitic acid (16:0), stearic acid (18:0), nonadecylic acid (19:0), arachidic acid (20:0), behenic acid (22:0), lignoceric acid (24:0) and unsaturated FAs such as linoleic acid (18:2), linolenic acid (18:3), oleic acid (18:1, *cis*-9), vaccenic acid (18:1 *trans*-11) were obtained from Sigma Chemicals (St. Louis, MO, USA). Also, polyoxyethylene sorbitan monolaurate (Tween 20) was obtained from Sigma. Trifluoroacetic acid and *N, N*`-dicylclohexylcarbodiimide were obtained from Alfa Aesar (Wardhill, MA, USA). Analytical grade sodium hydroxide was from EMD Chemicals Inc. (Darmstadt, Germany) and hydrochloric acid was purchased from Fischer Scientific Co. (Fair Lawn, NJ, USA). The derivatizing agent 6-aminoquinoline (6AQ) was obtained from Aldrich Chemicals (Milwaukee, WI, USA). Analytical grade chloroform was obtained from EM Science (Gibbstown, NJ, USA) and HPLC grade acetonitrile was obtained from Pharmaco-Aaper (Brookfield, CT, USA).

HPLC instrumentation and procedures

All HPLC separations were performed on a Waters (Milford, MA, USA) Alliance 2690 separations module, equipped with an in-line degasser, a quaternary pump, an auto sampler and a thermostated column compartment. The data acquisition was carried out by using Empower 2 (Build 2154) software (Waters Chromatography). The detection was carried out using a Waters fluorescence detector (Model 2475) with excitation

wavelength (λ_{exc}) set at 270nm and the emission wavelength (λ_{emi}) set at 495 nm. For stirring the samples and the FA standards a Titertek shaker from Titertek Instruments, (Huntsville, AL, USA) was used and for the extraction of FAs from the meat samples A Corning hot plate model PC 35 (Corning, NY, USA), a Vortex mixture (Baxter Diagnostics, Deerfield, IL, USA) and a Sorvall RC 5C plus centrifuge (Kendro Laboratory Products, Newtown, CT, USA) were also used.

Chromatographic separations were performed on two commercially available HPLC columns (15 cm x 4.6 mm i.d.) packed with 5 µm wide pore C4 functionalized silica particles (C4 column) (J.T Baker Inc., Phillipsburg, NJ, USA), a 5 µm Nucleosil CN functionalized silica (CN column) (15 cm x 4.6 mm i.d.) and an in-house synthesized naphthyl functionalized organic monolithic column (NMM column) (10 cm x 4.6 mm i.d.) based on our previous publication [20] (see also Chapter V).

The sample and the column compartments in the HPLC instrument were maintained at ambient temperatures. Water was filtered through a 0.45-µm membrane (Millipore, Bedford, USA) before use. During the gradient analysis, the columns were equilibrated with 10-15 column volumes with the mobile phase A before the next injection. Mobile phase A was used as sample diluent for all the gradient runs and the injection volumes were 10 µL and all the readings were measured in triplicate during the entire data collection process to ensure repeatability.

Extraction of FAs from oils

Triglycerides in the oil samples were hydrolyzed to free FAs using base catalyzed ester hydrolysis. A stirred solution containing a 1 g of sample in 5 mL of 0.05% Tween 20 prepared in 1.0 M aqueous NaOH in a 20.0 mL round-bottomed flask was refluxed in

a water bath at 70 ˚C for 3 h. The reaction mixture was cooled to room temperature, acidified with 6.0 M HCl solution (5.0 mL), extracted with chloroform (5.0 mL), dried over anhydrous sodium sulfate, and used as such for further derivatization.

Extraction of FAs from meat samples

A 1.0 g pulverized sample was weighed into a 50 mL extraction tube and 10 mL of extraction mixture (chloroform: methanol, 2:1, v/v) was added and gently shaken for 1 min to facilitate the proper mixing of the sample and solvent which were then vortexed for 1 min. The contents were filtered through a Whatman #1 filter paper to remove any suspended solid impurities and then aqueous impurities were removed by extraction with 6.6 mL of 0.73% aq NaCl solution. This extraction was repeated twice and the collected organic layer was centrifuged at 3000 rpm (22 ˚C) for 20 min. After the centrifugation, the supernatant layer was discarded and lipid fraction was dried with one scoop of sodium sulfate for 1 h. The contents were then transferred to a 10 x 125 mm Kimble and anhydrous sodium sulfate was washed with chloroform. This was followed by the evaporation of the organic layer by placing the tubes on a heating block at 45 ˚C under nitrogen for 2 h. The extracted fat was collected and stored in the refrigerator until the derivatization step.

Derivatization procedure

The derivatization reaction was performed according to the reaction scheme presented in Figure 1. To a standard FA or the sample solution in $CHCl_3$ in a 2.0 mL

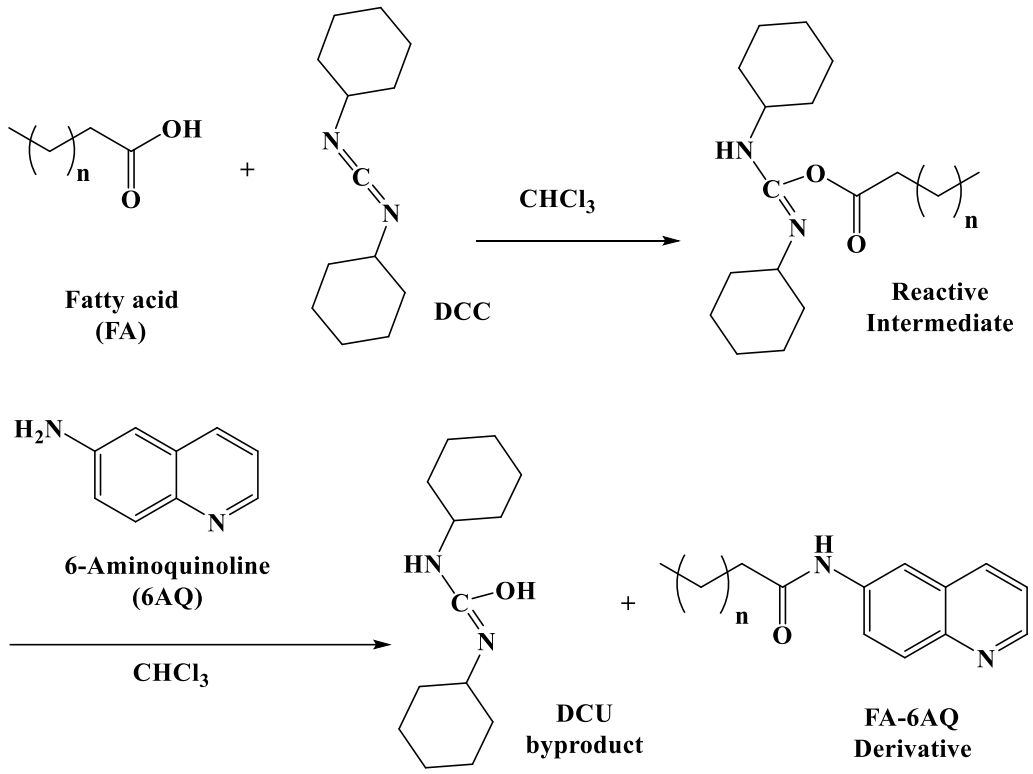

Figure 1. *Derivatization reaction pathway of FA by a direct condensation reaction between the FA and 6AQ promoted by DCC. (I) Activation of the FA by DCC. (II) Fluorescent labeling with 6AQ.*

amber colored vial, 100 µL of 500 mM DCC in chloroform was added and the solution was stirred at room temperature for 30 min. To this reaction mixture, 100 µL of 500 mM 6AQ was added and the stirring was continued for 12 h. The resulting reaction mixture was centrifuged and an aliquot of the supernatant was diluted using ACN that was further diluted with the mobile phase A before injecting into the HPLC system.

Quantification and validation of standard FA derivatives

Saturated standard FAs with varying chain lengths from 7:0 to 24:0 were chosen to establish the quantitation procedure. In addition, the most prevalent unsaturated FAs in food sample such as linolenic acid (18:3), linoleic acid (18:2) and oleic acid (18:1 *cis*-9) were also selected for the quantification process. Vaccenic acid (18:1 *trans*-11) was also quantified, which is a positional isomer for oleic acid (18:1 *cis*-9) with varying double bond position. In all cases, the aforementioned derivatization scheme was used.

The individual FA derivatives were identified according to the retention times of standards and chromatographic peak heights were used for the quantification. The relative retention times (RRT) of the FAs were calculated with respect to palmitic acid (16:0). Appropriate amounts of pure FA standards were derivatized according to the method outlined above in chloroform solvent and then diluted in acetonitrile which was further diluted with their respective mobile phase A before injection into the HPLC system.

Results and discussion

The maximum absorbance of FAs and its methyl esters are generally located at lower wavelengths (205 nm), which render their detectability very difficult, especially in

real food samples, which are associated with complex backgrounds. Previously, our lab has introduced a derivatization method for the sensitive detection of carbohydrates [21], and gangliosides [22]. Now, we demonstrate here a method where the carboxylic acid groups of the extracted FAs are tethered with 6AQ to form an amide in the presence of DCC. The feature of 6AQ derivatization is very promising in that the emission and excitation wavelengths of the derivatives are farther apart. In fact, 6AQ derivatives fluoresce (λ_{emi}) at 495 nm when excited at (λ_{exc}) 270 nm. Also, DCC's role is well known as a coupling reagent in peptide synthesis. Many reports were published where carbodiimide chemistry proved useful in the incorporation of a chromophore/fluorophore for UV and fluorescence detection [1]. The derivatization follows the reaction scheme shown in Figure 1, where the DCC and the carboxylic acid of the FAs react to form an anhydride, the reactive intermediate and subsequent nucleophilic attack of the amino group of 6AQ leading to the formation of an amide and insoluble by-product dicyclohexyl urea. In order to optimize the conditions for the derivatization reaction, especially the time of the reaction, a reaction monitoring experiment was performed between equimolar concentrations of FA and 6AQ. The progress of the derivatization reaction was monitored using HPLC, where peak areas of the unreacted 6AQ and the formed derivative (FA-6AQ) were recorded with respect to time. Equimolar concentrations of palmitic acid (16:0) and DCC reagents were added to 20 mL round-bottomed flask and stirred for 30 min. To this, equimolar amount of 6AQ was added and 10 µL aliquots were used as a representative sample for reaction monitoring and analyzed by HPLC for peak purity. The purity of the formed derivative FA-6AQ with respect to the reactant 6AQ was assessed by means of a gradient elution from mobile phase A (0.1

% (v/v) TFA in 5% ACN) to mobile phase B (0.1 % (v/v) TFA in 95% ACN). A flow rate of 1.00 mL/min was maintained with a linear gradient of 0-100 % B in 30 min. Typical overlay of obtained chromatograms is shown in Figure 2A.

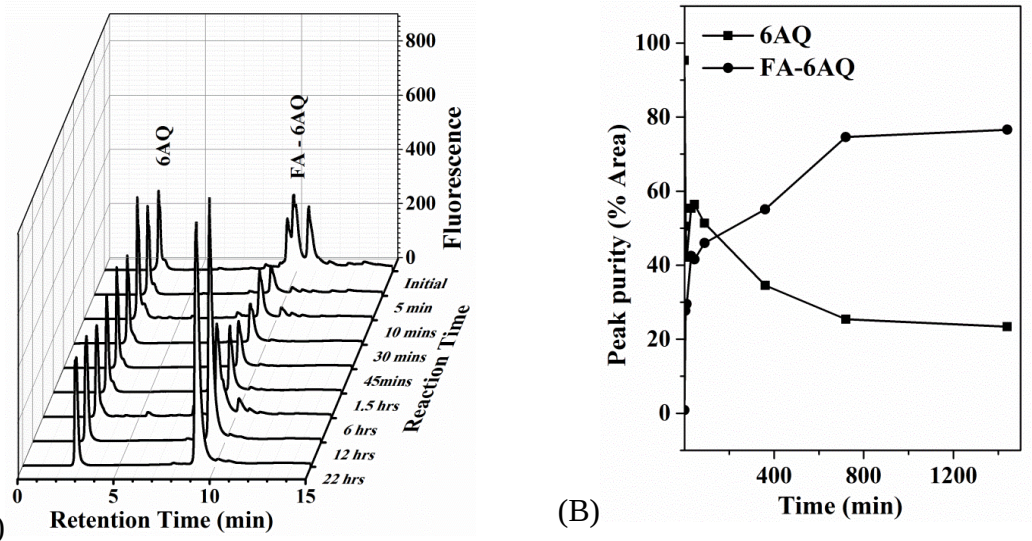

Figure 2. *Monitoring of the derivatization reaction of palmitic acid (16:0) with 6AQ in the presence of DCC. (A), Overlay of the chromatograms at various time intervals. (B), time course of the reaction in terms of % of the peak areas of both the reactant (6AQ) and the product (FA-6AQ). HPLC conditions: Mobile phase A, 0.1 %(v/v) TFA in 5% ACN, mobile phase B, 0.1% (v/v) TFA in 95% ACN; gradient program, 0-100 % B in 30 min; flow rate: 1.00 mL/min; fluorescence detection, excitation (λ_{exc}) at 270 nm and emission wavelengths (λ_{emi}) at 495 nm.*

The peak areas of the unreacted 6AQ and the derivative FA-6AQ were assessed to monitor the progress of the reaction. The progress of the reaction with respect to time is shown in Figure 2B, where peak purities of the reactant (6AQ) and product (FA-6AQ) are plotted versus the reaction time. The reaction reached a steady state in 12 h at

constant stirring with a % peak area of 74.63%, which was slightly increased to 76.60% at 24 h reaction time. Consequently, a 12 h reaction time was maintained for the derivatization process.

Chromatographic evaluation of FA-6AQ derivatives on the in-house naphthyl column

As per our first aim, the retention of FAs was studied on the napthyl functionalized organic monolithic column (NMM column), This column was designed in our laboratory, and was a "state of art" monolithic column which and has been explored for its application in the separation of both small and large molecules [20]. In general, monolithic columns are supposed to have a characteristic large pore size, which is appropriate for the separation of FAs especially these with a the long carbon chain. Also, the NMM column has an additional advantage of π-π interactions between the 6AQ tag of the solutes and the naphthyl functionality of the stationary phase making it an ideal separation column for FA-6AQ derivatives. Water and ACN were chosen as mobile phase solvents for the reversed-phase gradient elution with 0.05-0.1 % (v/v) TFA as a mobile phase additive. TFA facilitated the early elution of unreacted 6AQ (pKa = 5.63) with a sharp peak at $t_{0,}$ since it is positively charged at acidic pH. Therefore, it can be presumed that the retention of the FAs is primarily due to the hydrophobicity of the FA chain in the FA-6AQ structure. To study the retention behavior of the FA-6AQ derivatives on the NMM column, various saturated FAs with varying chain lengths from 3:0 to 24:0 were analyzed. The logarithmic retention factor (log k) of the saturated FA-6AQ derivatives was plotted versus the ACN concentration in the mobile phase (see Figure 3(A)). The plots were linear with R^2 values greater than 0.99 in all the cases indicating that the change in the ACN content of the mobile phase affected the retention

of the FAs from myristic acid (14:0) to lignoceric acids (24:0). Correspondingly, the dependence of log k on the carbon number in the FA chain at different ACN concentrations in the mobile phase is plotted in Figure 3(B). The slopes of the lines varied drastically at different ACN concentrations. At 30% ACN in the mobile phase the slope of the line is 0.4762, which changed substantially to 0.2736 at 35% ACN and gradually decreased to 0.1025 at 75 % ACN in the mobile phase. This plot gives us an estimate of the k values of various FAs based on their chain lengths and thus facilitates the design of the desired linear gradient program based on the nature of the FAs present in the sample.

The complete separation of saturated FA-6AQ derivatives is shown in Figure 4. The gradient program used was for 30 min with 95% ACN in the eluting mobile phase. Baseline separation was achieved for the studied FAs up to palmitic acid (16:0) at 15 min after which stearic (18:0), nonadecanoic (19:0), and arachidic (20:0) acids co-eluted at around 20 min. Thereafter, behenic (22:0) and lignoceric (24:0) acids were baseline separated and this may be due to the two carbon number difference in the chain length between the two acids. A gradient delay at 15- 20 min at 50% of mobile phase B did improve the separation of co-eluting FAs to some extent (for the gradient elution conditions see Figure 4). Therefore, the gradient elution should be carefully programmed to get maximum separation of all the available FAs present in the sample on the NMM column. The overall peak shapes were sharp for almost all the FAs and minimal broadening was observed for FAs of chain lengths greater than 20:0. This might be an attractive feature for the NMM column.

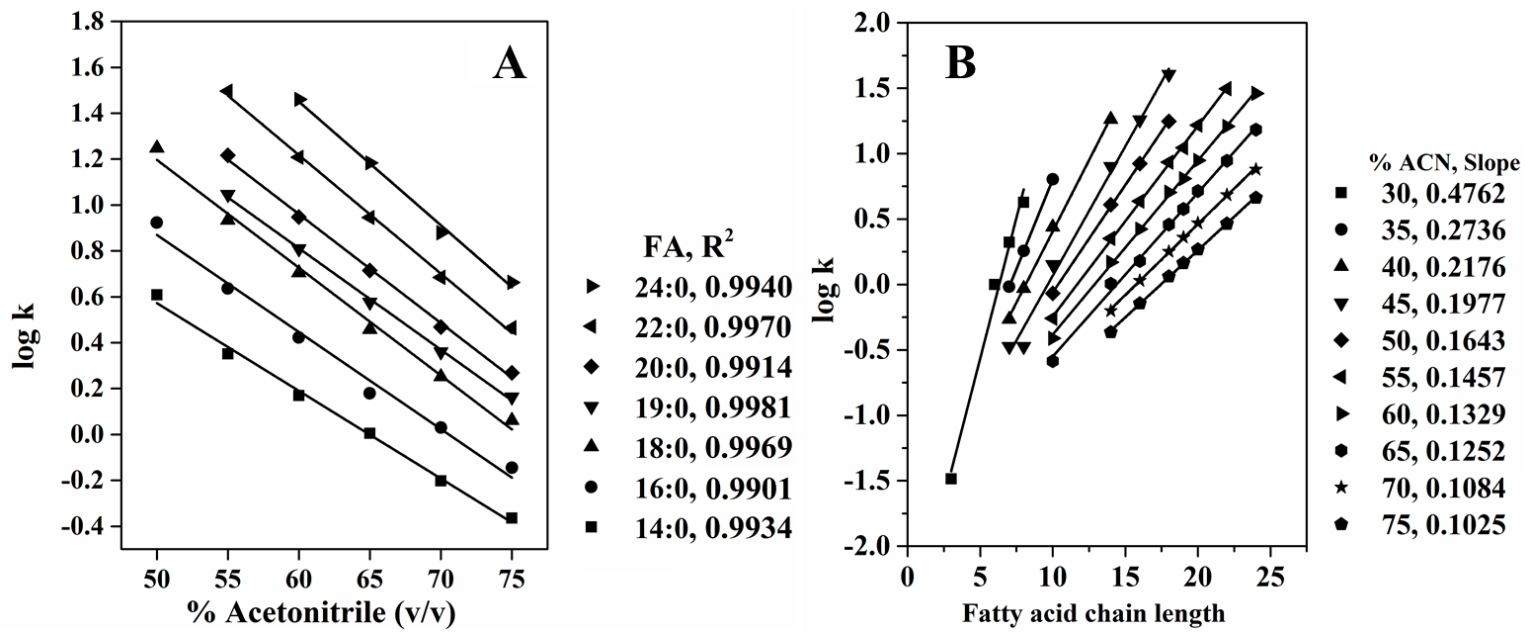

Figure 3. *(A), Plots of log k of FAs vs. %ACN in the mobile phase; column, NMM, 10 cm x 4.6 mm i.d. (B), Plots of log k of the FA-6AQ derivatives vs. the carbon number of the FAs at various acetonitrile concentrations in the mobile phase.*

Chromatographic evaluation of FA-6AQ on silica based columns

The retention of FA-6AQ derivatives were further investigated on commercially available silica based columns. The method development started by testing the separation of FA-6AQ on three columns, namely C18 Zorbax (8 cm x 6.2 mm i.d.) column packed with 3 µm end capped silica particles, C18 Spherisorb (15 cm x 4.6 mm i.d.) packed with 5 µm particles and C8 Zorbax (15 cm x 4.6 mm i.d) column packed with 5 µm silica particles. When tested in the separation of FA-6AQ, all of these columns proved ineffective even at high ACN concentrations (chromatograms not shown); meaning that virtually no elution of the FA-6AQ derivatives were obtained. The high surface area offered by silica particles along with the high hydrophobicity of C8 and C18 ligands on the stationary phase surface led to the irreversible binding of the FA-6AQ derivatives onto the nonpolar columns. So, the next step in the method development was the obvious choice for a butyl column and a cyanopropyl column, both with shorter alkyl chains, and consequently lower hydrophobicity. Columns (15 cm x 4.6 mm i.d.) packed with 5 µm silica particles functionalized with butyl (C4 column) and cyanopropyl (CN column) were tested in the separation of saturated FA-6AQ derivatives. Figure 4 shows the elution profile of saturated FA-6AQ derivatives. For the CN column, excellent baseline separation was obtained up to FAs equal to chain length of palmitic acid (16:0), which was at 8.80 min (for gradient program refer to Figure 4). Thereafter, the peaks of the higher chain length FAs broadened. The gradient program used was for 30 min, however a further increase in the gradient time did not improve the peak shapes and separation of FAs above 14:0. On the other hand, the C4 column gave baseline separation for all the FA-6AQ derivatives up to lignoceric acid (24:0). The delay in the eluting mobile phase

was carefully programmed for 25 min and 40 min as shown in Figure 4 to achieve an absolute baseline separation of all the FAs, especially FA-6AQ derivatives in the chain length region of 16:0 to 22:0. For the gradient conditions, refer to the respective figure captions. Based on the obtained results, it can be stated that so far, the NMM, CN and C4 column were effective in the separation of saturated FA-6AQ derivatives.

Along with the saturated FAs that were analyzed in the preceeding sections, the most common other unsaturated fatty acids such as linolenic acid (18:3), linoleic acid (18:2), oleic acid (18:1 *cis*-9) and vaccenic acid (18:1 *trans*-11) were also derivatized and analyzed on the NMM, CN and C4 columns. The separation of this total mixture of FAs was tested on all the three different columns and the chromatograms are shown in Figure 5. For the NMM column, a typical reversed phase behavior was observed in which an increased degree of unsaturation in the FAs resulted in the decrease of the retention times. Correspondingly, the induced dipole-dipole interactions between the double bonds of the FAs and the triple bond in the nitrile group of the acetonitrile may also play an important role in their early elution [9]. Here π-π interactions between the double bonds and the naphthyl stationary phase were dominated by the hydrophobic interactions present between the FA chain and the stationary phase. The chromatogram showing the complete separation of the total set of FAs chosen is shown in Figure 5. For the NMM column, the elution of 6AQ-FA derivatives was achieved in less than 60 min and the peak broadening of the highest FA was minimal and this is a desirable feature of NMM towards the separation of FAs, especially the one with high carbon chain lengths.

A partial separation of the FA-6AQ derivatives was observed on the NMM

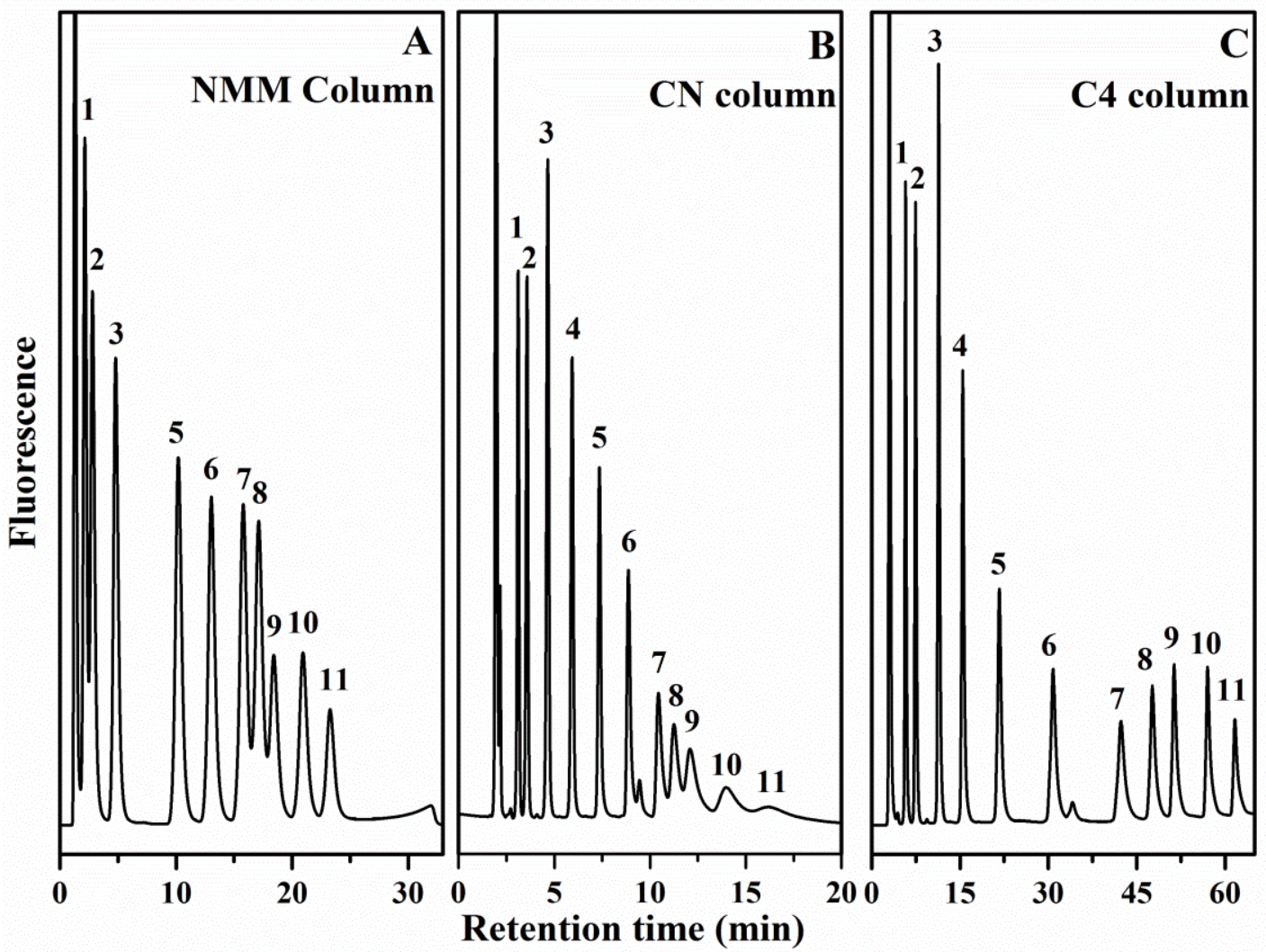

(Figure caption in the next page)

Figure 4. *Separation of saturated FA-6AQ derivatives. (A), NMM column, 10 cm x 4.6 mm i.d.; mobile phase A, 0.1 %(v/v) TFA in 40% ACN, mobile phase B, 0.1% (v/v)95% ACN; gradient program, % B 0/50/50/100 in 5/15/20/30 min. (B), CN column, 15 cm x 4.6 mm i.d.; mobile phases A and B, same as in (A); gradient program, % B 0/80/80 in 5/30/35 min. (C), C4 column, 15 cm x 4.6 mm i.d.; mobile phases A and B, same as in (A) and (B); gradient program, % B 0/25/40/90/90 in 0/10/40/65/75 min. For (A), (B) and (C); flow rate, 1.00 mL/min; fluorescence detection, excitation (λ_{exc}) at 270 nm and emission wavelengths (λ_{emi}) at 495 nm. Peak labels: 1, enanthic acid (7:0); 2, caprylic acid (8:0); 3, capric acid (10:0); 4, lauric acid (12:0); 5, myristic acid(14:0); 6, palmitic acid (16:0); 7, stearic acid (18:0); 8, nonadecanoic acid (19:0); 9, arachidic acid (20:0); 10, behenic acid (22:0); 11, lignoceric acid, (24:0).*

column. The elution of unsaturated FA derivatives that are used in the current study such as linolenic (18:3), linoleic (18:2) and oleic (18:1 cis 9) acid derivatives interferred with the retention times of FAs that elute between myristic (14:0) and stearic (18:0) acid derivatives in the chromatogram. Due to the characteristic broad peaks of the monolithic column, the FAs eluting in this region co-eluted and baseline separation was not achieved. When it comes to the separation of FA geometric isomers, the cis isomers are expected to elute before the trans isomers [23]. In the case of the NMM column, the separation between the positional isomers vaccenic acid (18:1, *trans*-11) and oleic acid (18:1 *cis*-9) is partial, where the vaccenic acid derivative retention peak shouldered with the derivative of oleic acid. By carefully tuning the gradient program the resolution

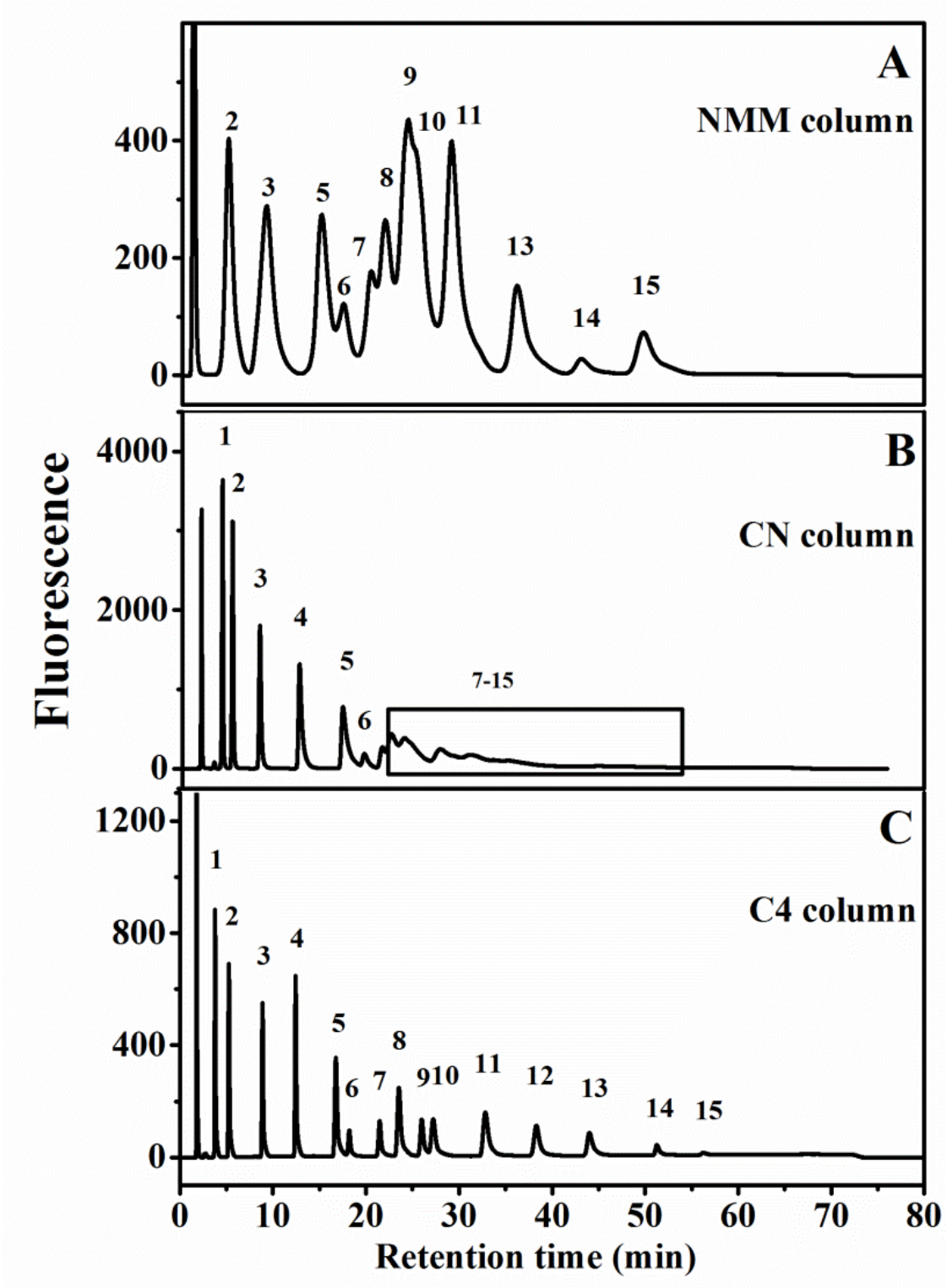

Figure caption in the next page

Figure 5. *Separation of 6AQ derivatives of total set of saturated and unsaturated FA. (A), NMM column, 10 cm x 4.6 mm i.d.; mobile phase A, 0.1 % (v/v) TFA in 35% ACN, mobile phase B, 0.1% (v/v) TFA in 80% ACN in water; gradient program, %B 10/90/90 in 0/60/70 min. (B), CN column, 15 cm x 4.6 mm i.d.; mobile phase A, 0.1 % (v/v) TFA in 30 % ACN, mobile phase B, 0.05% (v/v) TFA in 70% ACN; gradient program, % B 0-80 in 60 min. (C), C4 column, 15 cm x 4.6 mm i.d. ; mobile phase A, 0.1 % (v/v) TFA in 30% ACN, mobile phase B, 0.05% (v/v) TFA in 90%; gradient program, % B 025/40/90/90 in 0/10/40/65/70 min. For A, B and C; flow rate, 1.00 mL/min; fluorescence detection, excitation (λ_{exc}) at 270 nm and emission wavelengths (λ_{emi}) at 495 nm. Peak labels: 1, enanthic acid (7:0); 2, caprylic acid (8:0); 3, capric acid (10:0); 4, lauric acid (12:0); 5, myristic acid(14:0); 6, linolenic acid (18:3); 7, linoleic acid (18:2); 8 , palmitic acid (16:0); 9, oleic acid (18:1 cis-9); 10 trans-vaccenic acid (18:1 trans-11); 11, stearic acid (18:0); 12, nonadecanoic acid (19:0); 13, arachidic acid, (20:0); 14, behenic acid (22:0); 15, lignoceric acid, (24:0).*

between the palmitic acid (16:0), linoleic acid (18:2), linolenic acid (18:3) and oleic acid (18:1, *cis* -9) was greatly improved (chromatogram not shown) but the separation of geometrical isomers oleic acid and *trans*-vaccenic acid could not be achieved. The CN column gave no resolution for all FAs above 14:0 and the unsaturated FA derivatives gave characteristic broad peaks, which merged with the elution of FA derivatives of chain length greater that 16:0. So, for further analysis of the samples, the CN column was not used. Finally, excellent baseline separation was achieved for the combined mixture of both saturated and unsaturated FAs on the C4 column under optimized conditions with

ACN as eluting mobile phase and 0.1 % (v/v) TFA as the additive (for column dimension and the conditions refer to Figure 5). All of the 15 standard FA derivatives were effectively separated and baseline resolution was achieved. The positional isomers oleic acid (18:1, cis -9) and vaccenic acid (18:1 trans 11) were separated with baseline resolution, which eluted at 25.9 min and 27.3 min, respectively. The higher carbon chain FAs, which elute after 40 min, namely, arachidic acid, 20:0 (43.8 min), behenic acid, 22:0 (51.2 min) and lignoceric acid, 24:0 (56.4 min) have characteristic broad peaks due to the relatively narrow pore size of the silica column when compared to the NMM column.

The method validation included the establishment of the linearity of the detector response, quantification limits, and precision of the analytical procedure. The validation procedure was carried out for both the NMM and C4 columns. For the NMM column two FA standard mixtures were prepared, one with saturated FAs and the other mixture containing unsaturated FAs, namely, linoleic acid (18:2), linolenic acid (18:3) and oleic acid (18:1, *cis*-9) and were derivatized with 6AQ. The calibration solutions were diluted at 5 different levels and then analyzed under optimized conditions. For the NMM column, the two mixtures were analyzed in two different gradient elution conditions (refer to Table 1 for the calibration values). Excellent correlation coefficients were obtained for all of the FAs and are in the range of 0.9978-0.9993 and the % relative standard deviations (% RSD) of the intraday repeatability (n = 3) are also in the range of 0.3-10.6. Even the higher chain FA derivatives also produced acceptable % RSD values. The complete set of calibration curves for all the FAs is presented in Figure 6. The limit of detection of the saturated FA sample mixture was at concentration level of 5 nM,

which corresponds to a signal to noise ratio of 3. The limit of quantification was found to be 20 nM, which corresponds to a signal to noise ratio of 10.

A total number of 15 FA-6AQ derivatives were calibrated on the C4 column (for chromatographic conditions, refer to Figure 5).The linear regression equation, limit of detection and precision (intraday repeatability) were the method validation parameters that were evaluated in the current study. The values obtained are tabulated in Table 2. The R^2 values obtained are in the range 0.9964-0.9665, and the % RSD values for the intraday repeatability were in the range 0.1-28.2. The R^2 values gradually decreased from 0.9964 to 0.9665 as the length of the FA chain analyzed increased and the % RSD values were high, especially for behenic (22:0) and lignoceric acids (24:0), the % RSD values increased up to 23.2 and 28.2 at 10 µM sample concentration. This might be due to the strong interactions of the long chain FA with C4 functionalized silica particles. For the calibration graphs refer to Figure 7. As described in the preceding sections, a signal to noise ratio of 3 and 10 were used in calculating the limit of detection and limit of quantification, respectively, and the values are tabulated in Table 2. The calibration curves of all the FAs plotted along with their % RSD values are presented in Figure 7. The extent of linearity was determined by the limit of solubility of the FA mixture in the sample diluent (mobile phase A). A concentration of 40 µM was found to be the threshold limit of solubility for the FAs in the given sample diluent. Higher chain FAs such as behenic (22:0) and lignoceric (24:0) acids have detection limits up to only 20 µM.

TABLE 1

LOD AND LINEAR RANGE OBTAINED ON THE NMM COLUMN

FA derivative	Linear Range (µM)	y = mx + c	R^2	RSD (n=3) (intraday)^	LOD (nM)*
Caprylic acid(8:0)	0.02-40	y = 8379.4x + 183.29	0.9993	0.6-5.2	5
Capric acid(10:0)	0.02-40	y = 15518x - 578.54	0.9956	0.3-10.6	5
Lauric acid (12:0)	0.02-40	y = 17579x - 445.61	0.9977	0.7 4.9	5
Myristic acid(14:0)	0.02-40	y = 19641x - 312.69	0.9988	0.6-4.4	5
Palmitic acid (16:0)	0.02-40	y = 8047.2x - 213.34	0.9947	0.4-5.4	5
Stearic acid (18:0)	0.02-40	y = 19118x - 618.79	0.9979	0.6-7.9	5

*s/n ratio is 3 at 10 µL injection volume

^RSD: %relative standard distribution of the calibration plot

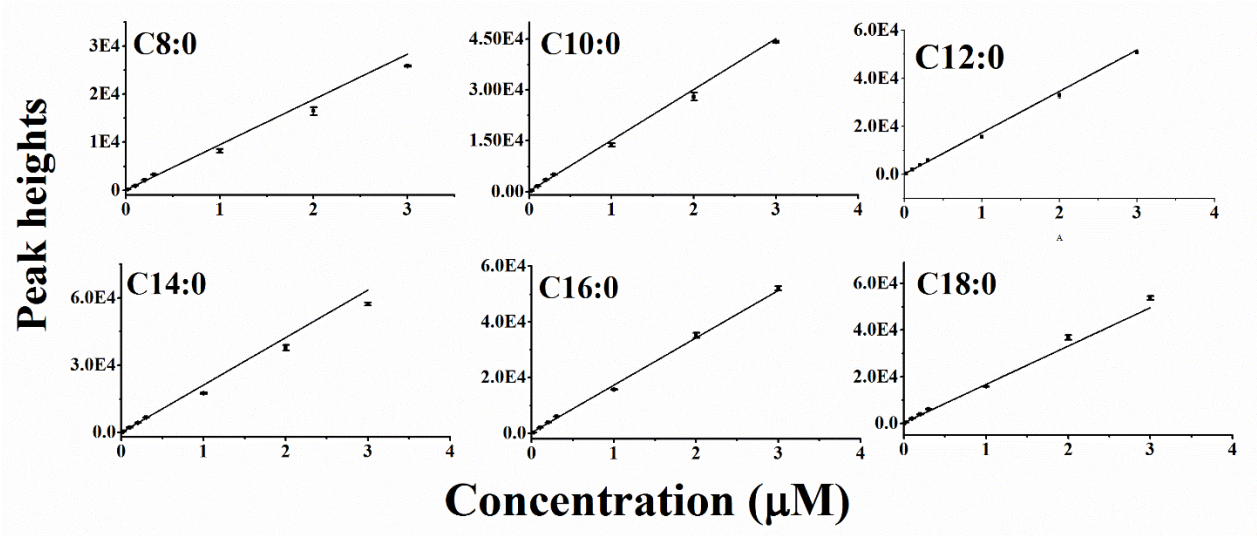

Figure 6. *Calibration of various FAs in the NMM column.*

TABLE 2

LOD AND LINEAR RANGE OBTAINED ON BUTYL SILICA COLUMN

FA derivative	Linear Range (µM)	y = mx+c	R^2	RSD (n=3) (intraday)^	LOD (nM)*
Capric acid(10:0)	0.02-40	y = 149655x - 37118	0.9927	1.8-11.4	5
Lauric acid (12:0)	0.02-40	y = 171642x - 24357	0.9974	0.3-10.4	5
Myristic acid(14:0)	0.02-40	y = 99978x - 41300	0.9981	0.1-13.9	5
Linolenic acid (18:3)	0.5-40	y = 22418x - 14853	0.9512	2.6-11.6	20
Linoleic acid (18:2)	0.5-40	y = 31976x - 18868	0.9912	0.4-9.9	20
Palmitic acid (16:0)	0.02-40	y = 68106x - 45031	0.9958	1.6-8.3	5
Oleic acid (18:1 *cis* 9)	0.02-40	y = 34461x - 29510	0.9858	2.7-13.5	5
Vaccenic acid (18:1 *trans* 11)	0.02-40	y = 36751x - 3301.8	0.9670	1.2-8.2	5
Stearic acid (18:0)	0.02-40	y = 50608x - 34695	0.9488	2.8-11.7	5

*s/n ratio is 3 at 10 µL injection volume

^RSD: % relative standard distribution of the calibration plot

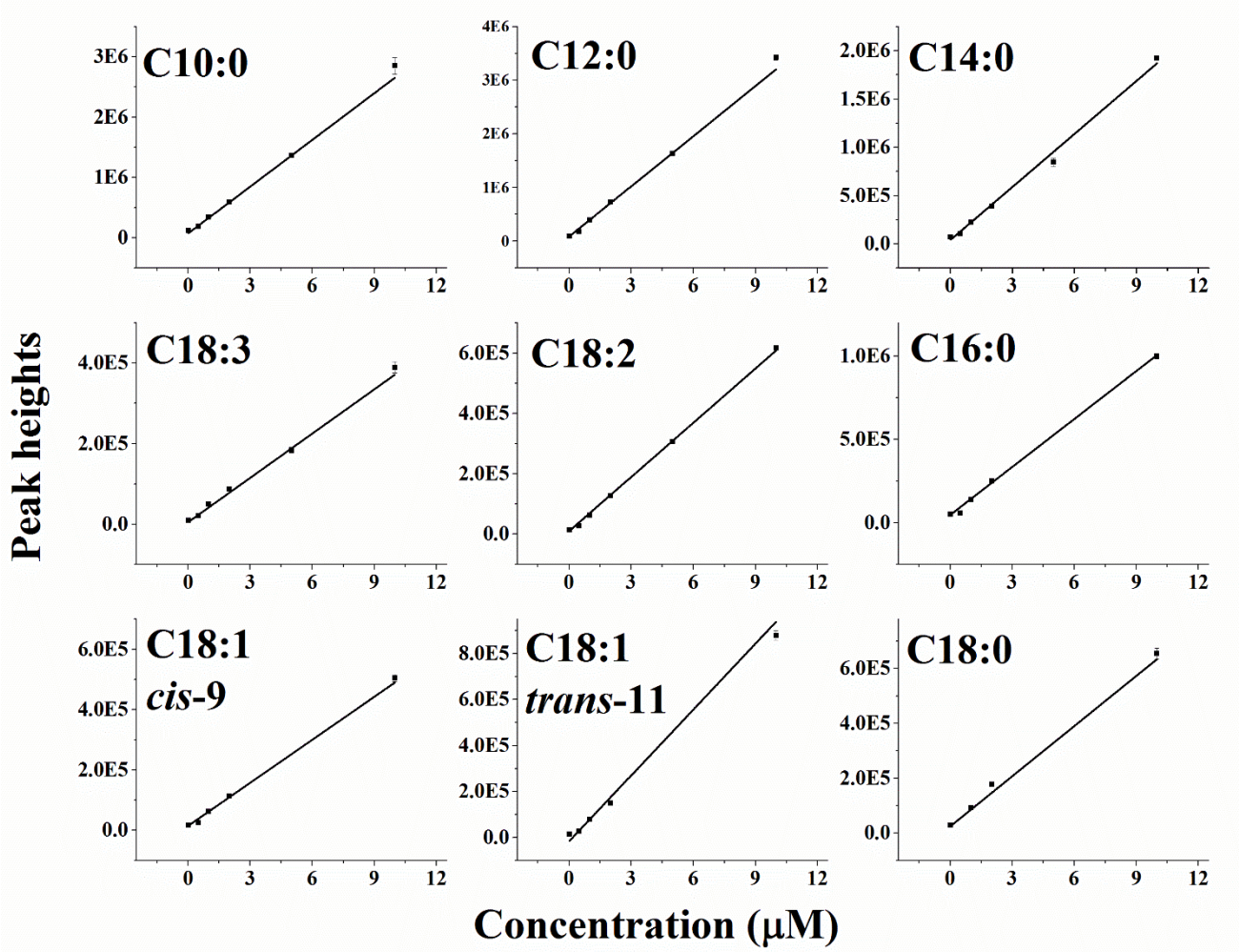

Figure 7. *Calibration curves of various FAs on the C4 column.*

FA profiles in the oil samples using the NMM column

After establishing the calibration curves for various standard FA-6AQ derivatives on the NMM and C4 columns, oil samples were analyzed for their FA content on the NMM column. Canola oil, which is rich in unsaturated FAs and coconut oil with high percentages of saturated FAs [24], were analyzed. Figure 8 depicts the separation of real oil samples on the NMM column. As the gradient program used for the separation of saturated FAs and the unsaturated FA mixtures is different, the samples of canola oil and coconut oil were analyzed by two different methods. For the canola oil sample, baseline separation was not achieved between linoleic acid (18:2) and oleic acid (18:1) and this might be due to high concentration of oleic acid relative to the other FAs. However, the chromatogram obtained is less cumbersome and the unreacted derivatizing agent 6AQ eluted at t_0 giving rise to an easily interpreted chromatogram. Similarly, baseline separation was achieved for all the analyzed FAs, and the chromatogram obtained for coconut oil sample is shown in Figure 8. Coconut oil, which is rich in saturated FAs, including lauric acid (12:0), myristic acid (14:0), palmitic acid (16:0) and stearic acid (18:0), attended a chromatogram free from complex sample background. The quantification results of the FAs present in the oil samples are listed in Table 3. Canola oil, which is rich in unsaturated FAs such as linolenic acid (18:3), linoleic acid (18:2), oleic acid (18:1) were quantified along with stearic acid (18:0). The total unsaturated FAs accounted for 82.7% including stearic acid (18:0), which is around 2.4%. On the other hand, coconut oil, which is composed of saturated FAs gave a clean chromatogram on the NMM column with baseline separation achieved for almost all the FAs. It is composed of FAs having a broad range of structures from caprylic acid (8:0) to stearic acid (18:0)

along with lauric acid (12:0) and myristic acid (14:0). A 40 min gradient run with increasing acetonitrile concentration is sufficient for the case of coconut oil sample. Refer to Table 1 for the observed FA content values.

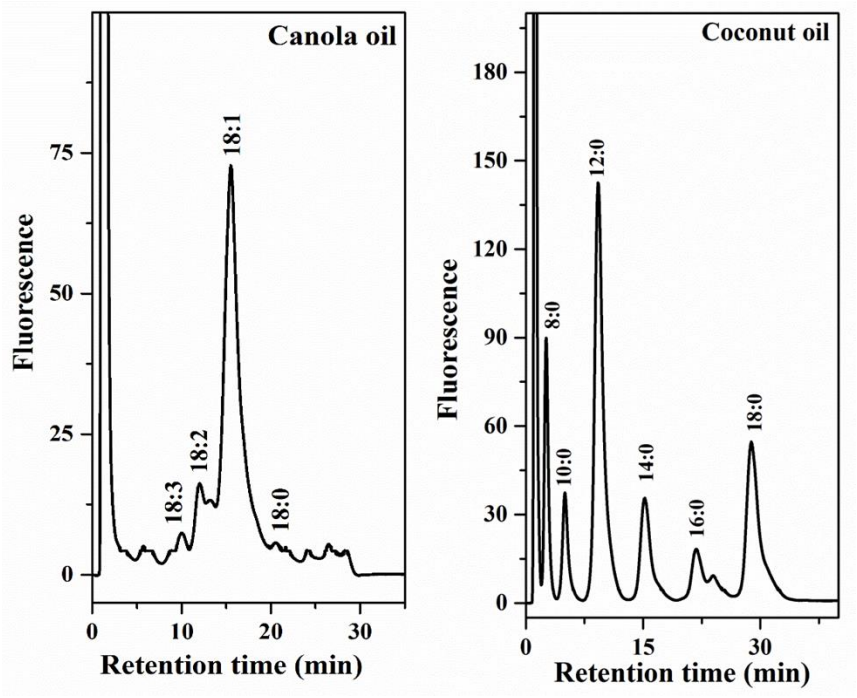

Figure 8. *Chromatograms of FAs from the oil samples. Conditions: Column, NMM column, 10 cm x 4.6 mm i.d.; mobile phase A, 0.1 % (v/v) TFA in 35% ACN in water, mobile phase B, 0.1% (v/v) TFA in 95% ACN in water, flow rate, 1.00 mL/min; fluorescence detection, excitation (λ_{exc}) at 270 nm and emission wavelengths (λ_{emi}) at 495 nm. Gradient conditions, 15/35/40/90/90 % B in 0/5/17/25/27 min and 10-90 % in 40 min for canola and coconut oil samples, respectively. Peak labels: caprylic acid (8:0); capric acid (10:0); lauric acid (12:0); myristic acid (14:0); linolenic acid (18:3); linoleic acid (18:2); palmitic acid (16:0); oleic acid (18:1); stearic acid (18:0).*

TABLE 3

ANALYTICAL RESULTS OF FAS IN OIL SAMPLES BY USING NAPTHYL MONOLITHIC COLUMN

COCONUT OIL	
FAs	*Concentration %w/w*
Caprylic acid (8:0)	12.01 ± 1.54
Capric acid (10:0)	6.61 ± 0.50
Lauric acid (12:0)	41.56 ± 1.05
Myristic acid (14:0)	10.15 ± 1.23
Palmitic acid (16:0)	5.12 ± 1.17
Stearic acid (18:0)	22.62 ± 4.38

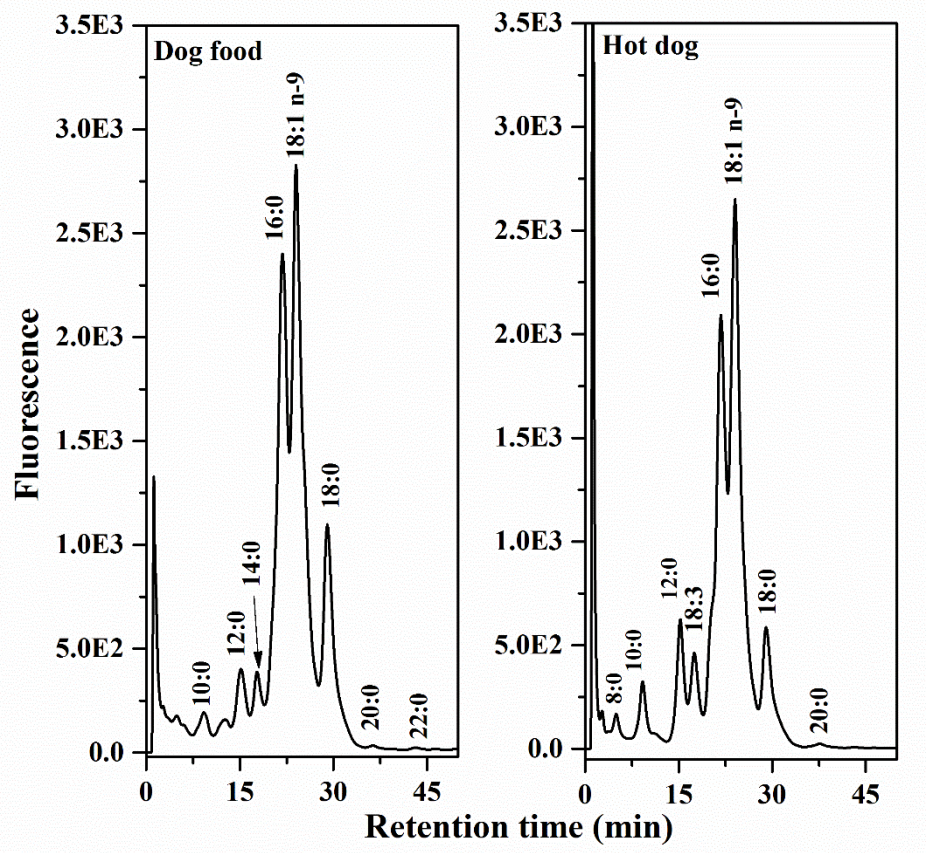

Figure 9. *Chromatograms of derivatized FAs from the food extracts of some selected food samples. NMM column, 10 cm x 4.6 mm i.d.; mobile phase A, 0.1 % (v/v) TFA in 35% ACN, mobile phase B, 0.1% (v/v) TFA in 95% ACN; flow rate, 1.00 mL/min. Fluorescence detection, excitation (λ_{exc}) at 270 nm and emission wavelengths (λ_{emi}) at 495 nm. Gradient elution, 10-90 %B in 45 min; for peak labels, refer to Figure 8.*

For further assessing the NMM column, the extracted fats from dog food and hot dog samples were derivatized based on the aforementioned derivatization method and analyzed by using a simple gradient program of 10-90% B in 60 min. The chromatograms are shown in Figure 9. Dog food and hot dog samples showed a similar pattern of FAs profiles, which are rich in oleic, palmitic acid and stearic acids. Baseline

separation of FAs was not observed due to the relatively high concentrations of these acids, which eluted in the time interval of 20-30 min. In addition to these FAs, several short chain FAs such as caprylic acid (8:0), capric acid (10:0), lauric acid (12:0), myristic acid (14:0) and long chain FAs such as arachidic acid (20:0) and behenic acid (22:0) were present in these samples and can be analyzed in less than 45 min. These results are a clear indication of the suitability of NMM column in real sample analysis of FAs in complex food samples.

FA profiles in meat samples and their quantification

As shown above, vaccenic acid and oleic acid in the FA mixtures were successfully separated on the C4 column. Consequently, by using the same method, FAs in meat samples were analyzed on the C4 column after subjecting the samples to the extraction and derivatization procedures mentioned in the preceding sections. The samples were analyzed in triplicate. The obtained chromatogram showing the FA profile of the meat sample is shown in Figure 10. In order to match the FAs with the standards, RRT were used for which palmitic acid (16:0) was used as a standard peak due to its presence in meat samples. A 70 min linear gradient was employed and carefully programmed to get optimum separation of all the FA derivatives. Almost all the FAs are effectively separated and distributed over the range from 10:0 to 18:0. The separation of vaccenic acid (18:1 *trans*-11) and oleic acid (18:1 *cis*-9) in the meat sample is different from the one obtained in the chromatogram of standards and this might be due to the relatively high concentration of oleic acid present in the meat sample. A total of 19 peaks were observed, of which the RRT of 9 FAs are matching with standards that are

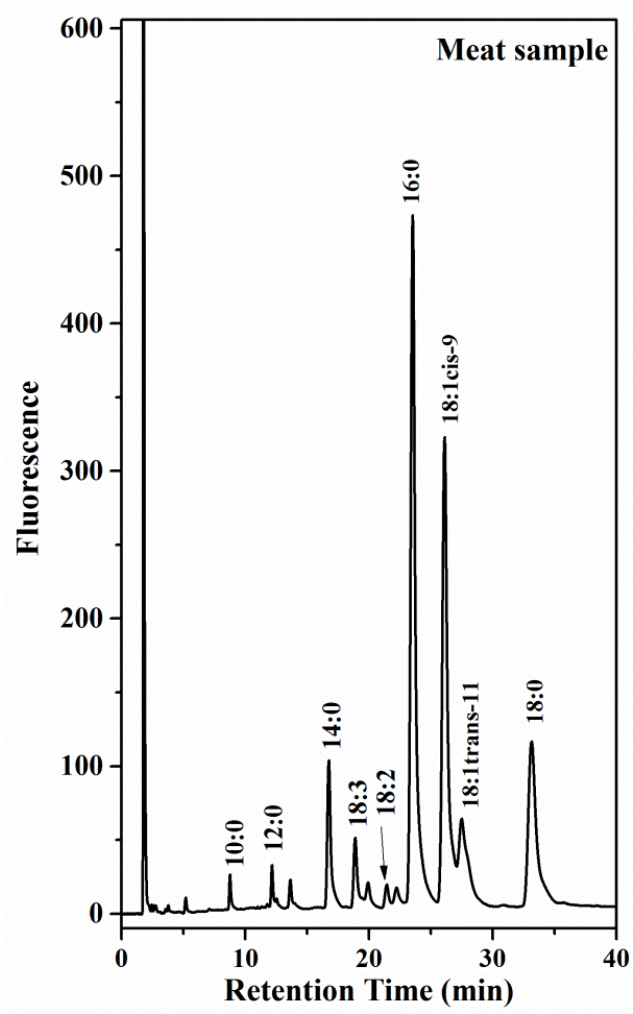

Figure 10. *Chromatogram of 6AQ derivatized FAs in the meat sample extract. C4 column, 15 cm x 4.6 mm i.d. Mobile phase A, 0.1 % (v/v) TFA in 30% ACN; mobile phase B, 0.05%(v/v) TFA in 90% ACN in water. Gradient program, % B 025/40/90/90 in 0/10/40/65/70 min; flow rate, 1.00 mL/min; fluorescence detection; excitation (λ_{exc}) at 270 nm and emission wavelengths (λ_{emi}) at 495 nm. Peak labels: capric acid (10:0); lauric acid (12:0); myristic acid(14:0); linolenic acid (18:3); linoleic acid (18:2); palmitic acid (16:0); oleic acid (18:1 cis-9); trans Vaccenic acid (18:1 trans-11); stearic acid (18:0).*

TABLE 4

FA CONTENT OF MEAT SAMPLES

FA derivative	*RRT**	*mg per 100 g of the meat*
Capric acid (10:0)	0.372	15.2 ± 1.3
Lauric acid (12:0)	0.532	13.8 ± 1.4
Myristic acid (14:0)	0.712	76.9 ± 0.3
Linolenic acid (18:3)	0.802	175.8 ± 7.7
Linoleic acid (18:2)	0.920	70.6 ± 2.6
Palmitic acid (16:0)	-	417.9 ± 36.8
Oleic acid (18:1 *cis* 9)	1.107	666 ± 21.1
Trans vaccenic acid (18:1 *trans* 11)	1.168	98.5 ± 24.8
Stearic acid (18:0)	1.407	227 ± 28.0
* Relative Retention Time with respect to 16:0		

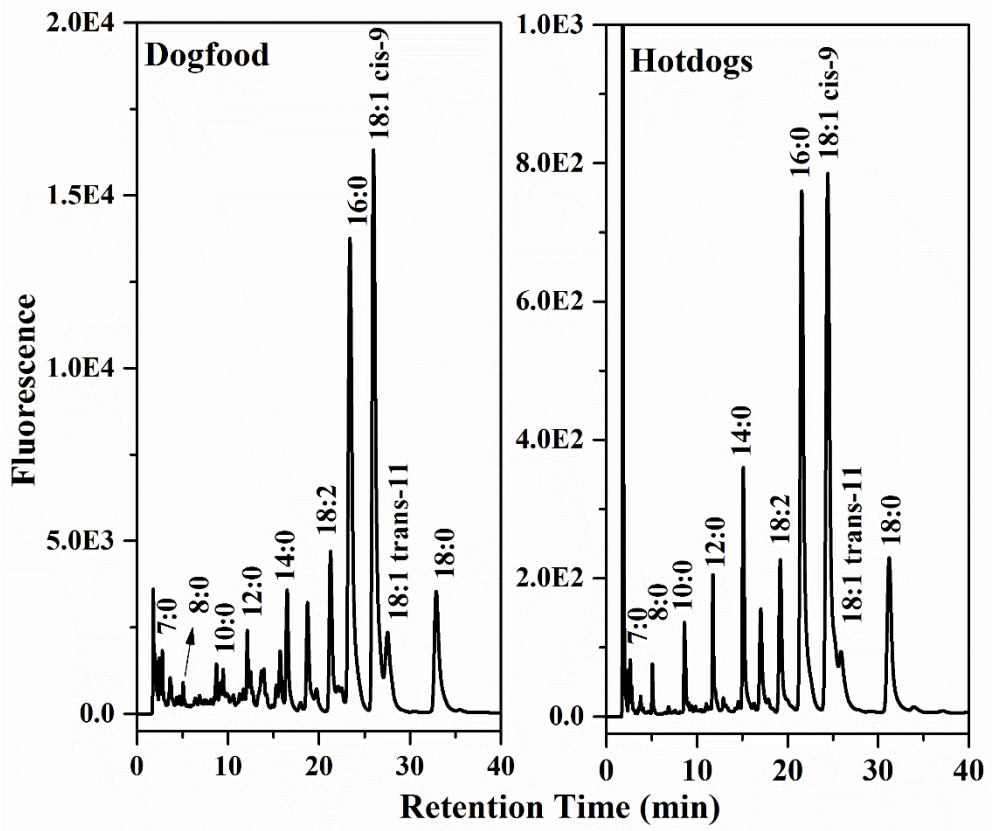

Figure 11. *Baseline separation of 6AQ FA derivatives present in the food sample extracts. Chromatographic condition and the peak labels were as in Figure 10.*

evaluated in the total separation of FAs on the C4 column. The quantification data obtained for the observed chromatograms along with the RRT values are listed in Table 4. Palmitic acid (16:0) was predominantly present in the sample followed by oleic and stearic acids. The vaccenic acid contents were quantified and the values were at the level of 98.5 mg in 100 g of the meat sample. The relative retention times for the observed FAs were also tabulated. To further validate the method, the meat samples were spiked with a known amount of lauric acid (12:0) and the experimental recovery values were in the

range 84.1-123.0 %. Apart from the meat samples, fats extracted from the most common food sample such as hot dogs and dog food were derivatized as per the preceding sections and analyzed on the C4 column using the same chromatographic procedure adopted for the meat samples. The obtained chromatograms are shown in Figure 11, which indicate the presence of a broad range of FAs from 7:0 to 18:0 present in both samples. The majority of FAs were baseline separated and the vaccenic acid peak was separated from the oleic acid peak.

Conclusions

In this study, a novel strategy for derivatizing FAs using 6AQ as a fluorescent tag in the presence of the coupling agent DCC was successfully developed and applied to the analysis of various oil and meat samples for their FA content. The chromatograms generated from the fluorescence detector were hassle-free and easy to interpret. The separation of the FA-6AQ derivatives were successfully established on the in-house synthesized naphthyl functionalized monolithic column. This column showed a promising behavior towards FA separation and could prove to be an efficient future tool for the fast, efficient and economical FA analysis, especially in the food industry. Finally, the 6AQ vaccenic and oleic acid derivatives were separated by employing a C4 functionalized silica column and their respective contents in the meat samples were quantified.

References

1. Wang, F.-H., X.-J. Xiong, X.-F. Guo, H. Wang, and H.-S. Zhang, *Determination of fatty acids in bio-samples based on the pre-column fluorescence derivatization with 1,3,5,7-tetramethyl-8-butyrethylenediamine-difluoroboradiaza-s-indacene by high performance liquid chromatography.* J. Chromatogr. A, 2013. **1291**: p. 84-91.
2. Rezanka, T. and J. Votruba, *Chromatography of very long-chain fatty acids from animal and plant kingdoms.* Anal. Chim. Acta, 2002. **465**(1–2): p. 273-297.
3. Gebauer, S.K., T.L. Psota, and P.M. Kris-Etherton, *The Diversity of Health Effects of Individual trans Fatty Acid Isomers.* Lipids, 2007. **42**(9): p. 787-799.
4. Field, C.J., H.H. Blewett, S. Proctor, and D. Vine, *Human health benefits of vaccenic acid.* Appl. Physiol. Nutr. Metab., 2009. **34**(5): p. 979-991.
5. *Natural Trans Fats Have Health Benefits, New Study Shows, www.sciencedaily.com/releases/2008/04/080402152140.htm.* ScienceDaily.
6. Tricon, S., G.C. Burdge, C.M. Williams, P.C. Calder, and P. Yaqoob, *The effects of conjugated linoleic acid on human health-related outcomes.* Proc. Nutr. Soc., 2005. **64**(02): p. 171-182.
7. Zhang, S., J. You, G. Zhou, C. Li, and Y. Suo, *Analysis of free fatty acids in Notopterygium forbesii Boiss by a novel HPLC method with fluorescence detection.* Talanta, 2012. **98**: p. 95-100.
8. Weatherly, C.A., Y. Zhang, J.P. Smuts, H. Fan, C. Xu, K.A. Schug, J.C. Lang, and D.W. Armstrong, *Analysis of Long-Chain Unsaturated Fatty Acids by Ionic Liquid Gas Chromatography.* J. Agric. Food. Chem., 2016. **64**(6): p. 1422-1432.

9. Aveldano, M.I., M. VanRollins, and L.A. Horrocks, *Separation and quantitation of free fatty acids and fatty acid methyl esters by reverse phase high pressure liquid chromatography.* J. Lipid Res., 1983. **24**(1): p. 83-93.

10. Montealegre, C., V. Verardo, A.M. Gómez-Caravaca, C. García-Ruiz, M.L. Marina, and M.F. Caboni, *Molecular Characterization of Phospholipids by High-Performance Liquid Chromatography Combined with an Evaporative Light Scattering Detector, High-Performance Liquid Chromatography Combined with Mass Spectrometry, and Gas Chromatography Combined with a Flame Ionization Detector in Different Oat Varieties.* J. Agric. Food. Chem., 2012. **60**(44): p. 10963-10969.

11. Hayashi, K., J. Kawase, K. Yoshimura, K. Ara, and K. Tsuji, *Determination of trace levels of fatty acid metal salts by high-performance liquid chromatography with fluorescence prelabeling.* Anal. Biochem., 1984. **136**(2): p. 314-320.

12. Brando, T., C. Pardin, J. Prandi, and G. Puzo, *Analysis of aminofluorescein–fatty acid derivatives by capillary electrophoresis with laser-induced fluorescence detection at the attomole level: application to mycobacterial fatty acids.* J. Chromatogr. A, 2002. **973**(1–2): p. 203-210.

13. Ichinose, N., K. Nakamura, C. Shimizu, H. Kurokura, and K. Okamoto, *High-performance liquid chromatography of 5,8,11,14,17-Eicosapentaenoic acid in fatty acids (C18 and C20) by labelling with 9-anthryldiazomethane as a fluorescent agent.* J. Chromatogr. A, 1984. **295**: p. 463-469.

14. ThomasáKarnes, H., *Reaction of 5-bromomethylfluorescein (5-BMF) with cefuroxime and other carboxyl-containing analytes to form derivatives suitable for laser-induced fluorescence detection.* Analyst, 1996. **121**(11): p. 1573-1579.

15. Toyo'oka, T., *Use of derivatization to improve the chromatographic properties and detection selectivity of physiologically important carboxylic acids.* J. Chromatogr. B Biomed. Sci. Appl., 1995. **671**(1): p. 91-112.

16. Li, G., J. You, Y. Suo, C. Song, Z. Sun, L. Xia, X. Zhao, and J. Shi, *A developed pre-column derivatization method for the determination of free fatty acids in edible oils by reversed-phase HPLC with fluorescence detection and its application to Lycium barbarum seed oil.* Food Chem., 2011. **125**(4): p. 1365-1372.

17. Chen, S.-H. and Y.-J. Chuang, *Analysis of fatty acids by column liquid chromatography.* Anal. Chim. Acta, 2002. **465**(1–2): p. 145-155.

18. Sun, Z., J. You, C. Song, and L. Xia, *Identification and determination of carboxylic acids in food samples using 2-(2-(anthracen-10-yl)-1H-phenanthro[9,10-d]imidazol-1-yl)ethyl 4-methylbenzenesulfonate (APIETS) as labeling reagent by HPLC with FLD and APCI/MS.* Talanta, 2011. **85**(2): p. 1088-1099.

19. Mehta, A., A.M. Oeser, and M.G. Carlson, *Rapid quantitation of free fatty acids in human plasma by high-performance liquid chromatography.* J. Chromatogr. B Biomed. Sci. Appl., 1998. **719**(1–2): p. 9-23.

20. Jonnada, M. and Z. El Rassi, *Robust naphthyl methacrylate monolithic column for high performance liquid chromatography of a wide range of solutes.* J. Chromatogr. A, 2015. **1409**: p. 166-172.

21. Nashabeh, W. and Z. El Rassi, *Capillary zone electrophoresis of linear and branched oligosaccharides.* J. Chromatogr. A, 1992. **600**(2): p. 279-287.

22. Mechref, Y., G.K. Ostrander, and Z. El Rassi, *Capillary electrophoresis of carboxylated carbohydrates I. Selective precolumn derivatization of gangliosides with UV absorbing and fluorescent tags.* J. Chromatogr. A, 1995. **695**(1): p. 83-95.

23. Dołowy, M. and A. Pyka, *Chromatographic methods in the separation of long-chain mono-and polyunsaturated fatty acids.* Journal of Chemistry, 2015. **2015**.

24. Aparicio, R. and R. Aparicio-Ruíz, *Authentication of vegetable oils by chromatographic techniques.* J. Chromatogr. A, 2000. **881**(1–2): p. 93-104.

VITA

Venkata Ramana Murthy Jonnada

Candidate for the Degree Of

Doctor of Philosophy

Thesis: DEVELOPMENT AND APPLICATIONS OF NOVEL MONOLITHIC STATIONARY PHASES FOR LIQUID PHASE SEPARATIONS

Major Field: Chemistry

Biographical:

Education:

Completed the requirements for the Doctor of Philosophy in Chemistry at Oklahoma State University, Stillwater, Oklahoma in July, 2016.

Completed the requirements for the Master of Science in Analytical Chemistry at Jawaharlal Nehru Technological University, Hyderabad, A.P., India in 2007.

Completed the requirements for the Bachelor of Science at Andhra University, Vishakhapatnam, A.P., India in 2005.

Experience:

Worked as Research Associate in Analytical Research and Development Laboratories, Aurobindo Pharma Ltd., Hyderabad, India from May 2010 to June 2011.
Worked as Senior Chemist in Analytical Development Laboratories in Mylan Labs, India from July 2007 to April 2010.